The RING domain of Nse1: roles in Smc5/6 complex stability and genome integrity in human cells

Sonia Nikolova Apostolova

Universitat de Lleida

TESI DOCTORAL

The RING domain of Nse1: roles in Smc5/6 complex stability and genome integrity in human cells

Sonia Nikolova Apostolova

Memòria presentada per optar al grau de Doctor per la Universitat de Lleida

Programa de Doctorat en Salut

Director/a

Jordi Torres Rosell

Neus Colomina Gabarrella

Tutor/a

Jordi Torres Rosell

2021

Doctoral thesis:

The RING domain of Nse1: roles in Smc5/6 complex stability and genome integrity in human cells

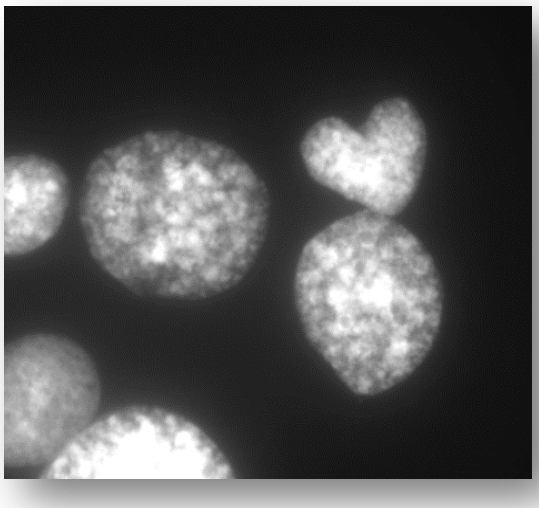

Sonia Apostolova, University of Lleida,

IRBLleida, Spain

2021

Dedicated to My Mother ♥

ACKNOWLEDGEMENTS

First, I would like to express my sincere gratitude to my supervisors Dr Jordi Torres Rosell and Dr. Neus Colomina Gabarrella for their guidance, patience and support throughout the years.

Jordi, thank you for giving me the opportunity to work on your research project and to do my PhD thesis in your lab, as well as for your time, constant support, motivation and constructive criticism.

Neus, thank you for everything you have taught me. I have learned a lot of new skills and scientific methods from you. Thank you also for your ongoing support in the scientific work, as well as outside the laboratory.

Many thanks to both of you for this great research and a life experience during these 5 years in which I have gained valuable knowledge and grew also as a person. I really appreciate it. Thank you also for making the completion of this thesis possible, despite the difficult times during COVID-19 outbreak.

Furthermore, I would like to thank to all previous and current members of the Cell Cycle group, especially Dr. Eloi Gari, Dr. Francisco Ferrezuelo, Dr. Neus Pedraza, Dr. Celia Casas, Dr. Gemma Belli, Dr. Marta Rafel, Sonia Rius, Roger Solé Soler, Marc Tarres, Eva Irene Ibars, Marta Guasch, Neus Lorite, Dr. Turi Monserrat and Dr. Mariel Zapatka for their help, valuable discussions and for creating a friendly atmosphere in the lab.

I would especially like to thank Dr. Marta Rafel for helping me with analyzing Crisp/Cas9 clones and for having taught me how to perform the SCE technique.

Thanks also to all colleagues from IRB Lleida for their kindness and for providing a good working environment.

I am also grateful to Prof. Dr. Neus Agell from University of Barcelona for giving me the opportunity to do a research stay in her department. And many thanks to Fernando Unzueta for his attention and tremendous help with DNA fiber analysis and BrdU/PI flow cytometry.

Many thanks also go to my friends Irina and Cvetan for their generosity, emotional support and encouragement during my PhD journey. Irina and Cvetan, thank you for all joyful moments and fun time spend together in Spain.

Finally, I would like to thank my ex-colleagues, friends and family in Bulgaria for their support during all these years.

Very special thanks to my father Nikola and my grandmothers Dimitrina and Tsveta for believing in me and for their love, patience and never-ending support.

I am particularly grateful to my sister Iva, for always being there for me and encouraged me not to give up no matter what difficulties I faced. Iva, thank you for your love and care, especially in the darkest days of my life.

SUMMARY

Eukaryotic cells need to accurately replicate and segregate chromosomes during cell division to maintain the stability of their genomes. Errors in these processes may lead to genetic disorders, pre-mature aging and cancer. The evolutionary conserved Smc5/6 complex is one of the three Structural Maintenance of Chromosomes (SMC) protein complexes with essential roles in preserving genomic stability during cell division, ensuring proper chromosome segregation and DNA repair. The function of this complex and its individual components is still not well understood, particularly in higher eukaryotes.

In this thesis we show that the RING domain in Nse1, one of the subunits of the Smc5/6 complex, has a crucial role in the maintenance of genomic integrity in human cells. By using CRISPR/Cas9 we created stable *NSE1* mutants in the C-terminal RING domain which show no detectable levels of Nse1 and other subunits of the complex, except Nse2. These mutant cells have a genomic instability phenotype, characterized by slow growth, prolonged mitosis, spontaneous endogenous DNA damage, slowdown of replication fork progression and sensitivity to MMS, a genotoxic drug. Our results suggest that *NSE1* mutant cells enter into mitosis with either under-replicated DNA or unresolved DNA structures consequently leading to chromosome breaks and genomic instability in the next generation.

The Smc5/6 complex is also known to prevent accumulation of toxic recombination structures by inhibiting Mph1 helicase in *Saccharomyces cerevisiae*. The suppression of Mph1 fork regression activity rescues *smc5/6* mutants, indicating that the Smc5/6 complex function in the same pathway as Mph1. However, it is unknown if this functional interaction is conserved in human cells. Our genetic interaction experiments suggest that the Smc5/6 complex and FANCM (homologue of Mph1), operate in distinct pathways as the loss of both causes synthetic sickness in human cells.

Finally, we identify novel interactors of the human Nse1 protein using a yeast two hybrid screen. Some of these interactors have cytoplasmic localization, suggesting that either the Smc5/6 complex has functions outside of the nucleus, or that Nse1 can also exert a function independently from the Smc5/6 complex. Although the function of these interactions is currently unknown, they could be useful for future analysis in order to better understand the role of human Nse1.

Altogether, our results demonstrate the importance of the RING domain in human Nse1 for the stability of the SMC5/6 complex and the maintenance of genomic integrity.

RESUM

La correcta replicació i segregació dels cromosomes durant la divisió cel·lular és essencial per al manteniment de l'estabilitat genòmica en cèl·lules eucariotes. Errors en aquests processos poden comportar el desenvolupament de diversos desordres genètics, envelliment prematur i càncer. El complex Smc5/6, conservat evolutivament en eucariotes, és un dels tres complexos de manteniment de l'estructura dels cromosomes (Structural Maintenance of Chromosomes, SMC), amb funcions essencials en el manteniment de l'estabilitat genòmica, assegurant una correcta segregació dels cromosomes i la reparació dels danys en el DNA. La funció d'aquest complex i la de les diferents subunitats que el formen, encara no és ben coneguda, particularment en eucariotes superiors.

En aquest treball de tesi es mostra que el domini RING de la subunitat Nse1 del complex SMC5/6, té un paper crucial en el manteniment de l'estabilitat genòmica en cèl·lules humanes. Mitjançant CRISPR-Cas9 hem creat mutants estables de *NSE1* en el domini RING C-terminal. En aquests mutants no es pot detectar la proteïna Nse1, ni altres subunitats del complex, excepte Nse2. Aquests mutants presenten un fenotip d'inestabilitat genòmica, caracteritzat per un creixement lent, mitosis més prolongades en el temps, dany endogen en el DNA, un alentiment en la progressió de les forquilles de replicació i sensibilitat a l'agent genotòxic MMS. Els nostres resultats suggereixen que els mutants en *NSE1* entren en mitosis amb la presència de zones del DNA no replicades o amb estructures de recombinació no resoltes, que porten al trencament de cormosomes i a inestabilitat genòmica en la següent generació.

En llevat, el complex Smc5/6 evita l'acumulació d'estructures de recombinació tòxiques mitjançant la inhibició de l'helicasa Mph1. La supressió de l'activitat de regressió de forquilles de Mph1 rescata els mutants *smc5/6*, indicant que el complex Smc5/6 funciona en la mateixa via que Mph1. Actualment, no es coneix si aquesta interacció funcional està conservada en cèl·lules humanes. Els experiments d'interacció genètica que hem realitzat suggereixen que el complex Smc5/6 i FANCM (homòleg de Mph1) operen en vies diferents ja que la pèrdua d'ambdós factors en cèl·lules humanes agreuja el fenotip dels mutants simples.

Finalment, mitjançant un cribratge amb un assaig di-híbrid, hem identificat nous interactors de la proteïna Nse1 humana. Alguns d'ells tenen localització citoplasmàtica, el que suggereix que el complex Smc5/6 podria tenir funcions fora del nucli, o bé, que Nse1 podria exercir algunes funcions independentment del complex Smc5/6. Tot i que encara no coneixem la funció d'aquestes interaccions, podrien ser d'utilitat per entendre millor la funció de la proteïna Nse1 en cèl·lules humanes en futurs estudis.

En conjunt, els resultats d'aquesta tesi demostren la importància del domini RING de la proteïna Nse1 en l'estabilitat del complex Smc5/6 i en el manteniment de la integritat genòmica en cèl·lules humanes.

RESUMEN

La correcta replicación y segregación de los cromosomas durante la división celular es esencial para el mantenimiento de la estabilidad genómica en células eucariotas. Errores en estos procesos pueden llevar a diversos desórdenes genéticos, envejecimiento prematuro y cáncer. El complejo Smc5/6, conservado evolutivamente en eucariotas, es uno de los tres complejos proteicos necesarios para el mantenimiento de la estructura de los cromosomas (Structural Maintenance of Chromosomes, SMC), con funciones esenciales en el mantenimiento de la estabilidad genómica, asegurando una correcta segregación de los cromosomas y la reparación del daño en el ADN. Aún no se conoce bien la función de este complejo y la de las diferentes subunidades que lo forman, particularmente en eucariotas superiores.

En este trabajo de tesis se muestra como el dominio RING de la subunidad Nse1 del complejo Smc5/6, tiene un papel crucial en el mantenimiento de la estabilidad genómica en células humanas. Hemos creado mutantes estables de *NSE1*, en el dominio RING C-terminal de la proteína, con la utilización de CRISPR-Cas9. En estos mutantes, no se puede detectar la proteína Nse1, ni otras subunidades del complejo, excepto Nse2. Presentan un fenotipo de inestabilidad genómica, caracterizado por un crecimiento lento, mitosis más prolongadas en el tiempo, daño endógeno del ADN, enlentecimiento en la progresión de las horquillas de replicación y sensibilidad al agente genotóxico MMS. Nuestros resultados sugieren que los mutantes en *NSE1* entran en mitosis con la presencia de zonas en el ADN no replicadas o con estructuras de recombinación no resueltas, lo que lleva a la rotura de cromosomas, y a inestabilidad genómica en la siguiente generación.

En levadura, el complejo Smc5/6 evita la acumulación de estructuras de recombinación tóxicas mediante la inhibición de la helicasa Mph1. La supresión de la actividad de regresión de horquillas de Mph1 rescata a los mutantes *smc5/6*, indicando que el complejo Smc5/6 y Mph1 son epistáticos en la estabilización de las horquillas de replicación dañadas. Actualmente, no se conoce si esta interacción funcional se mantiene en células humanas. Los experimentos de interacción genética que hemos realizado sugieren que el complejo Smc5/6 y FANCM (homólogo de Mph1) tienen funciones en vías diferentes, ya que la pérdida de ambos factores en células humanas agrava el fenotipo de los mutantes sencillos.

Finalmente, mediante un cribado con un ensayo di-híbrido, hemos identificado nuevos interactores de la proteína Nse1 humana. Algunos tienen localización citoplasmática, lo que sugiere que el complejo Smc5/6 podría tener funciones fuera del núcleo, o bien, que Nse1 podría ejercer algunas funciones independientemente del complejo Smc5/6. Aunque no conocemos la función de estas interacciones, podrían ser de utilidad para entender mejor la función de la proteína Nse1 en células humanas en futuros estudios.

En conjunto, los resultados de esta tesis demuestran la importancia del dominio RING de la proteína Nse1 en la estabilidad del complejo Smc5/6 y en el mantenimiento de la integridad genómica.

Contents

ACKNOWLEDGEMENTS IV
SUMMARY VI
RESUM VII
RESUMEN IX
List of Abbreviations i
INTRODUCTION 1
1.1 Eukaryotic cell cycle and genomic stability 1
1.1.1 S phase 2
1.1.2 Mitosis 6
1.2 Cell cycle checkpoints 7
1.2.1 G1/S checkpoint 10
1.2.2 G2/M checkpoint 10
1.2.3 Replicative stress and S phase checkpoint 11
1.2.4 Spindle checkpoint 13
1.3 DNA repair mechanisms 15
1.3.1 Homologous recombination (HR) 15
1.3.2 Non-homologous end joining (NHEJ) 16
1.3.3 Base-excision repair (BER) 17
1.3.4 Mismatch repair (MMR) 18
1.3.5 Nucleotide excision repair (NER) 19
1.3.6 Interstrand cross-link repair (ICL) 21
1.3.7 DNA damage tolerance (S phase specific) 24
1.4 Ubiquitylation pathway 27
1.4.1 Ubiquitylation in DNA repair 29
1.5 Structural maintenance of chromosomes 32
1.5.1 The Smc5/6 complex – structure 34
1.5.2 The Smc5/6 complex - function in eukaryotic cells 37
1.5.3 Nse1 ubiquitin ligase 41
1.5.4 Impaired Smc5/6 complex function and human diseases 44
OBJECTIVES 46

MATERIALS AND METHODS 47
3.1 Human cell lines methods 47
3.1.1 Cell lines and culture conditions 47
3.1.2 Freezing and thawing of cells 47
3.1.3 Generation of mutations in human *NSE1* by CRISPR/Cas9 technique . 47
3.1.4 Transient transfections of human cells 50
3.1.5 Lentiviral production and transduction for stable cell line generation 50
3.1.6 Cell proliferation analysis using trypan blue exclusion assay 51
3.1.7 Detection of apoptosis by double-staining with acridine orange and ethidium bromide (AO/EB) 51
3.1.8 Time-lapse microscopy 52
3.1.9 Immunofluorescence for detection of BLM foci 52
3.1.10 Micronuclei analysis 53
3.1.11 Sister chromatid exchange assay (SCE) 53
3.1.12 Clonogenic survival assay 53
3.1.13 Cell cycle analysis with propidium iodide (PI) 54
3.1.14 Cell cycle analysis with double staining with PI and BrdU and MPM-2 detection 54
3.1.15 DNA fiber technique for analysis of fork progression and dynamics . 55
3.2 Methods using yeast cells 55
3.2.1 Yeast strains 55
3.2.2 Yeast two hybrid assay 56
3.3 Bacterial methods 58
3.3.1 Plasmids 58
3.3.2 Transformation into competent E.coli cells 61
3.3.3 Plasmid Jet Prep (phenol-chloroform DNA extraction) 61
3.4 Nucleic acid methods 62
3.4.1 RNA isolation, cDNA synthesis and Real-time PCR (RT-PCR) 62
3.4.2 Site-directed mutagenesis (SDM) 62
3.4.3 Agarose-gel electrophoresis 63
3.4.4 Primers 63
3.4.5 Short hairpin and small interfering RNAs (shRNA and siRNA) 66
3.4.6 DNA sequencing 66
3.5 Protein methods 67

3.5.1 Immunoprecipitation 67
3.5.2 Sodium dodecyl sulphate-polyacrylamide gel electrophoresis (SDS-PAGE) 67
3.5.3 Western blot 68
3.6 Drugs and treatments 68
3.7 Antibodies 68
RESULTS 71
4.1 Analysis of the NH-RING domain in human cells 71
4.1.1 Generation of human *NSE1* mutants with impaired ubiquitin activity by CRISPR-Cas9 71
4.1.2 Phenotype characterization of the different *NSE1* mutants obtained (*NSE1-AA, NSE1-A, NSE1-ΔR*). 75
4.1.2.1 *NSE1* mutants show no detectable levels of Nse1 75
4.1.2.2 All *NSE1* mutants show slow growth phenotype and changes in cell morphology 77
4.1.2.3 No detectable cell cycle arrest, but higher number of cells with increased genomic instability in *NSE1* mutant cells 79
4.1.2.4 *NSE1* mutant cells display prolonged mitosis 80
4.1.2.5 *NSE1* mutants show higher levels of endogenous DNA damage 81
4.2 Rescue of *NSE1* mutants' phenotype by ectopic expression of wild type *NSE1.* 89
4.2.1 *NSE1* mutant cells are sensitive to genotoxic drugs. Ectopically expressed wild type *NSE1* restores the drug-sensitive phenotype. 91
4.2.2 *NSE1-ΔR* mutants show a reduction in the number of cells in S phase, which is normalized after expression of *NSE1* wild type 92
4.2.3 *NSE1-ΔR* mutants exhibit slowdown of replication fork progression. Ectopically expressed *NSE1* restores the normal fork progression 94
4.3 Genetic interaction between Smc5 and FANCM - Mph1 orthologue. 96
4.3.1 Depletion of Smc5 in FANCM KO results in synthetic sickness. 99
4.4. Identification of novel proteins interacting with human Nse1 using yeast two-hybrid screen. 103
4.4.1 Nse1 physically interacts with TRUSS and HMG-17 105
4.4.2 Validation of Y2H interactions *in vivo* 106
4.4.3 Nse1 interacts with different domains of TRUSS 107
4.4.4 TRUSS interacts with the N-terminal domain of Nse1 108

DISCUSSION 111

1. Usage of CRISPR-Cas9 to mutate the RING domain of NSE1 111

2. The NH-RING domain in Nse1: from an E3 ubiquitin ligase function to a structural role promoting the stability of the Smc5/6 complex 112

3. Role of human Nse1 and Smc5/6 complex in genomic stability 116

4. The Smc5/6 complex and FANCM maintain the genomic stability by regulating alternative repair pathways in human cells 121

CONCLUSIONS 125

REFERENCES 126

List of Abbreviations

3-AT - 3-Amino-1,2,4-Triazol
3D - three-dimensional
53BP1- p53-binding protein
AD - activation domain
Ade - adenine
Ala – alanine
AO - acridine orange
AP site - abasic site - apurinic or apyrimidinic
APC/C - Anaphase-Promoting Complex or Cyclosome
APE-1 - AP endonuclease 1
ATM - ataxia-telangiectasia mutated kinase
ATP - adenosine triphosphate
ATR - ataxia telangiectasia and Rad3-related kinase
ATRIP - ATR-interacting protein
BER - base-excision repair
BIR - break-induced replication
BLM - Bloom syndrome protein
BMF - bone marrow failure
bp -base pairs
BRCA1- breast cancer type 1 susceptibility protein
BrdU - Bromodeoxyuridine / 5-bromo-2'-deoxyuridine
BSA - bovine serum albumin
Bub3 - mitotic checkpoint protein
BubR1 - budding uninhibited by benzimidazole related 1 protein
cccDNA - covalently closed circular DNA
Cdc20 - cell-division cycle protein 20
Cdc25 - Cell division cycle 25 phosphatase
Cdh1 - Cdc20 homologue 1
CDK - cyclin-dependent kinase
CDKN1A - CDK-interacting protein 1 (p21)
cDNA - complementary DNA
Chk1 - Checkpoint kinase 1
Chk2 - Checkpoint kinase 2
Chr – chromatin fraction
CID - collision induced dissociation
CIdU – chlorodeoxyuridine
Co-IP - Co-immunoprecipitation
CPT – camptothecin
CRISPR-Cas9 - Clustered Regularly Interspaced Short Palindromic Repeats)/Cas9
CTP – camptothecin
Cys – Cysteine
DAPI - 4’,6-diamidino-2-phenylindole
DDB1 - DNA-damage binding protein 1
DDK - Dbf4-Dependent Kinase

DDR - DNA damage response
DDT - DNA damage tolerance
DMEM – Dulbecco's Modified Eagle's Medium
DMSO – dimethylsulfoxide
DNA - deoxyribonucleic acid
DNA-BD - DNA-binding domain
DNA-PKcs - DNA-dependent protein kinase, catalytic subunit
Dox - doxycycline
DSBR - double-strand break repair
DSBs - double-strand breaks
dsDNA - double stranded DNA
DUBs - deubiquitinases
EB - ethidium bromide
EDTA - ethylenediaminetetraacetic acid
eGFP - enhanced Green Fluorescent Protein
ES - enrichment score
EtBr - ethidium bromide
ETO – etoposide
Exo1 – exonuclease 1
FA - Fanconi anemia
FA - formic acid
FAAP24 - Fanconi Anemia associated protein of 24 kDa
FACS - fluorescence-activated cell sorting
FANCM - Fanconi anemia protein M
FBS - fetal bovine serum
FDR - False discovery rate
FEN1 - flap endonuclease 1
FLB - formamide loading buffer
GFP - green fluorescent protein
GGR - global genome repair
gRNA - guide RNA
H2AX - H2A histone family member X
HBV - Hepatitis B virus
HDR - homology-directed repair
HECT - Homologous to E6AP Carboxyl Terminus
HEK293T - Human embryonic kidney cell line
His - Histidine
HJs - Holliday junctions
HR - homologous recombination
HU - hydroxyurea
IAP - immunoaffinity purification
ICL - Interstrand cross-link
IdU – iododeoxyuridine
IMAC - immobilised metal ion affinity chromatography
IP - Immunoprecipitation
IR - ionizing radiation
ISG15 - interferon-stimulated gene 15

KAN - kanamycin
KITE - kleisin-interacting tandem winged-helix element
KO – knockout
LB - Luria Broth
LC-MS - Liquid chromatography–mass spectrometry
LEFs - loop-extruding factors
Leu - leucine
LTQ - linear ion trap
Lys - Lysine
mA – milliampere
Mad2 - mitotic Arrest Deficient protein
MAGE - melanoma-associated antigen
MAP - Mitogen-activated protein kinase
MCM - minichromosome maintenance helicase
MDC1 - mediator of DNA-damage checkpoint protein 1
MFH1/2 - histone fold protein complex
MMC - mytomicin C
MMR - mismatch repair
MMS - methyl methanesulfonate
MN – micronuclei
MPM-2 - mitotic protein monoclonal 2
Mps1 - monopolar spindle 1 kinase
mRNA - messenger RNA
NB - non bound
Nedd8 - neural precursor cell expressed, developmentally down-regulated 8
NEM - N-Ethylmaleimide
NER - nucleotide excision repair
NES - Normalised enrichment score
NF-κB - nuclear factor-κB
NHEJ - non-homologous end joining
Ni^{2+} - Nickel ion
NP-40 - Nonidet P40
Nse - non-structural maintenance of chromosome element
NSE1-A - single point mutant (C207A)
NSE1-AA – double point mutant (C204A-C207A)
NSE1-ΔR - Nse1 with truncated RING domain
OD_{600} - optical density measured at 600 nanometres-wavelength
one-way ANOVA – one way analysis of variance
ORC - origin recognition complex Orc1–6
ori – origins
P.D. Pull-Down
PAM - protospacer adjacent motif
PBS - phosphate-buffered saline
PCNA - proliferating cell nuclear antigen
PCR polymerase chain reaction
PEI – Polyethylenimine
PFA – paraformaldehyde

PI - propidium iodide
PIKK - phosphatidyl inositol 3' kinase-related kinases
PLK1 - polo-like kinase 1
PMSF - phenylmethylsulfonyl fluoride
Pol – polymerase
pre-RC - pre-replication complex
PrimPol - primase and DNA directed polymerase
PSM - peptide spectrum matches
PTMs - post-translational modifications
PVDF - Polyvinylidene difluoride
RBR - RING-in-Between-RING
rDNA - ribosomal DNA
RFC - replication factor C
RING - Really Interesting New Gene
RNA – ribonucleic acid
RNF8 - Ring finger protein 8
ROS - reactive oxygen species
RPA - replication protein A
RT – room temperature
RT-PCR - Real-time PCR
SAC - Spindle assembly checkpoint
SC - synthetic complete
Scc1 - sister chromatid cohesion protein 1
Scc3 - sister chromatid cohesion protein 3
SCE - Sister chromatid exchange
SDM - site-directed mutagenesis
SDSA - synthesis-dependent strand annealing
SDS-PAGE - sodium dodecyl sulphate-polyacrylamide gel electrophoresis
sgRNA - single guide RNA
shRNA – short hairpin RNA
siRNA - small interfering RNA
SLF1 - SMC5-SMC6 Complex Localization Factor 1
SLF2 - SMC5-SMC6 Complex Localization Factor 2
SMC - Structural Maintenance of Chromosomes
SMC1 - Structural maintenance of chromosomes protein 1
SN - supernatant
SN – soluble supernatant
SSBs - single strand breaks
ssDNA - single stranded DNA
ssODN - single-stranded oligodeoxynucleotide
SUMO - small ubiquitin-like modifier
T.E. – total extract
T7EI - T7 endonuclease I enzyme
TADs - topologically associated domains
TAE - Tris-acetate-EDTA
TB – trypan blue
TCA - trichloroacetic acid

TCEP - tris(2-carboxyethyl)phosphine
TCR - T-cell receptor
TCR - transcription-coupled repair
TEMED - tetramethylethylenediamine
TFA - trifluoroacetic acid
TFIIH - transcription factor IIH
TLS - translesion DNA synthesis
Top2 - topoisomerase II
TopBP1 - DNA topoisomerase II-binding protein 1
Topo IIIa - topoisomerase IIIa
Trp - tryptophan
TS - template switching
Ub – ubiquitin
UBLs - ubiquitin-like proteins
U-box - UFD2 homology
UDG - uracil DNA glycosylase
UQ - ubiquitinated
UV - ultraviolet
V – volts
WCE - whole cell extract
WT – wild type
XLF - XRCC4-like factor
XPA - Xeroderma Pigmentosum Complementation Group A Protein
XPB - Xeroderma Pigmentosum Complementation Group B Protein
XPD - Xeroderma Pigmentosum Complementation Group D Protein
XPG - Xeroderma Pigmentosum Complementation Group G Protein
XRCC4 - X-ray repair cross-complementing 4
Y2H - yeast-two-hybrid
YP - yeast peptone
YPD - Yeast Extract–Peptone–Dextrose
Zn - Zinc

INTRODUCTION

1.1 Eukaryotic cell cycle and genomic stability

The eukaryotic cell-division cycle is a fundamental tightly coordinated process that allows proliferation of cells and the development of multicellular organisms. Our current knowledge of cell division started with pioneering studies during the 19th century. It was first described in 1835 by the German botanist Hugo von Mohl, who observed dividing cells from green algae under the microscope. Thirty nine years later, the German cytologist Eduard Strasburger characterized the different stages of cell division in plants [Harashima et al., 2013, Baluška et al., 2012]. In the 1880s, the German biologist Walther Flemming identified somatic cell division with the term mitosis [Mitchison and Salmon, 2001].

Due to the intensive studying of cell division throughout the years, we now know in detail its different phases and the mechanisms involved in its regulation, which are highly conserved in all eukaryotes. The cell cycle is mainly divided in two stages: interphase and mitosis. Interphase involves the growth of the cell and the duplication of the genetic material. It is the longest phase of the cell cycle and includes G1, S and G2 stages. The G1 phase is a gap, during which the cell is preparing for DNA synthesis. In S phase the cell replicates DNA. After DNA replication, cells enter the second gap phase (G2) in preparation for mitosis. Mitosis corresponds to the nuclear division and requires equal segregation of chromosomes to daughter cells. Thus, S phase and mitosis are separated by two gap phases, G1 and G2, ensuring the temporal separation between DNA replication and chromosome segregation. After completion of one cell cycle, cells might enter successive cycles or enter quiescence (also known as G0 phase), a decision that normally depends on the presence or absence of mitogenic signals [Cooper, 2000, Li et al., 2015, Lalan et al., 2011].

The main regulators of the cell cycle are Cyclin-CDK (Cyclin-Dependent Kinase) complexes and checkpoints. CDKs are serine/threonine protein kinases that are activated by interaction with cyclin proteins. CDK4, CDK6 and CDK2 are activated during the G1 phase, CDK2 is active during the S phase, and CDK1 – during M phase [Vermeulen et al., 2003]. Activation of Cyclin-Cdk complexes promotes irreversible transitions between different phases of the cell cycle. On the other hand, these transitions are monitored by regulatory circuits known as cell cycle checkpoints. Checkpoints coordinate the proper order of cell cycle events thus ensuring, for example, that the genetic material is completely duplicated without errors before mitosis. In this way, checkpoints determine if cells can progress through the cell cycle or if they should delay or stop at specific phases, providing time to resolve unresolved issues [Cooper, 2000].

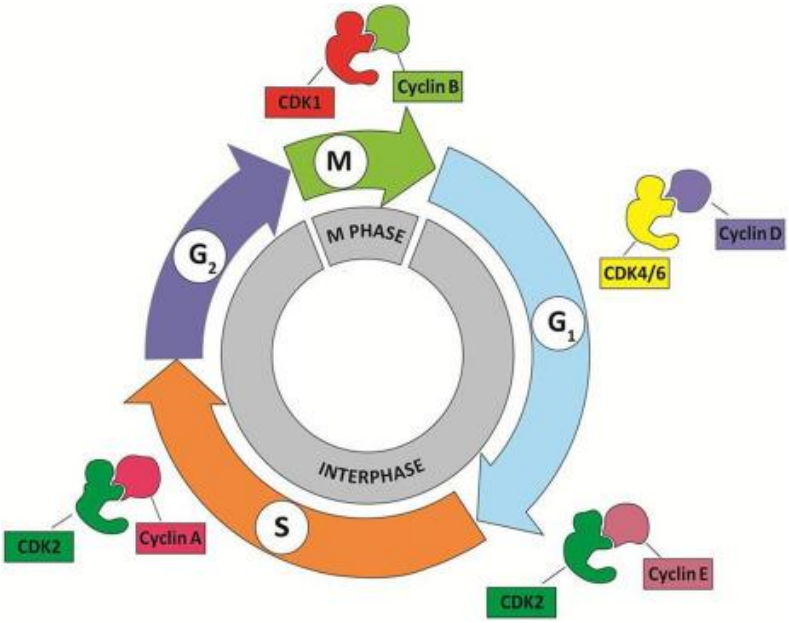

Fig.1 A schematic representation of eukaryotic cell cycle and its regulation. The cell cycle is divided in two main stages: interphase and M-phase. Interphase is subdivided into G1, S, G2 phases; M-phase includes mitosis. The progression of one phase to another is tightly controlled by Cyclin-CDK complexes (Yang, 2018).

1.1.1 S phase

The S phase is the period of the cell cycle in which DNA replication occurs. In eukaryotes, DNA replication is triggered and carried out by highly conserved enzymes and protein complexes that coordinate the accuracy of the process. DNA replication is mainly divided into three phases: initiation, elongation and termination.

DNA replication initiates at many chromosomal regions in the genome known as replication origin. To ensure that DNA is replicated only once per cell cycle, the initiation of replication is separated in two steps: licensing and firing. Origin licensing involves the formation of a pre-replication complex (pre-RC) during late mitosis and G1 phases of the cell cycle and subsequent loading of Mcm2–7 replicative helicase at replication origins. Once in S phase, the cell cycle machinery activates the replicative helicase becomes active and recruits the rest of replisome components to the origin, allowing the DNA synthesis to start. In addition, the cell cycle machinery prevents formation of new pre-replication complexes when cells

enter S phase. This is critical to avoid genome re-duplication events and to maintain the stability of the genome [Wu et al., 2014 (2), Fragkos et al., 2015, Yekezare et al., 2013, Reusswig and Pfander, 2019]. Although many origins are licensed, not all of them become finally activated. The inactive origins are called “dormant” and are used only in case of perturbations during DNA replication. Besides, the replication origins can be fired at different times in S phase. Some origins are replicated early and others late in S phase. This regulation of origin firing helps to guarantee genomic stability and to inhibit tumorigenesis [Yekezare et al., 2013, Kang et al., 2018, McIntosh and Blow, 2012].

Formation of Pre-RC complex is associated with the assembly of several replication factors, such as ORC (origin recognition complex Orc1–6), Cdc6, Cdt1, and minichromosome maintenance (MCM) replicative helicase complex, composed of six subunits Mcm2–7. ORC, Cdc6 and Cdt1 recognize the origin and load the Mcm2–7 helicase in a form of inactive double hexamers, which encircle the double stranded DNA in a specific orientation. The activation of the DNA helicase is triggered by a Cyclin-dependent kinase (CDK) and Dbf4-dependent kinase (DDK), which recruit and phosphorylate additional replication factors, including Cdc45 protein and a tetrameric GINS complex consisting of Sld5, Psf1, Psf2 and Psf3 subunits. These factors contribute to unwinding DNA from 3’ to 5’ direction by the DNA helicase and starting the initiation of DNA replication by further recruitment of several DNA polymerases, replication protein A (RPA), replication factor C (RFC), PCNA (proliferating cell nuclear antigen) and other replication proteins. During helicase activation, the double Mcm2–7 hexamer is converted into a single hexamer allowing bidirectional DNA replication. Each activated origin forms two bidirectional DNA replication forks. The multi-protein complexes that synthesize DNA are called replisomes and are highly conserved from yeast to humans [Fragkos et al., 2015, Kang et al., 2018, Burgers and Kunkel, 2017]. At least three polymerases (Pol α, Pol ε and Pol δ) associated with the CMG complex (formed by Cdc45, GINS and a single MCM hexamer), are required for DNA synthesis at the replication fork. The single stranded DNA (ssDNA) generated by the movement of the replicative helicase CMG complex along DNA is coated by RPA protein, which prevents rejoining of the single strands. The DNA Polα-primase complex binds to GINS complex through Mcm10 and Ctf4 cofactors and starts to synthesize short RNA primers [Kang et al., 2018, Burgers and Kunkel, 2017]. The primers are ribonucleotides needed to start DNA replication and are later replaced by DNA nucleotides. The leading and lagging DNA strands are both initiated by pol α but are synthesized in a different way. The leading strand is synthesized continuously, whereas the lagging strand is replicated discontinuously through smaller DNA fragments called Okazaki fragments. The extension of the synthesis of both DNA strands is carried out by Pol ε and Pol δ. The leading strand is mainly synthesized by Pol ε, whereas the lagging strand is synthesized by Pol δ [Burgers and Kunkel, 2017, Kang et al., 2018]. The binding of both polymerases to PCNA protein enhances their processivity. PCNA is a ring shaped sliding clamp which is loaded onto primer template junctions by the chaperone-like RFC complex. RFC binds PCNA forming a RFC-PCNA complex that recognizes the 3’ ends of the primer

template. Next, RFC loads PCNA at the primer-template junction and DNA polymerases are subsequently recruited to PCNA to start DNA polymerization [Moldovan et al., 2007, Kang et al., 2018].

The process of DNA synthesis terminates with the maturation of Okazaki fragments and displacement of each RNA-DNA primer by Pol δ. The generated displaced flap is cleaved by Flap endonuclease 1 (FEN1) (Rad27 in yeast) which in turn creates nicks between Okazaki fragments. DNA Ligase I ligates the gaps by joining together the Okazaki fragments [Kang et al., 2018, Zheng and Shen, 2011]. The recruitment of FEN1 and Ligase I to the Okazaki fragment is due to their interaction with PCNA [Kelman, 1997, Strzalka and Ziemienowicz, 2011]. In addition to its function in elongation and termination of DNA replication, PCNA also plays a key role in DNA repair pathways and chromatin assembly [Boehm et al., 2016, Strzalka and Ziemienowicz, 2011, Maga and Hubscher, 2003]. Finally, the termination of DNA replication occurs when the two replication forks which move in opposite directions meet each other causing fork convergence. The converging forks lead to disassembly of replication protein machinery from DNA by polyubiquitination of the MCM complex [Kang et al., 2018, Bailey et al., 2015].

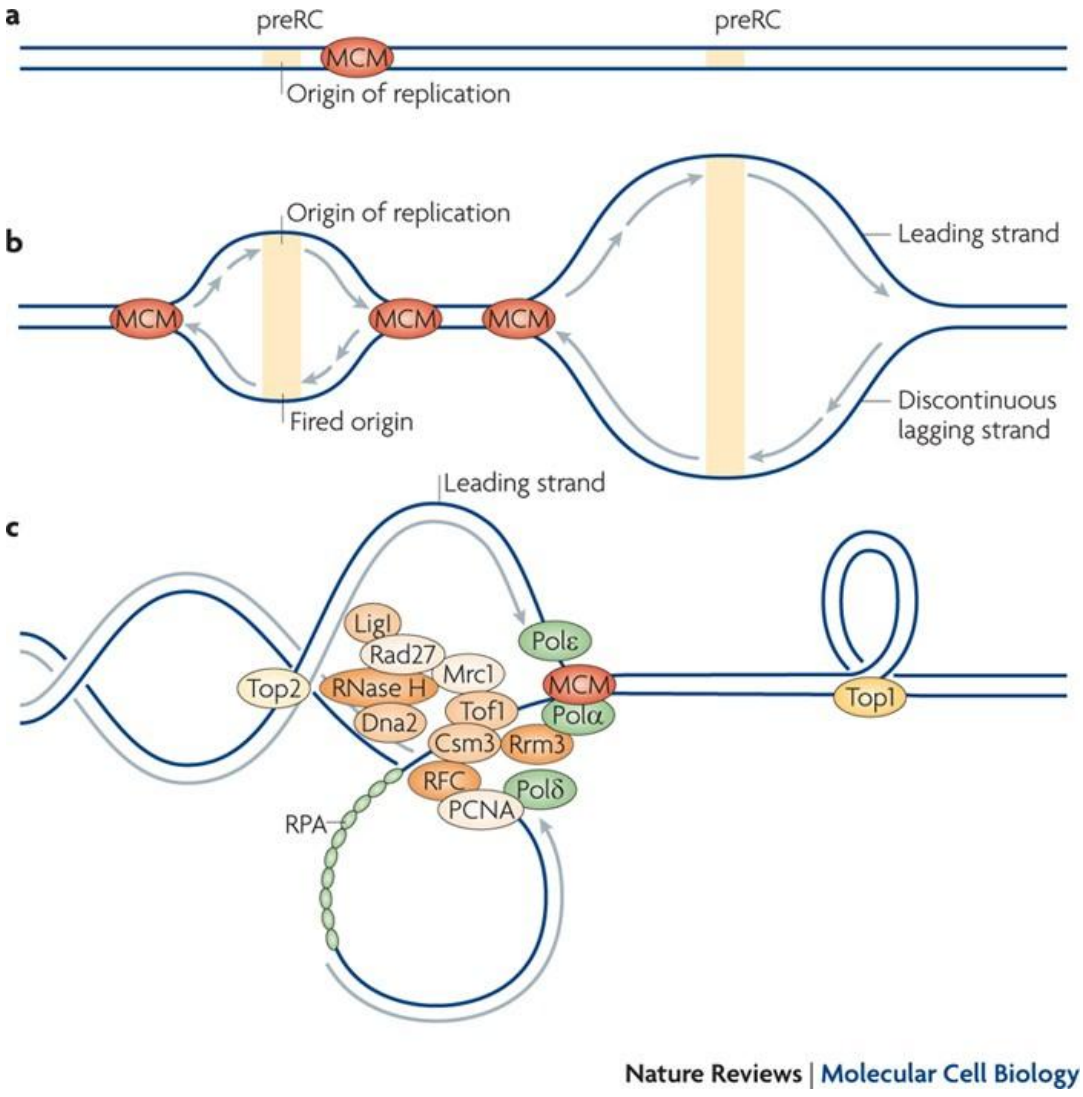

Fig.2 Initiation of DNA replication in eukaryotes. a) DNA replication initiates at many replication origins, forming a pre-replicative complex (preRC). b) The minichromosome maintenance (MCM) helicase complex is then loaded, starting to unwind DNA from 3' to 5' direction. The leading and lagging DNA strands are both initiated by pol α but are synthesized in a different way. The leading strand is synthesized continuously, whereas the lagging strand is replicated discontinuously through smaller DNA fragments called Okazaki fragments. c) Several replication factors (RPA, RFC, PCNA) required for DNA synthesis are assembled at the replication fork. The processing of Okazaki fragments involves the endonuclease Rad27 (FEN1 in humans), Dna2 helicase, RNase H, Polδ and DNA ligase I (LigI) (Branzei and Foiani, 2010).

1.1.2 Mitosis

The accurate segregation of chromosomes is of utmost importance for preserving the integrity of the genome. Mitosis begins with the condensation of chromosomes during prophase. Condensation involves tightly packaging of DNA into rod-shaped structures known as chromosomes. Each replicated chromosome consists of two identical DNA molecules, called sister chromatids with three main structural elements: telomeres, centromeres and chromosome arms [Rieder, 2011, Maeshima and Eltsov, 2008, Maddox et al., 2006]. Chromosome arms connect centromeres to telomeres and contain most of the genetic information. Telomeres are repetitive DNA sequences localized at both ends in each chromosome. They preserve chromosomal stability by protecting the chromosome ends from degradation and fusion with other chromosomes [Buchkovich and Greider, 1996, Khattar and Tergaonkar, 2016]. Each sister chromatid contains one single centromere. Depending on the localization of the centromere, chromosomes are classified as metacentric (centromere is located in the middle and both chromosome arms are of equal length), submetacentric (centromere is not located exactly in the center and the two arms are asymmetric in the length), acrocentric (centromere is localized near one end of the chromosome) and telocentric (centromere is located at the end of the chromosome) [O'Connor, 2008]. Importantly, centromeres direct the assembly of a large protein structure, called the kinetochore, which directly connects chromosomes to the cytoskeleton for chromosome segregation [Westhorpe and Straight, 2016].

Sister chromatids are physically cohesed to each other by a multisubunit protein complex called cohesin, which is loaded at centromeres and along sister chromatid arms. Cohesin is a member of a family of highly conserved SMC (Structural Maintenance of Chromosomes; see below). According to current models, cohesin has a ring-shaped structure able to topologically entrap the two sister chromatids [Makrantoni and Marston, 2018]. On the other hand, condensin, a cohesin-related SMC complex, reduces the overall length of chromosomes by entrapping two distant chromosome regions, thus promoting chromosome condensation [Antonin and Neumann, 2016].

During prometaphase spindle microtubules attach to kinetochores, allowing the microtubule-dependent pulling of sister chromatids [London and Biggins, 2014, Barnum and O'Connell, 2014, May and Hardwick, 2006]. Premature sister chromatid separation by microtubule pulling of sister kinetochores is prevented by cohesin. Following metaphase, the condensed chromosomes are aligned at the equatorial plate [McIntosh, 2016]. The progression into anaphase is triggered by the Anaphase-Promoting Complex or Cyclosome (APC/C) [Barnum and O'Connell, 2014, Bharadwaj and Yu, 2004]. APC/C is a multiprotein E3 ubiquitin ligase complex which ubiquitylates several proteins, including Cyclin B1 and the anaphase inhibitor Securin, targeting them for degradation. The destruction of Cyclin B

downregulates CDK activity in late mitosis, thus resetting the cell cycle. The degradation of securin leads to activation of separase, a protease that proteolytically cleaves cohesin molecules [Bharadwaj and Yu, 2004, London and Biggins, 2014, May and Hardwick, 2006]. Separase-dependent Inactivation of cohesin at the onset of anaphase allows the spindle to equally distribute sister chromatids, leading to the formation of two identical daughter nuclei. Although cohesin dissociates from chromosomes by proteolytic cleavage during anaphase in *S. cerevisiae,* the inactivation of cohesin follows a two-step process in human cells [Brooker and Berkowitz, 2014, Hauf et al., 2005]. First, during prophase the main bulk of cohesin is dissociated from chromatid arms through the phosphorylation activity of three mitotic kinases: CDK1, PLK1 and Aurora B [Eot-Houllier et al., 2018]. The prophase dissociation of cohesin is the cause for the observed X-shape of chromosomes during prometaphase and metaphase, as sister chromatids resolve and remain connected only at the centromere. The remaining pool of cohesin at centromeres is removed by separase-dependent cleavage of cohesin at the metaphase-to-anaphase transition. The activity of separase is strictly regulated. Its function is normally inhibited by the chaperone securin. When all chromosomes are properly aligned and bioriented on the mitotic spindle, APC/C triggers destruction of securin, thereby unleashing separase to cleave cohesin molecules at centromeres [Peters et al., 2008].

1.2 Cell cycle checkpoints

Eukaryotic cells activate specific surveillance mechanisms to ensure proper cell division, by monitoring cellular perturbations such as spindle damage, changes in temperature, osmotic stress and DNA damage among other defects. These control mechanisms, known as cell cycle checkpoints, are highly conserved signaling pathways which delay or arrest the cell cycle progression in response to DNA damage or stress factors. Once the problems are solved, checkpoints are inactivated, allowing cell cycle resumption. The main checkpoints are known as G1-S checkpoint, G2-M checkpoint and spindle checkpoint, based on the transition state which is inhibited. They are composed of several different proteins which act as sensors, signal transducers, mediators and effectors [Sancar et al., 2004]. The sensor and signal transducer proteins detect and signal troubles, with the help of mediators, to downstream effectors which arrest cell cycle progression and trigger repair [Visconti et al., 2016, Yoshiyama et al., 2013].

The DNA damage checkpoint monitors that the genetic material is in perfect state before chromosome replication or segregation [Donzelli and Draetta, 2003, Murakami and Okayama, 1997, Sancar et al., 2004, Barnum and O'Connell, 2014]. During the initial phase of checkpoint activation in response to DNA damage, sensor proteins aid in the activation of the signal kinases, ATM and ATR [Abraham, 2001]. ATM (ataxia-telangiectasia mutated) and ATR (ATM and Rad3-related) are the main regulators of the DNA damage response. ATM

signaling pathway is mainly activated in response to DNA double-strand breaks (DSBs, for example, in response to ionizing radiation), whereas ATR responds to various types of DNA lesions that are processed through generation of single-stranded DNA (ssDNA) [Awasthi et al., 2015, Abraham, 2001, Yoshiyama et al., 2013, Maréchal and Zou, 2013, Houtgraaf et al., 2006, Sancar et al., 2004].

Sensor proteins which transmit the signal to the transducers can detect different types of DNA damage. In case of DSBs, the first sensor factor recruited to these lesions is the MRE11/RAD50/NBS1 (MRN) complex. The MRN protein complex in turn recruits and activates the ATM kinase. RPA functions as a sensor protein in ATR activation. RPA coats single-stranded DNA (ssDNA), and is involved in different DNA repair pathways. ATR is activated by ATR-interacting protein (ATRIP) which interacts directly with RPA bound to ssDNA and thus localizes ATR to damaged sites. Another sensor which activates the ATR pathway is the RAD9/RAD1/HUS1 (9-1-1) ring complex, a PCNA-like complex that is loaded at primer-template damaged sites. 9-1-1 is loaded onto ssDNA-dsDNA junctions by the Rad17-RFC2-5 complex. After loading of the 9-1-1 complex on damaged DNA, its component RAD9 is phosphorylated. This phosphorylation allows the interaction of DNA topoisomerase II-binding protein 1 (TopBP1) with ATR and subsequent activation of the sensor kinase [Yoshiyama et al., 2013, Maréchal and Zou, 2013, Awasthi et al., 2015].

The mediator proteins interact with sensors and signal transducers and facilitate the activation of transducers. Several mediator proteins are known, including the mediator of DNA-damage checkpoint protein 1 (MDC1), p53-binding protein (53BP1), BRCA1, topoisomerase II-binding protein 1 (TOPBP1) and CLASPIN [Sancar et al., 2004, Yoshiyama et al., 2013, Houtgraaf et al., 2006]. MDC1, 53BP1 and BRCA1 are mainly involved in the ATM pathway, whereas TOPBP1 and CLASPIN facilitate the ATR pathway. In addition, H2AX, MRN complex and the SMC1 subunit in the cohesin complex have also been found to function as mediators, apart from their role in DNA repair and chromosome segregation [Sancar et al., 2004]. Histone variant H2AX is a subtype of H2A and is phosphorylated at Ser139 (*γ*H2AX) by ATM and ATR [Podhorecka et al., 2010]. In turn, phosphorylation of H2AX recruits repair and mediator proteins such as NBS1, BRCA1, MDC1, and 53BP1 at sites of DNA damage. Post-translational modifications of these proteins regulate specific DNA repair pathways. First, MDC1 initiates the ATM-dependent phosphorylation of H2AX and then interacts with γH2AX, forming a positive feed-back loop. γH2AX is an early sign of DNA damage whose levels are increased in DNA-damaging conditions. It has been suggested that the complex formed between ATM, γH2AX and MDC1 is critical for the activation of the checkpoint signal [Podhorecka et al., 2010, Yoshiyama et al., 2013].

The signal transducers transmit the signal to downstream proteins and activate them by phosphorylation. In response to DNA damage, ATM and ATR phosphorylate a large number

of protein substrates at Ser/Thr-Glu motifs, including NBS1, BRCA1, p53, Chk1 and Chk2 [Awasthi et al., 2015, Sancar et al., 2004]. Chk1 is phosphorylated specifically by ATR, whereas Chk2 is phosphorylated by ATM kinase. The activated checkpoint kinases in turn trigger downstream responses by phosphorylation of effector proteins [Patil et al., 2013, Maréchal and Zou, 2013]. Chk1 and Chk2 regulate the activity of the effectors: phosphotyrosine phosphatases - Cdc25A, Cdc25B and Cdc25C. In normal conditions, unphosphorylated Cdc25 phosphatases trigger G1/S and G2/M transitions by dephosphorylation of Cdks. Upon DNA damage, Cdc25 proteins are phosphorylated by Chk1 and Chk2, inactivating them and leading to cell cycle arrest [Sancar et al., 2004, Houtgraaf et al., 2006, Yoshiyama et al., 2013]. Another effector protein is the transcription factor p53 which is crucial for the fate of the cell. During DNA damage, p53 undergoes ATM/ATR and Chk1/Chk2 mediated phosphorylation, leading to its activation [Giono and Manfredi, 2006, Yoshiyama et al., 2013]. The activated p53 decides whether the cell undergoes cell cycle arrest and DNA repair or programmed cell death [Yoshiyama et al., 2013]. Another possible outcome of p53 activation is cellular senescence, which is a permanent cell cycle arrest [Marusyk et al., 2007].

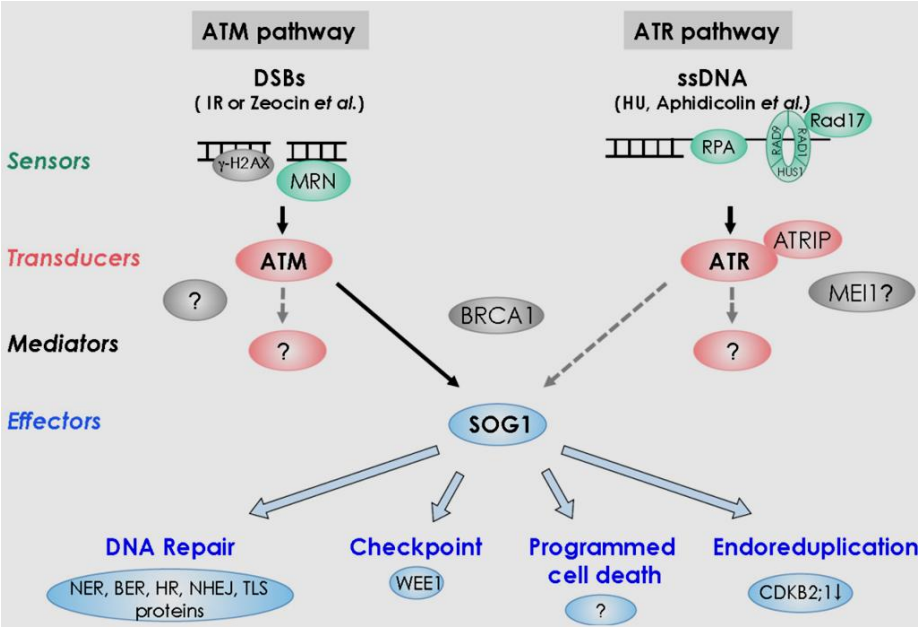

Fig.3 Cell cycle checkpoint signaling. In response to DNA damage, sensor proteins (shown in green) recruit and activate ATM and ATR signal transducers (shown in pink) which in turn transmit the damage signal to mediator proteins (shown in grey) and phosphorylate Chk2 and Chk1 kinases. ATM-Chk2 and ATR-Chk1 together transmit the signal to effector proteins (shown in blue). The latter leads to different cellular outcomes: DNA repair, cell cycle arrest, apoptosis or senescence (Yoshiyama et al., 2013).

1.2.1 G1/S checkpoint

The G1/S checkpoint blocks cell cycle progression into S-phase. The signaling pathway of cell cycle arrest depends on the type of damage and ultimately leads to activation of the tumor suppressor p53 [Wenzel and Singh, 2018, Houtgraaf et al., 2006, Abraham, 2001]. As mentioned above, the presence of DSBs in G1 phase activates ATM, which then phosphorylates H2AX and triggers the recruitment of repair factors at site of DNA damage. In addition, ATM phosphorylates and activates Chk2, initiating G1/S arrest [Shaltiel et al., 2015, Sancar et al., 2004]. Chk2 inactivates Cdc25A and thus inhibits the phosphorylation of S phase promoting cyclin A/Cyclin-dependent kinase (Cdk) 2 and cyclin E/Cdk2 complexes resulting in G1/S cell cycle arrest. If the DNA damage is caused by single strand breaks, another signal pathway is activated - ATR/Rad17-RFC/9-1-1, leading to phosphorylation of Chk1 [Sancar et al., 2004, Houtgraaf et al., 2006]. The initiated G1/S arrest by Chk1/Chk2 phosphorylation is maintained by the transcription factor p53 in both ATM and ATR pathways. ATM and ATR phosphorylate p53 at Ser15, whereas Chk1 or Chk2 at Ser20 which results in stabilization of the transcription factor. The stabilized p53 in turn activates transcriptional targets, including a cyclin-dependent kinase (Cdk) inhibitor protein p21 (also known as CDKN1A). The accumulated p21 binds and also inhibits the cyclin A/Cdk2 and cyclin E/Cdk2 complexes, preventing G1 to S phase progression. Surprisingly, the G1/S checkpoint is the only known checkpoint signal which is completely abolished due to the loss of function of p53 or p21 [Sancar et al., 2004, Caspari, 2000, Shaltiel et al., 2015, Abraham, 2001].

1.2.2 G2/M checkpoint

The G2/M checkpoint prevents cells from entering into mitosis upon DNA damage. In G2 phase, checkpoint kinases Chk1 and Chk2 inhibit the phosphatase Cdc25A and activate a protein kinase, called Wee1 by phosphorylation. Wee1 in turn prevents cells with unreplicated or damaged DNA from entering into mitosis by blocking the activity of Cdk1/cyclin B complex [Sancar et al., 2004, Rieder, 2011, Houtgraaf et al., 2006, Geenen and Schellens, 2017]. In contrast to G1/S, the maintenance of G2/M arrest in response to DSBs is not completely mediated by ATM, p53 and p21 signaling. It has been found that it mainly depends on ATR and Chk1 kinases [Shaltiel et al., 2015, Houtgraaf et al., 2006].

The G2/M checkpoint can be also controlled by another pathway, involving MAP kinase p38 and CHFR ubiquitin ligase. The MAP kinases p38γ and p38α are mainly activated in response to ionizing and UV radiation [Rieder, 2011, Sancar et al., 2004]. They can also suppress cyclin A- and B- dependent kinases by inhibiting the two phosphates Cdc25A and Cdc25B and can contribute to the maintenance of G2/M cell cycle arrest. The dependence of p38

pathway on ATM or ATR phosphorylation still remains unclear [Rieder, 2011, Shaltiel et al., 2015].

1.2.3 Replicative stress and S phase checkpoint

The S phase checkpoint, also known as intra-S checkpoint, is activated in response to DNA damage or replication stress during S phase. Replication stress is characterized by slowing or stalling of replication forks and is a major source of genomic instability [Zeman and Cimprich, 2014, Macheret and Halazonetis, 2015]. To prevent this, the S phase checkpoint, slows down DNA replication, blocks cell cycle progression and stabilizes replication forks [Willis and Rhind, 2009, Iyer and Rhind, 2017]. Persistent replication stress and failure to stabilize stalled forks may lead to fork collapse and production of broken DNA ends [Cortez, 2015, Allen et al., 2011]. The fork collapse results from destabilization of the replisome and can cause genomic instability and cell death [Zeman and Cimprich, 2014]. Therefore, the intact S phase checkpoint is crucial for cell survival and genome integrity [Segurado and Tercero, 2009].

Various exogenous and endogenous factors that block fork progression induce replicative stress. Exogenous sources include UV light, ionizing radiation (IR) and many genotoxic chemicals. To the endogenous sources can be attributed depletion of nucleotides, origin-poor regions, repetitive DNA sequences, chromosome fragile sites, oncogene activation, reactive oxygen species (ROS), etc. [Vesela et al., 2017, Zeman and Cimprich, 2014].

The majority of lesions encountered during DNA replication inhibit replicative polymerases, leading to stalled replication forks. However, replicative helicases continue to unwind the parental DNA, leading to uncoupling between the helicase and DNA polymerase activities [Iyer and Rhind, 2017]. The uncoupling can also appear between the leading and lagging strand polymerase activity [Pasero and Vindigni, 2017]. This replication fork uncoupling generates long stretches of ssDNA which activate the DNA replication stress response. The exposed ssDNA is immediately coated by RPA, which in turn leads to S phase checkpoint activation and recruitment of ATR kinase and downstream effector proteins [Zeman and Cimprich, 2014, Iyer and Rhind, 2013, Jossen and Bermejo, 2013, Gelot et al., 2015, Iyer and Rhind, 2017].

The intra-S checkpoint preserves genome stability by regulating origin firing, fork progression and transcription of G1/S genes [Segurado and Tercero, 2009, Iyer and Rhind, 2017]. Similar to other DNA damage checkpoints, the regulation of origin firing is originally considered as a global checkpoint mechanism in which the origins that are distant from the damaged sites are blocked from firing. On the contrary, the fork progression regulated by

the S phase checkpoint can be global or local. In the global response all of the replication forks are slowed, whereas in the local mechanism only the forks that encounter DNA damage are slowed down [Iyer and Rhind, 2013].

In addition, activation of the ATR protects stalled replication forks from degradation and prevents late origin firing and ssDNA formation [Zeman and Cimprich, 2014, Iyer and Rhind, 2017]. ATR first binds to ATRIP which recognizes RPA-ssDNA and then recruits several sensor and mediator proteins such as Rad9-Rad1-Hus1 (9-1-1), TopBP1, Claspin which are required for its activation. Then, activated ATR suppresses CDK activity, as explained above, and thus slows down S phase progression and inhibits mitosis, allowing time for restarting or repairing stalled replication forks [Jones and Petermann, 2012, Iyer and Rhind, 2017].

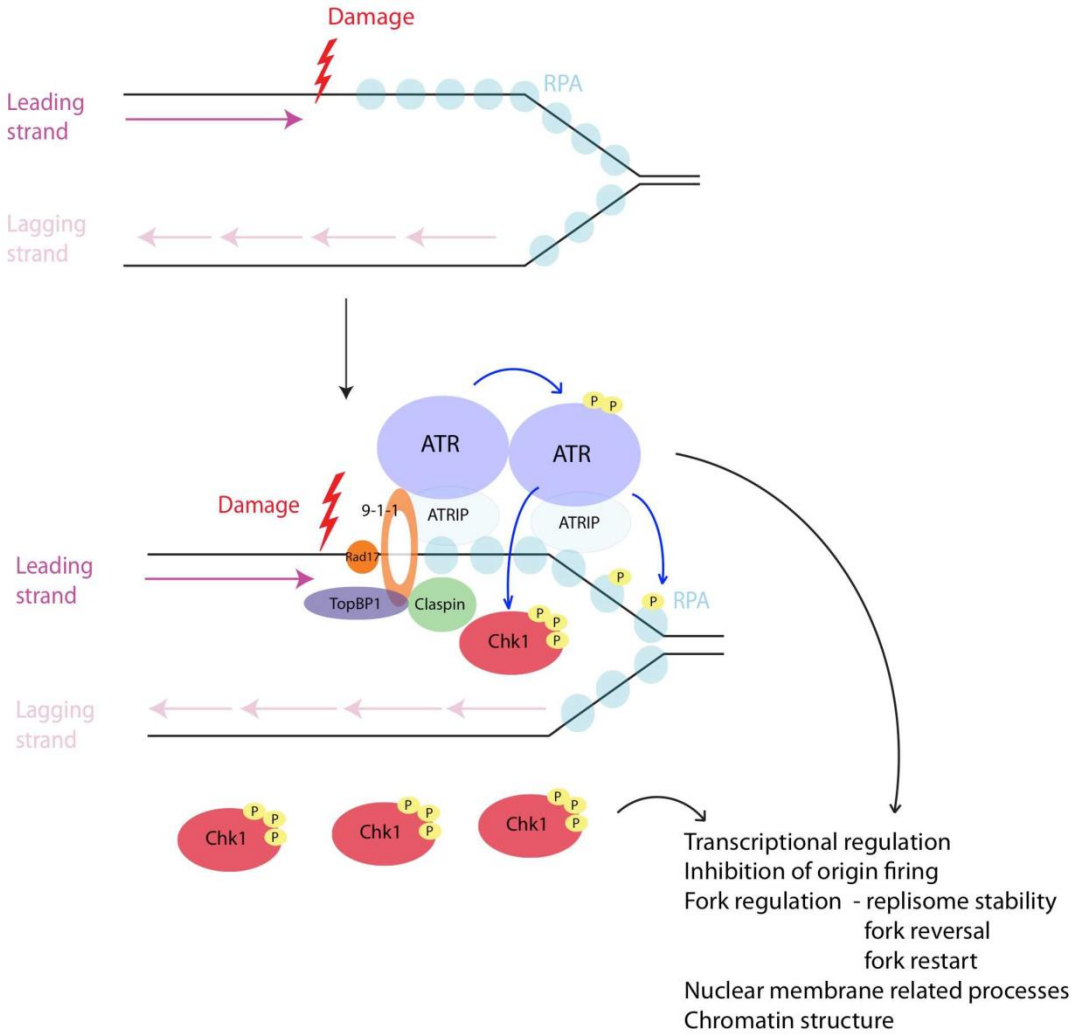

Fig.4 S phase checkpoint activation. Upon DNA damage or replication stress, DNA replication fork stalls leading to generation of ssDNA-RPA complex which recruits ATR kinase and downstream effector proteins (shown in purple, green and pink). The latter leads to activation of S phase checkpoint which stabilizes stalled forks by slowing down DNA replication and blocking cell cycle

progression. ATR-Chk1 pathway regulates several processes upon DNA damage (fork stabilization, transcription, origin firing inhibition, chromatin structure alteration and ect.) (Iyer and Rhind, 2017).

1.2.4 Spindle checkpoint

Spindle assembly checkpoint (SAC) ensures proper segregation of sister chromatids by delaying entry into anaphase until all chromosomes are properly attached to the mitotic spindle [Visconti et al., 2016, May and Hardwick, 2006].

The SAC detects unattached kinetochores, as well as lack of tension between sister kinetochores, and prevents chromosome segregation by inhibiting the Anaphase-Promoting Complex or Cyclosome (APC/C) and suppressing cyclin B and securin degradation. The latter keeps separase inactive, preventing cohesin cleavage [Barnum and O'Connell, 2014, Visconti et al., 2016]. Thus, it allows time for chromosomes to re-orient.

Spindle checkpoint is composed of multiple conserved proteins, which were first identified in yeast: Mad1, Mad2, BubR1, Bub1, Bub3 and Mps1. Most of them are recruited to kinetochores in a hierarchical manner and signal for checkpoint activation [London and Biggins, 2014]. Mad proteins accumulate at unattached kinetochores, whereas the Bub proteins can be recruited to kinetochores lacking microtubule attachment or tension [Hixon and Gualberto, 2000, May and Hardwick, 2006].

The activity of APC/C is mediated by its binding to two regulating proteins: Cdc20 and Cdh1. Cdc20 is the main target of SAC and can associate with some of the SAC components: BubR1, Bub3 and Mad2 [May and Hardwick, 2006, Barnum and O'Connell, 2014, Visconti et al., 2016]. In case of incorrectly attached kinetochores, Mad2 (Mitotic Arrest Deficient) binds to Cdc20 and forms a subcomplex, which interacts with Mad3/Bub1R-Bub3 subcomplex leading to the formation of a mitotic checkpoint complex (MCC). The latter inhibits Cdc20, resulting in the inactivation of APC/C complex and preventing cells from entering into anaphase [Lara-Gonzalez et al., 2012, May and Hardwick, 2006].

The conserved kinetochore kinase monopolar spindle 1 (Mps1) acts as a main effector of the spindle checkpoint, as well as in promoting chromosome bio-orientation [London and Biggins, 2014]. The Aurora B, Polo and NIMA-related (Nek) kinases also participate in the correction of the spindle defects [Barnum, and O'Connell, 2014]. Aurora kinase is particularly important to promote sister chromatid bi-orientation, as it disrupts other

unwanted microtubule-kinetochore configurations. For example, sister kinetochores can be mono-oriented when one or both sister chromatids are attached to the microtubules from the same pole, forming monotelic or synthelic attachment, respectively. Another unwanted possibility is the merotelic attachment, occurring when both sister kinetochores bind to microtubules from the same spindle pole. Importantly, if these defective attachments were left unresolved, they could lead to chromosome missegregation and chromosome instability [London and Biggins, 2014].

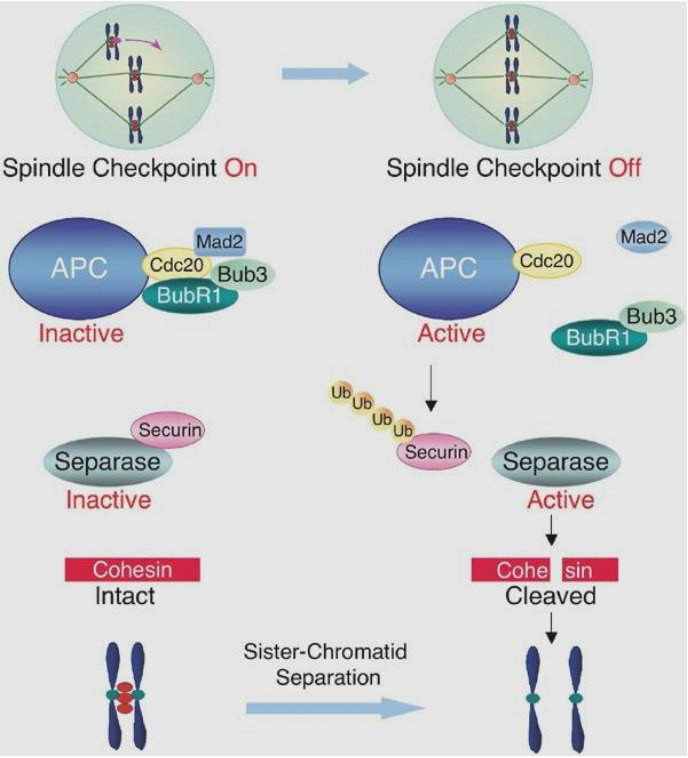

Fig.5 Spindle assembly checkpoint (SAC). The SAC delays anaphase onset until all chromosomes are correctly attached to the spindle by kinetochores. Recruitment of checkpoint proteins (BubR1, Bub3 and Mad2) to unattached kinetochores leads to inactivation of APC/C complex, which in turn inhibits cyclin B and securin degradation. Thus, the protease separase is kept inactive and cohesin is intact. Once kinetochores are properly attached to the mitotic spindle, the APC/C complex becomes active with the aid of the activator Cdc20. The activation of APC/C leads to degradation of securin and activation of the separase, which in turn cleaves cohesin and allows the separation of the sister chromatids (Bharadwaj and Yu, 2004).

1.3 DNA repair mechanisms

Our cells are challenged by hundreds of thousands of lesions every day. Accurate repair of these lesions is of utmost importance for maintaining genome stability. DNA repair pathways are highly conserved in evolution and require the coordinated action of multiple proteins. In eukaryotes, at least five diverse repair mechanisms are known to protect the genome from DNA damage: the double-strand break repair which involves homologous recombination and non-homologous end joining, base-excision repair, mismatch repair, nucleotide excision repair and interstrand cross-link repair.

1.3.1 Homologous recombination (HR)

Homologous recombination (HR) is a multistep repair mechanism which deals with lesions affecting both strands of DNA: double strand breaks (DSBs). DSBs are one of the most dangerous types of DNA damage. HR is promoted by the action of several proteins and takes place at the S or G2 phases of the cell cycle. HR repairs the DSBs in an error-free manner by using an intact homologous DNA template [Hakem, 2008, Wright et al., 2018]. The process requires 5'-3' resection of the DNA broken ends to produce 3'- single-stranded DNA (ssDNA). The end-resection is initiated by Sae2/CtIP nuclease and the MRN complex composed of Mre11, Rad50 and Nbs1 proteins. It is then continued by the action of the BLM helicase (Bloom syndrome, RecQ helicase-like), which opens up the double helix, and the Exo1 exonuclease, which extends resection [Rodgers and McVey, 2016, Dexheimer, 2013]. RPA then binds to ssDNA protecting it from degradation [Mladenov and Iliakis, 2011, Rodgers and McVey, 2016]. Next, RPA is replaced by Rad51, which forms a nucleoprotein filament on ssDNA, with the aid of mediator proteins Rad52, BRCA1/PALB2/BRCA2 and Rad51 paralogues: RAD51B, RAD51C, RAD51D, XRCC2 and XRCC3 in mammalian cells [Dexheimer, 2013]. Rad51 is a DNA-dependent ATPase which promotes invasion of a homologous repair template [Rodgers and McVey, 2016, Mehta and Haber, 2014]. In most cases a sister chromatid is used as a homologous repair donor. This is due to its physical proximity, provided by cohesin-dependent sister chromatid cohesion in the S and G2 phases [Rodgers and McVey, 2016]. The Rad51 nucleoprotein searches and invades a homologous sequence with the help of the motor protein Rad54 in an ATP-dependent manner. As a result, a new DNA strand is synthesized by Pol ε or δ using the 3'-end of the invading strand [Dexheimer, 2013, Mehta and Haber, 2014]. Following subsequent ligation by DNA ligase I, two Holliday junctions (four-way junction intermediate structures) are formed. These joint molecules can be further cleaved symmetrically or asymmetrically by structure-selective endonucleases Slx1/Slx4 and Mus81/Eme1, respectively or can be resolved by resolvases GEN1/Yen1 leading to formation of crossover or non-crossover products [Rodgers and McVey, 2016, Dexheimer, 2013]. The DSB repair can be completed by three different HR models: synthesis-dependent strand annealing (SDSA), double-strand break repair (DSBR),

which is the classical model for HR, and break-induced replication (BIR). Each of these models differs from each other by the strand invasion reaction and the outcome of the produced recombination intermediates [Pardo et al., 2009].

1.3.2 Non-homologous end joining (NHEJ)

Non-homologous end joining (NHEJ) is an alternative pathway for repairing the double-strand breaks (DSBs). In contrast to HR repair, NHEJ ligates the DSB ends without the need for a homologous template and is thought to be an error-prone mechanism which normally leads to the generation of small insertions and deletions (INDElS) [Pardo et al., 2009]. NHEJ operates throughout the cell cycle, but mainly at G1 phase [Hühn et al., 2013]. The process initiates with binding of Ku70-Ku80 (Ku) heterodimer to the broken ends of DNA. The resulting Ku-DNA complex subsequently recruits the catalytic subunit of DNA-dependent protein kinase (DNA-PKcs) and activates its kinase activity [Dexheimer, 2013, Fleck and Nielsen, 2004]. DNA-PKcs is a member of the phosphatidylinositol-3 (PI-3) kinase-like kinase family (PIKK), which includes also the main regulators of the DNA damage response (DDR): ATM and ATR [Davis et al., 2013]. During the recruitment to the Ku-DNA complex, DNA-PKcs undergoes autophosphorylation and activates the NHEJ-specific endonuclease called Artemis which is able to cut single-stranded or double-stranded overhangs [Chang et al., 2017, Dexheimer, 2013]. The DNA-PKcs-Artemis complex is also known to bridge DNA ligases to DSBs in the last step of the NHEJ by direct interaction between the C-terminal part of Artemis and the N-terminus of DNA ligase IV [Yang et al., 2016, Pardo et al., 2009, Chang et al., 2017]. Next, two DNA polymerases, Pol μ and Pol λ, are recruited to the Ku-DNA complex which re-synthesize the missing nucleotides. Other factors such as APE1, Tdp1, and PNKP and the exonucleases Exo1 and WRN can also participate in DNA re-synthesis. Finally the DNA ends are rejoined by XRCC4-DNA ligase IV complex with the aid of an additional factor XLF (XRCC4-like factor) [Fleck and Nielsen, 2004, Dexheimer, 2013]. The X-ray repair cross-complementing 4 (XRCC4) enzyme recruits several processing NHEJ factors to the DSBs ends and facilitates DSB bridging for efficient ligation [Pannunzio et al., 2017,]. XRCC4 interacts with DNA ligase IV and forms a subcomplex with XLF which stimulates ligase IV activity to carry out the ligation step [Yang et al., 2016, Davis et al., 2013, Chang et al., 2017].

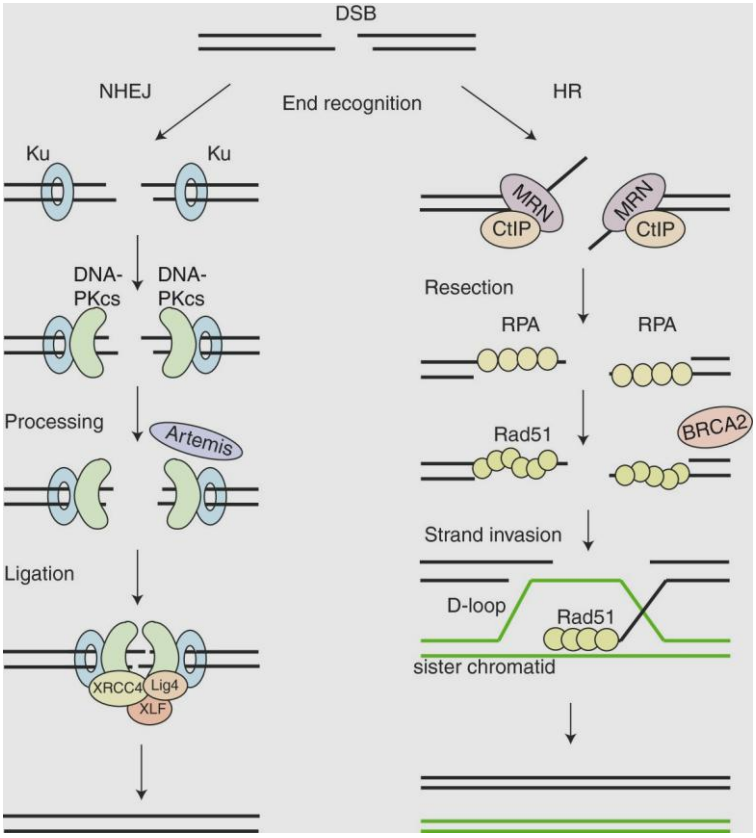

Fig. 6 Schematic overview of homologous recombination (HR) and non-homologous end joining (NHEJ). HR (on the right) uses a homologous DNA sequence as a template to repair DSBs. HR initiates with a resection, mediated by MRN/CtIP complex. The resection leads to formation of ssDNA, which is first coated by RPA and then replaced by Rad51 with the aid of mediator proteins. Rad51 filament promotes strand invasion on the homologous template which leads to generation of a D-loop. The formed D-loop intermediate can be processed by three different pathways: SDSA, DSBR or BIR. NHEJ (on the left) directly ligates the ends of the broken DNA. NHEJ starts with binding of the Ku heterodimer to the DNA ends and then recruits and activates DNA-PKcs. Non-compatible DNA ends are processed by endonucleases and the DSB is repaired by the Ligase IV XRCC4-XLF complex (Brandsma and Gent, 2012).

1.3.3 Base-excision repair (BER)

Base-excision repair (BER) repairs non-bulky lesions induced by alkylation, oxidation (ROS) and deamination of bases. BER recognizes and removes DNA lesions without distortion of the DNA helix by the enzymatic activity of several DNA glycosylases and specific endonucleases [Fleck and Nielsen, 2004, Dexheimer, 2013]. The synthesis and ligation steps are divided in two general pathways: short-patch and long-patch, depending on the number of nucleotides that are incorporated at the DNA damage site [Dexheimer, 2013]. The

specific DNA glycosylase removes only the damaged base from the sugar-phosphate backbone, leaving an abasic site - apurinic or apyrimidinic (AP site). The AP site is incised by AP endonuclease 1 (APE-1) which hydrolyses the phosphodiester backbone. Next, in case of short-patch BER repair the gap is filled by incorporation of nucleotides guided by DNA polymerase β (Pol β) and ligated by XRCC1/Ligase III complex. The long-patch repair fills the gap by Pol β, ε or δ with the help of PCNA (proliferating cell nuclear antigen) and RFC (replication factor C), which displace the 5' lesion into a flap intermediate. Finally, the generated flap structure is excised by FEN1 (flap-1 endonuclease) and the nick is sealed by DNA ligase I [Dexheimer, 2013, Giglia-Mari et al., 2011, Hakem, 2008].

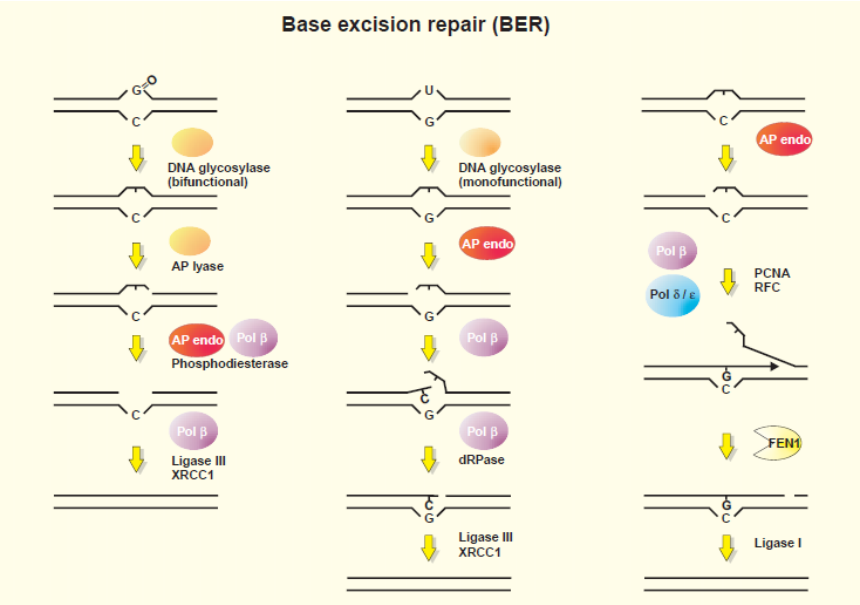

Fig.7 A schematic illustration of base-excision repair mechanism (BER). BER initiates with the aid of DNA glycosylases which excise only the damaged base, forming an AP site. The AP endonuclease cleaves the AP site, creating a single-strand break which can then be processed by short-patch or long-patch BER (see text for details) (Fleck and Nielsen 2004).

1.3.4 Mismatch repair (MMR)

Mismatch repair (MMR) removes mismatches and small insertion and deletion loops generated by replication errors during DNA replication. The mechanism is triggered by the evolutionary conserved MMR proteins and involves three steps: recognition, excision and gap filling by DNA resynthesis [Ambekar et al., 2017, Fleck and Nielsen, 2004]. First, human Msh2 forms a subcomplex with Msh3 and Msh6 and binds DNA mismatches. Then, the heterodimer Mlh1-Pms2 is recruited and cleaves mismatches by its endonuclease activity. In the end, exonuclease 1 Exo1 removes the DNA segment around the mismatch and the

single-strand gap is re-synthesized by DNA pol δ along with PCNA and RPA and is subsequently ligated by ligase I [Dexheimer, 2013, Fleck and Nielsen, 2004, Fukui, 2010].

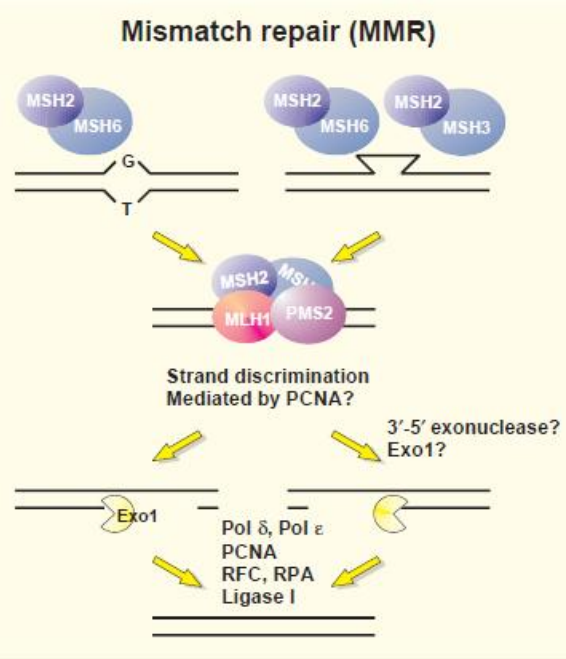

Fig.8 A schematic representation of mismatch repair (MMR). MMR is mediated by the help of MMR proteins (MSH2, MSH3, MSH6, MLH1, PMS2). First, MSH2 and MSH6 recognize the damaged site and recruit MLH1 and PMS2 which along with Exo1 excise mismatches. The single-strand gap is then repaired by Pol δ, PCNA and RFC and RPA. Finally, the DNA strand is re-ligated by DNA ligase I (Fleck and Nielsen 2004).

1.3.5 Nucleotide excision repair (NER)

Nucleotide excision repair (NER) is a multistep repair mechanism which recognizes and removes various types of bulky DNA lesions produced by UV irradiation, mutagens and chemotherapeutic agents [Dexheimer, 2013]. NER involves several steps to repair DNA: DNA damage recognition, unwinding of DNA, excision of a short single-stranded oligonucleotide around the lesion and filling of the generated gap by DNA synthesis [Ulrich, 2012, Dexheimer, 2013]. This mechanism is divided into two subpathways: global genome repair (GGR) and transcription-coupled repair (TCR) [Fleck and Nielsen, 2004]. GGR which is initiated by XPC-RAD23B and DDB1-DDB2/XPE proteins which detect and remove lesions

throughout the genome, whereas TCR is triggered by stalled RNA polymerase and CSA and CSB factors which specifically repair lesions that block transcription [Schärer, 2013]. After the distinct recognition step, both subpathways use a common mechanism to complete repair. First, a protein complex called transcription factor IIH (TFIIH) is recruited to the DNA damage site and with the help of two helicases XPB and XPD unwinds the DNA around the lesion. Next, XPA and RPA stabilize the unwound DNA leading to recruitment of the endonucleases XPG and ERCC1-XPF. ERCC1-XPF protein complex along with XPG incises the damaged strand 3' and 5' to the damage, respectively and creates ~30 base nucleotide single-strand gap which is filled by re-synthesis from DNA pol δ or ε together with the replication factors RFC, PCNA and RPA. Finally, the gap is ligated by DNA ligase I or III and the NER process is completed [Fleck and Nielsen, 2004, Dexheimer, 2013, Giglia-Mari et al., 2011].

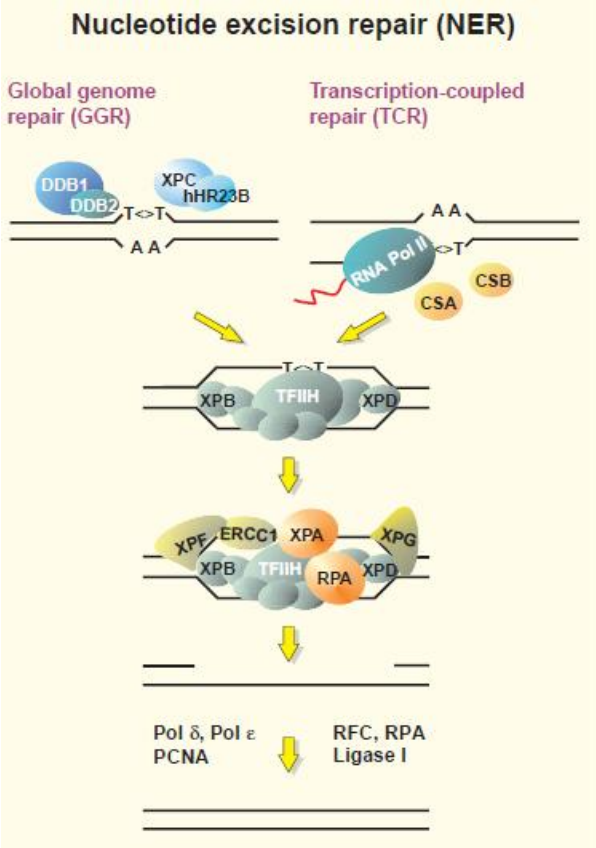

Fig. 9 A schematic illustration of nucleotide excision repair (NER). NER is mediated by two main pathways: global genome repair (GGR) and transcription-coupled repair (TCR). GGR detects the lesion by the aid of protein complexes (XPC-RAD23B and DDB1-DDB2/XPE). TCR recognizes stalled RNA polymerase II at a lesion and recruits CSA and CSB proteins. After lesion recognition both pathways follow the same mechanism to excise and repair the damage (see text for details) (Fleck and Nielsen 2004).

1.3.6 Interstrand cross-link repair (ICL)

Interstrand cross-link (ICL) repair occurs during the S phase of the cell cycle. It removes highly cytotoxic DNA lesions that covalently link two bases on complementary strands of DNA. These types of lesions prevent unwinding of two DNA strands and thus block critical DNA transactions such as replication and transcription, potentially leading to chromosomal breakage or cell death [Clauson et al., 2013, Noll et al., 2006, Muniandy et al., 2010]. ICLs can be produced by bifunctional alkylating agents, platinum compounds, mitomycin C or natural products such as psoralen [Noll et al., 2006]. These crosslinking agents can induce also base monoadducts, intrastrand crosslinks, and DNA-protein crosslinks [Chatterjee and Walker, 2017]. Due to the diversity of the crosslinking agents and the structural alterations that they cause in DNA, the exact mechanisms of ICL are still not well-understood [Muniandy et al., 2010, Legerski, 2010]. It is known that several DNA repair and tolerance pathways, including NER, HR and translesion DNA synthesis (TLS) are involved in the repair of ICLs [Muniandy et al., 2010, Andreassen and Ren, 2009]. During ICL repair the replication fork is stalled at the ICL and undergoes programmed collapse [Zhang and Walter, 2014]. The classical model of ICL pathway in replicating cells initiates with the incision of the fork by unhooking the ICL from the lagging strand, which in turn leads to the formation of a double-stranded DNA break (DSB). Next, the TLS tolerance pathway provides specific DNA polymerases to bypass the unhooked ICL, allowing DSB repair by HR and restoring the replication fork [Clauson et al., 2013, Zhang et al., 2015]. In non-replicating cells ICLs are repaired by TLS and NER systems using similar mechanisms [Clauson et al., 2013].

The ICL pathway is promoted by proteins of the Fanconi anemia (FA) pathway [Knipscheer et al., 2009]. Fanconi anemia is a rare genetic disease which was first described in 1927 by the Swiss pediatrician Guido Fanconi. It is an autosomal recessive disorder, a result of mutations in any of the 22 FA genes which is characterized by progressive bone marrow failure (BMF), aplastic anemia and cancer predisposition, mainly acute myeloid leukemia [Che et al., 2018, Sumpter and Levine, 2017, Kim and D'Andrea, 2012, Taniguchi and D'Andrea, 2006]. Cells from patients with FA show high sensitivity to agents that induce ICLs due to the failure in their repair capacity [Lopez-Martinez et al., 2016].

Depending on their function in the FA pathway, FA proteins are mainly divided into three main groups. The first group is composed of eight FANC proteins (FANCA, FANCB, FANCC, FANCE, FANCF, FANCG, FANCL and FANCM) along with three other proteins (FAAP20, FAAP24 and FAAP100) that form the FA core complex. The FA core complex is required for activation of DNA repair by ubiquitylation [Lopez-Martinez et al., 2016]. FANCM is the first protein that recognizes the ICL stalled fork facilitating the recruitment of the other FA proteins.

FANCM is an ATP-dependent helicase/translocase which is a member of ERCC1/XPF endonuclease family. It contains a C-terminal inactive nuclease domain which binds branched DNA structures and an N-terminal helicase domain with translocase activity which interacts with the FA core complex [Deans and West, 2011, Gari et al., 2008]. The translocase activity of FANCM can remodel stalled forks, facilitating DNA repair [Gari et al., 2008].

FANCM forms a complex with FAAP24 (Fanconi Anemia associated protein of 24 kDa) and MFH1/2 (histone fold protein complex), allowing the recruitment of the FA core complex to the stalled fork [Kim and D'Andrea, 2012, Clauson et al., 2013]. The FA core complex functions as an E3 ubiquitin ligase complex which along with the E2, UBE2T/FANCT subsequently monoubiquitylates the second group of FA proteins - FANCD2 and FANCI [Rodríguez and D'Andrea, 2017, Lopez-Martinez et al., 2016]. It is believed that FANCD2/FANCI complex is first recruited to ICLs and then monoubiquitylated. This monoubiquitylation is essential for activation of the FA pathway and for maintaining the genomic stability [Liang et al., 2016, Deans and West, 2011, Schwab et al., 2015, Lopez-Martinez et al., 2016]. Other proteins are also subsequently recruited to the damaged DNA, such as BLM helicase, Topo IIIa (topoisomerase IIIa) and RPA which form another large complex called BRAFT along with proteins of FA core complex (FANCA, FANCC, FANCE, FANCF and FANCG) [Lopez-Martinez et al., 2016].

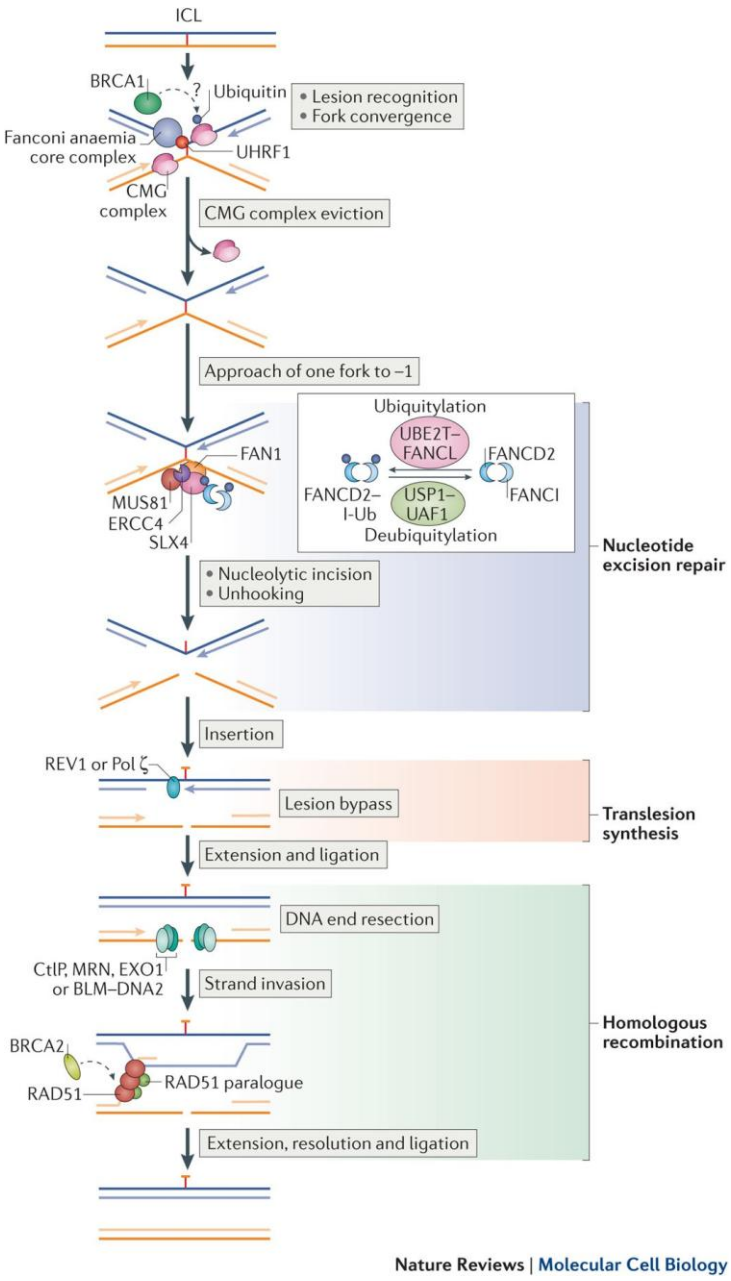

Fig.10 Interstrand cross-link (ICL) repair. ICL lesions are first detected by FANCM protein, which in turn recruits Fanconi anaemia (FA) core complex and monoubiquitylation of FANCD2–FANCI, as well recruits downstream FA proteins and DNA repair proteins. The ICL is repaired by incision of the damaged DNA strand by the nucleases FANCP (SLX4), FAN1 and ERCC4 (an endonuclease that also functions in nucleotide excision repair), creating a DSB. The unhooked ICL is then bypassed by TLS polymerases and the DSB is repaired by HR with the aid of BRCA2, RAD51 and RAD51 paralogue (RAD51C) (Ceccaldi et al., 2016).

The monoubiquitylation of the FANCD2/FANCI complex leads to the recruitment of downstream FA proteins from the third group and other DNA repair proteins. The third group of FA proteins comprises of FANCD1 (BRCA2), FANCJ (BRIP1), FANCN (PALB2), FANCO (RAD51C), FANCP (SLX4), FANCQ (XPF), FANCR (RAD51) and FANCS (BRCA1) [Lopez-Martinez

et al., 2016]. The FA pathway triggers the repair of ICL through incision of the damaged DNA strand by the nucleases FANCP (SLX4), FAN1 and ERCC4. Next, the unhooked ICL is bypassed by TLS polymerases and the DSB is repaired by HR with the aid of FANCD1, FANCR and FANCO proteins [Nalepa and Clapp, 2018].

1.3.7 DNA damage tolerance (S phase specific)

DNA lesions encountered in the wake of the replication fork cannot be repaired by most DNA repair pathways without incurring into double-strand breaks. In these cases, DNA lesions are bypassed through evolutionary conserved DNA damage tolerance pathways (DDT). There are two main pathways of DDT: translesion DNA synthesis (TLS) and template switching (TS) which are mediated by ubiquitylation or SUMOylation of PCNA [Ghosal and Chen, 2013].

TLS uses specialized DNA polymerases which can directly replicate across the lesion [Sale, 2012, Gao et al., 2016] In contrast to normal replicative polymerases, TLS polymerases lack proofreading activity and can incorporate wrong nucleotides during DNA synthesis. Therefore, TLS is mainly considered as an error-prone mechanism. However, growing evidence supports that TLS can be also error-free depending on the type of lesion and the type of the recruited polymerase [Chang and Cimprich, 2009, Ghosal and Chen, 2013]. Eukaryotic cells have eleven TLS polymerases (REV1, POL η, POL ι, POL κ, POL ζ, POL μ, POL λ, POL β, POL ν, POL θ), which are grouped in four families (Y, B, X and A) and PrimPol [Bi, 2015, Chatterjee and Walker, 2017, Ghosal and Chen, 2013, Chang and Cimprich, 2009]. Each of these polymerases has different substrate specificities depending on DNA lesion. TLS is initiated by monoubiquitylation of PCNA through the Rad6 E2 and Rad 18 E3, promoting the polymerase switch at the replication fork [Ghosal and Chen, 2013].

TS is an error-free pathway which is activated by the polyubiquitylation of PCNA through Rad5-Ubc13-Mms2 ligase complex. It uses the newly synthesized daughter strand as a homologous template to bypass the lesion via fork reversal or a recombination-based mechanism [Gao et al., 2016, Chang and Cimprich, 2009]. The latter process leads to the formation of sister chromatid junctions which resemble hemicatenane-like structures. These cruciform structures are later resolved by the RecQ helicase BLM syndrome protein (BLM) [Branzei, 2010]. The incorrect repair by DDT pathways leads to the formation of DSBs and subsequent replication fork collapse requiring HR to restart the replication [Sale, 2012].

The rescue of stalled replication forks includes their stabilization and restart. The ATR pathway stabilizes the stalled forks by preventing the loss of replisome. Additionally, it prevents fork collapse and subsequent formation of deleterious DSBs by regulating the

activity of DNA repair proteins Rad51 and fork remodeling helicase SMARCAL1. The latter mediates the replication fork reversal or regression. The replication fork reversal is a protective mechanism, which resume DNA synthesis without breakage [Errico and Costanzo, 2012, Liao et al., 2018, Couch et al., 2013, Quinet et al., 2017]

When the source of replication stress is removed, the ATR pathway allows the stalled replication forks to restart. There are several different models for replication fork restart, including fork restart by repriming, translesion synthesis (TLS) and template switching [Gelot et al., 2015, Iyer and Rhind, 2017].

The fork restart by repriming is a highly conserved mechanism in which DNA synthesis is resumed by repriming downstream the DNA lesion, leaving an unreplicated ssDNA gap behind the damaged forks, which should be repaired by postreplicative repair pathways. The lesion encountered on the lagging strand is directly bypassed due to the discontinuous nature of lagging-strand synthesis. However, the repriming of leading strand is more complex and it uses the primase-polymerase (PrimPol) which has primase and translesion polymerase activity in order to continue DNA synthesis [Pasero and Vindigni, 2017, Ait Saada et al., 2018, Guilliam et al., 2017, Iyer and Rhind, 2017].

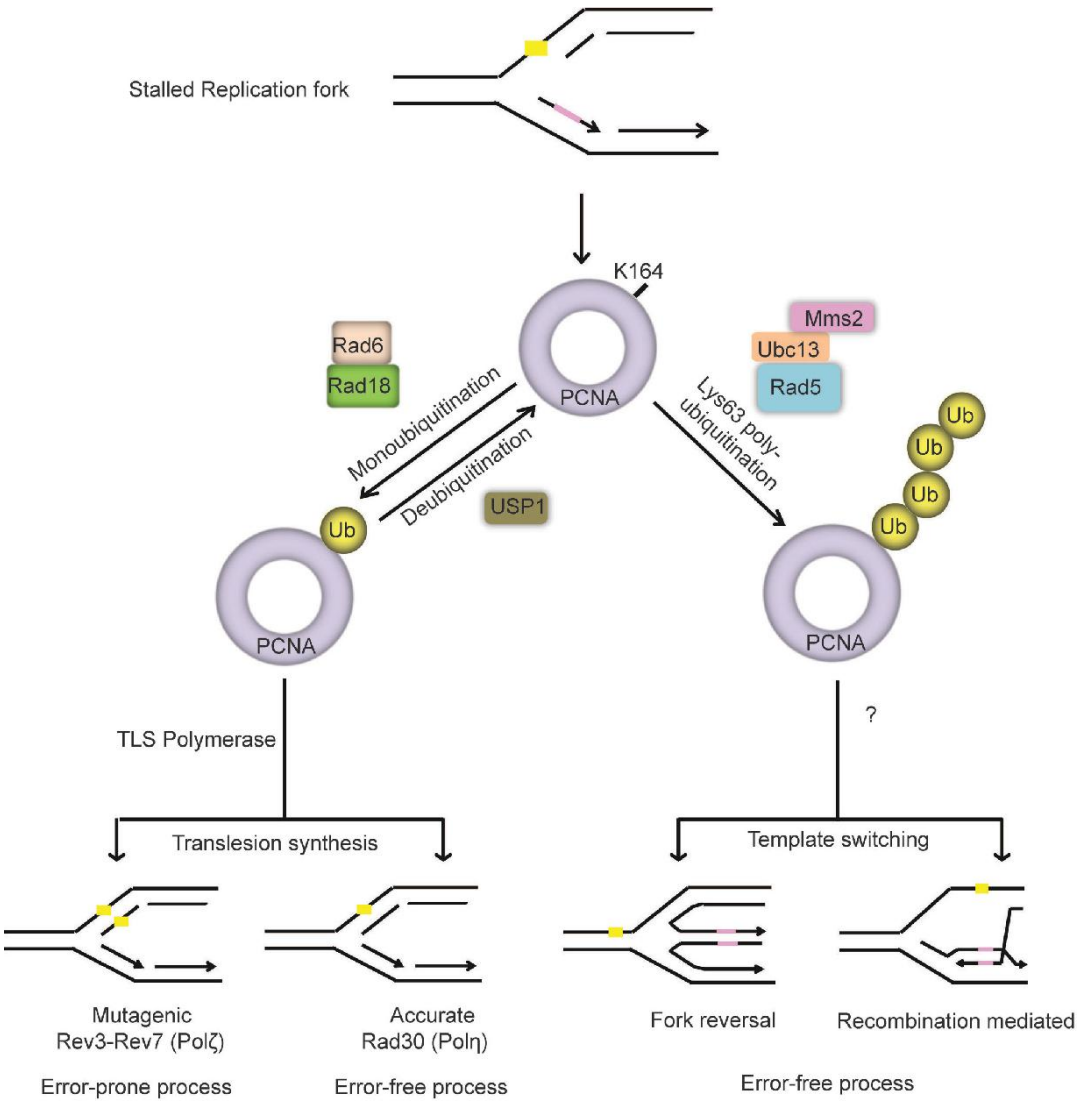

Fig.11 DNA damage tolerance pathway (DDT). A DNA lesion (yellow square) in DNA template stalls replication forks. DDT promotes bypass of the lesion by replicating across the lesion (translesion synthesis TLS, left) or by using the newly synthesized daughter strand as a homologous template (template switching TS, right). TLS is mediated by monoubiquitylation of PCNA through the Rad6-Rad18, inducing the polymerase switch at the replication fork, whereas TS is activated by the polyubiquitylation of PCNA through Rad5-Ubc13-Mms2. TS involves a structural rearrangement to bypass the lesion via fork reversal or recombination mediated mechanism. The fork reversal generates a four-way junction or "chicken-foot" intermediate (left), whereas recombination mediated mechanism generates a D-loop structure results in formation of sister chromatid junction (right) (Ghosal and Chen 2013).

1.4 Ubiquitylation pathway

Protein ubiquitylation, also called ubiquitination, is a post-translational modification that regulates crucial biological processes in eukaryotic cells. The main and most well-studied role of this modification is to target proteins for degradation by the 26S proteasome system [Stringer and Piper, 2011]. However, it is also involved in regulation of cell cycle, apoptosis, DNA repair, protein-protein interactions and is deregulated in some diseases such as cancer [Hershko and Ciechanover, 1998, Mourtzoukou et al., 2018].

Ubiquitylation is controlled by the action of three enzymes: E1, E2 and E3 [Stringer and Piper, 2011]. First, the C-terminal in ubiquitin is activated by E1 ubiquitin activating enzyme. This reaction requires ATP to form a high-energy thioester bond between a Cys residue in the catalytic site of the E1 enzyme and ubiquitin. Next, the activated ubiquitin is transferred by a transacylation reaction to a thiol group of Cys residue of E2 ubiquitin conjugating enzyme and finally transferred to the target protein by an E3 ubiquitin ligase. The attachment of ubiquitin to the protein substrate results in the formation of a covalent isopeptide bond between the carboxyl terminus of the ubiquitin and the ε-amino group of a Lys residue on the substrate protein [Huang and D'Andrea, 2006, Streich and Haas, 2010, Myung et al., 2001].

E3 ubiquitin ligases are essential for the ubiquitylation reaction, regulating the efficiency and substrate specificity. Eukaryotic cells contain hundreds of E3 ligases which can be grouped into four protein families: HECT (Homologous to E6AP Carboxyl Terminus), RING (Really Interesting New Gene), UFD2 homology (U-box) proteins and RING-in-Between-RING (RBR). The latter are RING/HECT hybrid type E3 ligases which were identified in the last few years. HECT, RING, U-box and RBR ligases can be a part of single proteins or multisubunit protein complexes. The most abundant in cells are the RING ligases. They contain RING finger domains with conserved Cys and His residues, which coordinate two zinc ions. Most of RING domains directly bind E2 enzymes and bring into close proximity the Lys of the substrate and the E2-ubiquitin intermediate [Bologna and Ferrari, 2013, Pickart and Eddins, 2004, Zheng and Shabek 2017, Pfoh et al., 2015]. The specificity of E3 ligases allows them to process different proteins and to coordinate distinct cellular signals [Zheng and Shabek 2017].

Ubiquitin was discovered for the first time in the 1970s as a small protein composed of 76 amino acids. It is constitutively expressed in all eukaryotic cells and shares evolutionary conservation [Herrmann et al., 2007]. Later, ubiquitin has been found to be a member of a family of highly conserved proteins, called ubiquitin-like proteins (UBLs). UBLs share a high structural similarity and also include small ubiquitin-like modifier (SUMO), interferon-

stimulated gene 15 (ISG15), neural precursor cell expressed, developmentally down-regulated 8 (Nedd8), and etc. All UBLs are involved in crucial cellular processes.

In vertebrates, ubiquitin is encoded by four different genes (*UBB*, *UBC*, *UBA52*, and *UBA80* (*RPS27A*)). It is synthesized as an inactive precursor which needs activation through proteolytic processing of its C-terminal tail [Kerscher et al., 2006, Pickart and Eddins, 2004, Pfoh et al., 2015]. The structure of ubiquitin and the other members of UBLs have a β-grasp fold that contains a five-stranded β-sheet and a central α-helix [Cappadocia and Lima, 2018]. Ubiquitin itself contains seven Lys residues (K) each of which can be ubiquitylated, by attaching to another ubiquitin molecule and forming different ubiquitin-chain linkages. Ubiquitin can be conjugated through one of its lysine residues (K6, K11, K27, K29, K33, K48 and K63) or the N-terminal methionine residue (M1) [Mourtzoukou et al., 2018]. The addition of a single ubiquitin molecule to a substrate is called monoubiquitylation. Monoubiquitylation signals for regulation of the receptor internalization, vesicle sorting, DNA repair and gene silencing [Huang and D'Andrea, 2006].

The attachment of more than one ubiquitin molecule to a target protein is referred to as polyubiquitination. Polyubiquitin chains, collectively called “ubiquitin code” signal for diverse cellular processes depending on the type of ubiquitin-chain linkage [Ohtake and Tsuchiya, 2017]. The most abundant types of ubiquitin-chain linkages in cells are K48 which target proteins for proteasomal degradation [Swatek and Komander, 2016]. The other types of chains can also trigger proteins for degradation, except the second most abundant K63-linkages, which are mainly involved in protein-protein interactions and DNA repair [Finley et al., 2012]. The specific functions of the other linkage types, also known as “atypical”, are not well understood. Recently, it has been found that K6-linkages are also implied in DNA damage response, whereas K11-linkages signal for the proteasomal degradation in cell cycle regulation [Swatek and Komander, 2016]. K27-chain linkages are one of the least studied and their role is related to the recruitment of proteins in DNA damage response. K29- and K33-linkages are both implicated in degradation of proteins by the proteasome and in regulation of AMPK protein kinases involved in cellular metabolism. Besides, K33-linkages are also associated with the regulation of the T-cell receptor (TCR). M1-linked chains play a key role in the regulation of the activation of the transcription factor NF-κB [Swatek and Komander, 2016, Zinngrebe et al., 2014, Akutsu et al., 2016].

Ubiquitin can be further modified by other modifications, including SUMOylation, phosphorylation and/or acetylation. The diversity of the different ubiquitin-chain linkages and regulation of ubiquitin by other post-translational modifications affects distinct signaling pathways in the cells. The covalent attachment of ubiquitin to a target protein is a reversible process. Due to the action of several families of proteases called deubiquitinases

(DUBs), ubiquitin is removed from its targets, and the free ubiquitin pool is recovered in the cell [Swatek and Komander, 2016].

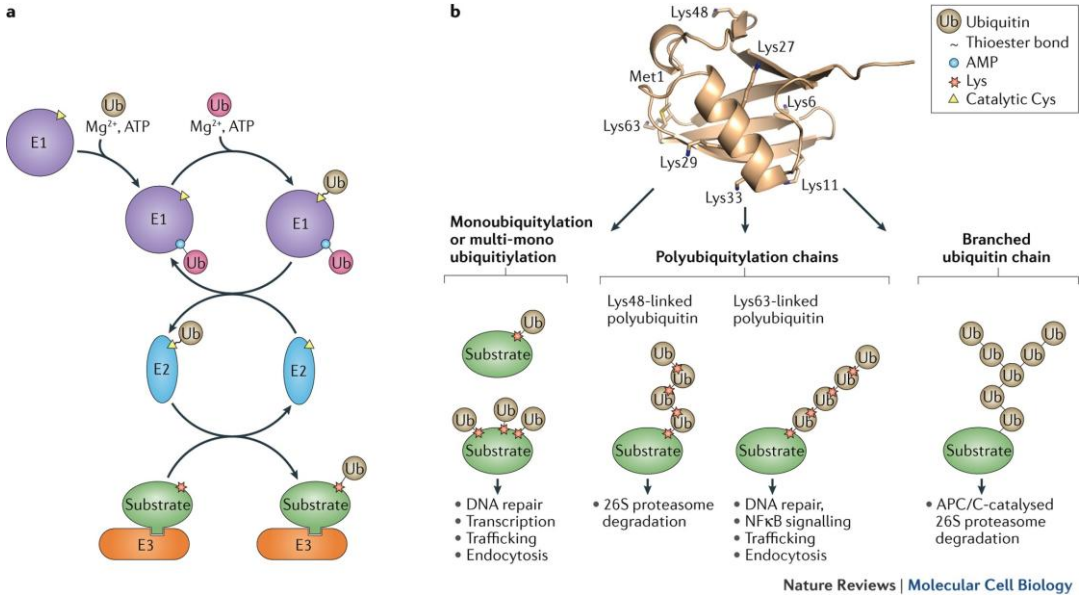

Fig.12 A schematic diagram of ubiquitylation pathway. a) Ubiquitylation involves three main steps. In the first step ubiquitin is activated by a ubiquitin-activating enzyme (E1) (shown in purple). The reaction is catalyzed by $Mg2^{+}$ and ATP to form a high-energy thioester bond between a Cys residue in the catalytic site of the E1 enzyme and ubiquitin. In the second step, the activated ubiquitin is transferred to a thiol group of Cys residue of E2 ubiquitin conjugating enzyme (shown in blue). In the third step, ubiquitin is finally transferred to a substrate protein by an E3 ubiquitin ligase (shown in orange). b) Substrate ubiquitylation classification. The ubiquitin molecule can be attached at one (monoubiquitylation) or multiple (multi-monoubiquitylation) lysine sites to a substrate. The attachment of several ubiquitin molecules to the substrate leads to formation of polyubiquitin chains, which can be homogenous (Lys48-linked and Lys63-linked) or heterogenous (branched ubiquitin chains). Different ubiquitin linkages signal for diverse cellular processes (Buetow and Huang, 2016).

1.4.1 Ubiquitylation in DNA repair

Eukaryotic cells have evolved distinct cellular mechanisms, collectively termed DNA damage response (DDR) to detect, signal and trigger repair of DNA lesions. This signaling network of cellular pathways, including cell-cycle checkpoint, DNA repair and DNA damage tolerance (DDT), ensures protection from DNA damage threats and thus maintains the integrity of the genome [Jackson and Durocher, 2013, Giglia-Mari et al., 2011].

DDR is tightly controlled by several post-translational modifications (PTMs) such as ubiquitylation, phosphorylation, SUMOylation, methylation, acetylation, and others. These modifications regulate the stability, localization and activity of proteins involved in DDR, facilitating the signaling pathway [Brown and Jackson, 2015].

Whereas the influence of some PTMs on DNA repair is well-studied, the implication of non-proteolytic ubiquitylation in DNA repair mechanisms has been recently described and is still a subject of considerable research. However, growing evidence has shown that ubiquitin modification has a crucial regulatory role in DNA damage tolerance (DDT), double-strand break repair, Fanconi anemia (FA) pathway and other DNA repair pathways [Al-Hakim et al., 2010, Ghosh and Saha, 2012, Jackson and Durocher, 2013, Cipolla et al., 2016, Pinder et al., 2013, Schwertman et al., 2016, Miles et al., 2015, Yu et al., 2020].

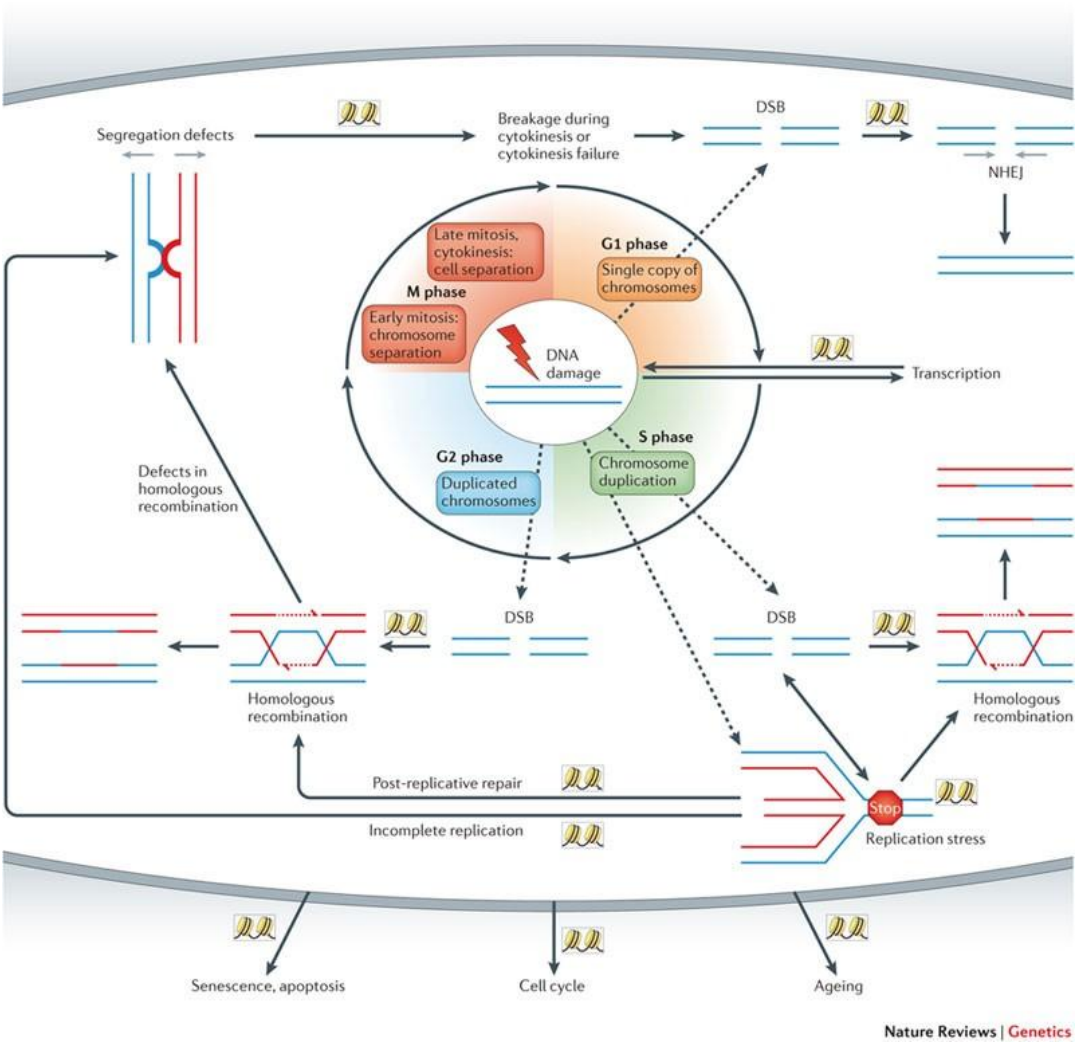

Fig.13 DNA damage response (DDR) and genomic stability. Upon DNA damage, the signaling network of cellular pathways, which connects cell-cycle checkpoint, DSB repair and DDT (Post-replicative repair) is activated in order to repair the damage and to preserve the integrity of the genome.

Failure in these processes can lead to accumulation of unrepaired DSBs and formation of aberrant chromatin structures between chromosomes. If these aberrant structures, which are derived from defects in homologous recombination or incomplete replication, are left unresolved, they can lead to segregation defects in mitosis or cytokinesis failure. As an active player in DDR is illustrated chromatin (indicated as nucleosomes) (Papamichos-Chronakis and Peterson, 2013).

The ubiquitin-mediated regulation of DNA repair, particularly DDT, was first illustrated with the discovery of yeast E2 and E3 enzymes, called Rad6 and Rad18. In response to DNA damage, Rad6-Rad18 ubiquitin ligase complex promotes monoubiquitylation of the sliding clamp PCNA at Lys164 and subsequent activation of translesion synthesis (TLS) mechanism of DDT [Brown and Jackson, 2015]. This modification was later found to be conserved from yeast to humans. Moreover, the monoubiquitylated PCNA can be further modified via K63-linked polyubiquitin chain, promoting the error-free DDT process. In yeast, PCNA polyubiquitylation is triggered by the Rad5 E3 ligase, along with the E2 dimer Mms2-Ubc13. In human cells, polyubiquitylation of PCNA is mediated by human homologs of the E2 complex and the joint activity of two functional Rad5 orthologs, named as HLTF and SHPRH [Cipolla et al., 2016, Ramaekers and Wouters, 2011]. PCNA ubiquitylation plays an essential role in DDT mechanisms, allowing bypass of blocking lesions and resuming normal DNA synthesis. It can be induced in response to replication stress, spontaneous DNA damage or genotoxic agents such as UV irradiation, methyl methanesulfonate (MMS), hydroxyurea (HU), aphidicolin and mytomicin C (MMC) that block replication fork progression [Fox et al., 2011]. Agents that directly generate DNA double strand breaks (DSBs), like bleomycin, camptothecin and ionizing radiation do not trigger PCNA ubiquitylation [Zhang et al., 2011, Chang et al., 2006]. Nevertheless, the repair of highly toxic DSBs has also been shown to be dependent on ubiquitin modification, although different ubiquitin ligases and substates are involved. The Ring finger protein 8 (RNF8) which is an E3 ubiquitin ligase has a central role in regulating the DNA double-strand break repair pathway. RNF8 localizes at DSB sites and along with the E2, Ubc13 and another E3 ubiquitin ligase, called RNF168 promotes ubiquitylation of histone H2A and H2A.X via K63-linked ubiquitin chain [Ulrich, 2014]. The RNF8/RNF168-mediated polyubiquitylation in turn recruits several DNA repair proteins, including 53BP1 and BRCA1, that are essential for non-homologous end joining (NHEJ) and homologous recombination (HR) repair [Brinkmann et al., 2015, Brown and Jackson, 2015, Zhao et al., 2014].

Besides polyubiquitylation, monoubiquitylation of histone H2A and H2B has also been found to be crucial for DNA repair [Uckelmann and Sixma, 2017]. Monoubiquitylation of H2A via Lys119 is the most abundant histone modification in mammalian cells and is critical for maintaining the genomic stability [Vissers et al., 2008]. H2B is monoubiquitylated at Lys120 and has a role in decompacting the structure of chromatin during DSB repair [Wojcik et al., 2018].

In mammalian and human cells, monoubiquitylation has also been observed to play an important role in the FA pathway, regulating the repair of interstrand crosslinks (ICLs). The activation of FA pathway in response to DNA crosslinks results in the recruitment and monoubiquitylation of FANCD2/FANCI heterodimer by the FA core multi-protein complex. FANCL is a component of the FA core complex, which functions as a RING E3 ubiquitin ligase and together with the E2, UBE2T monoubiquitylates FANCD2 and FANCI at Lys561 and Lys523, respectively. This ubiquitylation is essential for the subsequent ICL repair by recruiting downstream effector proteins at damaged sites [Liang et al., 2016, Al-Hakim et al., 2010, Ramaekers and Wouters, 2011, Yates and Maréchal, 2018].

Recently, in human cells it has been reported that RAD18 is recruiting SLF1-SLF2 proteins to DNA damage sites, which in turn, promote the recruitment of the Smc5/6 complex at these sites, during HR repair at stalled replication forks. Human SLF1 and SLF2 can be considered as functional homologs of Nse5 and Nse6, which facilitate the DNA repair function of the Smc5/6 complex by suppressing the accumulation of recombination intermediates [Räschle, 2015, Pebernard, 2006].

1.5 Structural maintenance of chromosomes

The functional and structural organization of eukaryotic chromosomes is regulated by a specific class of structurally related protein complexes, known as Structural Maintenance of Chromosomes (SMC) proteins [Hirano, 2006]. SMC proteins were first identified in budding yeast, where they showed to be essential for proper chromosome segregation during mitosis [Strunnikov et al., 1993]. Subsequently, the SMC protein family was also found in other organisms, demonstrating an evolutionary conservation from bacteria to humans. In addition to their function in chromosome disjunction, SMC proteins were found to be involved in mitotic chromosome condensation, sister-chromatid cohesion, recombinational repair and gene regulation [Harvey et al., 2002, Hirano, 2006].

A unique feature of SMC proteins is their common ring-shaped molecular structure, consisting of long antiparallel coiled-coil SMC subunits with an ATP-binding domain at their ends. Current models propose that SMC complexes use the energy of ATP hydrolysis to trigger conformational changes able to alter their topological interaction with DNA, thus regulating chromatin organization.

SMC proteins are composed of six different SMC subunits in eukaryotes (SMC1-SMC6) which are divided in pairs, constituting three different heterodimers: SMC1-SMC3, SMC2-

SMC4 and SMC5-SMC6. Each pair is composed of globular N- and C-terminal domains connected through long coiled-coils. These two SMC subunits interact with each other by their hinge domains, forming a V-shaped heterodimer complex. The connected N- and C-terminal domains form head domains which contain Walker A and Walker B motifs with ATPase activity. Head domains are bridged together by a kleisin subunit (non-SMC protein) leading to the conversion of the heterodimer's shape into a ring-like structure [Losada and Hirano, 2005, Kakui and Uhlmann, 2018, Harvey et al., 2002]. Heterodimers, together with non-SMC proteins assemble into three distinct large multiprotein complexes, called cohesin, condensin and Smc5/6 complex. Cohesin is composed of SMC1 and SMC3 and interacts with two non-SMC proteins (sister-chromatid cohesion proteins Scc1 and Scc3). It holds sister chromatids together from S phase until mitosis and is involved in organization of interphase chromosomes. Condensin, containing SMC2 and SMC4 form a complex with three non-SMC subunits and plays a crucial role in the compaction and elasticity of sister chromatids. The Smc5/6 complex comprises SMC5 and SMC6 and six non-SMC proteins. It is the least studied complex for which is known to be involved in DNA repair and chromosome stability [van Ruiten and Rowland, 2018, Dowen and Young, 2014, Gligoris and Löwe, 2016, Jeppsson et al., 2014 (2)].

Despite their role in distinct chromosomal functions, SMC complexes might share a common mechanism of action. One of the possible mechanisms that functionally join the SMC proteins is referred to as DNA loop extrusion. This mechanism is based on the formation of DNA loop structures by loop-extruding factors (LEFs). It has been suggested that SMC complexes function as LEFs due to their capacity to move along the DNA until an adaptor protein blocks this process. SMC complexes can mediate loop formation due to their ring-like structure, allowing them to bind and extrude DNA into extended loops. The latter is possible with the aid of ATPase hydrolysis allowing DNA translocation through the ring [Hassler et al., 2018, Baxter et al., 2019, Yuen and Gerton, 2018]. In support of this mechanism, both condensin and cohesin have been shown to act as LEFs using their ATPase motor activity *in vitro*. Condensin can extrude DNA in metaphase, suggesting its function in chromatin condensation depends on the loop extrusion process. Cohesin is able to generate loops by extrusion during interphase [Golfier et al., 2019, Ganji et al., 2018, Davidson et al., 2019]. Apart from its function in sister chromatid cohesion, cohesin has also been shown to be involved in the organization of the genome during interphase. It has been suggested that cohesin mediates compartmentalization of interphase chromosomes into topologically associated domains (TADs) and loops by cohesin-dependent loop extrusion [Mayerova et al., 2020]. The ability of cohesin and condensin to extrude DNA loops suggests that the loop extrusion principle might be also required for the Smc5/6 complex function.

1.5.1 The Smc5/6 complex – structure

The Smc5/6 complex is a nuclear protein complex composed of two core SMC proteins: Smc5 and Smc6 and six non-structural maintenance of chromosome element (Nse) proteins, known as Nse1, Nse2/Mms21, Nse3, Nse4/QRI2, Nse5 and Nse6. Human cells express four non-SMC subunits: NSMCE1, NSMCE2, NSMCE3, NSMCE4 which are homologs of the yeast Nse1-4. In addition they express two Smc5 localization factors: SLF1 and SLF2, which have been proposed to be the functional orthologues of Nse5 and Nse6 [Kegel and Sjögren, 2010, Taylor et al., 2008, Räschle et al., 2015].

The Smc5/6 complex was first discovered in *Schizosaccharomyces pombe,* where it was shown that Rad18 (Smc6) interacts *in vivo* with Spr18 (Smc5) forming a heterodimer. Later, the other non-SMC subunits (Nse1-6) of the complex were identified and it was found that all of them are essential and highly conserved between eukaryotes [McDonald et al., 2003, Pebernard et al., 2004, Hu et al., 2005, Morikawa et al., 2004, Pebernard et al., 2006]. Nse1 contains a RING domain (Really Interesting New Gene) with an E3 ubiquitin ligase activity and forms a subcomplex with Nse3 and Nse4 [McDonald et al., 2003, Sergeant et al., 2005]. Nse2, also known as Mms21, has an SP-RING domain, with SUMO (small ubiquitin-like modifiers) ligase activity [McDonald et al., 2003, Andrews et al., 2005]. In addition, Nse2 forms a subcomplex with Smc5 and Smc6 [Sergeant et al., 2005]. Nse3 is related to the melanoma-associated antigen (MAGE) protein family. One of their members, MAGE-G1 interacts with Nse1 and Nse4 in human cells, indicating that MAGE-G1 is the human homolog of Nse3 [Pebernard et al., 2004]. Nse4 is a kleisin subunit that bridges the head domains of Smc5 and Smc6 [Palecek et al., 2006]. The last two non-SMC proteins: Nse5 and Nse6 do not show evolutionary conservation in higher eukaryotes and are poorly studied [Pebernard et al., 2006]. The Smc5/6 complex can be subdivided into three subcomplexes, able to self-associate: Nse1-Nse3-Nse4, Nse2-Smc5-Smc6 and Nse5-Nse6.

The Nse1-Nse3-Nse4 subcomplex bridges the Smc5-Smc6 ATPase head domains and in fission yeast recruits the Smc5/6 complex at sites of DNA damage [Pebernard et al., 2008 (1)]. Nse1 and Nse3 are known as kleisin-interacting tandem winged-helix element (KITE) proteins, which are involved in kleisin bridging and DNA binding [Palecek, 2019]. The N-terminus of Nse3 interacts with the N-terminal part of Nse1, whereas the C-terminus of Nse3 binds the N-terminus of Nse4 [Hudson et al., 2011]. The C-terminal part of Nse1 contains the zinc finger RING domain, which stabilizes the formation of an Nse1-Nse3-Nse4 heterotrimer [Wani et al., 2018, Pebernard et al., 2008 (1)] (Fig.14).

Nse3 shares homology with the MAGE family of proteins, which are conserved in all eukaryotes. MAGE proteins are divided into two groups: MAGE I and MAGE II. MAGE I

proteins are highly expressed in tumor cells, whereas MAGE II are expressed in different types of cells. MAGE-G1 which is the human orthologue of Nse3 is a member of MAGE II proteins and it was found to enhance the ubiquitin ligase activity of Nse1 RING domain [Taylor et al., 2008, Lee and Potts, 2017, Doyle et al., 2010]. Although MAGE proteins share a high structural homology, it was reported that only MAGE-G1 and MAGE-F1 can interact with Nse1 [Taylor et al., 2008, Doyle et al., 2010] (Fig.14).

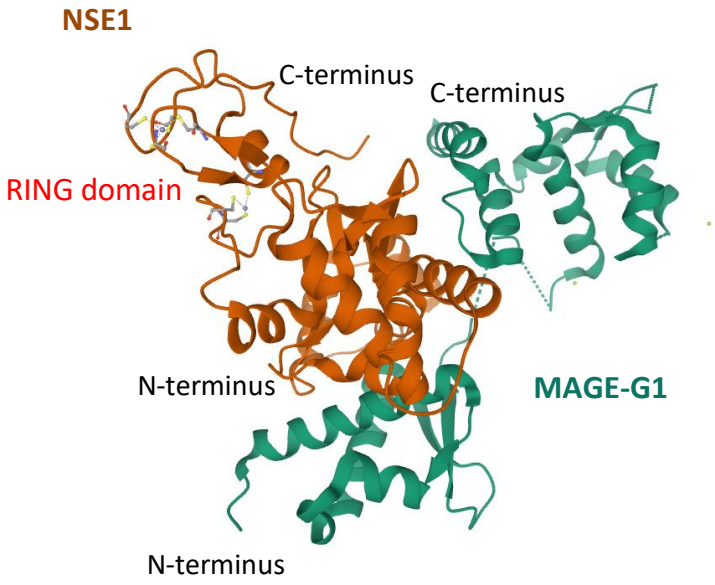

Fig.14 Crystal structure of Nse1 and MAGE-G1 (Nse3) and their interaction. Nse1 is indicated in brown, MAGE-G1 is labeled in green. At C-terminal part of Nse1 is shown the RING domain that coordinates two zinc ions. (*Image is created using Mol with the PDB ID and associated publication: Sehnal et al., (2018), Towards a common library and tools for web molecular graphics MolVA/EuroVis Proceedings and RCSB PDB, https://www.rcsb.org/3d-view/5WY5/1)*

The Smc5-Smc6 heterodimer forms the core of the Smc5/6 complex through the interaction between the Smc5 and Smc6 at their hinge domains [Fousteri and Lehmann, 2000, Sergeant et al., 2005, Diaz and Pecinka, 2018]. Nse2 interacts directly with the central part of Smc5 through its N-terminus. The C-terminal region of Nse2 contains a RING-like domain with a SUMO ligase activity allowing SUMOylation of different substrates [Sergeant et al., 2005]. Similar to ubiquitylation, SUMOylation is a post-translational modification in which a small ubiquitin-like modifier (SUMO) family of proteins is covalently attached to lysine (Lys)

residues in target proteins. SUMOylation regulates various biological functions such as cell growth and differentiation, protein stability, protein-protein interactions, protein trafficking and cell responses to stress [Wilson, 2017]. Nse2 can undergo auto-SUMOylation, as well as it can SUMOylate several subunits of the complex including Smc6, Nse3, Nse4 and Smc5 [Sergeant et al., 2005, Zhao and Blobel, 2005, Potts and Yu, 2005]. SUMOylation within the Smc5/6 complex is involved in response to DNA damage and inhibition of DNA replication [Sergeant et al., 2005, Andrews et al., 2005, Zapatka et al, 2019]. In our group, it has been described that the ATPase activity of Smc5 and binding to DNA, activate the SUMO-ligase activity of Nse2 in budding yeast [Bermúdez-López et al., 2015; Varejão et al., 2018].

The third known subcomplex of the Smc5/6 complex is the Nse5-Nse6. It is less studied and less conserved among eukaryotes. In different lower eukaryotes the Nse5-Nse6 subcomplex has been shown to be bound at different regions (hinge or heads) of the Smc5-Smc6 heterodimer [Sergeant et al., 2005, Pebernard et al., 2006, Duan et al., 2009]. In plants and humans, similar subcomplexes, termed as (ASAP1-SNI1) and (SLF1-SLF2), respectively were identified. They have been considered as the functional homologs of the Nse5 and Nse6 [Yan et al, 2013, Räschle et al., 2015].

Recently, the plant SNI1 has shown to be implicated in checkpoint activation and DNA damage response [Wang et al., 2018]. Also, mutations in ASAP1 or SNI1 cause severe growth defects and cell death [Yan et al., 2013, Wang et al., 2018]. As mentioned above, the human SLF1-SLF2 subcomplex interacts with RAD18 E3 ubiquitin ligase and recruits the Smc5/6 complex at DNA lesions in a ubiquitin-dependent manner [Räschle et al., 2015]. It has been suggested that all of the subunits of the Smc5/6 complex are essential for the structure and function of the complex.

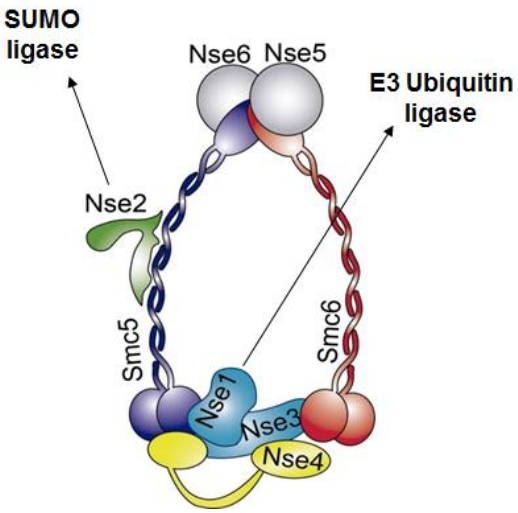

Fig. 15 Structure of the Smc5/6 complex in *Saccharomyces cerevisiae.* The Smc5/6 complex is composed of two SMC subunits (Smc5 and Smc6, shown in blue and red) and six non-SMC elements:

Nse1, Nse2, Nse3, Nse4, Nse5 and Nse6. Nse1, Nse3 and Nse4 (shown in blue and yellow) form a subcomplex. Nse5 and Nse6 (label in grey) form a dimer. Nse1 is a putative ubiquitin ligase, Nse2 is a SUMO ligase.

1.5.2 The Smc5/6 complex - function in eukaryotic cells

A large body of evidence demonstrates the implication of the complex in regulation of DNA repair and chromosome segregation. The first indications for the role of the Smc5/6 complex in DNA damage response came from a study which used *Schizosaccharomyces pombe* as a model organism. It has been found that point mutations in Rad18 (Smc6 in budding yeast) cause hypersensitivity to UV irradiation and ionizing radiation [Lehmann et al., 1995]. Consequently, the rest of the subunits of the Smc5/6 complex have also been found to be essential for viability and involved in DNA repair. Hypomorphic alleles of these proteins in budding yeast are extremely sensitive to a variety of DNA damaging agents, including UV and ionizing irradiation, methyl methanesulfonate (MMS), camptothecin (CPT) and hydroxyurea (HU) [Fujioka et al., 2002, Pebernard et al., 2004, McDonald et al., 2003, Andrews et al., 2005, Onoda et al., 2004, Hu et al., 2005, Pebernard et al., 2006].

Epistatic analysis with Rad51 indicated that the Smc5/6 complex is involved in DNA double strand-break (DSB) repair by homologous recombination (HR) [Lehmann et al., 1995, McDonald et al., 2003 Pebernard et al., 2004]. Besides, it has been shown that the Smc5/6 complex is essential for proper chromosome segregation of repetitive DNA regions [Torres-Rosell et al., 2005(1)]. Several studies using yeast, plant, chicken and human cells have confirmed the important role of the Smc5/6 complex in HR repair [Aragón, 2018]. The Smc5/6 complex was found to promote DSB repair by sister chromatid recombination in all of the tested species [De Piccoli et al., 2006, Mengiste et al., 1999, Watanabe et al., 2009, Stephan et al., 2011, Payne et al., 2014].

In budding yeast, recruitment of the Smc5/6 complex at DSBs depends on MRE11 (the first protein recruited to DSBs) during G2 and M phases [Lindroos et al., 2006, Ünal et al., 2004]. In human cells, this recruitment requires Rad18 and SLF1-SLF2 subcomplex, the functional homologs of yeast Nse5 and Nse6 during repair of DNA cross-links [Potts et al., 2006, Räschle et al., 2015].

Further studies with yeast and human cells have indicated that Nse2 SUMOylates Scc1 subunit of cohesin at several Lys residues, promoting sister chromatid HR [McAleenan et al., 2012, Wu et al., 2012]. This modification is not required for the recruitment of cohesin to DSBs, but Scc1 mutants deficient for SUMOylation are defective in sister chromatid HR and cannot mediate DNA damage-induced cohesion [Wu et al., 2012, McAleenan et al., 2012].

Related to this, Nse2-SUMOylation is also implicated in the maintenance of telomere length by HR in budding yeast and human cells. The impaired Smc5/6 function inhibits telomere HR leading to telomere shortening and subsequent senescence [Potts and Yu, 2007, Zhao and Blobel, 2005].

The Smc5/6 complex has also been found to be involved in stabilization and restart of stalled or collapsed replication forks, maintenance of ribosomal DNA (rDNA) and telomeres, as well as in chromosome topology regulation [Palecek, 2019]. More recently, another function of the Smc5/6 complex has also been described: its role as a host restriction factor against Hepatitis B virus (HBV) [Decorsière et al., 2016].

The function of the Smc5/6 complex at stalled and collapsed replication forks has been identified genetically, showing synthetic lethal interactions with mutations in genes involved in fork restart, such as *srs2*, the RecQ helicase *sgs1* (homolog of the human BLM helicase) and the endonuclease *mus81* [Branzei et al., 2006, Irmisch et al., 2009, Ampatzidou et al., 2006]. These findings suggest that the Smc5/6 complex, along with Sgs1/BLM helicase and Mus81 is involved in the recovery of stalled and collapsed replication forks by recombination. In addition, the *smc5/6* mutants show hypersensitivity to DNA damage drugs blocking replication, such as hydroxyurea (HU), which cause replication fork stalling [Hu et al., 2005, Torres-Rosell et al., 2005(1)]. During replication stress, stalled and collapsed forks give rise to aberrant recombination intermediates, also known as X-shaped Holliday junction (HJs) structures, which are normally removed during post-replicative repair. If HJs are left unresolved, they become toxic to cells, leading to chromosome missegregation or cell death [Mankouri et al, 2011, Aragón, 2018]. It has been found that the *smc5/6* mutants accumulate high levels of X-shaped DNA molecules, indicating a direct role of the complex in resolution of joint molecules [Torres-Rosell et al., 2005(1), Miyabe et al., 2006, Irmisch et al., 2009]. Moreover, the SUMO ligase activity of Nse2/Mms21 has also been implicated in preventing the accumulation of junction structures [Branzei et al., 2006, Bermúdez-López et al, 2010].

Recently, it has been indicated that sumoylation of different proteins implicated in repair (RPA, Rad52, Rad59, Smc5) by Nse2, would mediate the relocation of collapsed forks to the nuclear pore complex (NPC) to constrain recombination until they are localized at the NPC [Whalen et al., 2020]. Sumoylation by Nse2 was previously also implied in relocation of DSBs to the nuclear envelope in yeast cells, in order to be repaired [Horigome et al., 2016].

Furthermore, the Smc5/6-dependent SUMOylation of Sgs1/BLM mediates the removal of recombination intermediates [Bonner et al., 2016, Bermúdez-López et al., 2016, Pond et al., 2019]. On the other hand, in *Saccharomyces cerevisiae* the Smc5/6 complex reduces the presence of X-shaped recombination intermediates at blocked replication forks by

regulating the activity of the Mph1 helicase [Chen et al., 2009]. This suggests that the Smc5/6 complex can prevent the accumulation of X-shaped HJ molecules independently from Sgs1. Mph1 is the yeast orthologue of Fanconi anemia protein M (FANCM) in humans, that can dissociate DNA loop structures and catalyze the regression of stalled replication forks [Prakash et al, 2009, Xue et al, 2014, Gari et al., 2008]. The Smc5/6 complex has been proposed to be a negative regulator of Mph1, with the ability to inhibit the fork reversal activity of Mph1, but not its D-loop disruption function [Xue et al., 2014]. Moreover, deletion of *MPH1* rescues *smc5/6* mutants: inhibits the sensitivity to different DNA damaging agents and growth defects of these mutants, and also decreases recombination. To date, it is still unknown if this regulation is conserved in human cells.

In contrast to Sgs1, Mph1 does not depend on SUMOylation by the Smc5/6 complex [Chen et al., 2009]. The two helicases also differ in time of their action: Sgs1 resolves recombination structures, whereas Mph1 functions early during replication stress by promoting the formation of joint molecules [Palecek, 2019]. Recently, it has been shown that the Smc5/6 complex tightly controls the Mph1 activity at RNA-DNA hybrids, known as R-loops which can block replication forks and thus prevents deleterious accumulation of both RNA-DNA hybrids and X-shaped structures [Lafuente-Barquero et al., 2017].

Apart from its functions in replication stress and DNA damage, the Smc5/6 complex is also important in cells that are not exposed to sources of damage, during S and G2/M phases [Aragón, 2018]. In physiological unperturbed conditions, the yeast Smc5/6 complex is enriched at repetitive regions including ribosomal DNA (rDNA), centromeres and telomeres and is essential for their stability [Torres-Rosell et al., 2005(1), Torres-Rosell et al., 2005(2), Lindroos et al., 2006, Pebernard et al., 2008 (2)]. Moreover, mutations in the Smc5/6 complex cause rDNA missegregation, which results in incomplete replication [Torres-Rosell et al., 2007(1)]. Consistent with this, another study has shown that the Smc5/6 complex plays an essential role in removing DNA-mediated sister chromatid linkages, and thus promotes chromosome segregation during mitosis [Bermúdez-López et al., 2010]. The main participant in this process is the Nse2/Mms21 SUMO ligase activity that maintains the integrity of repetitive loci and their proper segregation [Takahashi et al., 2008, Bermúdez-López et al., 2010].

Yeast telomeres have also been found to require the SUMO ligase activity of the Smc5/6 complex for their proper organization [Zhao and Blobel, 2005]. Unlike them, centromeres do not depend on SUMOylating activity of the Smc5/6 complex. Probably, the Smc5/6 complex functions in centromeric regions in association with cohesin function [Pebernard, et al., 2008 (2)]. In addition, SUMOylation of cohesin subunits by the Smc5/6 complex suggests implication of the Smc5/6 complex in regulation of sister chromatid cohesion in lower and higher eukaryotes [Takahashi et al., 2008, Behlke-Steinert et al., 2009].

Another key function of the Smc5/6 complex is maintenance of the genomic stability by regulation of chromosome topology. During S phase, the Smc5/6 complex is localized on undamaged chromosomes, where it reduces the levels of DNA supercoiling, induced by replication or transcription [Lindroos et al., 2006, Kegel et al., 2011, Jeppsson et al., 2014 (1)]. It has been proposed that the Smc5/6 complex facilitates fork rotation and thus relieves the topological stress, allowing the progression of both DNA replication and transcription. Furthermore, the Smc5/6 also seems to be required for the resolution of the catenanes generated by fork rotation when topoisomerase II (Top2) is inactive [Jeppsson et al., 2014 (1)]. It has been shown that the frequency of the Smc5/6 chromosome interaction sites increases with the lengthening of chromosomes, as well as in chromosome circularization or non-functional Top2 [Kegel et al., 2011]. The resolution of topological tension ahead of the replication fork by rotational movement of the fork is essential for termination of replication when the two converging forks reduce the recruitment of the topoisomerases [Kegel and Sjögren, 2010].

The Smc5/6 complex also facilitates the replication termination in the rDNA arrays [Torres-Rosell et al., 2007(2)]. This finding confirms the importance of the Smc5/6 complex in releasing topological stress during replication and maintaining the integrity of the genome.

Recently, the Smc5/6 complex has also been shown to participate in restriction of DNA virus infections. It has been proposed that the Smc5/6 complex prevents the Hepatitis B virus (HBV) infection by binding the viral episomal DNA and thus suppressing viral transcription [Decorsière et al., 2016, Murphy et al., 2016]. The antiviral role of the Smc5/6 complex has also been reported in studies using herpes simplex virus 1 (HSV-1) [Xu et al., 2018] and human papillomavirus (HPV-31) [Gibson et al., 2020], although the exact mechanism of viral replication machinery inhibition is not yet understood. The function of the Smc5/6 complex as a restriction factor for HBV is thoroughly explained in (chapter 1.5.4).

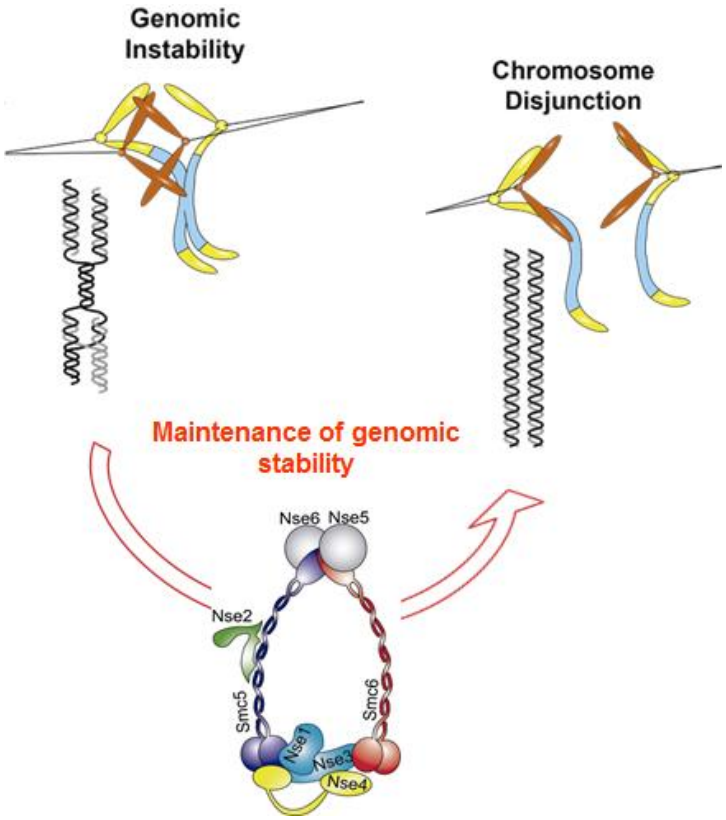

Fig.16 Function of the Smc5/6 complex in chromosome segregation and maintenance of genomic stability. The Smc5/6 complex promotes dissolution of recombination intermediates and the completion of genomes replication.

1.5.3 Nse1 ubiquitin ligase

Nse1 (also named NSMCE1 or NSE1 in mammalian cells), is part of the Smc5/6 complex and contains a RING domain (a zinc finger-like motif) with putative E3 ligase activity at its C-terminus. It forms a subcomplex with Nse3 and Nse4 [McDonald et al., 2003]. The RING (Really Interesting New Gene) domain is composed of eight conserved metal-binding cysteine and histidine residues which coordinate two zinc atoms in a cross-brace conformation [Pebernard et al., 2008 (1)]. The basic sequence of the RING domain: Cys-X2-Cys-X(9-39)-Cys-X(1-3)-HisX(2-3)-Cys-X2-Cys-X(4-48)-Cys-X2-Cys (where X is any amino acid) was first described by Freemont in 1991 [Freemont et al., 1991]. RING domains constitute a big family of RING variants found in functionally different proteins and widely spread among different species [Borden and Freemont, 1996]. Depending on the number of cysteine and

histidine residues (C_3HC_4 and $C_3H_2C_3$) RING domains can be mainly classified into two types of families: RING-CH and RING-H2 [Saurin et al. 1996, Deshaies and Joazeiro, 2009]. Outside these families, other RING variants have also been identified which share similar sequence and spacing between the conserved residues [Borden and Freemont, 1996]. The three-dimensional (3D) analysis of different RING domains showed that cysteine and histidine residues bind the two zinc atoms inside the core of the domain, and thus maintain the RING structure [Deshaies and Joazeiro, 2009]. The specific function of RING domains is still not well understood. Originally, it was thought that the RING domain facilitates the binding to DNA. Later, it was demonstrated that the RING motif of several proteins mediates ubiquitin E3 ligase activity and modulates the function of other proteins by ubiquitylation [Lorick et al., 1999, Deshaies and Joazeiro, 2009]. Also, it has been found that RING E3 ligases can function as monomers, homodimers, or heterodimers. Homo- and heterodimers can interact with other active or inactive RING domains in order to mediate ubiquitylation. In most cases, the inactive RING domain in heterodimers has a stimulatory effect, facilitating the interaction with the E2-congugating enzyme. Besides, some RING ligases can also function as multi-subunit complexes [Budhidarmo et al., 2012]. In addition, RING domains were found to be essential for the proper formation and structure of large protein complexes [Borden, 2000]. It is known that not all zinc-finger domains have an E3 ligase activity. For example, LIM and PHD type zinc finger domains are folded differently and do not show ubiquitin ligase activity. However, some proteins with a PHD-like RING domain have also been shown to act as E3 ubiquitin ligases [Yonashiro et al., 2006]. Currently, more than 600 proteins with RING type E3 ligase activity are identified in humans [Deshaies and Joazeiro, 2009].

Interestingly, Nse1 contains a different type of RING domain, Nse1 homology RING (NH-RING) which maintains the cross-brace structure of zinc coordinated residues (Cys or His) and shows a strong conservation among lower and higher eukaryotes [Pebernard et al., 2008 (1)] (Fig. 17). The Nse1 NH-RING shares a similar sequence with PHD RING domains (C_4HC_3) which are mainly involved in protein-protein interactions and chromatin remodelling [Pebernard et al., 2008 (1), Bienz, 2006]. However, it is still not well understood if the Nse1 RING domain can promote ubiquitylation of protein substrates and/or has another function. Ubiquitin-ligase activity was described *in vitro*, using human proteins MAGE-G1 and Nse1 [Doyle et al., 2010], but not using the corresponding yeast proteins [Pebernard et al., 2008 (1)]. Later, one *in vivo* substrate for MAGE-F1 and Nse1 has been described, MMS19, implied in assembling iron-sulfur proteins, some of them implied in DNA repair [Weon et al., 2018]. Therefore, *in vivo* ubiquitin ligase activity of Nse1, depending on Smc5/6 complex, has not been described yet.

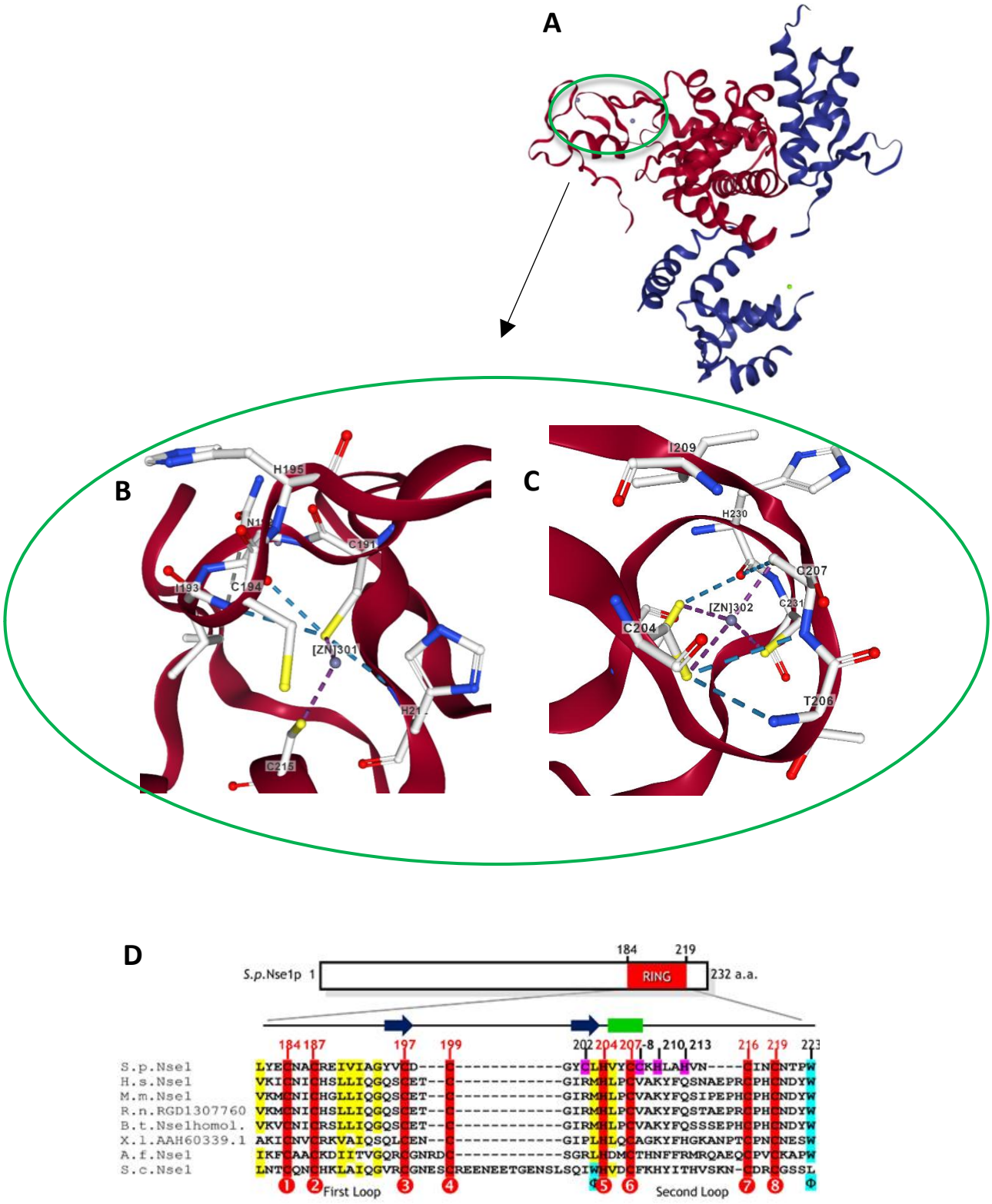

Fig. 17 The crystal structure of human Nse1-MAGE-G1 (Nse3) protein dimer and sequence alignment of Nse1 RING domain. A. Crystal structure of Nse1-Nse3 dimer. Nse1 protein is labeled in red, MAGE-G1 is indicated in blue. Zinc ions are indicated with blue dots (RCSB Protein Data Bank, 5WY5). B. and C. Two zinc (II) coordinating ligands in Nse1 RING domain. Hydrogen bonds are shown

in blue lines, metal Interactions are illustrated with purple lines. Cysteine and histidine residues that coordinate the two zinc ions are shown. D. Sequence alignment of Nse1 RING domain in different eukaryotes. The conserved residues that coordinate the zinc atoms are labeled in red. *(A, B and C. Images are created with the PDB ID and associated publication, NGL Viewer (AS Rose et al. (2018) NGL viewer: web-based molecular graphics for large complexes. Bioinformatics doi:10.1093/bioinformatics/bty419), and RCSB PDB, https://www.rcsb.org/3d-view/5WY5/1* D. (Pebernard et al., 2008 (1)).

1.5.4 Impaired Smc5/6 complex function and human diseases

The integrity and function of the Smc5/6 complex is essential for human health and survival. Mutations in some of the subunits of the complex show severe genetic disorders with different clinical characteristics. Patients carrying heterozygous mutations in *NSMCE2 (NSE2)* show microcephalic primordial dwarfism, accompanied by extreme insulin resistance and gonadal failure as well as chromosome breaks [Payne et al., 2014]. A later report showed that newborn babies with heterozygous and homozygous mutations in *NSMCE3 (NSE3)* developed chromosome breakage syndrome with progressive pulmonary disease, leading to death [van der Crabben et al., 2016]. Besides, it has been found that patients with Kabuki syndrome which is characterized with growth retardation, distinct facial appearance, skeletal and dermatoglyphic abnormalities, carry a mutation in *SMC5,* along with mutations in other genes. Thus, it is possible that impairments in Smc5/6 function contribute to some of the clinical features of this syndrome [Kuniba et al., 2009]. Moreover, the disturbed function of the Smc5/6 complex has been also associated with the processes of premature aging and carcinogenesis. *In vivo* studies in mice demonstrated that mutations in *NSMCE2* lead to accelerated aging and a high incidence of tumors. Mouse embryos with heterozygous mutations in *NSMCE2* displayed dwarfism with a loss of thymic cellularity, whereas adult mice share characteristics similar to those observed in patients with Bloom syndrome, such as severe anemia, altered pigmentation and reduced subcutaneous fat, associated with elevated levels of micronuclei. Homozygous mutations in *NSMCE2* are lethal for the organism whereas the heterozygous mutations cause a high incidence of different types of tumors in mice, due to defects in chromosome segregation and increased mitotic recombination [Jacome et al., 2015]. The strong gene conservation between mice and humans suggest that these effects can be also detected in humans with mutations in the Smc5/6 complex. In accordance with this, another recent work revealed that mutations in *SMC5* contribute to the development of brain metastases in patients with different types of cancers [Saunus et al., 2015].

On the other hand, it has been recently described that the Smc5/6 complex helps the organism to overcome the infection with hepatitis B virus (HBV), serving as a host restriction factor. HBV is a member of the Hepadnaviridae family with a small partially double stranded DNA (ds) genome. It is a major global threat leading to chronic hepatitis B, liver cirrhosis, and hepatocellular carcinoma. The virus uses reverse transcriptase from an RNA intermediate to replicate its genome in the host cell [Seeger and Mason, 2000]. During virus entry in the nucleus of the cell, the viral genome is converted to episomal covalently closed circular DNA (cccDNA), serving as a template for viral transcription. It has been found that the Smc5/6 complex recognizes and binds this episomal DNA and thus prevents viral transcription and inhibits the infection [Mitra and Guo, 2016, Decorsière et al., 2016].

Upon infection, HBV expresses a regulatory protein, called HBx which enhances viral transcription, by triggering the Smc5/6 complex for degradation by the proteasome system. The HBx protein interacts with DNA-damage binding protein 1 (DDB1), which is part of a Cullin-RING E3 ligase complex (CUL4) and targets the Smc5/6 complex for degradation. However, the mechanism of this HBx-DDB1 interaction remains unclear [Mitra and Guo, 2016, Murphy et al., 2016]. It has been found that HBx is required for viral transcription from the episomal cccDNA but not from an integrated copy in the host cell genome. Based on this observation it has been proposed that in the absence of HBx, the Smc5/6 complex interacts and inhibits only the viral episomal DNA [Mitra and Guo, 2016]. Probably, the Smc5/6 complex restricts HBV during the initial phase of the infection, before occuring the integration of viral DNA in the genome of the host cell [Furuta et al., 2018]. The molecular mechanism of the Smc5/6 complex-dependent restriction of HBV still remains unclear. It has been proposed that it may be related to the topology of the viral cccDNA and the DNA binding activity of the Smc5/6 complex [Aragón, 2018, Palecek, 2019].

OBJECTIVES

The Smc5/6 complex is essential in recombinational repair and accurate chromosome disjunction. As a component of the Smc5/6 complex, Nse1, which contains a RING domain with putative ubiquitin ligase activity, is supposed to contribute to Smc5/6 function. Despite the increasing number of investigations regarding the Smc5/6 complex and its biological role in yeast cells, the function of the complex and specifically the role of each of its components is still not well understood in both lower and higher eukaryotes. Therefore, in this doctoral thesis we aimed to reveal and characterize the role of Nse1 in DNA repair and genomic stability by using human cell lines as model systems. To achieve this goal, we defined the following objectives:

a) Generation of *NSE1* mutant cells with impaired RING domain and characterization of their phenotype.

b) Revealing if the functional interaction, identified in yeast between the Smc5/6 complex and Mph1 helicase (FANCM) is conserved in human cells

c) Identification of novel interactors of human Nse1

MATERIALS AND METHODS

3.1 Human cell lines methods

3.1.1 Cell lines and culture conditions

Human embryonic kidney (HEK293T) cell line was purchased from the American Type Culture Collection (ATCC, USA). SV-40 immortalized human fibroblasts, originally derived from a patient, carrying a *FANCM* homozygous mutation c.1506_1507insTA; p.Ile503* (FANCM knockout (KO) cells) were a gift from Prof. Jordi Surrallés, Department of Genetics and Microbiology Autonomous University of Barcelona, Cerdanyola del Vallès (UAB), Spain. *FANCM* gene expression was re-established by transduction of a lentiviral vector expressing FANCM wild-type using Tet-ON 3G expression system. HEK293T and human fibroblast cells were cultured in complete Dulbecco's modified Eagle's medium - DMEM (Gibco) supplemented with 10% fetal bovine serum (FBS), 20 units/ml penicillin and 20µg/ml streptomycin. In order to induce the expression of *FANCM* in FANCM KO cells, the antibiotic doxycycline (Dox) at a final concentration of 1µg/ml was added to the culture medium. All cell lines were mycoplasma-negative and were grown in thermostat at 37^{o}C and 5% CO_2.

3.1.2 Freezing and thawing of cells

All cell lines used were kept frozen in cryopreservation solution containing 90 % FBS and 10 % dimethylsulfoxide (DMSO) and stored at -80^{o}C or in liquid nitrogen for long term storage. Briefly, cells at a confluence of 70-80% were harvested by trypsinization with 0,25% trypsin/EDTA, counted using a hemocytometer and centrifuged for 5min at 1000 rpm. Pellet cells were resuspended in proper volume of cryopreservation solution and 1ml of cell suspension at a concentration of 1 x 10^6/ml or 2 x 10^6 cells/ml were quickly aliquoted into cryovials. For thawing cryovials were placed into a water bath at 37^{o}C for a few seconds. Then 1 ml thawed cells were diluted in 9 ml of culture medium and centrifuged for 5min at 1000 rpm. The supernatant was aspirated and pellet was resuspended with pre-warm at 37^{o}C culture medium and seeded into an appropriate culture vessel.

HEK293T cells (wild type) were passaged in a ratio of 1:10 every two-three days, whereas *NSE1* mutant cells were subcultured in a ratio of 1:5 because of their decreased doubling time by approximately half. Human fibroblasts FANCM KO and FANCM KO expressing *FANCM* WT were divided every 48 h in a ratio of 1:3 and 1:5, respectively.

3.1.3 Generation of mutations in human *NSE1* by CRISPR/Cas9 technique

Genome edition in HEK293T cell line using CRISPR-Cas9

To create human cell lines with disrupted RING domain of *NSE1*, the CRISPR-Cas9 system was used. CRISPR (Clustered Regularly Interspaced Short Palindromic Repeats)/Cas9 is a novel versatile tool for genome editing, based on the adaptive immune system of prokaryotes. The technique utilizes the Cas9-gRNA complex to bind and cleave double-stranded DNA at a specific region, creating DSBs.

First, a single guide RNA (sgRNA) sequence (fusion between tracrRNA and crRNA) was designed to target exon 7 of *NSE1* using Benchling CRISPR-sgRNA design tool (https://www.benchling.com). Then, chimeric sgRNA was cloned by annealed oligonucleotides (CYO2275 and CYO2276, Table 3) into plasmid pX458 (#48138, Addgene) containing Cas9 endonuclease, fused to enhanced Green Fluorescent Protein (eGFP). Cloning procedure was performed as described in Ran et al., 2013. The expression vector obtained, p4093 (shown in Table 2), was next used to deliver Cas9-sgRNA complex into HEK293T cells.

To generate a deletion or point mutations in the *NSE1* RING domain, two CRISPR-Cas9-based approaches were applied. The first approach is based on NHEJ repair of Cas9-induced DSBs, leading to deletions or insertions. Cells at 70-80% confluency were transfected with 1 µg of p4093, using Lipofectamine 2000 (Invitrogen), as described previously (chapter 3.3.4).

In the second approach, a specific single-stranded oligodeoxynucleotide (ssODN), CYO2295 (shown in Table 3) was used as a template to repair DSBs by homologous recombination. The donor DNA, carrying desired point mutations (c.[610_612delinsGCT; 618_620delinsAGC], p.[Cys204Ala; Cys207Ala]) was designed, according to instructions from IDT (Integrated DNA Technologies, USA), (https://eu.idtdna.com/pages/education/decoded/article/megamer-single-stranded-donor-templates-(ssdna-or-ssodns)-for-successful-homology-directed-repair-(hdr)-in-genome-editing-applications).

To increase the transfection efficiency, 1 x 10^6 HEK293T cells were transfected by nucleofection with 2,5 µg of p4093 and 0,5 µM ssODN using Nucleofector Solution V (Lonza) and program A-023 in Nucleofector I (Amaxa, Lonza). After nucleofection, cells were plated in a 6 well plate and incubated for 24h at 37°C and 5% CO_2.

After 24h, transfected cells from both approaches were observed under fluorescent microscopy for GFP signal. Cells were then trypsinized, counted and diluted in complete DMEM up to 5 cells/ml (0,5 cells/100µl). To isolate single clones, 100 µl of diluted cells were seeded in each well of 96-well plates (4 and 15 different 96-well plates were used in the first and second CRISPR-Cas9 approach, respectively). After 24 h, each well, containing one single cell, was analyzed by fluorescence microscopy. Only wells with GFP-positive cells were marked and followed for 2 weeks to obtain a monoclonal cell population. Clones that grew more rapidly were characterized as big. Clones that showed slower growth were

labeled as small or very small. Only in slow growth clones, mutations in *NSE1* were observed.

Edition analysis

To analyze obtained individual clones of both approaches for target mutations, first the genomic DNA was extracted and the genomic region surrounding the Cas9 cleavage site was amplified by PCR. To obtain genomic DNA, cells from each well were trypsinized and diluted in complete DMEM: one half of the sample was seeded again in a 24-well plate and the other half was centrifuged and diluted in 100 µl of genotyping buffer (150mM TRIS-HCl pH 8,5, NaCl 200mM, EDTA 5mM, SDS 0,2%) with 1mg/ml Proteinase K. Samples were incubated at 54^{o}C for 1 hour and then boiled at 95^{o}C for 5 min, to inactivate Proteinase K. Next, 500 µl of chilled ethanol (-20^{o}C) was added immediately to samples to precipitate DNA. After inverting 4-5 times the tube, DNA fibers could be observed and were collected by centrifugation at 4^{o}C and maximum speed for 10 min. DNA pellet was dissolved in MilliQ water and was used for the PCR amplification with primers listed in Table 3 (CYO2277; CYO2278). The PCR reaction was performed at annealing of 60^{o}C and 35 seconds for elongation, during 35 cycles and a PCR product of 826 bp was obtained.

a) Surveyor Assay

In the first approach, in order to test for genetic modifications in the *NSE1* RING sequence result of NHEJ repair, the Surveyor Assay using T7 Endonuclease I (M302, NEB) was performed. 200ng of the PCR product were mixed with NEB Buffer 2 and MilliQ water to a final volume of 19 µl. Samples were then denatured at 95^{o}C for 5 min, followed by re-annealing at decreasing temperature from 95^{o}C to 85^{o}C at -2^{o}C/second and a ramp decreasing temperature from 85^{o}C to 25^{o}C at -0.1^{o}C/second. After re-annealing, 1 µl of T7 Endonuclease I was added to PCR products and samples were incubated for 15 minutes at 37^{o}C. PCR products from untransfected with the CRISPR plasmid cells were used as controls. For heteroduplex formation, equal amounts of PCR products, amplified from transfected cells were mixed with PCR products, obtained from untransfected cells. After denaturation and re-annealing, heteroduplexes were digested or not with T7 Endonuclease. PCR products were separated on 1% agarose gels and indels were detected by the positive cleavage of T7 Endonuclease I: the 826 bp band should be cleaved into two smaller bands around 400 bp each one. Details of this analysis are explained in results section.

b) Restriction analysis

For detecting incorporated point mutations in *NSE1* RING sequence by the ssODN in the second HDR-based approach, a restriction analysis was conducted. PCR products were restricted with PvuII enzyme for 1 hour at 37^{o}C and analyzed by electrophoresis on 1% agarose gels. If both strands contain the point mutation, two bands of 384 bp and 306 bp would be observed. Details of this analysis are explained in results section.

3.1.4 Transient transfections of human cells

Transfection experiments were performed by two different transfection protocols using polyethylenimine (PEI) (408727, Sigma) or Lipofectamine 2000 (Invitrogen). For PEI transfection method, human cell lines (HEK293T) were seeded in 60 mm plates, previously coated with collagen (100µg/ml) in order to enhance cell adhesion and let them grow overnight at 37^{o}C and 5 % CO_2. After 24 h, cells were washed with 2 ml Opti-MEM I reduced serum media (Gibco) and then the medium was replaced by the previously prepared mixture of plasmid DNA and PEI in a ratio: 1µg :10µl, diluted in Opti-MEM I reduced serum media, vortex-mixed and incubated for 10 min at RT. The transfected cells were incubated for 45 min in the incubator at 37^{o}C and 5 % CO_2. After incubation, the Opti-MEM I reduced serum media was changed with a fresh normal culture medium (DMEM, supplemented with 10 % FBS, streptomycin and penicillin) and cells were incubated overnight for overexpression of the target gene.

Lipofectamine 2000 transfection method was performed according to the manufacturer's instructions. Similar to the PEI method, cells were seeded in plates, previously coated with collagen (100µg/ml) and incubated for 24 h. Before transfection with Lipofectamine, a normal culture medium without antibiotics (DMEM with 10% FBS) was added to cells and they were incubated at 37^{o}C and 5 % CO_2 during the preparation of the transfection mixture (DNA:Lipofectamine). After 5 min incubation at RT, DNA and Lipofectamine in a ratio 1µg :1µl, diluted in Opti-MEM I reduced serum media were added drop by drop onto cells. The plates were incubated for 24 h. The overexpression of the target genes was assessed by Western blot analysis, using specific antibodies shown in Table 5.

3.1.5 Lentiviral production and transduction for stable cell line generation

For generation of stable cell lines downregulated for a target gene, a lentiviral vector packaging system 3rd generation was used. Lentiviral particles were produced by co-transfection of HEK293T cells with PEI and opti-MEM. 3 x 10^5/ml cells were plated in a 100 mm plate, previously coated with collagen (100µg/ml) and let to obtain good adherent monolayer for 24 h at 37^{o}C and 5% CO_2. After incubation, cells were co-transfected with 12 µg pLKO.1-Neo, containing controlshRNA or Smc5shRNA, 6 µg envelope plasmid pVSV-G and 6 µg packaging plasmid pMDLg/pRRE using polyethylenimine (PEI) standard transfection protocol. After 48 h, the produced lentiviruses were harvested, filtered through a 0.45 µm syringe filter and stored at -80^{o}C. For lentiviral transduction SV40-transformed FANCM knockout (KO) and FANCM KO with expression of *FANCM* wild type human fibroblasts derived from a patient were seeded in 60 mm plates at a concentration of 5 x 10^5/plate. 2.5 ml of viral supernatant and 2.5 ml culture medium (DMEM + 10% FBS, P/S) were added directly to cells, along with polybrene at a concentration of 8 µg/ml in order to increase the binding between the lentiviral envelope and plasma membrane. After 24 h the

medium containing polybrene was changed and after 48 h, cells were split and selected for 5-10 days with Neomycin at a concentration of 800 µg/ml. The downregulation efficiency of *SMC5* was detected by Western blot analysis.

3.1.6 Cell proliferation analysis using trypan blue exclusion assay

For analysis of proliferation rate and cell viability, HEK293T (wild type), *NSE1-ΔR* mutants, *nse1* double and single point mutant cells and *NSE1-ΔR* mutants with ectopic expression of wt *NSE1* were seeded at a concentration of 1 x 10^5/ml (only viable cells) in 6 well plate. Cells were cultured in DMEM with 10% FBS, penicillin and streptomycin and incubated at 37 ^oC and 5% CO_2. The cell proliferation was followed during 3 days and analyzed under light microscopy using trypan blue exclusion assay. Trypan blue assay can directly distinguish the viable and dead cells. The method is based on the ability of the dye to pass through the compromised cell membranes, entering in cytoplasm and staining only the dead cells in blue. The viable cells with intact membranes are impermeable for the dye and remain unstained. After trypsinization and centrifugation at 1000 rpm for 5 min, cell suspensions were diluted with 0.4% trypan blue solution (T8154, Sigma) in ratio 1:1 and incubated for 5 min. Cells were counted with a haemocytometer counting chamber after 24h, 48h and 72h. The growth curve graphs are representative from three independent experiments.

3.1.7 Detection of apoptosis by double-staining with acridine orange and ethidium bromide (AO/EB)

For detection of apoptosis by evaluating the nuclear morphology using acridine orange and ethidium bromide (AO/EB) live staining, HEK293T (wild type) at a concentration of 4 x 10^4 cells per well and double point mutant cells (*NSE1-AA*) at a concentration of 1.2 x 10^5 per well, were grown onto coverslips (12mm in diameter), coated with collagen (100µg/ml) into 24 well plates. Only viable cells were seeded using trypan blue exclusion assay. After 24 h of incubation at 37^oC and 5% CO_2, cells were washed once with PBS and stained with a mixture of fluorescent dyes acridine orange (AO) (A6014-10G, Sigma) 10 µg/ml and ethidium bromide (EB) (32813, USB) 10 µg/ml (1:1), diluted in PBS. The stained cells were immediately observed under fluorescent microscope Olympus IX71 and camera DP70, within 30 minutes, before the color started to fade. The principle of the technique is based on the ability of AO to pass through plasma membranes of viable and early apoptotic cells, staining the cells in green. In contrast, EB can cross only the plasma membrane of late apoptotic and necrotic cells, whose integrity is compromised and stains the cells in orange to red. The nuclei of viable cells with intact cell membrane are stained in dark green, whereas the early apoptotic cells show bright green nucleus with condensed chromatin and membrane blebbing. The late apoptotic cells show orange nucleus with chromatin fragmentation, whereas the necrotic cells display orange shrinkage nucleus without DNA fragmentation.

3.1.8 Time-lapse microscopy

To assess cell cycle progression by time-lapse video microscopy, HEK293T (wild type) at a concentration of 6 x 10^4 cells and *NSE1-ΔR* mutants with a concentration of 8 x 10^4 cells were plated in collagen (100µg/ml) coated 35µm µ-dish (ibidi high). Cells were cultured in Dulbecco's modified Eagle's medium (DMEM), (Gibco) supplemented with 10% fetal bovine serum (FBS), 20 units/ml penicillin and 20µg/ml streptomycin. After 48 hours cells (~60% confluent) were transfected with mCherry-H2B for chromatin labelling using PEI and OptiMEM (according to a standard protocol, previously described). After 24 hours, the transfection efficiency was ~50% and cells were analyzed by time-lapse imaging for 48 hours, due to the slower growth of mutant cells. Cells were monitored by confocal microscope Olympus FV1000 equipped with 37^{o}C and 5%CO_2 chamber. Six fields were examined for each cell line and each microscope image was acquired every 10 min using 20X objective. The cell cycle progression of transfected cells was unable for measuring/tracking due to cell death in wild type and mutant cells after mCherry-H2B expression. In non-transfected wild type and mutant cells only the mitosis duration could be measured based on the specific morphological characteristics of mitosis. The duration of mitosis was quantified by using ImageJ Software (NIH, USA). The result is representative of counting cells from three different fields.

3.1.9 Immunofluorescence for detection of BLM foci

BLM foci formation was determined by immunofluorescence analysis according to a previously described protocol (Chan et al., 2018). HEK293T (wild type), *NSE1-ΔR* mutants and double point mutant cells (*NSE1-AA*) were cultured in Dulbecco's modified Eagle's medium (DMEM), (Gibco) supplemented with 10% fetal bovine serum (FBS), 20 units/ml penicillin and 20µg/ml streptomycin, and seeded onto coverslips, coated with collagen (100µg/ml) in six well plates. After 24h, cells were fixed with PTEMF buffer (20 mM PIPES pH 6.8, 0.2% Triton X-100, 1 mM $MgCl_2$, 10 mM EGTA and 4% paraformaldehyde) for 10 min. After incubation, cells were washed once with PBS and permeabilized with 0.2 % Triton X-100 diluted in PBS for 5 min. After washing with PBS, cells were blocked with 3% BSA in PBS for 30 min and incubated with primary antibody rabbit anti-BLM (1:1000, Abcam ab2179), diluted in 3% BSA in PBS for 1h. After washing with PBS twice, cells were stained with the secondary antibody Alexa Flour 488 goat anti-rabbit (1:1000) diluted in 3% BSA in PBS for 1h. Cells were washed twice with PBS and stained with DAPI (5µg/ml) (D-9542, Sigma) for nuclei visualization for 10 min. in dark at RT. The coverslips were washed once with PBS and mounted with Mowiol. The microscopic images were examined under a fluorescent microscope Zeiss Axio Observer microscope Z1 with 60X objective. The BLM foci were counted by ImageJ Software (NIH, USA). More than 200 cells were counted in each cell line. Results are representative of two (for *NSE1-AA*) and three (for *NSE1-ΔR* mutants) independent experiments.

3.1.10 Micronuclei analysis

HEK293T (wild type) at a concentration of 1.5 x 10^5 cells, *NSE1-ΔR* mutants and double point mutant cells (*NSE1-AA*) with a concentration of 3 x 10^5 cells were seeded in 6 well plate, on coverslips coated with 100µg/ml Collagen (diluted in 0,02N acetic acid). After 48h, cells were washed with PBS and fixed with 4% paraformaldehyde (PFA) in PBS buffer for 20 min. at RT. After fixation, samples were washed twice with PBS and permeabilized with 0.1% Triton X-100 (diluted in PBS) for 5 min. The permeabilized cells were washed twice with PBS and stained with DAPI (5µg/ml) for 10 min. at the dark. Then, samples were washed once with PBS, mounted with Mowiol (20µl per slide) and covered with coverslips. The glass slides were observed directly or kept at 4^{o}C. The nuclei and micronuclei were observed using fluorescent microscope Olympus IX. Micronuclei were counted by ImageJ Software (NIH, USA).

3.1.11 Sister chromatid exchange assay (SCE)

SCE is a useful sensitive method for detection of recombination activity and chromosome instability. For visualization of SCE, HEK293T (wild type) and *NSE1-ΔR* mutants have been incubated with BrdU (Sigma) at a concentration of 50µM for two cell cycles. The duration depends on the proliferation rate of tested cell lines (32h for HEK293T and 72h for *NSE1-ΔR* mutants, respectively). Cells were blocked at metaphase with KaryoMAX Colcemid (0.05µg/ml) (Thermo Fisher Scientific) for 2 hours. After washing with PBS, cells were trypsinized, centrifuged and exposed to hypotonic shock with 0,03M sodium citrate for 25 min at 37^{o}C. Chromosomes were fixed with a solution of methanol and acetic acid 3:1 and metaphase spreads were prepared onto glass slides. Metaphase chromosome spreads were stained with 0.1mg/ml acridine orange (Sigma), diluted in distilled water and incubated for 5 min. at RT. The stained slides were carefully rinsed with distilled water, incubated for 1 min in Sorenson buffer pH 6,8 (0.1 M Na_2HPO_4, 0.1 NaH_2PO_4) and mounted with Mowiol. The slides with metaphase spreads were immediately observed under fluorescent microscope Olympus BX51 using a filter with the wavelength range (467 – 556nm). The number of reciprocal exchange events per chromosome was quantified. More than 2000 chromosomes were counted in each sample. SCE events were quantified using ImageJ software (NIH, USA).

3.1.12 Clonogenic survival assay

For analyzing the drug sensitivity, wild type cells, truncated *NSE1* mutants, and truncated mutant cells with ectopic expression of *NSE1,* were left untreated or exposed to methyl methanesulfonate (MMS), a DNA alkylating agent, at a dose of 250µM, for 2 hours at 37^{o}C. After removing the drug, cells were trypsinized, counted and replated (500 cells/well) in a 12 well plate and let them grow for 10 days. After 10 days, the obtained colonies were fixed with 10% formalin solution (Sigma) in PBS 1x for 30 min., and stained with 0,01% crystal

violet diluted in milliQ water for 30 min. Excess of stain solution was removed by washing with milliQ water. The clonogenic signal intensity was measured using ImageJ Software (NIH, USA).

3.1.13 Cell cycle analysis with propidium iodide (PI)

For cell cycle analysis by DNA content measurement, 1 x 10^6 cells were washed twice with PBS and fixed with cold 70% ethanol for 24 hours. After washing with PBS two times, cells were centrifuged and DNA content was stained by incubating pelleted cells with 50µg/ml propidium iodide (PI) (P-4170, Sigma) and 50µg/ml RNase A (Invitrogen) diluted in PBS for 15 min at 37^{o}C. Samples were analyzed by Flow Cytometer FACS - Canto II (Becton Dickinson).

3.1.14 Cell cycle analysis with double staining with PI and BrdU and MPM-2 detection

For double-staining flow cytometry exponentially growing cells (80% confluent) were treated or not (used as a control) with bromodeoxyuridine (BrdU) at a concentration of 10µM for 30 min. at 37^{o}C. Cells were harvested, along with the supernatant. Then they were centrifuged and fixed with 70% cold ethanol for 24 hours at -20 ^{o}C. After centrifugation and washing with PBS-T (PBS 1x with 0.05% Tween20) to remove the traces of ethanol, pelleted cells were treated with 2M (2,16M) HCl with 0,1 Triton X-100 for DNA denaturation and incubated for 15 min at RT. Then, the HCl was neutralized with 100mM $Na_2B_4O_7$ (pH 8.5). After centrifugation, cells were washed with PBS-T and centrifuged again. The obtained pellets were resuspended and blocked with 3% BSA with PBS-T for 45 min. Next, after centrifugation, pelleted cells were incubated with anti-BrdU (1:250) and anti-MPM-2 (1:250) antibodies for 1 hour at RT (rotating at a rolling machine). Samples were washed with PBS-T, spin for 2 min at 3000rpm and incubated with secondary Alexa Fluor 647 anti-mouse (1:400) and Alexa Fluor 488 anti-rat (1:500), respectively for 45 min in dark. After incubation, cell pellets were washed with PBS-T and stained with propidium iodide (PI) (1% PI with 0,1µg/µl RNase in PBS) and then subjected to flow cytometry analysis for measuring total DNA content (PI), S phase (BrdU) and mitotic cells (MPM-2). The results are representative of three repeats. The double-staining flow cytometry was performed in the laboratory “Signaling and checkpoints of cell cycle” headed by Prof. Dr. Neus Agell, Department of Biomedical Sciences, Faculty of Medicine and Health Sciences, University of Barcelona, Spain.

3.1.15 DNA fiber technique for analysis of fork progression and dynamics

For DNA fiber analysis 8 x 10^4 cells per well for HEK293T and *NSE1-ΔR* mutants with re-expressed *NSE1* and 1.6 x 10^4 cells per well for *NSE1-ΔR* mutants were plated in 12 well-plate, previously coated with collagen (100 μg/ml in 0,02N sodium azide) for better adhesion. Cells were left unlabelled or pulse-labelled with CIdU (25μM) for 30 min., washed with pre-warmed at 37 ^{o}C PBS 1x and labelled or not with IdU (250μM) for 30 min. Cells were washed three times with cold PBS and harvested by trypsinization. Labelled and unlabelled cells were mixed 1:1 for dilution of the sample. After centrifugation, the pelleted cells were resuspended with 200μl cold PBS. Then, 4μl of cell suspensions were added quickly onto a glass slide and mixed with 8μl of spreading buffer (0,5% SDS, 200mM Tris-HCl pH 7,5 and 50mM EDTA). After 2 min. incubation, the glass slides were tilted at 15^{o} angle. Then, the slides were incubated 2-5 min, in order the drop to flow along the slides and DNA fibers to be stretched onto slides. The obtained DNA fibers were quickly dried for 10 min. and fixed with methanol/acetic acid 3:1 for 10 min. After fixation, slides were washed three times with PBS 1x and DNA fibers were denatured with 2,5M HCl for 80min. at RT. Then, fibers were washed four times with PBS and blocked with a blocking buffer (1%BSA, 0,1% Triton X-100 and 1x PBS) for 45 min. DNA spreads were incubated with rat anti-BrdU antibody (Abcam Ab6326) which recognizes CIdU (1:1000 in blocking buffer) and mouse anti-BrdU antibody (BD Biosciences, clone B44) which identifies IdU (1:200), diluted in blocking buffer. The red and green DNA tracks were detected after 1 hour incubation with the secondary fluorochrome-conjugated antibodies – Alexa Fluor anti-rat 555 (1:500) and Alexa Fluor anti-mouse 488 (1:500) diluted in blocking buffer. Slides were washed five times with PBS, quickly dried onto a paper and mounted with Mowiol (50μl per slide), covered with coverslips (24x60mm) and after 2 hours sealed with nail polish. DNA fibers were observed immediately under laser scanning confocal microscope Zeiss LSM 880. The progression and dynamics of replication forks were measured by ImageJ Software (NIH, USA). The statistical analysis was implemented by GraphPad Prism Software using Mann-Whitney test to evaluate statistical significance (*$p<0.05$, **$p<0.01$ and ***$p<0.001$). The results are representative of three independent experiments. The DNA fiber technique was carried out in the laboratory “Signaling and checkpoints of cell cycle” headed by Prof. Dr. Neus Agell, Department of Biomedical Sciences, Faculty of Medicine and Health Sciences, University of Barcelona, Spain.

3.2 Methods using yeast cells

3.2.1 Yeast strains

All yeast strains (*Saccharomyces cerevisiae*) used in this thesis are presented in Table 1.

Table 1. Yeast strains

Strain	Genotype	Procedure
Y3628	*MATa, trp1-901, leu2-3, 112, ura3-52, his3-200, gal4D, gal80D, LYS2::GAL1UAS-GAL1TATA-HIS3, GAL2UAS-GAL2TATA-ADE2 URA3::MEL1UAS-MEL1TATA -lacZ MEL1*-pGBKT7 (TRP1)	Strain YNC3628 was created by transforming AH109 strain with an empty pGBKT7 plasmid.
Y3629	*MATa, trp1-901, leu2-3, 112, ura3-52, his3-200, gal4D, gal80D, LYS2::GAL1UAS-GAL1TATA-HIS3, GAL2UAS-GAL2TATA-ADE2 URA3::MEL1UAS-MEL1TATA -lacZ MEL1*pGBKT7 (TRP1)-hNSE1 (*NSMCE1*)	Strain YNC3629 was created by transforming AH109 strain with plasmid pGBKT7 expressing *NSMCE1.*
Y3632	*MATα ura3-52, his3-200, ade2-101, trp1-901, leu2-3, 112, gal4Δ, met−, gal80Δ, URA3::GAL1UAS-GAL1TATA-lacZ* pACT2 (LEU2)	Strain YNC3632 was created by transforming Y187 strain with pACT2

3.2.2 Yeast two hybrid assay

For the identification of new putative interactors for human Nse1, a standard yeast-two-hybrid (Y2H) screen was performed, using the Matchmaker GAL4 Two-Hybrid System 3 protocol (Clontech). The principle of this method is based on the interaction between the "bait" protein, which is fused to DNA-binding domain (DNA-BD) and library "prey" proteins, fused to activation domain (AD) of the GAL4 transcription factor. The interaction brings BD and AD into close proximity and activates transcription of reporter genes. Human *NSMCE1*

cDNA was cloned into pGBKT7 vector and used as “bait”, whereas cDNA libraries from a mouse embryo (11-day) were cloned into pGADT7 vector and used as “prey”. Human *NSMCE1* ORF was amplified by PCR using primers (CYO2130) and (CYO2131), shown in Table 3. The plasmids encoding bait and prey proteins were transformed into AH109 and Y187 yeast strains, respectively. To detect interactions both plasmids were introduced into one single cell by mating two haploid yeast strains from the opposite mating types. A haploid strain (MATa) expressing the fusion bait protein was mated with haploid strains (MATα) expressing cDNA library prey proteins. For mating, 50 ml of AH109 strain carrying pGBKT7-*NSMCE1* ORF were grown on synthetic complete medium (SC) lacking tryptophan (Trp) overnight at 30 ^{o}C. In addition, 50 ml of Y187 strain carrying empty pGADT7 vector were grown on SC, lacking leucine (Leu) and were used as a negative control. The bait and negative pre-cultures were first diluted and then grown to 2 OD_{600} in yeast extract peptone glucose (YPD) supplemented with adenine (Ade). The bait culture (10^{9} total cells) were thoroughly mixed with the prey library and incubated at 30^{o}C for 20-24 hours, at 30 rpm shaking velocity. Negative control cells were mixed with bait strains and incubated in the same conditions. After mating, diploid zygotes expressing both the bait and prey plasmids were grown in a selective medium (SC), supplemented with Ade and lacking Leu, Trp and histidine (His).

In parallel, to estimate the mating efficiency, $10^{-3}$and 10^{-4} dilutions were prepared and 100 µl of each dilution were plated in SC agar plates with Ade, lacking Trp and Leu . After incubating for 3 days at 30^{o}C, the mating efficiency was calculated by counting the number of colonies. The efficiency was found to be 7.1%, which was high enough for a successful Y2H screen. Before screening, the self-activation background of the *HIS3* reporter gene in GAL4 system was determined using different concentrations of 3-Amino-1,2,4-Triazol (3-AT) (Sigma). 3-AT is an inhibitor of *HIS3* gene product that allows selection for specific interactions. The minimal inhibitory concentrations of 2mM and 5 mM 3-AT that suppress growth on histidine-deficient medium were selected as the optimal ones. After 5-6 days of selection for Nse1 specific interactors, bigger colonies were picked up and grown under low stringency conditions (SC-His-Leu-Trp + 2 mM 3-AT) for 2-3 days. Then, colonies were replica-plated in selective plates, lacking His with 5mM and 10mM 3-AT and in high stringency plates, lacking both His and Ade (SC-His-Leu-Trp-Ade + 5 mM 3-AT, SC-His-Leu-Trp-Ade + 10 mM 3-AT) in order to select only the strong interactors.

To identify the potential candidates, library plasmid DNA was isolated from positive clones and amplified by PCR using specific primers 5’AD (CYO847) and 3’AD (CYO637), listed in Table 3. PCR reaction was performed using SupraTherm Taq DNA Polymerase (GeneCraft). Positive PCR fragments were subjected to sequencing and analyzed using the BLAST database (https://blast.ncbi.nlm.nih.gov).

Overall, from 194 positive clones analyzed, 27 clones were classified as strong interactors, and from them, only 17 clones were in the correct reading frame. After DNA sequencing, 10

different genes were identified. Potential new interactors for NSE1 were first validated in yeast and then confirmed in human cells.

a) Confirmation of positive interactions in yeast

To confirm the positive interactions detected in the Y2H screen, the library plasmids isolated from Y2H diploid yeasts were co-transformed in AH109 strain with the pGBKT7-hNse1 plasmid or pGBKT7 empty vector. The transformants were then grown on (SC-Leu-Trp), (SC-Leu-Trp-His + 10 mM 3-AT), and (SC-Leu-Trp-His-Ade) plates and incubated for 2-3 days at 30^{o}C. Only clones grown on SC without adenine were selected and sequenced. From them, six were confirmed as specific interactors for *NSE1*. Amino acid sequences were compared against the mouse (Mus musculus) protein sequence database using BLAST alignment. UniProt database (https://www.uniprot.org/uniprot/) was used for identification of protein names and function.

b) Confirmation of positive interactions in human cells

To verify positive interactors in human cells, a co-immunoprecipitation (Co-IP) technique was performed using HEK293T cell line. Briefly, inserts from potential candidates were cloned into pNBM470 expression vector, allowing N-terminal tagged proteins with a 6HA epitope. . The new constructs were then transformed into *E. coli* DH5-alpha and different clones were analyzed by sequencing. Only two candidates, HMG-17 and TRUSS were used for *in vivo* experiments. HEK293T cells were seeded in 6 well plates and transfected with 2 µg of plasmid, expressing the Y2H candidates tagged with HA (p4016 and p4018) and 2 µg of plasmid, expressing Nse1 tagged with GFP at the N-terminus (p3853), using PEI polymer. Co-immunoprecipitation procedures were carried out as described in (chapter 3.6.1) using anti-HA agarose beads. Proteins were detected by immunoblot using polyclonal anti-human Nse1 (NSE1) and monoclonal anti-HA antibodies (shown in Table 5).

3.3 Bacterial methods

3.3.1 Plasmids

The plasmids used in this thesis are listed in Table 2.

Table 2. Plasmids.

Name	Description	Source
p2111	pLKO-Puro-TRC2 scramble shRNA	MISSION shRNA

p2323	pH2B-mCherry	EUROSCARF
p3567	pGBKT7-human *NSE1*	This study
p3573	pLKO1-Puro shRNA human SMC5 TRCN0000147918	MISSION shRNA
p3854	pEGFP-C1-human *NSE1*	This study
p3935	pCbetaS plasmid with 3HA epitope	MD Cole' lab
p3936	pCbetaS-3HA-*TRUSS* 1-797 (full length)	MD Cole' lab
p3937	pCbetaS-3HA-*TRUSS* 73-797	MD Cole' lab
p3938	pCbetaS-3HA-*TRUSS* 1-383	MD Cole' lab
p3939	pCbetaS-3HA-*TRUSS* 73-537	MD Cole' lab
p3940	pCbetaS-3HA-*TRUSS* 539-797	MD Cole' lab
p3941	pCbetaS-3HA-*TRUSS* 1-147	MD Cole' lab
p3942	pCbetaS-3HA-*TRUSS* 73-283	MD Cole' lab

p3943	pCbetaS-3HA-*TRUSS* 73-284	MD Cole' lab
p3944	pCbetaS-3HA-*TRUSS* 73-311	MD Cole' lab
p3957	pCMV6-*Ndln2* (Myc-DDK) (*NSE3*)	OriGene Technologies
p3981 (pX458)	pSpCas9(BB)-2A-GFP	Addgene
p4093	pX458+sgRNA human *NSE1* on exon 7	This study
p4224	pEGFP-C1-human *NSE1* 183-266 (Cter)	This study
p4227	pEGFP-C1-human *NSE1* 1-187 (Nter)	This study
p4269	pLenti CRISPR v2-Puro	Addgene
p4539	pLVX-tre3G-*FANCM*	Jordi Surrallés' lab
p4595	pLenti EF1alpha promoter-human *NSE1*	This study
p4589	pLKO1-Neo shRNA human *SMC5*	This study

p4706	pLKO1-Neo shRNA Scramble	This study
p4787	pLVX-CMV promoter-human *NSE1*	This study
p4988	pEGFP-C1-human *NSE1-AA* (C204A C207A)	This study
p4997	pEGFP-C1-human *NSE1* 183-266 (Cterminal)-AA (C204A, C207A)	This study

3.3.2 Transformation into competent E.coli cells

Plasmid DNA was transformed into competent DH5α cells (Thermo Fisher) by a heat shock method. Briefly, 50 µl competent cells were gently mixed with 1-5 µl plasmid DNA and incubated on ice for 30 min. After incubation, cells were heat shocked at 42^{o}C for 20 sec. and immediately incubated on ice for 2 min. Then, 1 ml of LB media was added and samples were incubated at 37^{o}C for 1 hour. After short spin for 1 min., pellet cells were resuspended in 150 µl LB media and plated on LB agar plates, supplemented with the required antibiotic for plasmid selection.

3.3.3 Plasmid Jet Prep (phenol-chloroform DNA extraction)

For screening of positive clones after bacterial transformation a phenol-chloroform method (Jet Prep) was used. Briefly, six colonies from each transformation were picked up and dissolved in 100 µl distilled water. After short spun at 8000 rpm for 1 min., 50 µl BT buffer (2% Triton X-100, NaOH pH 12.4) was added to the pellet cells, followed by the addition of 50 µl phenol-chloroform mixture. Samples were then mixed well by shaking and centrifuged at 13000 rpm for 5 min. Then, 5 µl of supernatant, containing DNA were mixed with FLB (25% Bromophenol Blue, 0.25% xylene cyanol, 25% ficoll-400) loading buffer and loaded onto 0.8% agarose gel, along with the original plasmid used as a control. The positive clones were selected by comparing the sizes of mutated plasmids and original plasmid.

3.4 Nucleic acid methods

3.4.1 RNA isolation, cDNA synthesis and Real-time PCR (RT-PCR)

For analysis of relative mRNA expression levels of *NSMCE1*, quantitative RT-PCR was used. First, total RNA was isolated from HEK293T cells (wild type), truncated nse1 mutant cells, double and single point mutant cells using an RNeasy Mini kit (Qiagen, Germany) according to the manufacturer's instructions. The cDNA synthesis was performed with SuperScript Reverse Transcriptase (Invitrogen). Briefly, 1 µg of total RNA was diluted in miliQ water, combined with random hexamers (Invitrogen) and 10 mM dNTP, and incubated at 65^{o}C for 5 min. Samples were chilled on ice for 15 min, short spun down and 4 µl of 5x First Strand buffer (Invitrogen), 2 µl 0,1M DTT (Invitrogen) and 1 µl RNaseOUT (Invitrogen), for mRNA protection were added to the reaction. Samples were then incubated at 25^{o}C for 10 min and heat shocked at 42^{o}C for 2 min. After incubation, 1 µl SuperScript Reverse Transcriptase was added and reverse transcription was carried out at 42^{o}C for 50 min, followed by 15 min incubation at 70^{o}C. cDNA samples were stored at -20^{o}C. The specific primers for RT-PCR designed by software Primer3 (version 0.4.0) are indicated in the list of primers (CYO2372, CYO2373). The PCR reactions were performed using SYBR select Master Mix (Applied Biosystems). The PCR cycling conditions were as follows: uracil DNA glycosylase (UDG) activation at 50^{o}C for 2 min., followed by activation of the SureStart Taq DNA polymerase at 95oC for 2 min., 40 cycles of denaturation at 95^{o}C for 15 sec., annealing at 55^{o}C for 15 sec., extension at 72^{o}C for 1 min. The mRNA expression levels were measured using Bio-Rad CFX-96 real-time PCR detection system. Relative mRNA quantification was calculated using the ΔΔCq method [Haimes, 2014]. The mRNA levels of *NSE1* were normalized against β-actin mRNA levels. Three independent experiments were carried out per each cell line.

3.4.2 Site-directed mutagenesis (SDM)

Site-directed mutagenesis was used to generate RING domain and N-terminal deletions in human *NSE1*. Both types of mutations were introduced by PCR using QuikChange II Site-Directed Mutagenesis Kit (Agilent Technologies) with some modifications. The PCR primers with specific mutations - (CYO2291, CYO2292 and CYO2293, CYO2294) are shown in the list with primers (Table 2). The PCR reaction was performed using Phusion DNA polymerase (New England Biolabs) and 100ng/µl of template DNA. The same PCR mixture without DNA polymerase was used as a control. The thermal cycles were as follows: denaturation at 98^{o}C for 3 min, followed by 20 cycles at 98^{o}C for 10 sec, 58^{o}C for 15 sec., 72^{o}C for 4 min. The final elongation was performed at 72^{o}C for 7 min. The efficient mutagenesis was verified by 0.8 % agarose-gel electrophoresis. The PCR-SDM products were purified using QIAquick PCR purification kit (Qiagen) and then ligated using Rapid DNA ligation Kit (Roche). Ligated PCR products have been digested by DpnI, which cleaves only non-mutated and methylated parental DNA. Finally, the DpnI digested products were transformed in 50 µl DH5α competent cells and plated on LB agar plates, supplemented with 100 µg/ml kanamycin.

The efficiency of the transformation was checked by isolation of plasmid DNA from E. coli using a Jet Prep protocol (six clones from each transformation were tested). The plasmid DNA was purified by QIAprep Spin Miniprep Kit (QIAGEN) and digested by NdeI for identification of the mutated clones. Two positive clones were then transfected into HEK 293T cells using Lipofectamine 2000 (Invitrogen) and the expression of mutated Nse1 proteins was analyzed by Western blot.

3.4.3 Agarose-gel electrophoresis

Agarose-gel electrophoresis was used for separation of DNA by size using 0,8-1,5% agarose gels, depending on the sizes of DNA fragments. The different concentrations of gels were prepared by mixing of agarose powder type D1 low EEO (Pronadisa) with 1x TAE buffer and boiled in a microwave for around 1 min., until the agarose if fully dissolved. The prepared solution was poured into a gel caster and the gel was allowed to solidify for 30 min. Then, 1-2 µl of DNA were mixed with FLB loading buffer (25% Bromophenol Blue, 0.25% xylene cyanol, 25% ficoll-400) and the samples were loaded on the gel electrophoresis, performed in 1x TAE buffer (40 mM Tris-HCl, 20 mM acetic acid, 1 mM EDTA, pH 8.0), constant voltage (100 V) and 400mA for 30-40 min or more depending on the size of the gel. In order to visualize DNA the gel was stained with the fluorescent dye ethidium bromide (EtBr) for 10-15 min and observed under a UV transilluminator system.

3.4.4 Primers

The list of primers used in the thesis is shown in Table 3.

Table 3. Primers.

Number	Description	Sequence
CYO2130	Forward primer human *NSE1*, EcoRI and NdeI	GGAATTCCATATGCAGGGCAGCACAAGGAGAATGGGCGTCATGACTGATG
CYO2131	Reverse primer human *NSE1*, BamHI	CGGGATCCAGCAGGGCACGATGGCTAATG
CYO2291	Forward primer for RING domain deletion in human *NSE1*	ATGCCATCGTGCCCTGCTGGATCC

CYO2292	Reverse primer for RING domain deletion in human *NSE1*	ATGTCACGTCTCCCGGATGTATTGCTC
CYO2293	Forward primer for N-terminal deletion in human *NSE1*	ATGTACCCCGACGCGGTGAAGATC
CYO2294	Reverse primer for N-terminal deletion in human *NSE1*	ATGAGCTCGAGATCTGAGTCCGGA
CYO2396	Forward primer pLKO1-NeoR	TTCTTGACGAGTTCTTCTGACGCCCGCCCCACGACCCGCA
CYO2397	Reverse primer pLKO1-NeoR	AATCCATCTTGTTCAATCATGGTAAGCTCCGGTGGATCCC
CYO2398	Forward primer NeoR-pLKO1	GGGATCCACCGGAGCTTACCATGATTGAACAAGATGGATT
CYO2399	Reverse primer NeoR-pLKO1	TGCGGGTCGTGGGGCGGGCGTCAGAAGAACTCGTCAAGAA
CYO847	Forward primer for pGADT7-Rec cDNA (5'AD Sequencing primer SHORT)	CTATTCGATGATGAAGATACCC
CYO637	Reverse primer for pGADT7-Rec cDNA (3'AD Sequencing primer)	AGATGGTGCACGATGCACAG

Primers used for RT-PCR analysis		
CYO2372	Forward primer human *NSE1*	CATGGCGTGCTAGAGGAATG
CYO2373	Reverse primer human *NSE1*	TTGTTGATGAAGTCCTCCAACTT
hACTBF	Forward primer human β-actin gene	GCACAGAGCCTCGCCTT
hACTBR	Reverse primer human β-actin gene	GTTGTCGACGACGAGCG
CYO2686	Forward primer human *FANCM*	AGATCGAGGCTTGCTACCAG
CYO2687	Reverse primer human *FANCM*	GCACTCTCTTACTGCACCATATT
Primers used for CRISPR-Cas9 technique		
CYO2275	sgRNA Forward primer human *NSE1* BbsI site cloning	CACCGTAAGTGCATCCTGATCCCAC
CYO2276	sgRNA Reverse primer human *NSE1* BbsI site cloning	aaacGTGGGATCAGGATGCACTTAC
CYO2277	Forward primer human *NSE1* (31378), genomic DNA	CGGAGTTTCTGGGACAAAGTGC

CYO2278	Reverse primer human *NSE1* (32182), genomic DNA	GCAGAGTTAGCCCCAGTTCAGA
CYO2295	ssODN, human *NSE1* encoding C204A, C207A mutations	GCCCATTTCCCTTGTGGCTTCCCCGGAGGTTTGCAGAACAT GGAGGTGTGCACCAGCTCCGCCGTCATTGGCCTTTCCTGTT TCAGGGTCAAAGCGCTGAAACAGCTGGGATCAGGATGCAC TTACCCTGCGTGGCCAAGTACTTCCAGTCGAATGCTGAACC GCGCTGCCCCCACTGCAACGACTACTGGCCCCACGAG

3.4.5 Short hairpin and small interfering RNAs (shRNA and siRNA)

Table 4. Short hairpin RNAs (shRNAs) and small interfering RNAs (siRNAs)

shRNA and siRNA used for gene silencing		
Gene	**Target sequence**	**Source**
SMC5	GAGGTGAAAGAAGTGTTTCTA	MISSION shRNA TRCN0000147918, verified
FANCM	AAGCUCAUAAAGCUCUCGGAA	siRNA sequence from Castella et al., 2015

3.4.6 DNA sequencing

DNA sequencing was conducted by StabVida (Portugal) through the Scientific and Technical Service of Proteomics and Genomics (SCT-P&G) of the University of Lleida, Spain.

3.5 Protein methods

3.5.1 Immunoprecipitation

For immunoprecipitation (IP), co-transfected human HEK293T cells with indicated plasmids, were washed twice with ice-cold PBS 1x and 2 mM phenylmethylsulfonyl fluoride (PMSF). Total protein was extracted with 300 µl lysis buffer (50 mM HEPES-NaOH, pH 7.5, 300 mM NaCl, 1% (v/v) Nonidet P40 (NP-40), 10 mM $MgCl_2$, 1 mM PMSF, 10 mM N-Ethylmaleimide (NEM) and Protease Inhibitor Cocktail Tablet, Roche), using dounce homogenization and further centrifugation for 10 min at 13000 rpm and 4^{o}C, in order to separate soluble (supernatant) and insoluble protein (pellet). For Nse1 IP, 3 µl homemade rabbit polyclonal antibody against human Nse1 was added to 30 µl protein A magnetic beads (Dynabeads, Novex) and then the mixture was first washed and then incubated in wash and bind buffer, containing 0,1 M Na_3PO_4, pH 8 and 0.05% Tween-20 for 30 min on a rolling machine. After incubation, soluble protein was added to the antibody-coupled magnetic beads previously washed twice with lysis buffer. Protein samples were immunoprecipitated for 1 h on a rolling machine. After washing five times with washing buffer (25 mM HEPES-NaOH, pH 7.5, 300 mM NaCl and 0.2% (v/v) NP-40), immunoprecipitated samples were boiled in 4% SDS sample buffer at 95^{o}C for 2 min. Proteins were separated by SDS-PAGE electrophoresis and detected by Western blot analysis, using specific antibodies. The homemade Nse1 antibody was kindly provided by Dr. Raimundo Freire, Hospital Universitario de Canarias, Spain. For FLAG and HA IP, protein samples were immunoprecipitated overnight at 4^{o}C with Anti-FLAG M2 Agarose Beads (Sigma) and Anti-HA agarose Beads (Pierce, Thermo Scientific), respectively. After incubation, the same IP protocol was used.

3.5.2 Sodium dodecyl sulphate-polyacrylamide gel electrophoresis (SDS-PAGE)

SDS-PAGE is a technique for separation of proteins based on their molecular weight. Protein samples were separated using 7.5% - 15% SDS-polyacrylamide gels depending on the size of the target protein. The resolving gel was prepared at different percentages from 30% acrylamide/bis-acrylamide, 1,5 M Tris-HCl pH 8.8, 10% SDS, 10% ammonium persulfate and (tetramethylethylenediamine) TEMED. 5% stacking gel was prepared from 30% acrylamide/ bis-acrylamide, 1 M Tris-HCl pH 6.8, 10% SDS, 10% ammonium persulfate and TEMED. Equal amounts of protein, previously boiled and short spun, were loaded into the wells of SDS-PAGE gel. 5 µl of a protein molecular weight marker (Prestained Protein Ladder) was loaded in one of the wells of the gel in order to determine the size of the target protein. Electrophoresis was performed in 1x Running buffer, prepared from 10x Running buffer (Tris 25mM; Glycine 192mM; SDS 0.1%, pH 8.3) and 20 mA/gel for 70 - 90 minutes, using vertical mini-PROTEAN tetra cell gel apparatus (BioRad).

3.5.3 Western blot

For western blot analysis, cells were harvested and lysed with lysis buffer (2% SDS, 5% glycerol, 0,06M Tris-HCl, 4% β-mercaptoethanol, 0.0025% bromophenol blue). After separation of the proteins by SDS-PAGE electrophoresis, they were transferred onto a PVDF membrane (Millipore), previously activated by soaking in methanol, washed with distilled water twice and soaked in transfer buffer, containing 10% or 20% methanol or ethanol for better detection of big and small proteins, respectively. The transferring of the proteins was performed at 60 mA/gel for 1 hour by semi-dry blotting procedure using Semi-Dry transfer system TE 77 (Pharmacia Biotech). After incubation, the membrane was blocked with 5% non-fat milk or 3% bovine serum albumin (BSA) in PBST (PBS 1x, 0.1% Tween-20) for 1 h at RT in order to prevent non-specific binding. The membrane was then incubated with the primary antibody, diluted in 0.25% milk in PBST or 1% BSA overnight at 4^{o}C. After washing two times with PBST for 10 min and once with PBST with 0.25% milk or 1% BSA for 8 min, the membrane was incubated with the secondary antibody, diluted in 0.025% milk or 1% BSA for 1 h at RT. After incubation, the membrane was washed 4 times with PBST for 5 min each and then incubated with Immobilon Western Chemiluminescent HRP Substrate (Millipore) for 2-3 min and wrapped in transparency film. The protein bands were detected by ChemiDoc™ MP imaging system (BioRad). The antibodies used in this study are listed in detail in Table 5.

3.6 Drugs and treatments

Several drugs were used in this thesis: the proteasome inhibitor MG132 (carbobenzoxy-Leu-Leu-leucinal) (C221) was purchased from Sigma and MLN-4924, NEDD8-activating enzyme inhibitor (505477) was purchased from Merck Millipore. The DNA damaging agents: etoposide (E1383), hydroxyurea (H8627-25G) and methyl methanesulfonate (MMS) (129925-25) were obtained from Sigma. Phleomycin (BI3852) was obtained from Apollo chemicals and camptothecin (C1495) was obtained from TCI (Tokio Kasei). The synthetic analog of thymidine bromodeoxyuridine (BrdU) was purchased from Sigma.

3.7 Antibodies

The list of antibodies used in this study is shown in Table 5.

Table 5. List of antibodies

Antibodies used for Western blot			
Primary antibody	**Company**	**Dilution**	**Secondary antibody**

yH2AX (Ser139)	Millipore	1:500	anti-mouse
NSE1	Raimundo Freire's Lab	1:1000	anti-rabbit
NSE1 D2	Santa Cruz	1:1000	anti-mouse
SMC5 N2N3	GeneTex	1:500	anti-rabbit
SMC5	Raimundo Freire's Lab	1:1000	anti-rabbit
SMC6	Raimundo Freire's Lab	1:1000	anti-rabbit
SMC6 A3	Santa Cruz	1:500	anti-mouse
NSE3	Raimundo Freire's Lab	1:500	anti-rabbit
NSMCE4A	Sigma-Aldrich HPA037459	1:1000	anti-rabbit
NSE2	Oscar Fdez-Capetillo's Lab	1:200	anti-mouse
Actin C4	Millipore	1:5000	anti-mouse
FLAG M2	Sigma-Aldrich	1:5000	anti-mouse
Vinculin	Sigma-Aldrich, Vin-11-5	1:200	anti-mouse
High Affinity (HA) tag 3F10	Roche	1:5000	anti-rat
Hexokinase, yeast	USBiological	1:5000	anti-rabbit

Antibodies used for immunofluorescence, flow cytometry			
BLM	Abcam, ab2179	1:1000	Alexa Fluor anti-rabbit 488
BrdU	Abcam, ab6326	1:1000 1:250	Alexa Fluor anti-rat 555
BrdU	BD Biosciences, clone B44	1:200	Alexa Fluor anti-mouse 488
MPM-2	Millipore	1:250	Alexa Fluor anti-mouse 647

RESULTS

4.1 Analysis of the NH-RING domain in human cells

4.1.1 Generation of human *NSE1* mutants with impaired ubiquitin activity by CRISPR-Cas9

Yeast cells with mutations in the RING domain of Nse1 show slow growth and are hypersensitive to DNA damage drugs [Wani et al., 2018, Pebernard et al., 2008 (1)]. These findings suggest an important role of Nse1 in DNA repair and chromosome segregation. Since we know that NSE1 RING domains in yeast and humans share a strong conservation in evolution, we wanted to confirm these observations in human cells. We created stable cell lines with mutations in the RING domain by CRISPR/cas9 technology. Using two different approaches we generated *NSE1* mutants with a deletion - (*NSE1ΔRING* or *NSE1ΔR*) or specific point mutations (C204A-C207A) on RING motif (*NSE1-AA*). In Fig.1 is shown the workflow of the method.

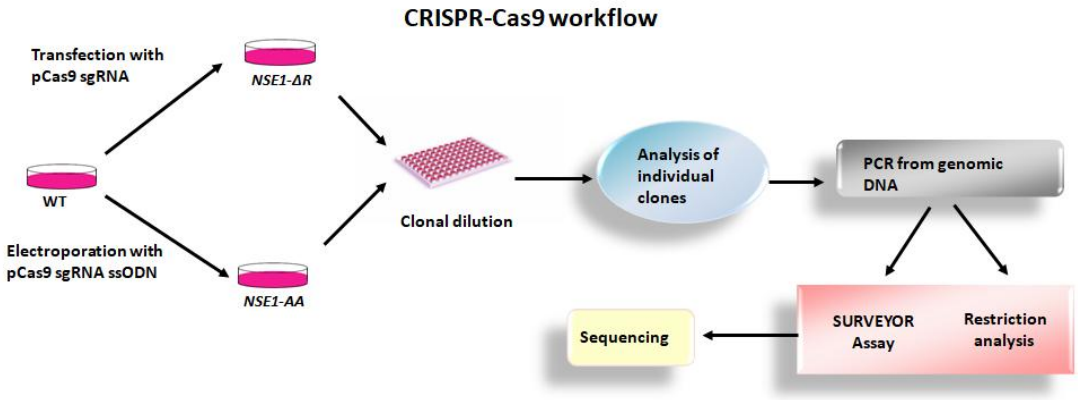

Fig.1 CRISPR-Cas9 workflow for generating mutations in the RING domain of human *NSE1* (hNse1) in HEK293T cells. The experimental procedure is detaily explained in the text. The individual clones, positive in the analysis of genome edition were finally sequenced.

In order to create a deletion, we used the CRISPR/Cas9 method to create directed DNA double strand breaks (DSBs) that can be repaired either by homologous recombination (HR) or by non-homologous end joining (NHEJ). In case this last mechanism is used for repair, this could lead to the occurrence of insertions or deletions (INDELs) and subsequent gene disruption. In this approach, we transfected HEK293T cells with a plasmid carrying the guide RNA (sgRNA), Cas9 endonuclease and GFP, used as a fluorescent marker (Fig.2).

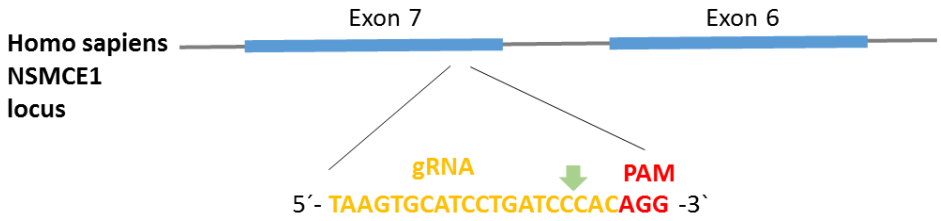

Fig.2 CRISPR/Cas9 generation of a mutation on exon 7 of *NSMCE1* (human *NSE1*) A schematic illustration of the guide RNA (gRNA) targeting exon 7, where the C-terminal part of the RING domain is codified. The gRNA is indicated in yellow, the protospacer adjacent motif (PAM) sequence is shown in red. The Cas9 cleavage site is pointed with a green arrow.

To insert point mutations at the target locus of *NSE1* we used the CRISPR/Cas9-based ssODN to induce homology-directed repair (HDR). A homologous DNA donor - single strand oligodeoxynucleotide (ssODN) carrying the desired point mutations - was used as a template by HDR to repair the DSBs. For this approach, we electroporated with nucleofection HEK293T with the same plasmid carrying sgRNA, Cas9 endonuclease and GFP, and in addition, the ssODN was also included (Fig.3).

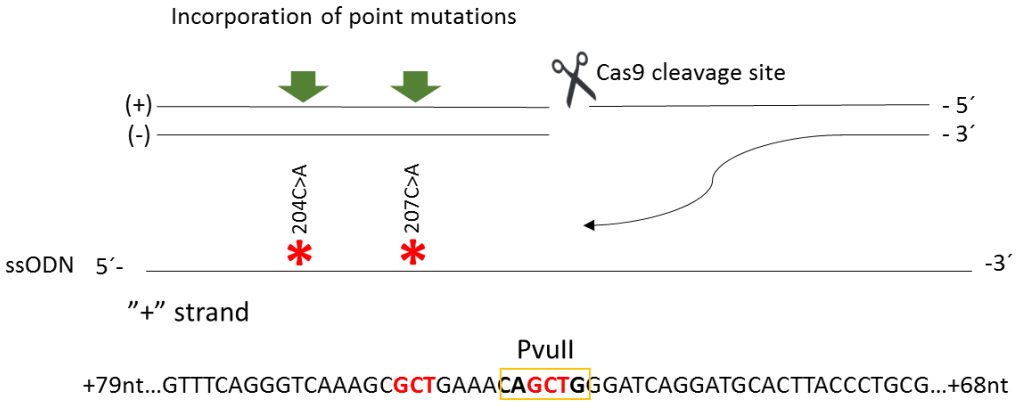

Fig.3 Design to generate point mutations on *NSE1* using CRISPR/cas9-based ssODN. A schematic representation for introducing two point mutations at *NSMCE1* locus (human *NSE1*) using CRISPR cas9 strategy with ssODN. The ssODN with a size of 200bp has been designed to carry the desired point mutations. Two cysteine residues at positions 204 and 207 were changed to alanine. The letters in red indicate the two substitutions. In a yellow box is labelled the introduction of PvuII restriction site.

Then we performed clonal dilution to isolate only single cell clones. Next, we analyzed the individual clones by PCR amplification from genomic DNA. Clones with a deletion were further examined by SURVEYOR assay to detect the target mutation (Fig.4), whereas clones with point mutations were analyzed by restriction analysis to distinguish which of them are repaired by the ssODN (Fig.5).

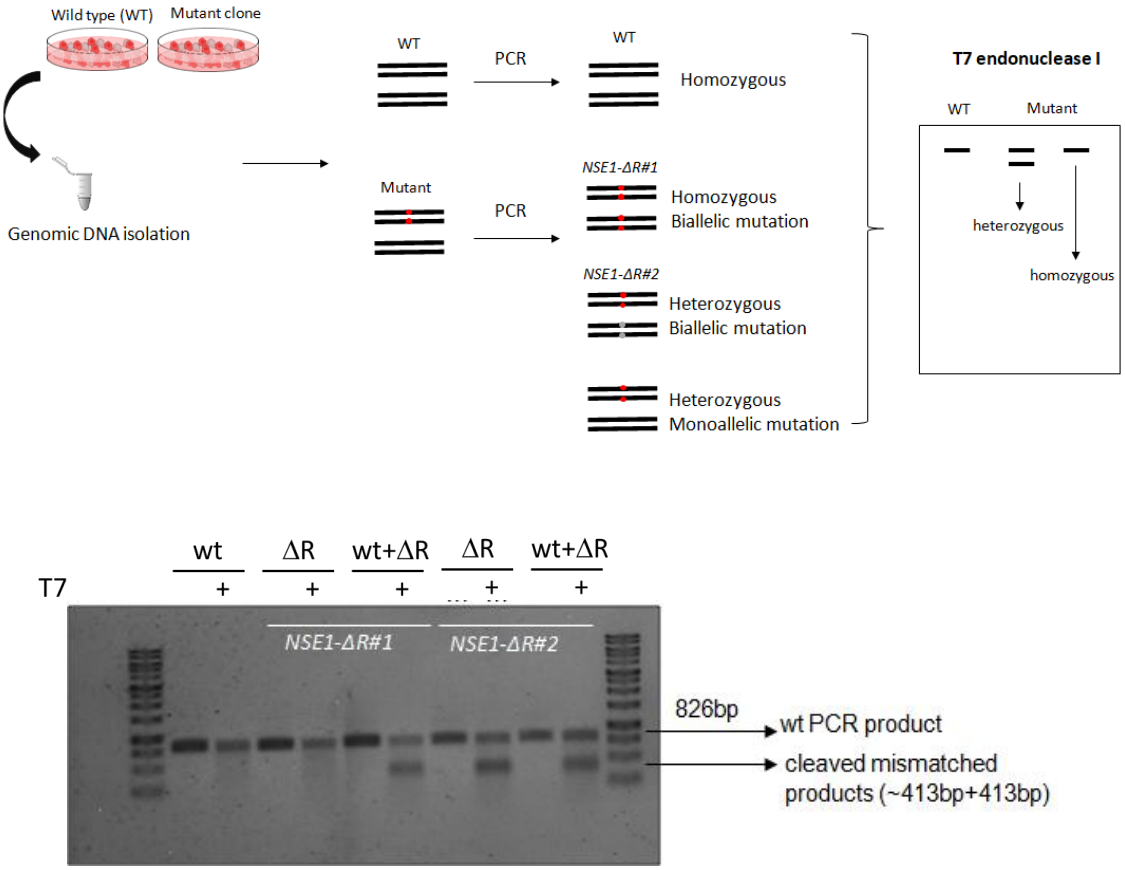

Fig.4 Detection of genome edition at human *NSE1* target locus using T7 endonuclease I cleavage assay. A. Scheme of the method. Genomic DNA has been isolated from HEK293T wild-type and mutant cells previously transfected with a plasmid carrying sgRNA, Cas9 and GFP. The target region was amplified and the PCR products were denatured, re-annealed and treated with T7 endonuclease I enzyme (T7EI) to detect the Cas9 induced mutation. The result was visualized by gel electrophoresis. T7EI recognizes and cleaves non-perfectly matched DNA. The enzyme can recognize only heterozygous mutations but it cannot distinguish the homozygous biallelic mutant clones from wild-type cells, neither if the mutation is monoalleic or biallelic. To create heteroduplex molecules, we mixed DNA from WT and mutant clones and analyzed the fragments by T7EI. The cleaved PCR products indicate the presence of INDELs exactly at the place where Cas9 should cleave the target sequence. Two different types of *NSE1-ΔR* mutants have been identified – *NSE1-ΔR*#1 has a homozygous genotype, whereas *NSE1-ΔR*#2 is heterozygous. *NSE1-ΔR*#1 has been further used in the experiments.

The presence of NHEJ indels and precise editing by HR were further confirmed by DNA sequencing (Fig.6 A and B).

Among different clones analyzed, DNA sequencing revealed that *NSE1-ΔR* and *NSE1-A* mutants have a homozygous genotype, i.e. all alleles carry the corresponding mutations, whereas *NSE1-AA* is a heterozygous mutant that carries a mutant allele with the desired point mutations and an allele with an insertion corresponding to the ssODN sequence.

Therefore, this clone presents three different bands when analyzed by PCR from genomic DNA and further PvuII restriction (as shown in Fig. 5).

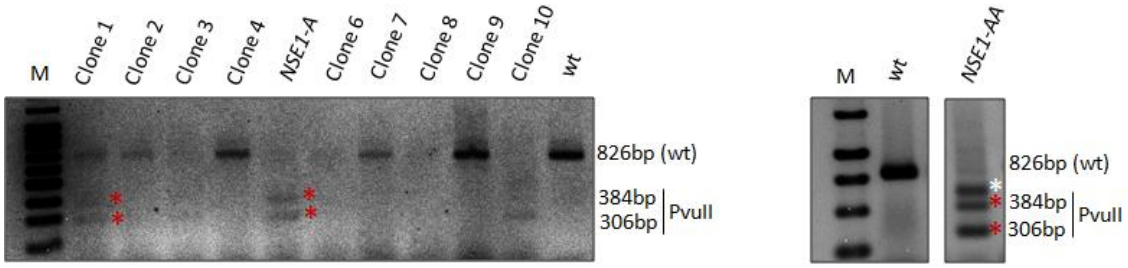

Fig.5 Identification of the CRISPR cas9-ssODN induced point mutations at human *NSE1* locus by restriction analysis. Genomic DNA was isolated from wild type HEK293T and mutant cells, previously transfected with plasmid containing sgRNA, Cas9, GFP and ssODN. The *NSE1* analyzed region (826bp) was amplified and the PCR products were digested with a PvuII restriction enzyme to detect the created point mutations by homology-directed repair. PvuII site has been introduced in the position of one of the point mutations (207C>A) that are codified by the ssODN donor (204C>A, 207C>A).
Several clones were analyzed and only three of them showed the desired mutations in homozygosis. Most of the clones were repaired by NHEJ leading to the occurrence of truncated mutants. The red asterisks illustrate the PvuII digestion products. The white asterisk indicates the appearance of an unexpected band with a higher size in clone *NSE1-AA*, which was further analyzed by DNA sequencing.

A

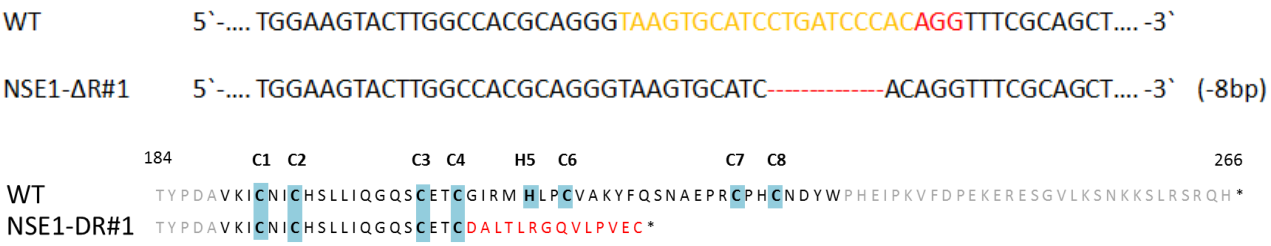

B

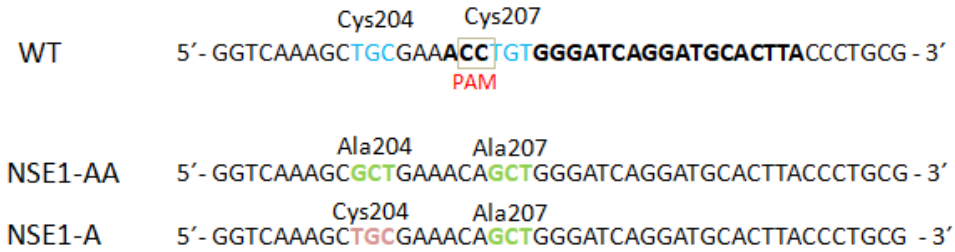

Fig.6 Verification of the genome edition by DNA sequencing. A. Alignment of DNA sequences of wild type and *NSE1* mutant clone - *NSE1-ΔR*#1. Red dashes point the identified mutation with 8 deleted nucleotides. Below, the corresponding protein sequences of NSE1 WT - wild type Nse1 C-terminal part (RING domain is labelled in black) and *NSE1-ΔR#1* (Nse1 with truncated RING domain) are shown. Conserved cysteine and histidine residues are highlighted in blue. B. Alignment of DNA sequences of wild type and two point mutant clones. In blue letters are shown the targeted cysteine residues in wild type sequence. The first analyzed mutant clone

shows the two expected substitutions 204C>A and 207C>A, indicated with green letters (*NSE1-AA*). The second mutant clone received only one 207C>A substitution (*NSE1-A*), highlighted in pink and green, respectively.

4.1.2 Phenotype characterization of the different *NSE1* mutants obtained (*NSE1-AA, NSE1-A, NSE1-ΔR*).

4.1.2.1 *NSE1* mutants show no detectable levels of Nse1

To study the phenotype of the identified mutant clones, we first conducted western blot analysis to check expression levels of Nse1. Due to the missing amino acids in *NSE1-ΔR* mutant, we predicted a smaller size of Nse1. Surprisingly, we could not detect Nse1, neither in the truncated mutants, nor in the point mutants (Fig.7 A). Based on these results, we supposed that Nse1 in mutant clones is highly unstable and rapidly degraded. In addition, we also found a loss of expression levels of different subunits of the complex in our mutants (Fig.7 B e) and Fig.18), suggesting that the entire Smc5/6 complex is destabilized.
In order to test whether the mutant Nse1 is targeted for proteasomal degradation, we treated wild type and mutant cells with an inhibitor of the proteasome. After overnight treatment with MG-132, the levels of Nse1 were partially restored in the double and single point mutant (*NSE1-AA* and *NSE1-A*). This result confirms our assumption that mutant Nse1 is degraded by the proteasome (Fig.7 B a) and b)). We have to note the appearance of a higher band in the MG-132 treated *NSE1-AA* sample corresponding to an aberrant form of the protein, including the insertion of the ssODN sequence into *NSE1* exon 7 during the genome edition.

In contrast, MG-132 exposure did not increase the protein expression level in *NSE1-ΔR* mutant (Fig.7 B c)). We also tried to recover the Nse1 expression level using MLN4924, a NEDD8-activating enzyme inhibitor which avoids the neddylation of Cullin complexes, and therefore, their activation. After 24 hours of treatment with the inhibitor we could not detect any restoration of the protein levels (Fig.7 B d)).

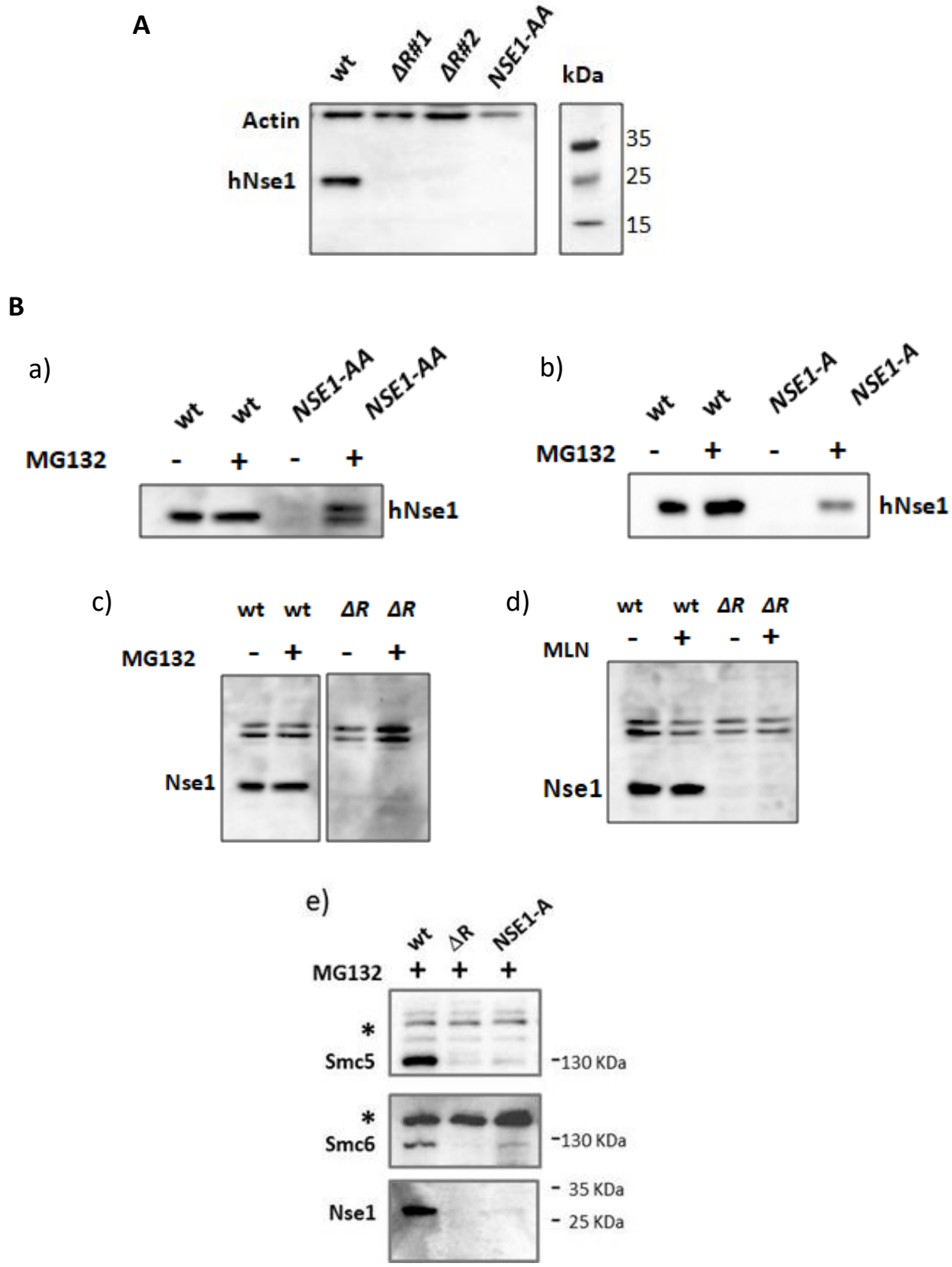

Fig.7 Characterization of *NSE1* mutants by western blot analysis. A. All mutant clones show no detectable Nse1 levels. B. Western blot analysis of wild type, *NSE1-AA, NSE1-A* and *NSE1-ΔR* mutant (a), b) and c)) treated

or not with MG132 proteasome inhibitor (10μM) for 24 hours. The addition of MG132 prevents degradation of Nse1 in the single and double point mutants, but not in the truncated one, showing that *NSE1-AA* and *NSE1-A* mutants are targeted for proteasomal degradation. d) Treatment of wild type and *NSE1-ΔR*#1 (*ΔR*) mutants with MLN inhibitor (1 μM) for 24 hours. The MLN inhibitor did not restore levels of Nse1 in truncated mutants. e) Treatment of wild type, *NSE1-ΔR#1* (ΔR) and *NSE1-A* mutants with MG132 as described above. Smc5 and Smc6 subunits were not expressed or expressed at very low levels in mutant cells.

In order to verify that *NSE1* mRNA levels or stability in mutant clones were not affected, we performed RT-PCR. Comparing mRNA expression levels of *NSE1* in wild type and different mutants we could detect slightly reduced *NSE1* mRNA levels in truncated and point mutant AA, and around 40-50% of expression in *NSE1-A* mutant, compared to control WT cells (Fig.8). Although Nse1 expression in mutant cells will be decreased due to lower levels of mRNA, we think that this would only partially explain the observed decrease in mutant protein levels. The increased protein instability would also help to explain the complete absence of these mutant proteins.

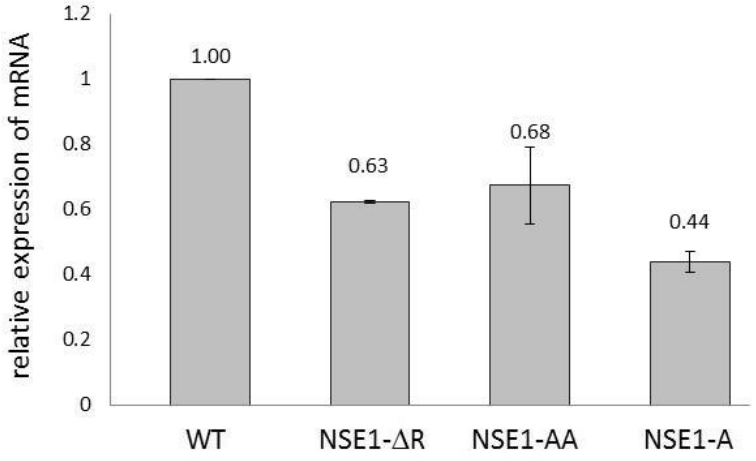

Fig. 8 Real-time PCR analysis measuring relative mRNA expression levels of *NSE1*. The mRNA levels of *NSE1* in wild type and mutant clones were quantified by RT-PCR and normalized to the mRNA levels of β-actin gene (*ACTB*), used as an internal control. The graph shows that *NSE1* mRNA levels were partially reduced in *NSE1-ΔR* and *NSE1-AA*, and more decreased in *NSE1-A*. Means and SEM values of three independent experiments are shown.

4.1.2.2 All *NSE1* mutants show slow growth phenotype and changes in cell morphology.

To test whether the cellular growth in our *NSE1* mutants is disturbed, we investigated cell proliferation of wild type and four different mutant clones (*NSE1-AA, NSE1-A, NSE1-ΔR*#1 and *NSE1-ΔR*#2) during 3 days using the trypan blue (TB) assay. The growth curve analysis

showed that all analyzed *NSE1* mutant cells were viable but grew much slower compared to wild type cells (Fig.9 A).

Additionaly, we detected cellular morphological alterations in our mutants using light microscopy. Comparing the cell morphology of wild type and *NSE1* mutant cells we observed bigger cells with changes in the shape and a high presence of cytoplasmic vacuoles that were presented only in the double point and truncated *NSE1* mutants, but not in wild type cells (Fig.9 B).
In accordance, cells depleted for NSMCE2 demonstrated accumulation of vacuoles in the cytoplasm [Verver et al., 2016]. The strong slow-growth phenotype and the appearance of vacuoles is a sign of cellular stress as a result of disruption of Nse1 and subsequent impaired Smc5/6 function.

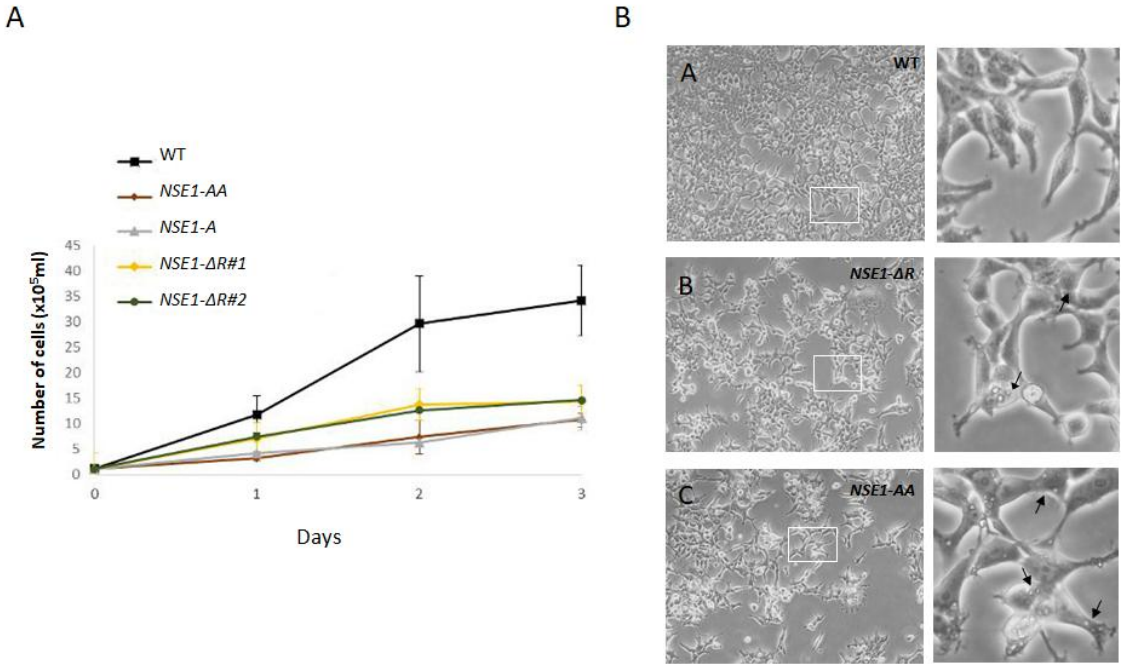

Fig.9 Analysis of growth rate and cell morphology in *NSE1* mutants. A. Growth curve analysis of wild type cells and four individual *NSE1* mutants. All of the analyzed *NSE1* mutants demonstrate slower growth in comparison with wild type cells. The cell proliferation was followed during 3 days using trypan blue (TB) exclusion assay. The values are representative of three independent experiments. B. *NSE1-AA and NSE1-ΔR*#1 show a change in cell morphology and high presence of cytoplasmic vacuoles. Phase contrast of wild type cells and two different *NSE1* mutants. A. Wild type cells show the normal cell morphology for HEK293T. B. and C. Both *NSE1* mutant cells display changes in cell morphology: bigger cells and accumulation of vacuoles in the cytoplasm, a sign of cellular stress. The black arrows indicate the formation of vacuoles. The images are obtained with 10x objective.

4.1.2.3 No detectable cell cycle arrest, but higher number of cells with increased genomic instability in *NSE1* mutant cells

Since we found that *NSE1* mutant cells exhibit slower growth, we wanted to assess whether this phenotype is associated with the arrest of the cell cycle at a specific phase. We conducted cell cycle analysis by flow cytometry (FACS) measuring the DNA content with propidium iodide (PI). Although the result did not show big alterations in the distribution of the cell cycle in wild type and two different mutant clones, a higher number of cells with less than G1 DNA content and with more than G2 DNA content that presented only in the mutant cells were detected. These cells most probably are apoptotic and polyploid cells, suggesting an increased genomic instability (Fig.10 A, B, C and D). In order to confirm the presence of apoptotic cells in *NSE1* mutants we performed a live-staining assay with acridine orange (AO) and ethidium bromide (EtBr) for detection of apoptosis. Using fluorescence microscopy we compared morphological nuclear changes of wild type and double point mutant cells. The result demonstrated normal nuclear morphology in wild type and indications for early apoptotic and necrotic cells in mutant cells (Fig.10 E).
The increased cell death is indicative of spontaneous endogenous DNA damage in *NSE1* mutants although cell cycle arrest or accumulation of cells at a specific cell cycle phase could not be detected by the FACS analysis. Consistent with our result, induction of apoptosis, as well as accumulation of polyploid cells have also been observed in mouse embryonic stem cells deficient for Smc5 [Pryzhkova and Jordan, 2016].

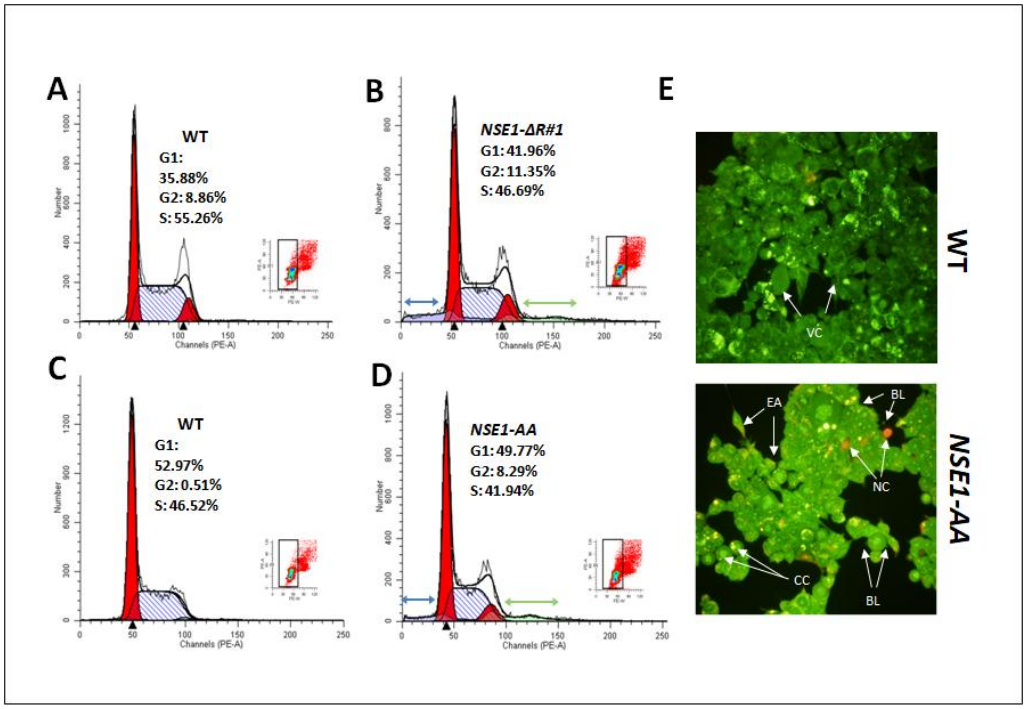

Fig.10 *NSE1* mutants show slight alterations in cell cycle distribution and increased number of apoptotic cells. On the left, the figure shows the cell cycle distribution of wild type HEK293T cells (A and C) and two different *NSE1* mutants (B. *NSE1-ΔR*#1 and D. *NSE1-AA*). Cells were harvested, fixed with 70% ethanol,

followed by propidium iodide (PI) staining of DNA and analyzed by flow cytometry. Both types of mutants show a higher number of cells with less than G1 DNA content (blue arrow) and more than G2 (green arrow), referring to putative apoptotic and polyploid cells, respectively. Cell cycle distribution was analyzed using ModFit software. E. Representative fluorescent microscopy image of wild type cells and *NSE1-AA* mutant cells stained with acridine orange (AO) and ethidium bromide (EtBr) for detection of apoptosis. Wild type cells show normal nuclear morphology without observation of apoptosis and necrosis. Double point mutant cells show signs of early apoptosis and necrosis. Early apoptotic cells display light green nucleus with chromatin condensation and membrane blebbing. Necrotic cells - orange shrinkage nucleus without DNA fragmentation. AE: early apoptosis VC: viable cells; CC: chromatin condensation; BL: blebbing of the cell membrane; NC: necrotic cells.

4.1.2.4 *NSE1* mutant cells display prolonged mitosis

The presence of cells with increased genomic instability signals for abnormal mitosis. Therefore, in order to monitor the mitotic progression in *NSE1* mutants we used *in vivo* confocal time-lapse microscopy. The cell cycle progression of wild type and truncated mutant cells (*NSE1-ΔR*#1*)* was followed for 48 hours instead of 24 hours, due to the slower growth rate of the mutant cells. Before the analysis, wild type and mutant cells were transfected with a plasmid expressing a fusion of the histone H2B with mCherry for chromatin labeling (the transfection efficiency was ~50%). Due to the occurrence of cell arrest or cell death in both wild type and mutant cells that were positive for H2B-mCherry, we could not track mitosis progression. Therefore, we could measure only the non-transfected cells for morphological changes that appear during mitosis after analyzing the fluorescent images. To examine the duration of mitosis we quantified the time when the cells start to round up, which is concurrent with chromatin condensation (prophase) until the time where they spread and divide (telophase and cytokinesis). The obtained result indicated that *NSE1* truncated mutant cells underwent mitosis for a longer period compared to wild type cells. The *NSE1* mutant showed a ~1 hour delay difference in the duration of mitosis, probably due to defects in chromosome segregation or aneuploidy (Fig.11 A and B). The duration of the entire cell cycle could not be determined due to the fast moving of the cells and difficulties in following them in each field. However, the aberrant mitotic progression correlates with the presence of genomic instability, and could partially explain the slower proliferation rate of our *NSE1* mutants. Similar to our data, cells deficient for HR proteins exhibited prolonged metaphase arrest [Wilhelm et al., 2014]. Regarding these findings and our results, we can suggest that *NSE1* mutant cells enter into mitosis with under-replicated or not completely repaired DNA which leads to aberrant mitosis.

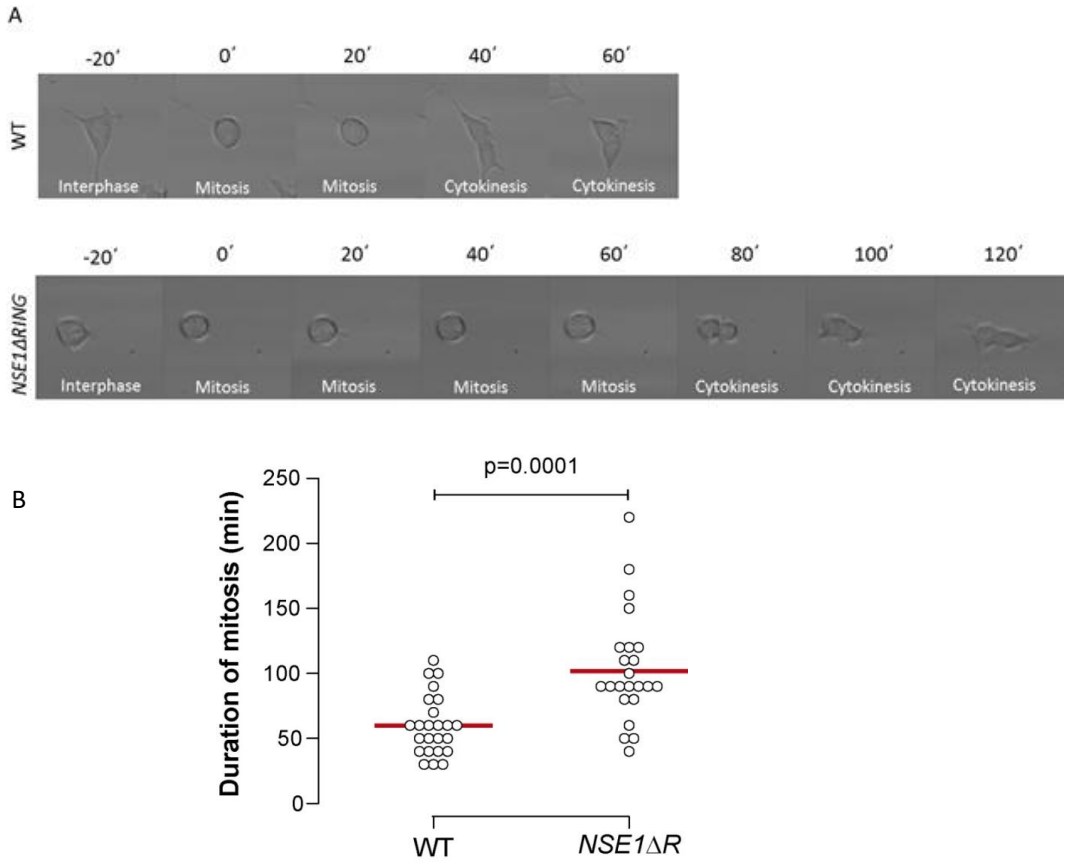

Fig.11 *NSE1ΔRING* mutant cells show prolonged mitosis. Time-lapse microscopy of wild type (HEK293T) and *NSE1ΔRING* (*NSE1ΔR*) mutant cells. A. Representative time-lapse images of a wild type cell showing a normal mitotic progression (about 60 min) on the top and *NSE1ΔRING* mutant cell showing abnormal timing of mitosis (about 2h and 40 min) below. The longer period of both mitosis and cytokinesis in mutant cells suggests a delay in the entire cell cycle. The time of mitosis is counted at the point where cells start to round up (0 min) until they divide (cytokinesis). The representative images show the duration of mitosis at every 20 min. At time -20 min is shown the interphase stage. B. A quantification of the duration of mitosis in wild type and *NSE1-ΔR (NSE1-ΔR*#1*)* mutants. Mitotic progression in wild type and *NSE1* mutant cells was followed for ~48h hours using *in vivo* confocal time-lapse microscopy. Images were taken every 10 minutes and the mean mitotic time is shown. For each sample, 8 cells from 3 different fields were counted. Each dot represents the entire duration of mitosis of one cell. *NSE1-ΔR* is referred to as *NSE1-ΔRING.* The images were analyzed by ImageJ Software (NIH, USA). Statistics were performed by one-way ANOVA, using Bonferroni-Holm post-hoc test. P value<0.05 was considered statistically significant.

4.1.2.5 *NSE1* mutants show higher levels of endogenous DNA damage

One expected phenotype for *SMC5/6* mutants is the accumulation of high levels of endogenous DNA damage [Gallego-Paez et al., 2014], therefore we wanted to know whether the lack of Nse1 would cause the same phenotype in our cellular model. To achieve this and to confirm our predictions from result obtained above, we started to evaluate the initial DNA damage in *NSE1* mutant clones using various biomarkers for genomic instability, such as γH2AX, BLM foci formation, micronuclei (MN) and sister chromatid exchange (SCE) assays.

To test the endogenous DNA damage in our *NSE1* mutant clones we first conducted western blot analysis of wild type and two truncated mutants using anti-phosphorylated histone antibody (γH2AX). The phosphorylation of histone on Ser139 is a useful marker for early DNA damage response as a result of DNA double-strand breaks (DSBs). Our data clearly showed that the levels of γH2AX are higher in both truncated mutants in comparison with those in wild type cells (Fig.12).

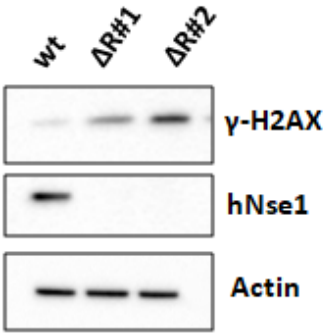

Fig.12 *NSE1-ΔR* mutants show higher levels of γH2AX, a sign of endogenous DNA damage. Western blot analysis of wild type, *NSE1-ΔR*#1 and *NSE1-ΔR*#2 mutant cells using anti-γH2AX and anti-human Nse1 antibodies. α-actin was used as a loading control. Both types of truncated mutants show elevated endogenous γH2AX levels, compared to wild type cells. *ΔR*#1 and *ΔR*#2 referred to as *NSE1-ΔR*#1 and *NSE1-ΔR*#2, respectively.

Next, we examined BLM foci formation in *NSE1* mutants and wild type cells. BLM (Bloom) is a RecQ helicase which is highly conserved between different species and is essential for maintaining genomic stability. Mutations in this protein in humans cause Bloom syndrome (BS), a rare genetic disease associated with higher incidence of cancer. In normal conditions BLM is localized to promyelocytic leukemia protein (PML) nuclear bodies but in response to DNA damage caused by stalled replication forks and double-strand breaks (DSBs) it accumulates into nuclear foci. Thus, BLM facilitates DNA repair along with other proteins at the early steps of homologous recombination (HR) and by resolution of recombination intermediates in the final steps of HR [Bischof et al., 2001, Chu et al., 2010]. To determine if there is a higher spontaneous induction of BLM foci in *NSE1* mutant cells, we performed immunofluorescence using fixation and extraction technique at the same time, which allows a better detection of the foci. Wild type, *NSE1-AA* and *NSE1-ΔR* mutants have been stained with an antibody that recognizes specifically BLM. The immunofluorescent analysis showed bigger and more intense foci in both types of mutants compared to wild type cells (Fig.13 A and 14 A). BLM foci quantification analysis showed that the average number of BLM foci in *NSE1-AA* has been 22% higher than those in wild type (Fig.13 B) and 16% higher in *NSE1-ΔR* mutant than in wild type cells (Fig.14 B). Since our wild type cells are SV40-transformed, it was not a surprise that they also showed some levels of an initial DNA damage, according to the BLM foci quantification. Nevertheless, both types of *NSE1* mutant cells showed a significantly higher number of BLM foci, that is probably associated with the formation of DNA DSBs or stalled replication forks, a hallmark of genomic instability.

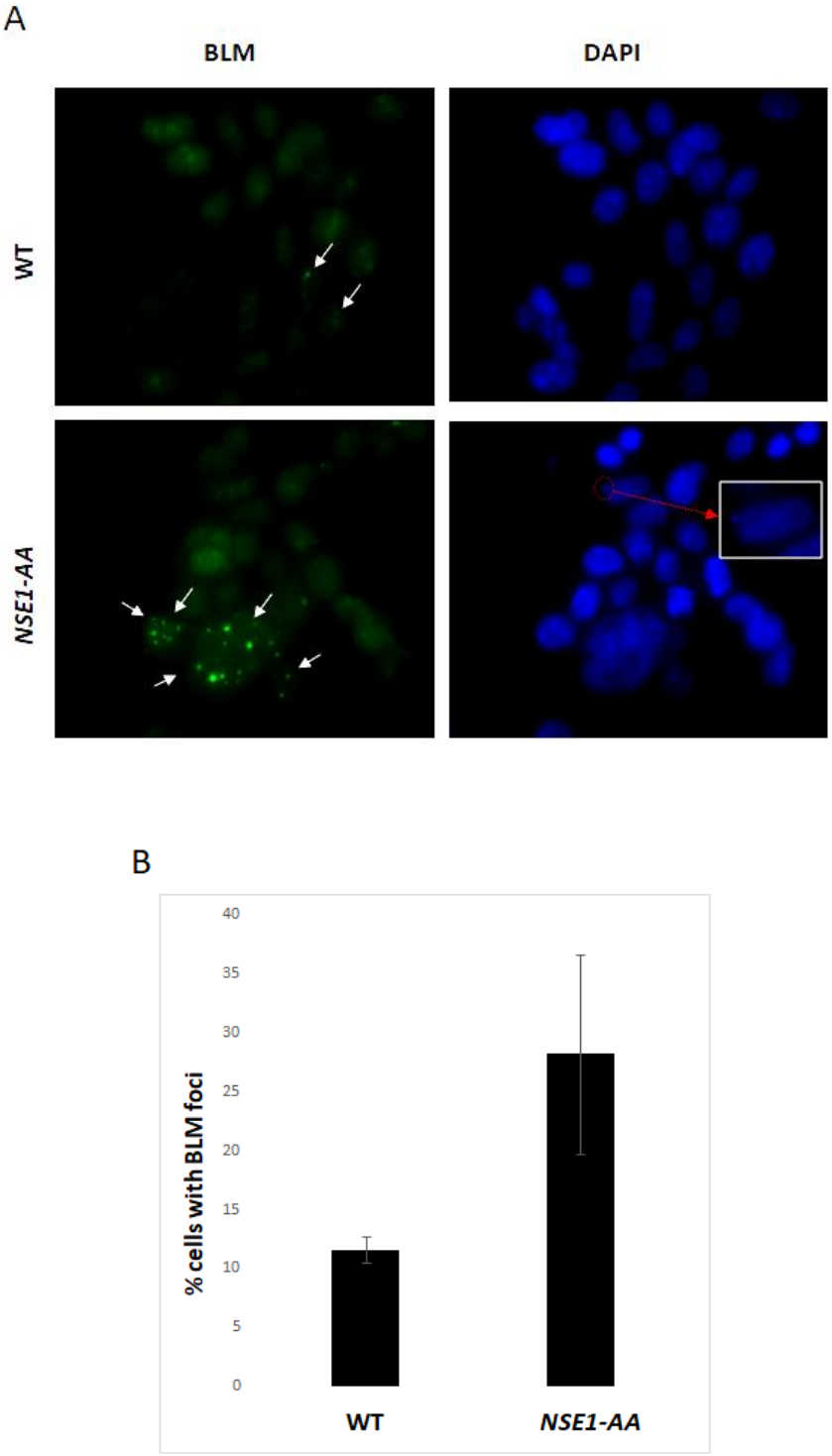

Fig.13 *NSE1-AA* shows an increased number of BLM foci – a sign of endogenous DNA damage A. Immunofluorescence of wild type and mutant cells. Cells were fixed and extracted and further stained with

anti-BLM antibody, and with DAPI to visualize the nuclei. White arrows point BLM foci, the red arrow indicates the appearance of micronuclei. B. A quantification of the average number of BLM foci in wild type and mutant cells. In each sample, ~200 cells were counted. Values are representative of three independent experiments. The BLM foci quantification was performed using ImageJ Software (NIH, USA).

Next, we conducted a micronuclei assay to reveal whether *NSE1* mutant cells show defects in chromosome segregation during mitosis. Micronuclei (MN) are chromosomal fragments resulting from DNA breaks or chromosome lagging. They remain in the cytoplasm, nearby nucleus and are transmitted to daughter cells during cell division [Fenech et al., 2011]. The high presence of MN is a sign of genomic instability. To be able to observe the micronuclei we stained wild type and *NSE1* mutant cells with DAPI and analyzed them by fluorescent microscopy. The result indicated a higher presence of MN in the double point mutant compared to wild type (Fig.13 A). The quantification of the average number of MN in truncated mutant cells was also higher than in wild type (Fig.14 B).

The finding that both types of *NSE1* mutants showed a higher number of micronuclei indicated that the endogenous DNA damage is due to the absence of Nse1. The high frequency of MN can also explain the observed abnormal mitosis in *NSE1* mutants and may be related with defects in chromosome segregation.

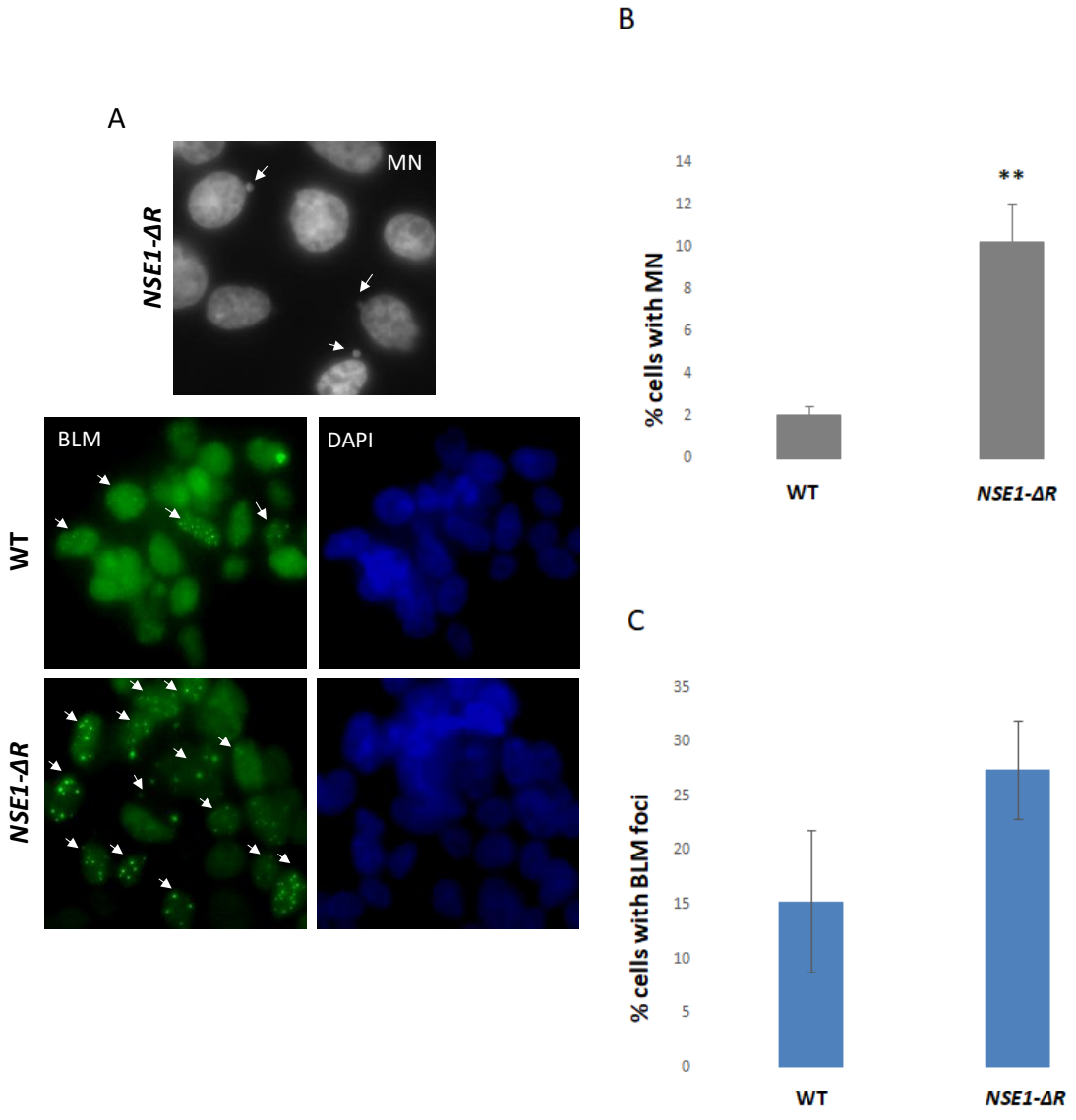

Fig.14 *NSE1-ΔR* mutant cells show an increased number of micronuclei and BLM foci. A. Immunofluorescence of wild type and mutant cells. Cells were fixed and extracted, and stained with an anti-BLM antibody. The nuclei were visualized using DAPI staining. The white arrows indicate micronuclei (MN) and BLM foci. B. and C. A quantification of the average number of MN and BLM foci in wild type and *NSE1-ΔR* cells. In each sample, ~200 cells were counted. Values are representative of three independent experiments. BLM foci and MN quantifications were conducted by ImageJ Software (NIH, USA). Statistical analysis was performed by one-way ANOVA, using Bonferroni-Holm post-hoc test (*p<0.05, **p<0.01 and ***p<0.001).

To confirm that *NSE1* mutant cells exhibit chromosome instability we used another sensitive marker – the sister chromatid exchange (SCE) assay. Sister chromatid exchange is a reciprocal exchange of DNA between sister chromatids during mitosis. The method is based on the incorporation of the thymidine analogue 5-bromodeoxyuridine (BrdU) into DNA during two cell divisions. The labeling of both DNA strands of one sister chromatid with BrdU allows the cytological visualization and differentiation of the chromatids in metaphase of the cell cycle after DNA staining. The high presence of SCE signals for chromosomal DNA damage. To observe the spontaneous levels of SCE in wild type and *NSE1* truncated mutant cells we have grown cells in the presence of BrdU for two cell cycles. The workflow of this method is shown in Fig.15.

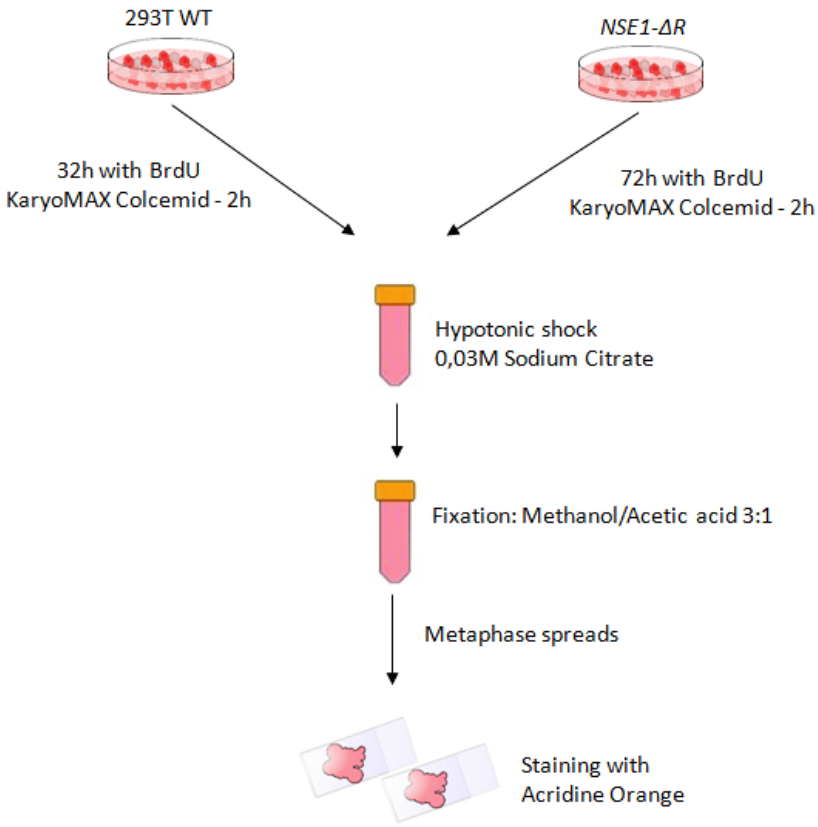

Fig.15 Workflow of Sister chromatid exchange (SCE) assay. Wild type and *NSE1* mutant cells have been grown in the presence of BrdU (50μM) for 2 cell cycles and blocked in metaphase with KaryoMAX Colcemid (0,05μg/ml). Then, cells were exposed to hypotonic shock with 0,03M sodium citrate and fixed with a solution of methanol and acetic acid 3:1. Slides with metaphase spreads have been further stained with acridine orange (AO) (0,1mg/ml) and immediately observed under fluorescent microscope using FITC filter.

The SCE analysis showed significantly elevated endogenous levels of SCE in *NSE1-ΔR* mutant cells compared to wild type cells (Fig.16). Similar to elevated SCEs in cells with mutation in *BLM*, probably higher levels of SCE in *NSE1* mutants are due to accumulation of recombination molecules and defects in DNA repair mechanisms.

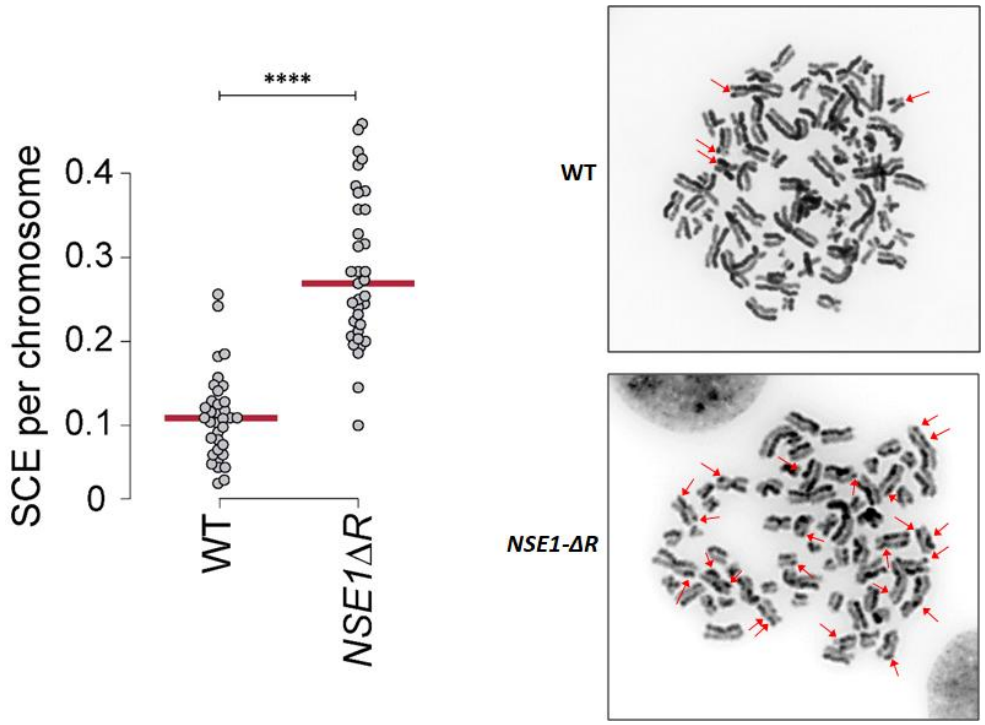

Fig.16 *NSE1-ΔR* mutant cells show higher levels of spontaneous sister chromatid exchanges (SCE). SCE assay of wild type and *NSE1* mutant cells. The graph shows the quantification of SCE per chromosome in wild type and *NSE1-ΔR* mutant, each dot represents one metaphase. For each cell type line, more than 2000 chromosomes were counted. The SCE events were quantified by ImageJ Software (NIH, USA). Statistics was performed by one-way ANOVA, using Bonferroni-Holm post-hoc test (*p<0.05, **p<0.01 and ***p<0.001). *NSE1-ΔR* is referred to as *NSE1-ΔRING* mutant. Microscopic photographs on the right indicate metaphase spreads of wild type and *NSE1* mutant cells. Red arrows point crossover events between the sister chromatids. The images are obtained with 60x objective.

Based on the used combination of DNA damage markers, we can suggest that the primary cause of genomic instability in *NSE1* mutants is due to obstacles during DNA replication and recombination that cannot be eliminated properly because of the lack of functional Nse1 and Smc5/6 complex.

Additionally, we constructed different *NSE1* mutant versions in expression vectors as GFP fusions to Nse1 wild type (Nse1 WT), Nse1 point mutated in C204 and C207 (Nse1 AA), N-terminal part of Nse1 (Nse1 Nter), C-terminal part of Nse1 (Nse1 Cter) or C-terminal region with point mutations (Nse1 Cter AA). To test the effect of *NSE1* mutations in terms of subcellular localization and protein stability, we used *in vivo* fluorescence microscopy and

immunoblotting. These results showed that overexpressed full length Nse1 fused to GFP was localized not only in the nucleus, but also in cytoplasm, whereas mutant constructs (Nse1 AA and Nse1 Nter) were mainly distributed to the cytoplasm (Fig. 17 A and B). However, expression of GFP construct fused to the C-terminal part of Nse1, with the same point mutations, did not alter the localization of Nse1 fusion protein (Fig. 17 A). Moreover, immunoblot analysis demonstrated that protein levels of Nse1 AA were consistently slightly lower than those of Nse1 WT. On the contrary, Nse1 Cter AA were very similar to those in Cter construct or full length Nse1 (Fig.17 C), indicating that the C- terminal part of Nse1 with the AA mutations is not unstable. Based on this, we can assume that double point mutations on RING are not itself a cause for altering the stability of the protein. It seems that the N-terminal half of Nse1, is responsible for the altered subcellular localization of double point mutant versions. Regarding truncated mutants, lacking the RING domain (GFP-Nse1 Nter) probably destabilizes the fusion protein, since protein levels are much lower than either full length Nse1 or Cter part (Fig. 17 C). In agreement, the same *NSE1* mutation created by CRISPR (ΔR mutant) expressed extremely unstable endogenous Nse1. Taken together, we can suggest that mutant Nse1 protein is being degraded very rapidly and therefore its interaction with the Smc5/6 complex is impeded. Another possibility could be that mutant Nse1 is able to interact with the complex and thus destabilizes the rest of subunits, leading to the Smc5/6 complex degradation.

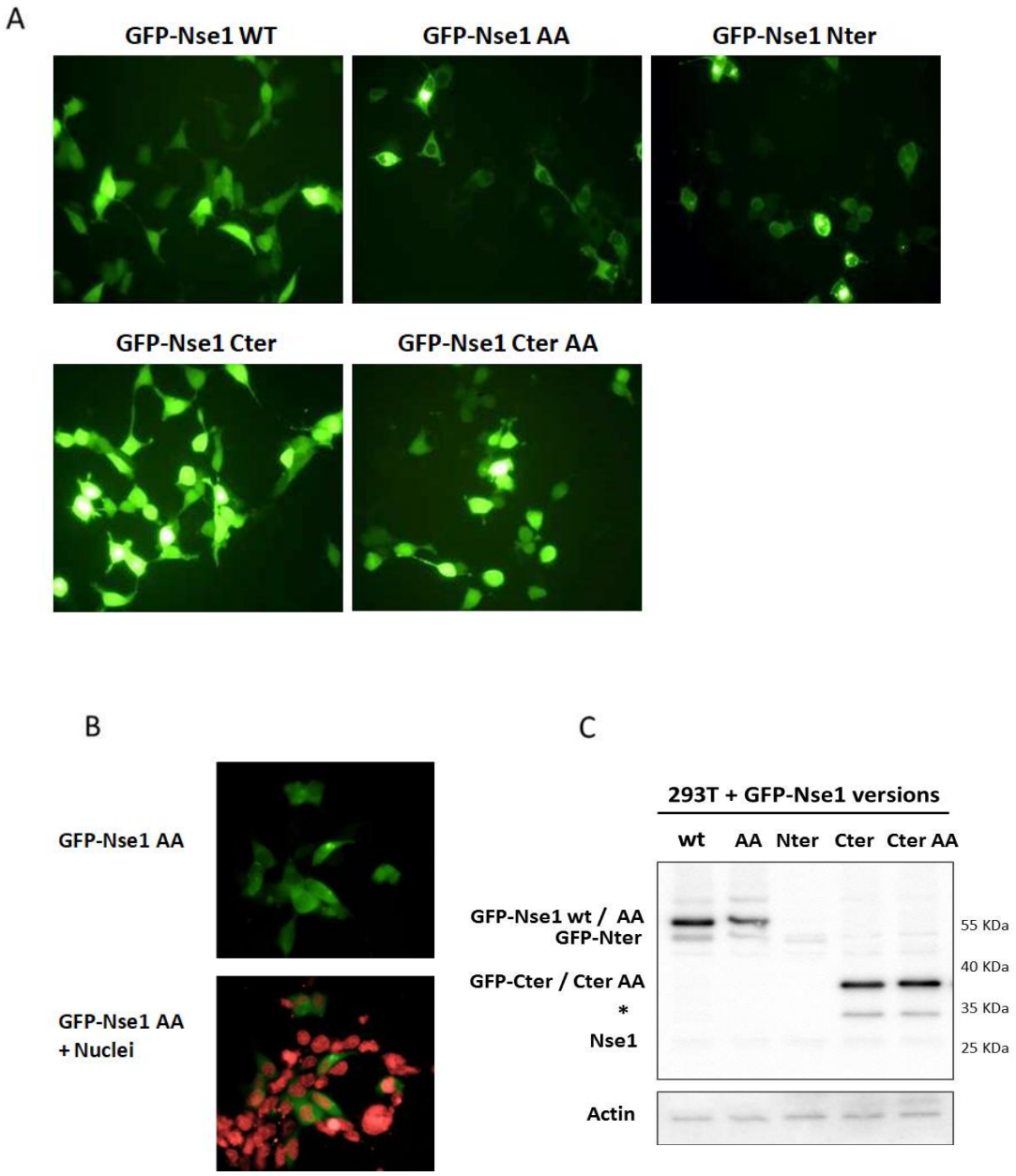

Fig. 17 Mutations on the RING domain alter the subcellular localization of Nse1. A. *In vivo* fluorescence microscopy of 293T cells/truncated mutant cells expressing different versions of fusion proteins GFP-Nse1. AA indicates point mutations on Cysteine (residues C204 and C207) changed to Alanine, either in full length Nse1 or in the Cter part (residues 183-266). Nter includes residues 1-187. GFP-Nse1 and GFP-Cter localize in both cytoplasm and nucleus. The lack of RING domain (Nter) or point mutations on this domain in full length Nse1 (AA) decreases the accumulation of protein into the nucleus. This is not observed when the mutant Cter part of the protein is expressed. B. *In vivo* nuclei staining and fluorescence microscopy in cells expressing full length Nse1 with point mutations on the RING domain (GFP-Nse1 AA), showing that the area with lower accumulation corresponds to the nucleus. C. Western blot analysis of the fusion proteins. The fusion protein with the Nter domain of Nse1 (1-187) (GFP-Nter) shows much lower protein levels, compared to wild type Nse1.

4.2 Rescue of *NSE1* mutants' phenotype by ectopic expression of wild type *NSE1.*

Although the CRISPR-Cas9 system is an accurate method for creating target mutations in the gene, one undesired side effect could be an edition of *loc*i different from the specifically targeted one. Therefore, it is important to determine that the phenotype observed is only due to the edition of the desired gene. Based on this, *NSE1* mutant cells should recover the wild type phenotype if *NSE1* would be expressed in these cells.

As explained above, the phenotype observed for *NSE1* mutants was identical with phenotypes in mutants lacking the Smc5/6 function, as described in the literature. In order to test whether the ectopic expression of *NSE1* can restore wild type phenotype in *NSE1* mutants, we transduced homozygous *NSE1-ΔR* mutant cells with a lentiviral vector that expressed the ORF of human *NSE1* gene under the control of the EF1 alpha promoter. Cells were grown for two days, divided and further grown for four more days. Next, we performed growth curve analysis comparing the cell proliferation during three days in wild type, *NSE1* truncated mutants and *NSE1* truncated mutants complemented with *NSE1* wild type (WT). The result showed that the ectopic expression of *NSE1* almost completely rescued the slow growth phenotype of the mutant cells (Fig.18 A).

We also performed western blot analysis to examine the levels of Nse1, Smc5 and γH2AX in truncated mutants with ectopically expressed *NSE1*. The results demonstrated that Nse1 and Smc5 levels were restored and the levels of γH2AX were reduced, similar to those observed in wild type cells (Fig.18 B). Moreover, we observed that protein levels of other subunits of the complex, such as Smc6 and Nse4A, were also restored. We could also observe that Nse2 was present in mutant cells, indicating that the stability and/or the expression regulation of this subunit behaves differently than the rest. To investigate whether the ectopically expressed *NSE1* in truncated mutants can interact with Smc5 we conducted Nse1 immunopurification (Co-IP). We compared wild type cells, used as positive controls, cells expressing the truncated mutant *NSE1*, as negative controls, and mutant cells with wild type *NSE1*. Our data proved that ectopically expressed Nse1 protein does interact with Smc5 with a similar efficiency as in wild type cells (Fig.19). Based on these findings we can assume that severe phenotypic effects observed in *NSE1* mutants are certainly a result of the loss of Nse1.

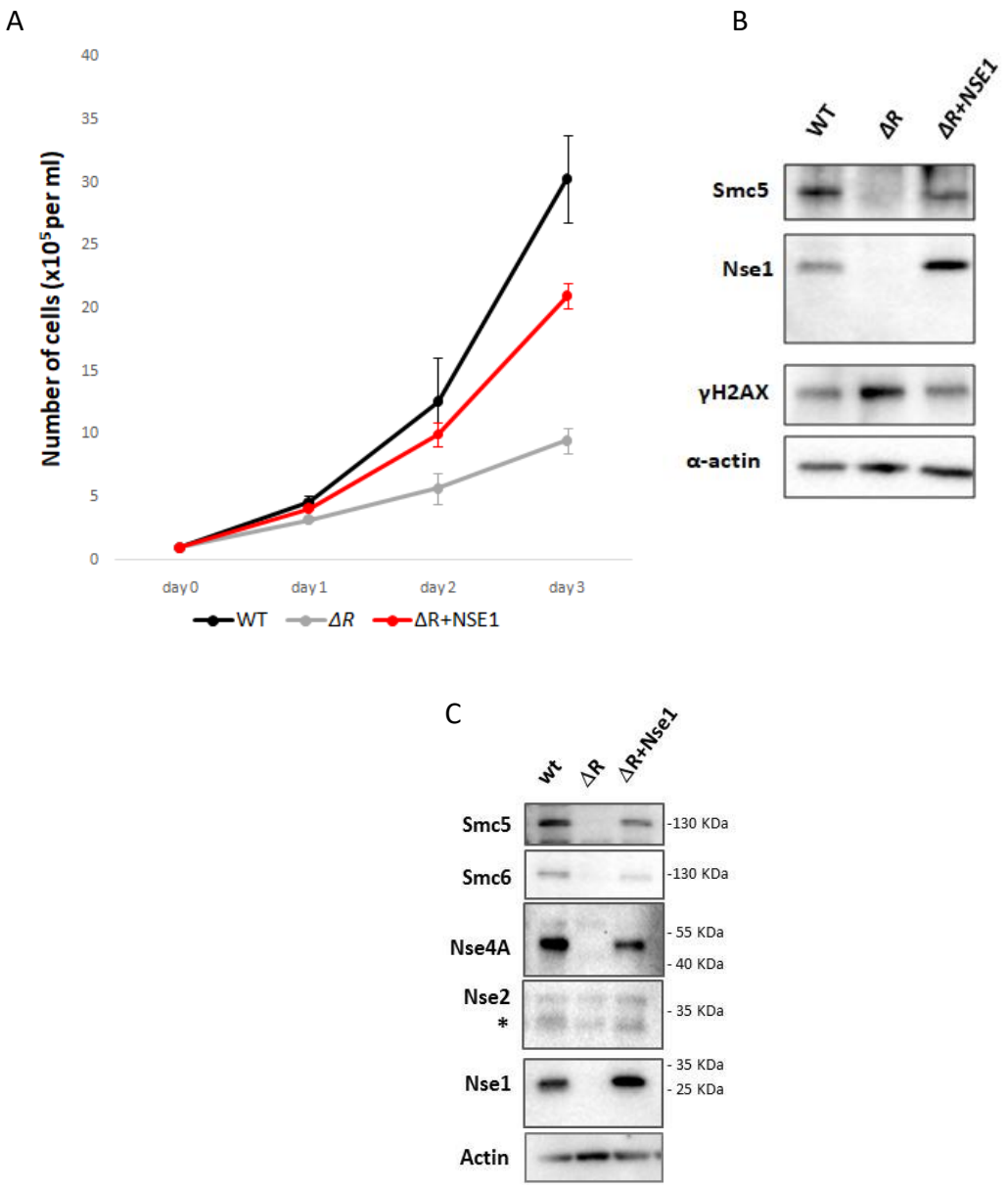

Fig.18 Phenotype rescue of *NSE1* mutant cells by ectopic expression of wild type (WT) *NSE1*. A. The slow growth of *NSE1* mutants is partially recovered after re-expression of Nse1. Growth curve analysis of wild type, *NSE1-ΔR (ΔR)* mutant and *NSE1-ΔR* mutant cells with re-expressed Nse1 (*ΔR+NSE1*). The cell proliferation has been followed for 3 days using Trypan blue (TB) exclusion assay. Values are representative of three independent experiments. B. *NSE1-ΔR* mutant with re-expressed Nse1 recovered Smc5 expression levels and normalize γH2AX levels, similar to those in wild type cells. Western blot analysis of Nse1 in wild type, *NSE1-ΔR* and *NSE1-ΔR* mutant with ectopic expression of wild type *NSE1*, using antibodies against Smc5, Nse1, γH2AX and α-actin as a loading control. C. In addition to Smc5, the ectopic expression of Nse1 recovered the expression of other subunits as Smc6 and Nse4A. Notice that Nse2 levels were maintained in *NSE1* mutants.

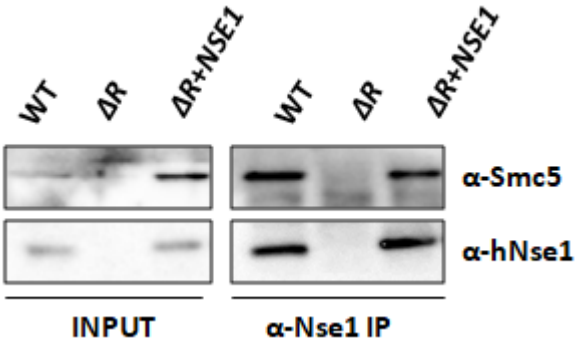

Fig.19 Nse1 immunoprecipitation and interaction between ectopically expressed Nse1 and Smc5 in *NSE1-ΔR* mutant cells. The Nse1 IP clearly shows that after re-expression of Nse1 in mutant cells (ΔR+*NSE1)*, the interaction between both proteins is recovered. Nse1 wild type was ectopically expressed in *NSE1* mutant cells using a lentiviral vector. The cell lysates were immunoprecipitated with anti-human Nse1 antibody and were analyzed by western blot with antibodies against Smc5 and Nse1. Input- soluble sample, IP- immunoprecipitated fraction.

4.2.1 *NSE1* mutant cells are sensitive to genotoxic drugs. Ectopically expressed wild type *NSE1* restores the drug-sensitive phenotype.

Yeast *nse1* RING mutants are hypersensitive to genotoxic stress revealing that Nse1 contributes to the Smc5/6 complex function [Pebernard et al., 2008 (1), Wani et al., 2018]. In order to evaluate whether our *NSE1* mutant cells show higher sensitivity to external DNA damage, we treated wild type cells, truncated *NSE1* mutants, and truncated *NSE1* mutant ectopically expressing wild type *NSE1* gene with the DNA damaging agent, MMS at indicated doses (Fig.20). MMS is an alkylating drug which induces different types of DNA lesions, inhibiting replication and transcription progression [Lundin et al. 2005]. We found that truncated mutant cells displayed hypersensitivity to MMS compared to wild type cells. Our observation is in agreement with previous studies using yeast, plant, chicken and human cells deficient for the Smc5/6 complex [Wani et al., 2018, Diaz et al., 2019, Stephan et al., 2011, Taylor et al., 2008].

The re-introduction of the *NSE1* gene in mutant cells alleviated this sensitivity, indicating that the phenotype observed in *NSE1* mutant cells is directly due to the absence of Nse1 and the Smc5/6 complex, since an important percentage of mutant cells are not capable of recovering their growth after short treatment with the genotoxic drug and further re-seeding. The higher sensitivity of *NSE1* mutants to MMS supports the requirement of the

Smc5/6 complex in homologous recombination (HR) and replication fork restart after exogenous DNA damage.

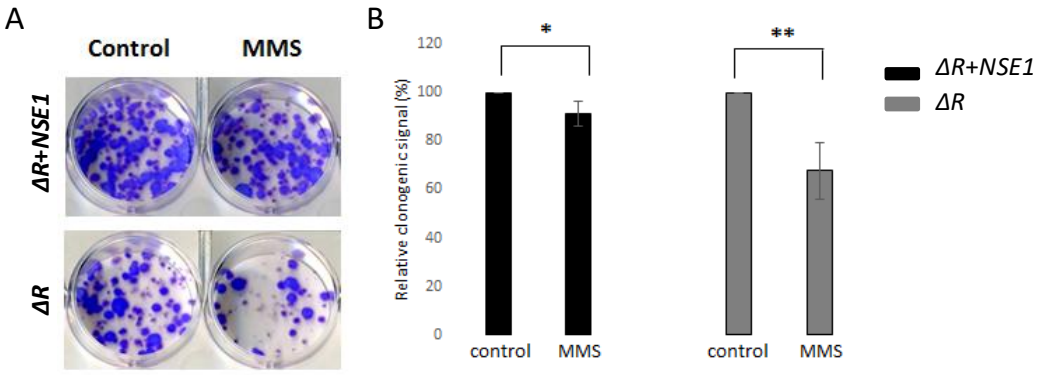

Fig.20 *NSE1-ΔR* mutant cells display differential sensitivity to MMS. Ectopic expression of wild type *NSE1* alleviates this susceptibility. A. Clonogenic survival assay of *NSE1-ΔRING* (*ΔR)* mutant and *NSE1-ΔR* mutant cells with re-expressed Nse1 (*ΔR+*Nse1*)* without and after 10 days of treatment with 250µM MMS for 2 hours. After drug removing, cells were divided and seeded at the same cell density for analyzing the cell survival by measuring the clonogenic signal. B. An average quantification of clonogenic signal intensity relative to control in *NSE1-ΔR* with ectopically expressed *NSE1* and *NSE1-ΔR* mutant cells. The graphs are representative of four independent experiments. Statistical analysis was conducted by One-way ANOVA, using Bonferroni-Holm post-hoc test (*p<0.05, **p<0.01 and ***p<0.001).

4.2.2 *NSE1-ΔR* mutants show a reduction in the number of cells in S phase, which is normalized after expression of *NSE1* wild type.

Based on the observed genome instability phenotype in *NSE1* mutants and since we could only detect slight differences in the distribution of cell cycle phases by FACS and PI staining, we therefore wanted to measure more precisely the cell cycle kinetics in wild type and *NSE1* mutants. To achieve this we used a more sensitive tool, double-staining flow cytometry with PI and bromodeoxyuridine (BrdU), along with mitotic protein monoclonal 2 (MPM-2) detection of different phosphoproteins such as MAP2, HSP70, cdc25 and DNA topoisomerase IIa, most of which are phosphorylated at the onset of mitosis. BrdU is a thymidine analog, which incorporates into the newly synthesized DNA during the S phase. Thus, cells that are in S phase, can be easily distinguished and measured. MPM-2 is a biomarker for mitotic cells, whose increase is a signal for G2/M transition. Similar to our previous flow cytometry analysis, comparing wild type cells, *NSE1-ΔR* mutants and *NSE1-ΔR* with ectopic expression of *NSE1* wild type, we could not detect significant differences in DNA content, stained with PI. Again, we observed an increased number of cells with less than G1 DNA content and more than G2 in truncated mutants, but not in wild type, neither in *NSE1-ΔR* mutants ectopically expressing Nse1 (Fig.21 A). The flow cytometric analysis of BrdU incorporation showed a decrease in the population of BrdU positive cells with ~10% in

NSE1-ΔR mutants, compared to wild type cells and truncated mutants expressing wild type Nse1 (Fig.21 B). The restoration of wild type phenotype in *NSE1-ΔR* mutants led to an increase of the proportion of BrdU positive cells, similar to that in wild type cells. This indicates DNA replication defects in the absence of Nse1. The analysis of MPM-2 activity did not show significant changes in population mitotic cells, comparing wild type cells, *NSE1-ΔR* mutants and Nse1 recovered mutants. The MPM-2 positive cells in *NSE1-ΔR* were few and very similar to those in wild type cells, as well as in Nse1-recovered mutant cells (Fig.21 C), although we could detect prolonged mitotic duration in truncated mutants by live time-lapse microscopy.

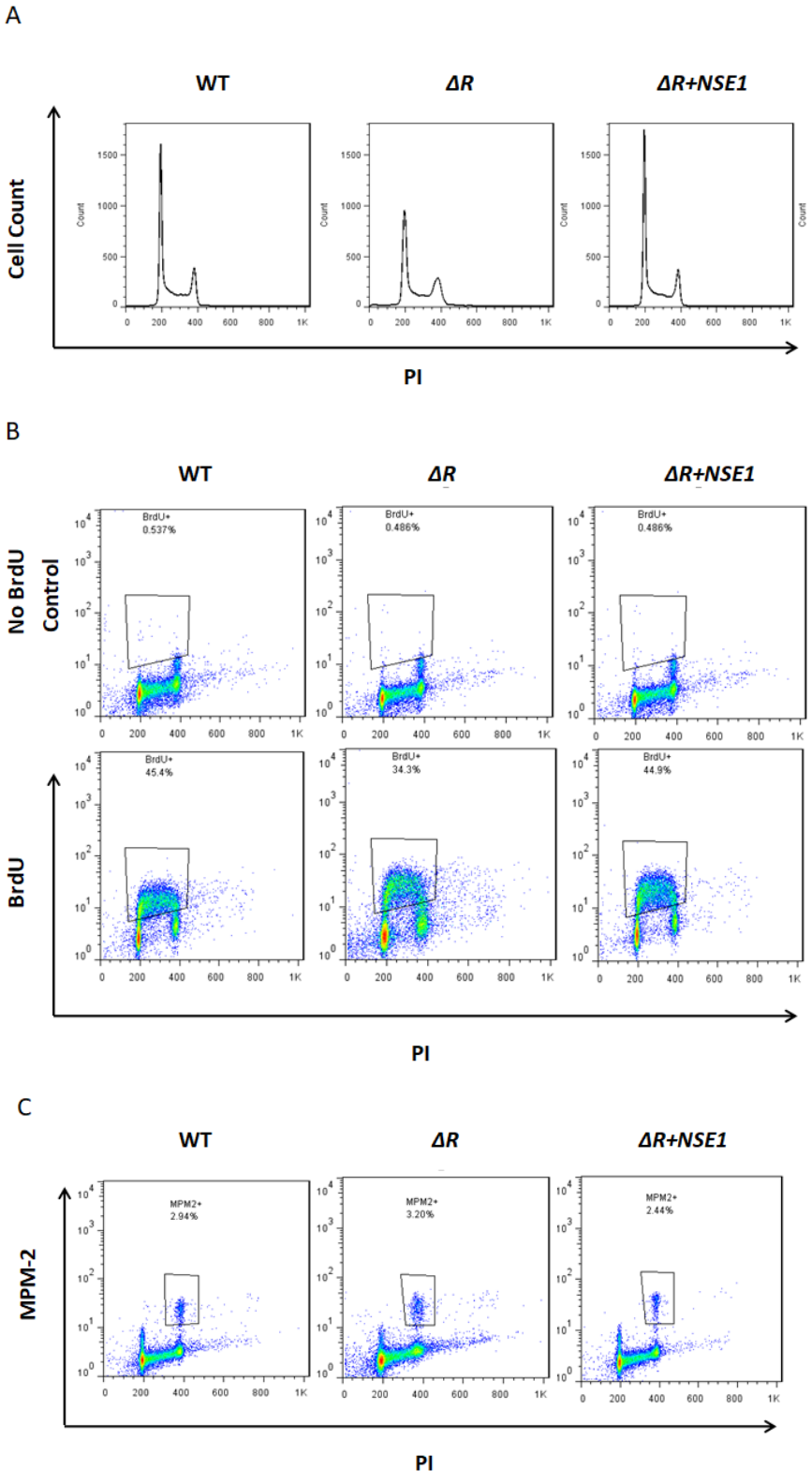

Fig.21 *NSE1-ΔR* mutant cells show a decrease in S phase, but do not exhibit delayed mitotic entry. The ectopic expression of *NSE1* restores the normal S phase progression. Flow cytometry analysis using PI and BrdU, combined with MPM-2 marker. A. Flow cytometric analysis of DNA content by PI staining. B. S phase progression analysis by BrdU incorporation C. Flow cytometry of MPM-2 mitotic activity. MPM-2 specifically recognizes phosphorylated proteins during early mitosis.
Exponentially growing cells at a confluence of 80% (HEK293T - wild type, *NSE1-ΔR* mutant and *NSE1-ΔR+NSE1* wild type were left untreated (used as a control) or treated with BrdU at a concentration of 10μM for 30 minutes. BrdU incorporated cells were subsequently stained with anti-BrdU and anti-MPM-2 antibodies, as well as with PI DNA dye and analyzed by flow cytometry. Histograms indicate the mean of three repetitions (Panel A), flow cytometry plots are representative of three repeats (Panel B and C). *ΔR* corresponds to *NSE1-ΔR, ΔR+NSE1* is referred to as *NSE1-ΔR+NSE1*.

4.2.3 *NSE1-ΔR* mutants exhibit slowdown of replication fork progression. Ectopically expressed *NSE1* restores the normal fork progression.

In order to further study DNA replication in *NSE1-ΔR* mutants and *NSE1-ΔR* mutants complemented with Nse1*,* we performed DNA fiber analysis. The DNA fiber analysis is a useful technique for monitoring the progression and dynamics of DNA replication. The principle of the technique is based on the incorporation of two different thymidine analogs chlorodeoxyuridine (CIdU) and iododeoxyuridine (IdU) into newly synthesized DNA and their detection in the individual DNA molecules by specific fluorochrome-conjugated antibodies. In our analysis, we first pulse-labelled DNA synthesis with CIdU for 30 minutes, followed by 30 minutes labeling with IdU. After cell lysis, the DNA fibers were spread onto glass slides and visualized through immunofluorescence with anti-BrdU antibodies which recognize CIdU in red and IdU in green, indicating the direction of fork movement. The double labeling with CIdU and IdU allows the identification of ongoing forks, replication terminations and new origin firing, as well as the measurement of fork velocity (Fig.22 A). First, we assessed the DNA replication fork progression in wild type, *NSE1-ΔR* mutants and *NSE1-ΔR* mutants with re-expressed *NSE1*. The fork speed was evaluated by measuring the length of the green replication tracks. The result clearly showed that *NSE1-ΔR* mutants displayed slower fork progression, compared to wild type cells. Moreover, ectopically expressed *NSE1* in mutant cells restores fork progression, similar to that in wild type cells (Fig.22 B). This indicates that loss of Nse1 causes DNA replication stress in *NSE1* mutants.

Slowing of replication forks is a hallmark of replication stress and in most cases is a result of intra-S phase checkpoint activation which allows time DNA lesions to be repaired. As a consequence, replication forks are stalled/collapsed or origin firing is suppressed [Iyer and Rhind, 2017].

Therefore, in order to further reveal the cause of the slow DNA synthesis in *NSE1* mutants, we analyzed the replication fork dynamics by quantification of the percentage of ongoing forks, stalled/terminated forks and new origins. *NSE1-ΔR* mutant cells did not show a significant increase in the percentage of stalled/terminated forks, neither a decrease in origin firing, compared to wild type and complemented with Nse1 mutant cells. The quantification of ongoing replication forks also did not show any significant differences, comparing wild type, truncated mutants and Nse1 recovered mutant cells (Fig.22).

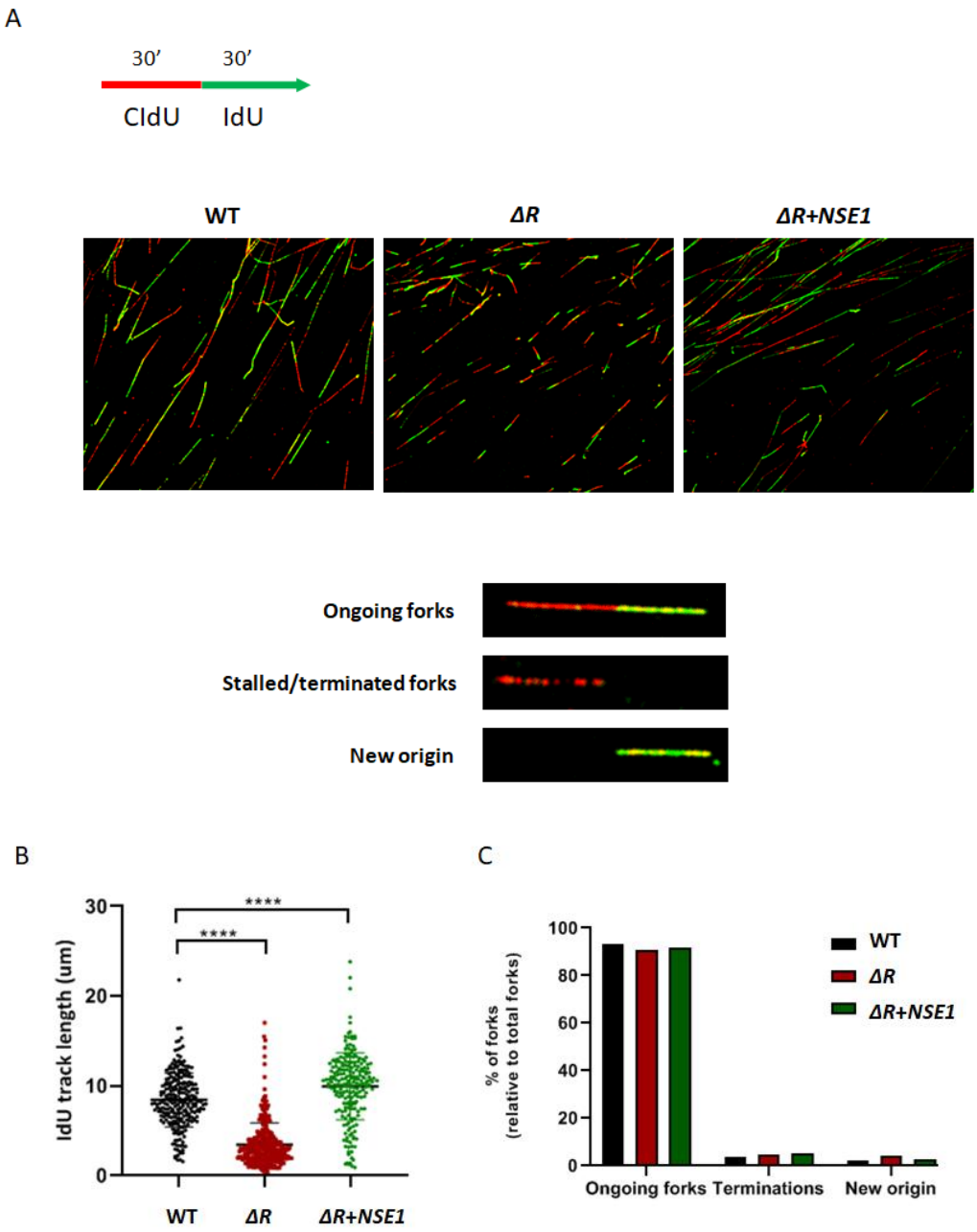

Fig.22 *NSE1-ΔR* mutants show slower replication fork progression. Ectopic expression of *NSE1* suppresses the replication fork slowdown. A. Experimental design of DNA fiber analysis. HEK293T (WT), *NSE1-ΔR* mutants and *NSE1-ΔR*+Nse1 cells were pulse-labelled with CIdU (25μM) for 30 minutes, washed with PBS and pulse-labelled with IdU (250μM). Cells were harvested and lysed. The obtained DNA fibers were spread onto glass slides, fixed and immunostained with anti-BrdU which recognizes CIdU (red) and IdU (green), respectively. The

DNA fibers were visualized by fluorescent confocal microscopy. Representative images of DNA fibers are shown in the upper panel. B. Analysis of replication fork rate. *NSE1-ΔR* mutants exhibit a significant slower fork progression, compared to WT. The ectopic expression of *NSE1* wild type in truncated mutants normalizes the fork speed, similar to that in WT. The length of the green tracks (IdU) was measured by ImageJ Software (NIH, USA). Each dot represents one DNA fiber. More than 200 DNA fibers were counted per each cell line. C. Analysis of replication fork dynamics. There were no significant changes in fork dynamics between WT, *NSE1-ΔR* mutants and recovered with Nse1 mutant cells. The ongoing replication forks, stalled/terminated forks and new origin firing were characterized and evaluated using ImageJ Software (NIH, USA). More than 500 events were counted per each cell line. *ΔR* corresponds to *NSE1-ΔR, ΔR+*Nse1 is referred to as *NSE1-ΔR*+Nse1. Both graphs are representative of three independent experiments. Statistical analysis was performed by Mann-Whitney test (*p<0.05, **p<0.01 and ***p<0.001) using GraphPad Prism Software.

These results correspond to one of the three repetitions that were performed. In the other two experiments differences between wild type and mutant cells were maintained but, due to the labour-intensity of the method, values obtained in mutant cells with ectopic expression of *NSE1*, could not be compared. Although our result was unexpected, it supports our previous notion that probably *NSE1* mutants accumulate moderate levels of DNA damage that might not be able to activate surveillance mechanisms.

4.3 Genetic interaction between Smc5 and FANCM - Mph1 orthologue.

The Smc5/6 complex is involved in homologous recombination repair and stabilization of stalled replication forks [Palecek, 2019]. In *Saccharomyces cerevisiae*, Smc5 physically interacts with Mph1, a DNA helicase that triggers fork regression at stalled replication forks and inhibits mitotic crossover events, resulting from DNA DSBs. Smc5 regulates Mph1 by preventing the formation of recombination intermediates. Yeast cells with mutations in the Smc5/6 complex showed high levels of X-shaped DNA molecules and hypersensitivity to DNA damage drugs, whereas the inactivation of Mph1 in these mutants reduced the recombination intermediates incidence and recovered the slow growth without and after DNA damage induction [Chen et al., 2009]. Mph1 is a homolog of human FANCM (Fanconi anemia M) protein which has a crucial role in interstrand-crosslink repair. Mutations in FANCM are associated with Fanconi anemia, a rare genetic disease characterized by defects in development, bone marrow failure and cancer predisposition [Ceccaldi et al.,2016]. Currently, it is unknown whether the functional interaction between Smc5 and Mph1 is conserved in higher eukaryotes or not.

Since the mutant cell lines we had generated showed endogenous DNA damage and genomic instability hallmarks, we analyzed whether the down-regulation of FANCM would alleviate these phenotypes. For this purpose, expression of FANCM was downregulated with a specific siRNA [Castella et al., 2015] for 72 hours, either in wild type or in *NSE1* mutant cells (expressing ΔR mutant). By Real time PCR (RT-PCR) we observed that treatment with the specific siRNA caused a 70% reduction in FANCM mRNA levels. Samples were fixed and

stained with DAPI and their nuclei morphology was analyzed. We quantified the frequency of micronuclei as a marker for genomic instability, as well as the presence of fragmented nuclei or very big nuclei, that we grouped as abnormal nuclei (Fig. 23 A).

The frequency of DNA bridges was analyzed as a marker for the impairment of DNA repair or replication. We observed that in wild type 293T cells and in mutants that ectopically expressed *NSE1*, the downregulation of FANCM did not significantly increase, neither decrease, the levels of the different markers quantified (Fig. 23 B and C). As previously mentioned, mutants showed higher levels of micronuclei and DNA bridges in anaphase or telophase, than wild type or mutant cells ectopically expressing *NSE1*. In addition, we observed a higher frequency of abnormal nuclei. The downregulation of FANCM in *NSE1* mutants caused a significant increase in the frequency of abnormal nuclei, compared to mutants not treated with siRNA (Student T test). Although the rest of markers did not show a significant change, all of them increased as well.

A

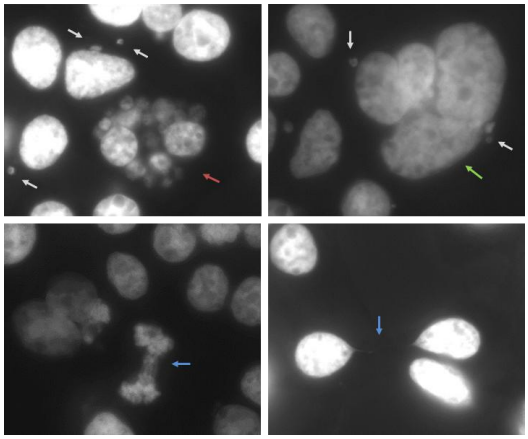

B

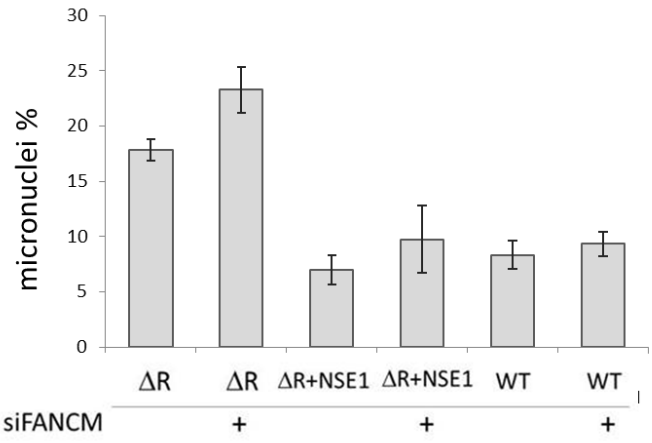

C

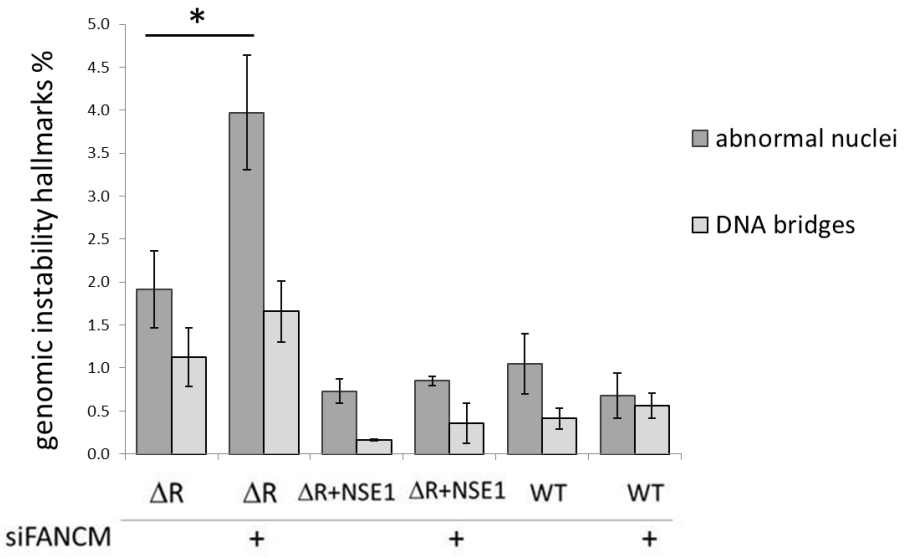

Fig. 23 Down-regulation of FANCM is deleterious in *NSE1* mutant cells. Wild type 293T cells, mutant *NSE1ΔR* cells, or mutant cells with ectopic expression of wild type Nse1, were transfected with a specific siRNA to down-regulate FANCM expression and were compared with not transfected cells. After 72 hours, DNA was stained with DAPI and nuclei morphology was analyzed. A. Fluorescence microscopy images of mutant *NSE1ΔR* cells, treated with FANCM siRNA. White arrows indicate the presence of micronuclei, magenta arrow points out a fragmented nucleus, green arrow shows an aberrant nucleus, and blue arrows indicate an anaphase (left) and a post-telophase (right) DNA bridge. B. A quantification of micronuclei frequency in all cell lines analyzed. Double mutant cells show a higher number of micronuclei, compared to wild type 293T cells or mutant cells expressing wild type NSE1. FANCM downregulation did not significantly increase the frequency of micronuclei. C. A quantification of abnormal nuclei (dark grey) and DNA bridges (light grey) frequencies in all cell lines analyzed. Student-T test analysis showed a significant increase in the frequency of abnormal nuclei when mutant *NSE1ΔR* cells were treated with FANCM siRNA ($p<0.05$). The downregulation of FANCM did not imply any significant change in wild type 293T cells or mutant cells with ectopic expression of wild type NSE1. Three independent experiments were analyzed and 500 nuclei were quantified in each sample. Mean and SEM values are represented.

This result indicated that *NSE1* mutants depleted for FANCM accumulated higher levels of genomic instability and DNA damage hallmarks, instead of diminishing them. This would suggest that in human cells, *FANCM* depletion would not rescue the phenotype of *SMC5/6* mutants and, therefore, *SMC5* would not directly regulate *FANCM* activity, as observed in budding yeast.

Since our result was in contradiction with what has previously been described in yeast, and in order to further confirm this result in human cells, we used different human cells as a model system.

To evaluate the genetic interactions between Smc5/6 complex and FANCM in another human cell line we used primary fibroblasts, originally derived from a patient with a FANCM homozygous mutation (described in materials and methods) kindly provided by Prof. Dr. Jordi Surrallés. Since FANCM protein was not detected by western blot, cells were further named as FANCM knockout (KO). FANCM expression was re-established by transduction of

a lentiviral vector expressing FANCM wild-type under the control of doxycycline (1µg/ml) using Tet-ON 3G expression system. Due to the endogenous DNA damage, FANCM KO cells exhibit a slight decrease in cell viability and cell morphology changes such as bigger cells compared to normal wild type fibroblasts. In this approach, we transduced human fibroblasts, wild type or KO for FANCM, with the lentiviral vector expressing a shRNA against SMC5 (pLKO1Neo-shSMC5). The SMC5 shRNA has been validated ensuring minimization of off-target effects and complete gene knockdown. Both fibroblasts lines were also transduced with a lentiviral vector expressing a scrambled shRNA (pLKO1Neo-shcontrol) and were used as controls.

4.3.1 Depletion of Smc5 in FANCM KO results in synthetic sickness.

After 10 days of a selection with Neomycin, we performed growth curve analysis and immunoblotting with anti-Smc5 antibody in parallel, comparing wild type and FANCM mutant cells depleted or not for Smc5. Although we do not show these results in the thesis, in a first attempt, the western blot analysis showed that the expression level of Smc5 was partially reduced (Smc5 was downregulated ~70%), compared to controls, and cell proliferation analysis followed for 3 days indicated a slower growth in wild type cells partially depleted for Smc5 in comparison with wild type control cells. Moreover, a higher inhibition of cell proliferation was observed in FANCM KO cells with partially reduced Smc5. Surprisingly, in contrast to what has been observed in *smc5/6* mutant yeast cells depleted for Mph1, our data suggested that in human cells FANCM mutants showed synthetic sickness in combination with partially impaired Smc5/6 complex. Next, we analyzed the nuclear morphology by DAPI staining. The reduction of Smc5 induced a high number of micronuclei, aberrant nuclei and cytokinetic bridges in FANCM WT cells and dramatically raised the frequency of these markers in FANCM KO, compared with control cells.

To give more insight into the genetic interaction between FANCM and Smc5, we used human fibroblasts FANCM WT and KO, completely deficient or not for the Smc5. We noticed that, when we were selecting cells for 10 days, as recommended, FANCM KO cells completely deficient for Smc5 failed to undergo cell division, and FANCM WT lacking Smc5, exhibited extremely slow growth. Therefore, we repeated exactly the same experiment but resistant cells were selected for 5 days with 800µg/ml Neomycin, which was enough for complete downregulation of Smc5, and we maintained the selection antibiotic at low concentration in all samples during the phenotype analysis. Three independent experiments were conducted and although we could not find statistical differences in the growth curves (Fig. 24 A), it is worth noting that double mutants (FANCM KO, shSMC5) showed a slower growth rate regarding single mutants in all repetitions. Clearly, cell proliferation was more affected in double mutants, which also displayed a higher percentage of genomic instability hallmarks. The same tendency could be observed in all of the experiments. One representative experiment is shown in Fig. 24 B and C, and Fig.25. We performed western blot using anti-Smc5 antibody to confirm that the expression level of Smc5 were reduced and then, we conducted growth curve analysis. The immunoblot showed a complete loss of

Smc5 in FANCM WT and KO transduced with plasmid expressing *SMC5* shRNA, compared to controls (Fig.25 C). The growth curve result demonstrated that the loss of Smc5 reduces cell proliferation in FANCM WT and strongly inhibited it in FANCM KO, as they grew extremely slow, compared to control cells (Fig. 24 A). To measure cell death in these mutants we used Trypan blue assay. The result clearly showed that on the 3rd and 4th days of growth FANCM WT deficient for Smc5 showed a high death rate whereas the percentage of cell death in FANCM KO cells depleted for Smc5 was even higher (~25%), compared to control cells, where it was less than 10% (Fig.24 B). As mentioned above, it should be taken into account that after three passages, FANCM KO cells lacking Smc5 failed to undergo cell division and FANCM WT lacking Smc5 exhibited extremely slow growth.

To further characterize the cellular phenotype of wild type and FANCM KO fibroblasts deficient for Smc5 we used DAPI staining to score changes in nuclear morphology. Our results demonstrated an increase in the number of cells with micronuclei in FANCM WT depleted for Smc5 and in FANCM KO lacking Smc5, compared to control cells (Fig.25 A). Also, we observed an increased number of cells with cytoplasmic bridges in both types of cells with impaired Smc5/6 complex, which was again raised in FANCM and Smc5 deficient fibroblasts (Fig. 25 A). Cytoplasmic bridges between daughter cells, with the presence of DNA bridges in them, appeared as a result of cytokinesis failure. These DNA bridges would lead to defects in chromosome segregation and production of aneuploidy cells. In addition, we detected a significant increase of abnormal nuclei in FANCM KO cells depleted for Smc5 compared to FANCM WT cells, comparing three independent experiments. These abnormal nuclei included fragmented and big nuclei (at least 3 fold bigger than the mean nuclei size in FANCM WT samples). The number of aberrant nuclei in FANCM WT cells depleted for Smc5 was similar to that in FANCM KO cells and higher than FANCM WT cells (Fig. 25 A), but lower than double mutant cells. In order to have an objective way to measure and quantify the aberrant shape of nuclei, we used ImageJ software and circularity measure as a reference. Nuclei with ellipsoidal shape got a high score in circulariy and elongated or lobulated nuclei got a low score. We observed that in double mutants, circularity values were always lower than in the rest of samples. An example of nuclei with low or high values in circularity is also shown (Fig. 25 B). Taken together, our results emphasize a synthetic sickness interaction between FANCM and Smc5 indicating that both proteins exert independent functions in DNA repair machinery and are essential for the maintenance of genomic stability in human cells.

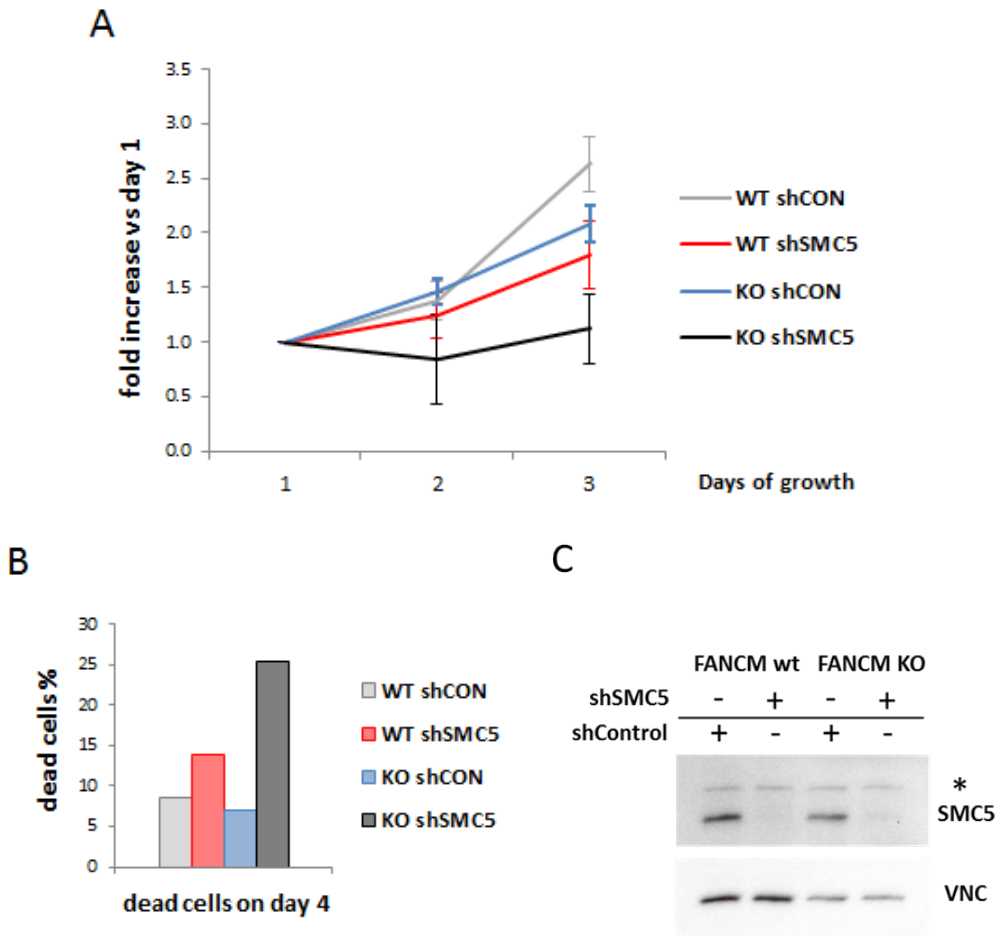

Fig.24 Depletion of Smc5 induces a severe genomic instability in FANCM WT and synthetic sick phenotype in FANCM KO. A. Growth curve analysis of FANCM WT and FANCM KO depleted or not for SMC5. Human fibroblasts wild type (WT) or knockout (KO) for FANCM were transduced with lentiviruses expressing SMC5 shRNA or scrambled shRNA control. Cell proliferation was followed during 3 days using Trypan blue (TB) exclusion assay. The downregulation of SMC5 reduces the growth of FANCM WT and this reduction is stronger in FANCM KO cells compared to controls. Means and SD from three independent experiments are shown.B. FANCM WT+ shSMC5 and FANCM KO + shSMC5 show an increased rate of cell death in comparison with controls. The percentage of cell death has been evaluated by Trypan blue assay. Results from one representative experiment are shown. C. Western blot analysis of FANCM WT shControl, FANCM WT + shSMC5 and FANCM KO + shSMC5 using anti-Smc5 and anti-Vinculin antibodies. Wild type and FANCM KO cells + shSMC5 show no expression level of Smc5.

A

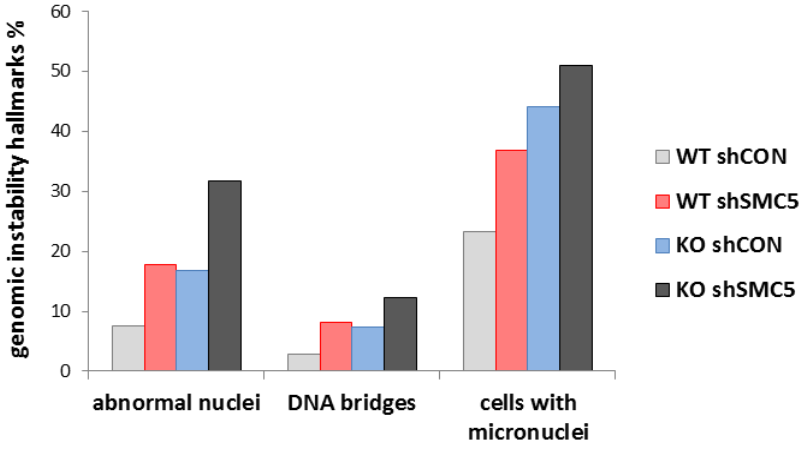
genomic instability hallmarks %
60
50
40
30
20
10
0
abnormal nuclei
DNA bridges
cells with micronuclei
WT shCON
WT shSMC5
KO shCON
KO shSMC5

B

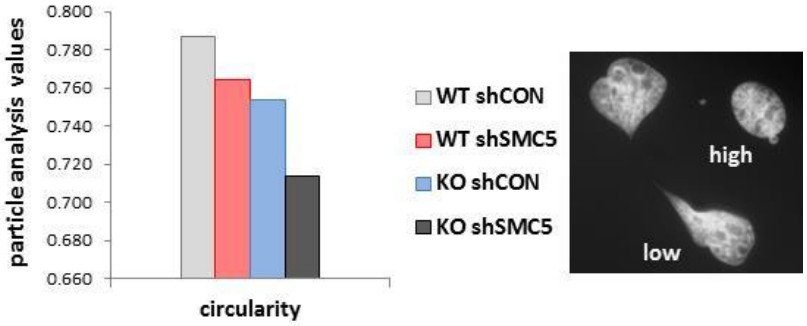
particle analysis values
0.800
0.780
0.760
0.740
0.720
0.700
0.680
0.660
circularity
WT shCON
WT shSMC5
KO shCON
KO shSMC5
high
low

C

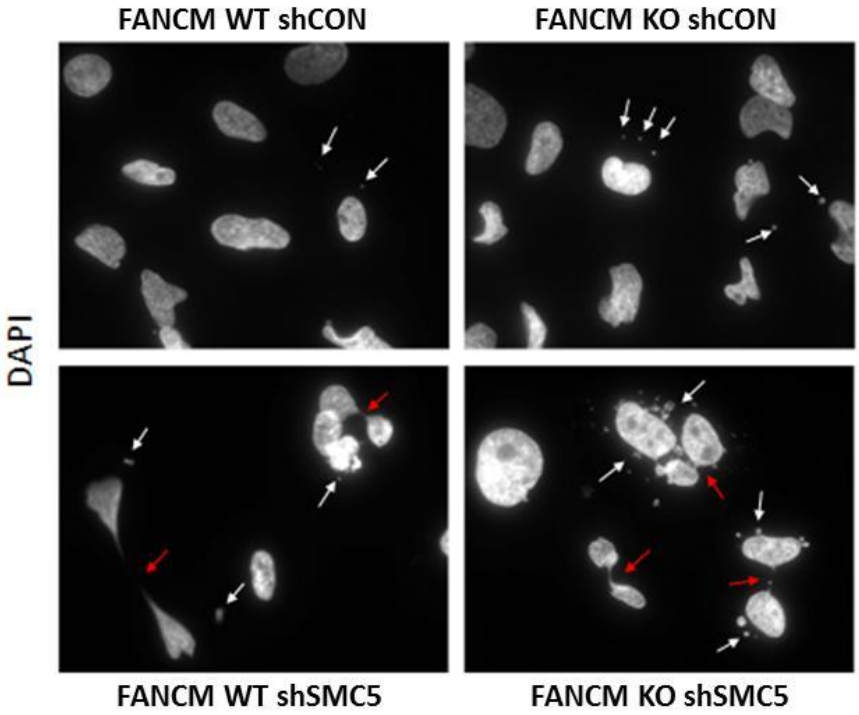
FANCM WT shCON
FANCM KO shCON
DAPI
FANCM WT shSMC5
FANCM KO shSMC5

Fig.25 The depletion of Smc5 in FANCM KO and FANCM WT show increased level of chromosome instability
A. A representative experiment for the quantification of the number of cells with abnormal nuclei, DNA bridges and micronuclei in FANCM WT and FANCM KO, depleted or not for Smc5. 250 cells were counted in each condition. B. Circularity measure of nuclei using ImageJ software. Particle analysis data are shown from 100 cells counted in each condition. Examples of a nucleus with a low score for circularity and another one with a high score are shown. Nuclei were stained with Hoescht. C. Microscopic photographs of FANCM WT and FANCM KO depleted or not for SMC5. White arrows indicate the micronuclei formation and red arrows point to DNA bridges. The nuclei were stained with DAPI. Images are obtained with 60x objective.

4.4. Identification of novel proteins interacting with human Nse1 using yeast two-hybrid screen.

Currently, Nse1 is known to interact with Nse3 in the Smc5/6 complex. Outside the Smc5/6 complex, only one physical interactor of Nse1 in human cells has been described, MAGE-F1, *in vitro* and *in vivo* [Hudson et al., 2011, Weon et al., 2018]. Therefore, to give more insight of Nse1 function, we performed yeast two hybrid assay for detecting novel interacting partners of human Nse1.

A yeast two hybrid screen was performed by cloning the cDNA of human *NSE1* (also named *NSMCE1*) into a vector that expressed the fusion to Gal4 DNA-binding domain, used as "bait". A mouse embryonic cDNA library cloned into vectors that expressed the fusion to Gal4 activation domain were used as "preys". The specific interaction of "bait" and "prey" proteins allows growth on selective medium lacking histidine. To select only the strong interactors, the obtained colonies were grown in high stringency conditions lacking histidine and adenine (Fig.26). To identify the potential candidates we further conducted colony PCR and subsequent DNA sequencing. Some candidates were identified as positive interactors from which TRUSS, HMG-17 and LRPAP1 were detected more than once (Table 1).

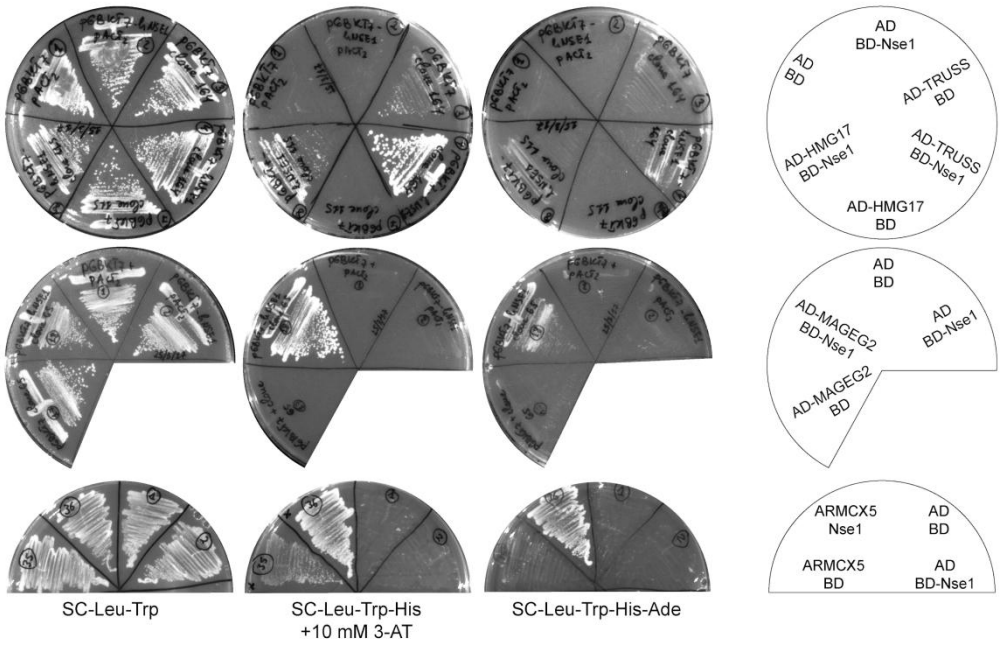

Fig.26 Validation of the observed interactions in the yeast two-hybrid assay by mating. Selection of only strong interactors by plating the obtained colonies in high stringency conditions lacking histidine and adenine. HMG-17, TRUSS (A), MAGEg2 (B) and ARMCX5 (C) were some of the identified positive interactors of hNse1. Nse1 cDNA was cloned into a vector containing the Gal4 DNA-binding domain (BD), that is used as a "bait". Interactor candidates were fused to Gal4 activation domain (AD) (mouse embryonic cDNA library) used as a "prey".

Table 1. List of proteins that specifically interact with human Nse1. Abbreviations, complete names, number of independent clones showing the specific interaction, as well as the specific function of the proteins are shown in the table.

Positive interactor	Number of clones	Function
TRUSS Tumor necrosis factor receptor (TNF-R)-associated ubiquitous scaffolding and signaling protein	**3**	Protein ubiquitination
HMG-17 (HMGN2) Non-histone chromosomal protein	**3**	Regulation of transcription, replication, recombination and DNA repair
MAGE-G2 Melanoma-associated antigen G2	**1**	A testis-specific protein, highly homologous to MAGE-G1 (Nse3), of unknown function

VPS41 Vacuolar protein sorting 41	**1**	Vacuolar assembly and vacuolar traffic/ sorting of proteins into vacuoles
LRPAP1 Low density lipoprotein receptor-related protein associated protein 1	**5**	Endocytosis and phagocytosis
ARMCX5 Armadillo Repeat Containing X-Linked 5	**1**	Unknown function

4.4.1 Nse1 physically interacts with TRUSS and HMG-17

From all of the identified proteins that interact specifically with human Nse1 (NSE1), we focused only on TRUSS and HMG-17 which could be probably associated with the Smc5/6 complex function. TRUSS protein (Tumor necrosis factor receptor-associated ubiquitous scaffolding and signaling protein) also known as TRPC4-associated protein (TRPC4AP) is a big scaffolding protein that can promote ubiquitylation and degradation of different proteins. However, its regulation still remains unclear. TRUSS is part from the DDB1-CUL4A E3 ligase complex and targets the oncoprotein c-Myc for degradation [Choi et al. 2010]. Additionally, it can interact with IκBα kinase (IKK), triggering its degradation and leading to activation of the nuclear factor-κB (NF-κB) immune signaling pathway [Terry Powers et al. 2010, Yu et al. 2018]. As well as, TRUSS can interact with TNF receptor associated factor-2 (TRAF2), a RING E3 ligase which also regulates TNF immune pathway [Au et al. 2007]. These interactions indicate a role of TRUSS in cell survival, immune- and inflammatory responses. Besides, it has been found that Skp2 E3 ligase triggers TRUSS for degradation, but in the presence of the hepatitis B viral protein, HBx, the degradation of TRUSS is abolished and the protein is stabilized [Jamal et al. 2015]. On the other hand, recently it has been reported that the Smc5/6 complex is a restriction factor for hepatitis B virus, binding the viral episomal DNA and avoiding transcription, and thus preventing the infection. Interestingly, the viral protein HBx leads to degradation of the Smc5/6 complex [Decorsière et al. 2016]. We can speculate that a functional interaction among these proteins could exist.

The functional relationship between human Nse1 and the non-histone chromosomal protein HMG-17 is probably due to the role of HMG-17 in DNA replication, recombination and DNA repair [Hock et al. 1998]. It has been found that HMG-17 (HMGN2) takes part in nucleotide excision repair (NER) pathway supposing that it facilitates the ability of DNA repair proteins to access and repair the DNA lesion. It is known that HMG-17 undergoes different post-translational modifications which regulate its function. Apart from phosphorylation and acetylation, it has been demonstrated that HMG-17 can also be SUMOylated. At present, there is no evidence if HMG-17 can be modified by ubiquitin [Subramanian et al. 2009, Wu et al. 2014 (1)].

The other interactors of Nse1 have distinct functions, predominantly in the cytoplasm of cells. It has been described that in human cells, overexpressed Nse1 is localized not only in the nucleus but also into cytoplasm vesicles [Hou et al. 2012], supposing that Nse1 can exhibit other functions independently from the Smc5/6 complex. This could explain the interaction of Nse1 with TRUSS, which is localized in the cytoplasm, and the rest of the interacting proteins that are involved in vacuolar traffic and endocytosis. In order to further study the function of Nse1 within the Smc5/6 complex we started to validate the interactions between Nse1 and TRUSS and Nse1 and HMG-17 in human cells.

4.4.2 Validation of Y2H interactions *in vivo*

To confirm the observed interactions from yeast two-hybrid screening, we performed immunoprecipitations (IP) on protein extracts from human cells. First, we confirmed that we could observe the interaction between Nse1 and the previously known interactor Nse3. In HEK293T cells a FLAG-tagged version of mouse Nse3 (NDNL2) was overexpressed. We either immunoprecipitated Nse3 using an anti-FLAG antibody, or we conducted an IP against the endogenous Nse1. In both cases we could detect the interaction between Nse1 and Nse3 (Fig.27).

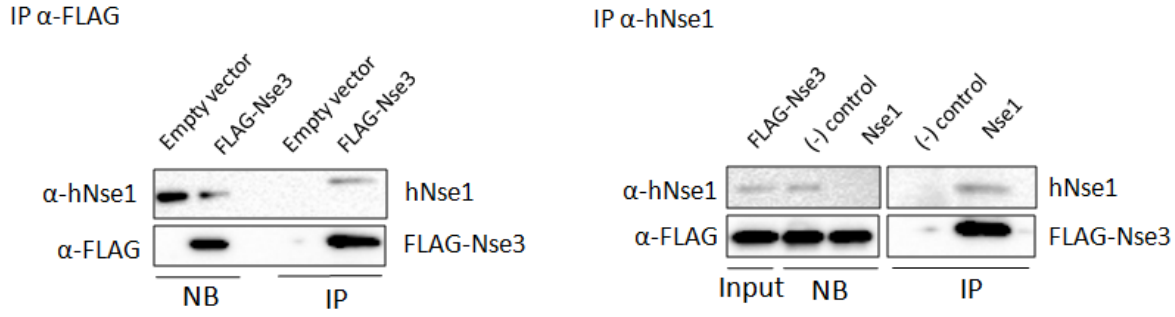

Fig.27 Confirmation of Nse1 and Nse3 interaction *in vivo* by co-immunoprecipitation (Co-IP). Nse1 interacts with Nse3. A- IP anti FLAG; B- IP anti Nse1. HEK293T cells were transfected with a plasmid encoding FLAG-epitope tagged Nse3 or with an empty plasmid. The cell lysates were immunoprecipitated with anti-FLAG beads (A) or anti-human Nse1 antibody (B), and were analyzed by western blot with antibodies against hNse1 and FLAG. NB - non bound sample, Input- soluble sample, IP – immunoprecipitated fraction.

Next, we started to verify the interactions between Nse1 and TRUSS or HMG-17. We co-expressed either TRUSS or HMG-17, tagged with a 3HA epitope and GFP-tagged Nse1 in HEK293T cells. Then, cells were lysed and proteins were immunoprecipitated with anti-HA agarose beads, followed by western blot analysis using antibodies against HA and Nse1. Our results confirmed that Nse1 can interact specifically with both proteins *in vivo* (Fig.28).

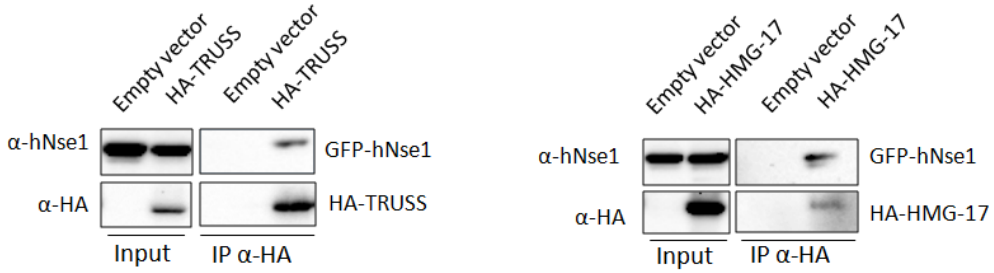

Fig.28 Confirmation of the interaction between Nse1 and TRUSS or HMG-17 *in vivo* by co-immunoprecipitation (Co-IP) in human cells . Nse1 interacts specifically with TRUSS and HMG-17. HEK293T cells were co-transfected with plasmids encoding HA-epitope tagged TRUSS or HMG-17 and GFP-tagged Nse1. The transfection with empty plasmid was used as a control. The cell lysates were immunoprecipitated with anti-HA agarose beads and subjected to western blot analysis using anti-hNse1 and anti-HA antibodies. Input - soluble sample, IP- immunoprecipitated fraction.

4.4.3 Nse1 interacts with different domains of TRUSS

To reveal which region of TRUSS is required for the interaction with Nse1 we used different deletion mutants of TRUSS and we performed Co-IP. The results demonstrated that Nse1 can interact with all of the mutated constructs (Fig.29). The Y2H result and subsequent sequencing showed that Nse1 interact with the middle domain of TRUSS (residues 342-642) *in vitro*, but the exogenous immunoprecipitation analysis indicated that Nse1 can interact physically with different regions of TRUSS *in vivo* (residues 1-147, 1-383, 73-284, 73-537, 73-797 and 539-797). However, it seems that when Nse1 interacts with the N-terminal part of TRUSS (residues 1-147 and 1-383), as well as with the C-terminal residues (539-797) the interaction is a bit stronger, in comparison with the interaction between Nse1 with TRUSS residues (73-284, 73-537 and 73-797). The experiment has been repeated two times and the same result has been obtained. This unexpected result could be explained by the fact that both proteins were over-expressed and therefore, the conditions differ from the physiological ones in living cells. It has been described that TRUSS can interact with TRAF2 through an interface that implies different domains of TRUSS [Terry Powers et al., 2010]. Based on this, several fragments of TRUSS are necessary for the interaction of both proteins. Similarly, our result could reflect that the interaction with Nse1 also requires different domains of TRUSS.

Regarding the ratio of HA-TRUSS that was purified and the levels of GFP-Nse1 that were co-purified, we could infer that, although the Y2H interaction was detected with the C-terminal half of TRUSS, in this experiment the N-terminal half seems to be more efficient in binding to Nse1.

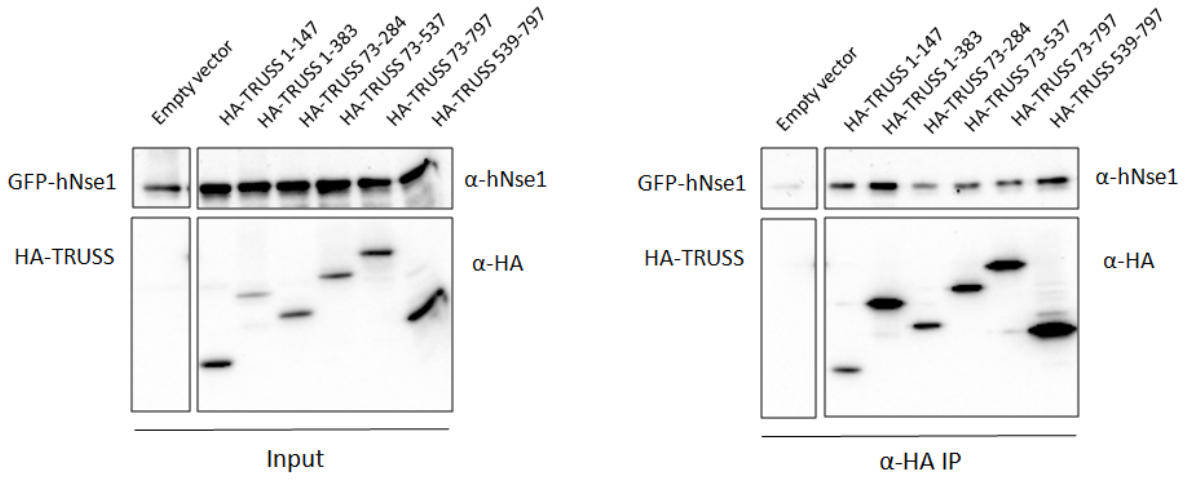

Fig.29 Nse1 interacts with different domains of TRUSS. Co-immunoprecipitation of Nse1 of TRUSS deletion versions. HEK293T cells were co-transfected with plasmids encoding HA-epitope tagged TRUSS deletion constructs and GFP-tagged Nse1 or with empty plasmid. The cell lysates were immunoprecipitated using anti-HA agarose beads and were analyzed by western blot with antibodies against human Nse1 and HA. Numbers indicate the residues included in each deletion version. Input - soluble sample, IP – immunoprecipitated fraction.

4.4.4 TRUSS interacts with the N-terminal domain of Nse1

To reveal which region of Nse1 was necessary for the interaction with TRUSS, we created two Nse1 mutant constructs: one lacking the RING domain (N-terminal (Nter), residues 1 to 187) and the other containing the RING domain, residues 188 to 234, and the rest of C-terminal residues, next to the RING (Cter, 183 to 266). In this experiment we used a previously generated by CRISPR-Cas9 cell line derived from HEK293T, where cells express a truncated version of Nse1, lacking the C-terminal part (explained in the previous section of results). The Co-IP analysis showed that TRUSS interacts with the full length Nse1 and Nter domain, but very weakly with the Cter domain of Nse1 (Fig. 30 A). As observed in Input samples, levels of the Nter fusion were much lower than Nse1 or the Cter domain, indicating that the fusion protein GFP-Nse1 Nter is more unstable and/or less soluble. However, the levels of co-immunopurification were similar to Nse1, indicating that Nter domain is sufficient for interacting with TRUSS, and suggesting that maybe this interaction could be even stronger. Using fluorescent microscopy, we tested the subcellular localization of Nse1. The microscopic analysis demonstrated that the overexpressed GFP-Nse1 is localized all over the cell, but when TRUSS is co-expressed, big foci are formed, indicating that TRUSS binds and accumulates Nse1 at discrete points in the cytoplasm. The same effect was observed when GFP-Nter fusion was co-expressed with TRUSS. It should be noted that Nter part of Nse1 has shown a more cytoplasmic localization than full length Nse1, and has a tendency to aggregate in the cytoplasm, although the presence of TRUSS exacerbated this fact. The GFP-Cter fusion protein did not show foci, accumulated in cytoplasm when TRUSS

was co-expressed, as expected, since in IP experiments the level of Cter Nse1 co-immunoprecipitated withTRUSS was very low (Fig. 30 B). Therefore, we can conclude that the interaction of Nse1 with TRUSS causes its cytoplasmic retention. In order to confirm that these foci were located in the cytoplasm, we stained nuclei *in vivo*. The fluorescent images supported that the foci caused by the co-expression of TRUSS were localized in the cytoplasm of cells (Fig. 30 C).

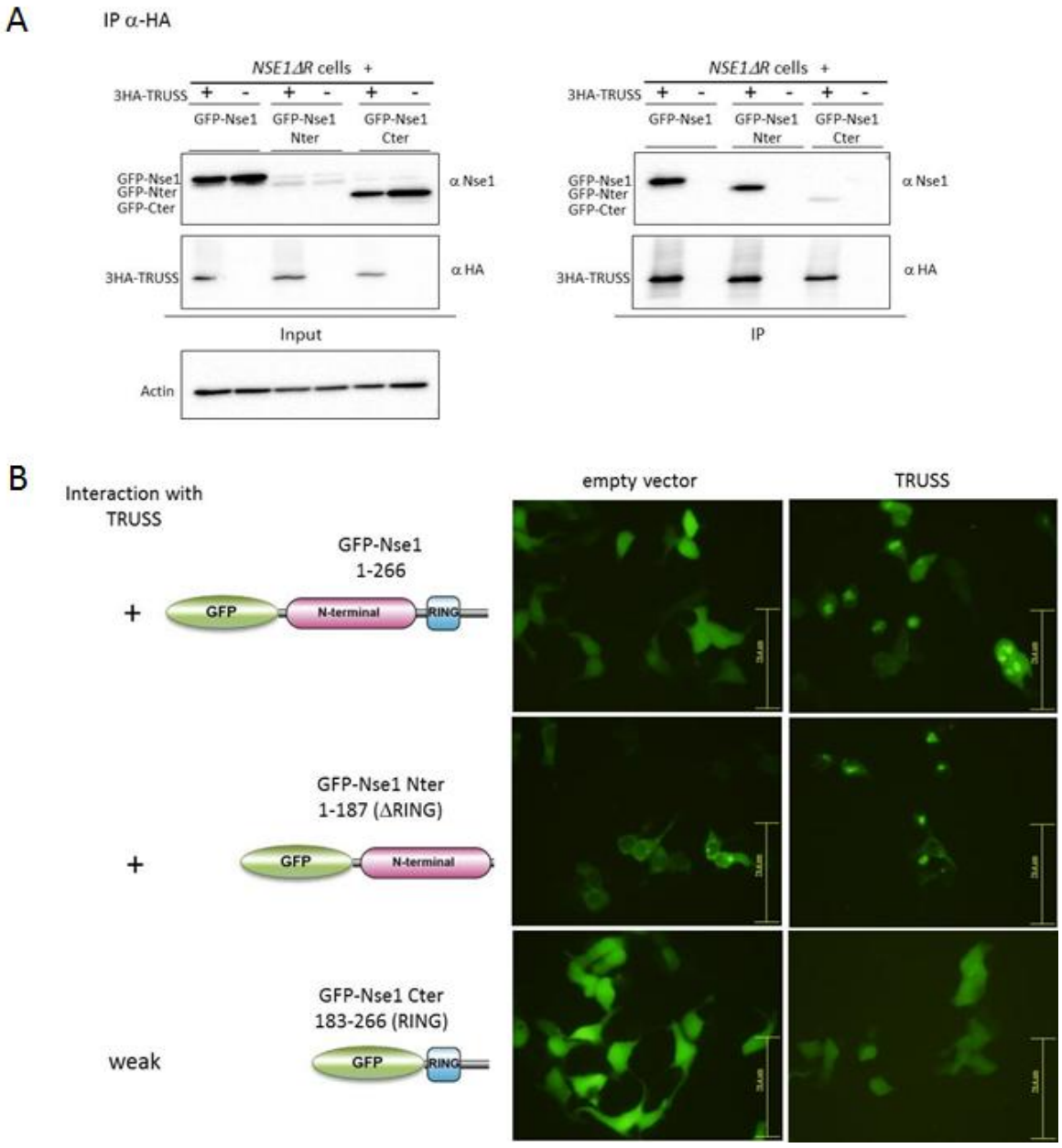

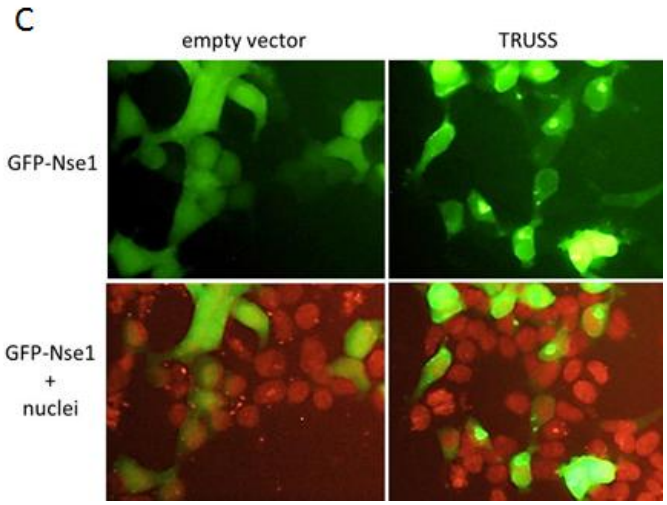

Fig.30 TRUSS interacts with the N-terminal domain of Nse1. *NSE1-ΔR* cells were transfected to express the GFP-Nse1 fusion protein or GFP fused to the Nter domain (1-187 aa) or the Cter domain (183-266 aa) of Nse1. In each case, cells were co-expressing 3HA-TRUSS or not. A. Western blot of protein extracts (Input) and anti-HA immunopurification (IP) showing Nse1 Co-IP. Full length Nse1 and Nter domain interact with TRUSS, whereas the Cter domain of Nse1 shows a very weak interaction with TRUSS. B. *In vivo* fluorescence microscopy images showing cytoplasmic foci of Nse1 and Nter domain when TRUSS is overexpressed, but not observed with the Cter domain. C. Merge images of GFP signal and *in vivo* nuclei staining with Hoescht indicate that foci with TRUSS overexpression have a cytoplasmic localization.

These results indicate that TRUSS interacts with high affinity with the Nter domain of Nse1 and that the RING domain is not necessary for this interaction. Co-immunoprecipitation efficiency seemed to be higher with the Nter region. Regarding these findings, we could suggest that either, the more cytoplasmic localization of the Nter version would favour the interaction with TRUSS, or that the lack of RING domain-Cterminal end would enhance the interaction. Then, in turn, we could suggest that the RING domain and/or the Cterminal end would somehow regulate the interaction of Nse1 with TRUSS.

DISCUSSION

In this doctoral thesis, we have addressed the role of the human Smc5/6 complex in genome stability through the study of the NH-RING domain of the Nse1 subunit. This domain has been proposed to act as an E3 ubiquitin ligase, but also to play a role in protein-protein interactions within the Smc5/6 complex [Doyle et al., 2010, Weon et al., 2018, Pebernard et al., 2008 (1)]. To study the role of this domain in human cells, we have introduced frameshift and point mutations in the C-terminal domain of Nse1, with the idea to either delete or unfold the RING. Our results indicate that this domain is essential to maintain the stability of the Smc5/6 complex and the integrity of the human genome.

1. Usage of CRISPR-Cas9 to mutate the RING domain of NSE1.

CRISPR-Cas9 has become the most popular technology for the manipulation and edition of genes in living cells. This is due to the wide availability of vectors and protocols for the introduction of site-specific double stranded DNA breaks in the genome. Their subsequent repair by the error-prone non-homologous end joining pathway leads to insertions and deletions that potentially affect the functionality of the gene. This simple procedure allowed us to obtain various mutant HEK293T clones with truncations in the RING domain of NSE1. In the presence of a homologous DNA sequence, the DSB may be repaired by homologous recombination, opening up the possibility to edit the sequence of the genome. The use of ssDNA as a donor template for recombinational repair is recommended to increase the efficiency of point mutations [Ran et al., 2013]. Although the procedure for genome edition using Cas9 might seem straightforward, we did not isolated clones with the anticipated mutant genotype. In fact, we obtained some puzzling results, which we think are derived from the use of the ssODNs.

A first analysis, based on restriction analysis, indicated that 6 out of the 39 clones isolated after addition of the ssODN contained the expected mutation: 4 of them were heterozygotes, containing wild type and mutant *NSE1* genes, and 2 were homozygotes. However, a more in depth analysis indicated that 3 of these 6 mutant clones contained an insertion of the ssODN sequence at the DSB site. In fact, one of the two clones initially classified as homozygotic was heterozygotic, bearing one copy of the *NSE1* gene with the designed mutations, and a second copy with an ssODN insertion at the Cas9 cut site. We think that this insertion must derive from the following set of reactions. First, Cas9 introduced a DSB. The break was then resected at 5' ends, exposing a 3' overhang complementary to the ssODN on the right side of the DSB. Next, the ssODN hybridized with the 3' overhang. Then, the 5' end of the ssODN was ligated to the 3' end on the left side of the DSB. Finally, the remaining stretch of single stranded ssODN sequence was used as a template to polymerize a complementary strand. This hypothesis requires that (i) the 5' end of the ssODN is not degraded after annealing to the resected right side of the DSB and (ii)

that a ssDNA 5' end is ligated to a 3' end, on the left side of the DSB. While 5' ends are degraded for recombinational repair in the context of dsDNA, it is possible that 5' ends are more stable when they are single stranded, what could explain the first requirement. It is also possible that the NHEJ machinery may ligate a ssDNA substrate. In any case, the observation that 50% of the mutant clones contained the insertion suggests that this product may be more frequent than previously anticipated. It remains to be tested if this is a particular condition of the HEK293T cells used in this work.

However, and even more surprising than the insertion of the ssODN was the finding that the second homozygotic clone only included one of the two designed C-A mutations in the RING domain (C207A). This result is unexpected as the recombination event had to occur in a short stretch of DNA between positions codifying for C204 and C207. This product could be explained by a partial resection or a recombination event that would change the DNA sequence downstream of the position codifying for C204, but not upstream of this position.

In any case, it is worth noting that despite we could not obtain the expected mutations in *NSE1*, the truncated alleles, the single C207A and the heterozygous cells expressing alleles with ssODN insertions and the double C204A C207A mutations had very similar phenotypes.

2. The NH-RING domain in Nse1: from an E3 ubiquitin ligase function to a structural role promoting the stability of the Smc5/6 complex

The Smc5/6 complex is the only known SMC protein complex with two RING domains, each of them potentially able to modify other proteins/complexes through SUMO and ubiquitin [Solé-Soler and Torres-Rosell, 2020]. The activity of Nse2 as a SUMO ligase has been extensively documented *in vivo* and *in vitro* and several SUMO targets are known [Almedawar et al., 2012, Bonner et al., 2016, Solé-Soler and Torres-Rosell, 2020]. In this thesis, we aimed to study the function of the putative E3-ligase activity of the RING domain in Nse1 by generating mutant HEK293T cell lines using CRISPR. We designed two sets of mutants predicted to destroy the putative RING-E2 interaction interface: one of them would truncate the RING domain, while the C-A mutations would unfold it. To our surprise, both type of mutations severely reduced the Nse1 protein levels. This prevented the intended use of RING domain mutants as a tool to specifically disrupt RING-E2 inteactions. In spite of this, the analysis CRISPR-derived *NSE1* mutant cells indicated that the primary function of the RING domain in Nse1 is directly related to its stability. It is worth nothing that this does not discard a possible role in ubiquitylation. In fact, it is even possible that both functions (stability and ubiquitylation) might be even connected.

The idea that Nse1 has ubiquitin ligase activity comes mainly from *in vitro* experiments. For example, Nse1 functions as an E3 ubiquitin ligase *in vitro* in human and mammalian cells

[Doyle et al., 2010, Hou et al., 2012,]. In striking contrast, this activity could not be observed using the fission yeast Nse1 protein [Pebernard et al., 2008 (1)]. The RING-E2 interaction typically requires a set of hydrophobic residues at particular position in the RING domain. This interface involves: an Ile/Leu residue between the first two zinc-coordinating Cys in the RING domain; a Trp/Tyr/Leu residues at short distance from the 6th zinc-coordinating Cys; and a Pro-Phe motif separating the last two Cys residues [Garcia-Barcena et al., 2020]. While most of these residues are present in the mammalian Nse1 RING domains, they are absent from their yeast othologs [Perbernard et al 2008 (1), Figure 1A], suggesting that the ubiquitin ligase activity of Nse1 might have been gained in higher eukaryotes or lost in yeast species.

A recent study also attributes an E3 ubiquitin ligase activity to Nse1 *in vivo*, although this function is not coordinated with the Smc5/6 complex [Weon et al., 2018]. Human Nse1 interacts with MAGE-F1 and promotes ubiquitylation and subsequent degradation of MMS19 *in vivo*. MAGE-F1 is highly expressed in tumor cells and shares similarities with MAGE-G1 (the human homolog of Nse3), although it is not part of the Smc5/6 complex, whereas MMS19 is involved in regulation of DNA repair. Probably, in cancer cells MAGE-F1 interacts with Nse1 to trigger degradation of MMS19, reducing the DNA repair capacity. It has been proposed that human Nse1 can interact with distinct proteins outside the Smc5/6 complex, mediating different cellular functions [Weon et al., 2018]. It might be possible that Nse1 is able to exert ubiquitin ligase activity only when it is not in a complex within the Smc5/6 complex.

Despite the large body of evidence showing a presence of an active ubiquitin ligase activity in many RING finger proteins [Lorick et al., 1999, Deshaies and Joazeiro, 2009, Metzger et al., 2014], we should also take into account that some RING domains do not function as ubiquitin ligases. PHD-type domains, which have the same distribution of residues that coordinate zinc as C4HC3 RING domains, have been shown not to function as an E3 ligase and are mainly implicated in nuclear protein-protein interactions [Bienz, 2006]. Several RING domains have been found to be essential for proper formation and structure of large protein complexes [Borden, 2000]. Consistent with this, the NH-RING domain of Nse1 has also been shown to be essential for the structural stability of the Nse1-Nse4-Nse3 subcomplex [Pebernard et al., 2008 (1)]. The function and folding of RING domains depends on the specific arrangement of the zinc coordinated residues and their integrity [Metzger et al., 2014, Borden and Freemont, 1996]. Moreover, the presence of zinc ions contributes to the stability of proteins [Kluska et al., 2018].

Based on these findings, it is probable that the Nse1 RING domain is also essential for the stability of the Nse1 protein, as well as for the stability of the whole Smc5/6 complex. In agreement with this, we have shown that *NSE1* mutant cells carrying a point mutation or a deletion in the RING domain result in lower levels of Nse1. Our results suggest that the low

Nse1 protein level in point mutants is due to a shorter half-life, relative to its wild type counterpart and depends on an active proteasome. On the other hand, our finding that MG132 inhibitor has no significant effect on the accumulation of wild type Nse1, suggests that the wild type Nse1 is stable and has a long turnover in cells. In contrast, the truncated Nse1-ΔR protein could not be detected after treatment with the proteasome inhibitor MG132 or the NEDD8-activating enzyme inhibitor MLN (Fig. 7). *NSE1* mRNA levels are substantially lower in RING mutants than in wild type cells, although we currently do no understand why. In any case, the presence of a mutant NSE1 mRNA gene suggests that the mutant Nse1 protein is translated but is probably very rapidly degraded. Since the protein levels of Nse1 point and truncated mutants differs in their proteasome dependency, we propose that each type of mutant is degraded through different pathways. The main pathways that control the proteolysis in eukaryotic cells are ubiquitin-proteasome system (UPS) and autophagy-lysosome system (ALS). UPS is normally involved in degradation of short-lived proteins, whereas ALS degrades long-lived proteins. Even though the two pathways are distinct, they are functionally related. Recently, it has been shown that the proteasome inhibition activates the autophagic degradation pathway [Ji and Kwon, 2017]. In addition, some proteins can be targeted for degradation by both pathways [Korolchuk et al., 2010]. Based on this, we suggest that the Nse1 protein in *NSE1-ΔR* mutants accumulates into aggresomes and is degraded by autophagy. Another possibility could be that the Nse1-ΔR protein accumulates to such extremely low levels that cannot even be detected after proteasome inhibition. An analogous effect has been previously observed upon expression of mutant versions of the yeast Nse1 protein in insect cells, where the protein truncated in the RING domain is expressed at much lower levels than point mutants in zinc-coordinating residues [Pebernard et al., 2008 (1)].

The inhibition of UPS normally leads to accumulation of polyubiquitinated proteins. However, we could not detect Nse1-ubiquitylated forms in *NSE1* mutant cells. Based on previous studies showing that prolonged proteasome inhibition increases protein insolubility [Pilecka et al., 2011], and promotes formation of protein aggregates [Ardley et al., 2003, Xiong et al., 2013] we suppose that long-term treatment with MG132 might alters the solubility of the mutant Nse1-ΔR protein, leading to formation of ubiquitylated insoluble protein aggregates.

We also found that mutations in the Nse1 RING domain cause the loss of Smc5, Smc6 and Nse4 (but not Nse2) protein levels. This probably suggests that the RING domain is essential not only for Nse1 stability, but also for the stability of most subunits in the Smc5/6 complex. In fact, earlier studies in yeast and human cells have shown that the loss of only one subunit in the Smc5/6 complex leads to decreased levels of the rest of subunits [Zhao and Blobel, 2005, Taylor et al., 2008]. Moreover, mutations in the *NSMCE3* gene, leading to a chromosome breakage syndrome, also destabilize most Smc5/6 subunits [van der Crabben et al., 2016]. One exception to global Smc5/6 depletion upon loss of a subunit seems to be

Nse2. The observation that Nse2 protein levels are not affected in *NSE1* mutant cells suggests that Nse2 and Smc5/6 protein levels in human cells are regulated independently. In accordance, various studies in chicken and human cells have shown that downregulation of Nse2 (*NSMCE2*) does not reduce expression of Smc5 and Smc6, indicating that the stability of the Smc5/6 complex is probably not affected by Nse2 [Kliszczak et al., 2012, Taylor et al., 2008, Verver et al., 2016, Pond et al., 2019]. A possible explanation for this could be that Nse2 binds to the arm of Smc5 and contrary to the other subunits, may not be directly involved in ATPase-dependent loading of the complex onto DNA [Jeppsson et al. 2014 (2)].

Based on the observations presented here, one possibility is that most subunits in the Smc5/6 complex are degraded after loss of the Nse1 protein. However, it is also possible that the lack of a properly folded RING domain in Smc5/6 targets the entire complex for proteasomal degradation. Our study also indicates that an unfolded RING domain is not intrinsically unstable. This is supported by the observation that the levels of expression of an Nse1 C-terminal RING domain (lacking the N-terminus), are not affected by C-A mutations in the RING domain (Fig. 17), while an Nse1 protein lacking the C-terminal RING domain is more unstable (Fig. 17). Thus, it is not the RING mutations per se that destabilize *NSE1-A* mutants. We speculate that the RING could hinder a degron sequence in the N-terminal domain of the protein (or somewhere else in the Smc5/6 complex). Unfolding, truncation or physical relocation of the RING domain would expose this sequence, leading to ubiquitylation and destruction. Hence, it would be very interesting to test at what point RING mutants are targeted for destruction. We hypothesize that this could require (i) interaction with Nse3; (ii) assembly of an Nse1-Nse3-Nse4 subcomplex; or (iii) incorporation into the Smc5/6 complex. This degradation could be part of a quality control mechanism to ensure the presence of properly folded and active Smc5/6 complexes. However, it is also intriguing to speculate that targeted degradation of Smc5/6 might be physiologically relevant, even in wild type complexes. For example, the association and dissociation of Smc5/6 from DNA, which is probably linked to chromosome disjunction, might require the targeted desctruction of specific Smc5/6 molecules. This destruction could depend upon displacement of the RING domain from its normal position within the Smc5/6 complex. This situation would be mimicked by Nse1-RING mutants but this time leading to complete destruction of the Smc5/6 cellular pools.

Another interesting finding of this thesis connecting Smc5/6-Nse1 to ubiquitylation and degradation is the observation that Nse1 can interact with the TRUSS protein. Recently, the hepatitis B viral protein HBx has been shown to interact with the DDB1-CUL4 E3 ligase complex and trigger ubiquitylation of the Smc5/6 complex for proteasomal degradation [Decorsière et al., 2016]. On the other hand, TRUSS is targeted for degradation by the Skp2 ligase. However, in the presence of HBx protein, TRUSS is stabilized [Jamal et al., 2015]. Thus, it could be possible that, similar to Skp2, Nse1 promotes ubiquitylation and

degradation of TRUSS. If this was true, HBx would interact with DDB1-CUL4 E3 ligase complex during HBV infection, promoting degradation of the Smc5/6 complex and thus stabilizing TRUSS. However, a recent study has proposed a model in which the PJA1 RING E3 ligase competes with Nse1 for interaction with Smc5/6 complex during HBV infection, to facilitate the binding of the Smc5/6 complex to episomal viral DNA [Xu et al., 2018]. Since TRUSS can also trigger ubiquitylation, another possibility is that TRUSS binds to Nse1 and other proteins to promote Smc5/6 degradation. However, the levels of endogenous Nse1 are not lowered after TRUSS overexpression, what suggests that TRUSS does not normally alter Nse1 stability. Nevertheless, all these hypotheses remain to be further elucidated to understand the possible functional relationships between Smc5/6 complex, TRUSS and HBx.

To our surprise, we could not detect a specific region of TRUSS required for the TRUSS-Nse1 interaction. Our immunoprecipitation analysis indicates that Nse1 can interact physically with different regions of TRUSS. Besides, TRUSS interacts with the N-terminal region of Nse1 and does not require the RING domain. As Nse3 and TRUSS interact with the same region of Nse1, it is possible that the function of the Nse1-TRUSS interaction is not directly related to the Smc5/6 complex, as it is the case with Nse1-MAGE-F1 interaction. However, if both proteins compete for binding to Nse1 and are mutualy exclusive, the TRUSS-Nse1 interaction might directly affect the number of active Smc5/6 molecules in the cell, altering its function. Consistent with this is the observation that overexpression of Nse1 and TRUSS show a cytoplasmic localization. A cytoplasmic retention mechanism could have an impact in nuclear Smc5/6 availability.

3. Role of human Nse1 and Smc5/6 complex in genomic stability

The Smc5/6 complex plays essential roles in chromosome segregation and in post-replicative DNA repair [Aragon, 2018, Palecek, 2019]. The function of this evolutionary conserved protein complex has been mainly studied in budding and fission yeast, which are more amenable to genetic manipulation. Although recent efforts have allowed the development of conditional Smc5/6 mutants in human cells [Venegas et al., 2020], very little is known about the roles of this protein complex in humans. Based on our immunoblot analysis, expression of Smc5/6 complex subunits is severely impaired in *NSE1* RING mutant cells (Fig. 7 e). This observation allowed us to explore the use of HEK293T *NSE1* mutant cells as a model for (almost) complete Nse1 knockdown. This experimental approach has enabled us to study the role of the Smc5/6 complex in genome stability in human cells.

Mutation of the RING domain in Nse1 affects cell cycle proliferation and genomic integrity
All core subunits in the Smc5/6 complex are essential for cell survival in yeast, plant and mammalian cells [Harvey, 2004, Li et al, 2017, Ju et al., 2013]. The only exceptions are Nse5 and Nse6 subunits in fission yeast, which seem not to be essential for viability [Pebernard et

al., 2006]. The loss of any subunit results in destabilization and impaired cellular function of the Smc5/6 complex. For example, homozygous mutations in *NSMCE2* and *SMC6* cause lethality in mouse embryos [Jacome et al., 2015, Ju et al., 2013]. In contrast to these findings, *NSE1* mutant cells are viable. This apparent contradiction may be explained by the fact that HEK293T is a SV40-T transformed human cell line with a severe and unstable aneuploid karyotype. It is possible that copy number alterations present in this cell line can genetically interact with the *NSE1* mutations, allowing cellular growth. In fact, it is even possible that a particular genotype was preferentially picked up during selection and amplification of CRISPR-derived *NSE1* mutant clones, allowing their survival. In any case, HEK293T *NSE1* mutant cells display a very slow growth phenotype, which is dependent upon low Nse1 protein expression. In agreement with this, a previous study showed that Smc5-depleted DT-40 chicken cells, which also have a slight abnormal karyotype, display slower growth compared to wild type cells [Stephan et al., 2011].

Further characterization of *NSE1* mutants showed that all the clones analyzed share a similar phenotype. Besides slow growth, which was previously observed in yeast and mammalian cells downregulated for the Smc5/6 complex [McDonald et al., 2003, Hu et al., 2005, Ampatzidou et al, 2006, Ni et al., 2012, Verver et al., 2016], we also detected changes in cell morphology, such as bigger cells and presence of cytoplasmic vacuoles, indicating increased cellular stress. In striking contrast to the slow-growth phenotype, FACS analysis revealed no particular arrest at any phase of the cell cycle in *NSE1* mutant cells. Even though flow cytometry did not show gross changes in cell cycle distribution, we observed that *NSE1* mutants have more cells with less than G1 DNA content and more than G2 content. These abnormal DNA content most probably reflect defects in chromosome segregation as well as apoptotic and polyploid cells. Since *NSE1* mutant cells proliferate more slowly without substantially alteration of the FACS profile, it seems logical to conclude that all cell cycle phases are elongated to a similar extent. It is worth keeping in mind that the appearance of non-viable cells also contributes to a longer doubling time. However, time-lapse analysis of cells undergoing mitosis shows that the duration of this phase is almost doubled in mutant relative to wild type cells. Overall, these observations are surprising, as most alterations in cell cycle progression normally trigger the activation of checkpoints, promoting arrest at specific phases, something that was not observed in the FACS analysis with propidium iodide staining or using the mitosis-specific MPM-2 marker. Therefore, we propose that *NSE1* mutants have partially activated checkpoint responses, which transiently arrest cells in G1, in mitosis and slow down S phase. In agreement, sub-threshold DNA damage levels do not elicit a full checkpoint response, allowing cell cycle progression [Fragkos and Naim, 2017]. Thus, we cannot exclude that the levels of endogenous DNA damage in *NSE1* mutants might not be sufficient to activate a full checkpoint response and promote cell cycle arrest.

It is currently unclear what causes the accumulation of endogenous DNA damage in *NSE1* mutant cells, although we can attribute it to defects in recombinational repair and chromosome segregation, based on previous studies in yeast. Interestingly, a recent study has shown that Smc5/6 depletion in G1-arrested cells does not alter S phase or mitotic entry, despite leading to chromosome non-disjunction during the first anaphase [Venegas et al, 2020]. Thus, the consequences of Smc5/6 inactivation are similar in humans and in budding yeast, and are most probably related to the formation of pathological structures during DNA replication in the absence of the Smc5/6 complex [Torres-Rosell et al., 2005 (1), Torres-Rosell et al., 2007(1), Bermúdez-López et al, 2010]. Analogously to the yeast situation, chromosome segregation defects do not stem from an inability to activate the DNA damage checkpoint, as treatment with DNA damage induces a mitotic arrest in Smc5/6-depleted cells [Venegas et al., 2020]. In addition, the sustained lack of the human Smc5/6 complex promotes mild endogenous DNA damage, detected as increased Chk2 and γH2AX phosphorylation and increased p53 and p21 expression, resulting in cellular senescence [Venegas et al., 2020]. This would occur in ensuing cell cycles, because of anaphase bridges and chromosome breakage in the first mitosis after Smc5/6 inactivation. From this point of view, HEK293T *NSE1* mutants must represent a chronification of a pathological state of chromosome segregation and repair deficiency. Previous studies have also shown that cells depleted for Smc5/6 complex have increased levels of γH2AX foci, suggesting stalled or collapsed replication forks and accumulation of DSBs [Gallego-Paez et al., 2014, Verver et al., 2016]. In accordance, here we show that *NSE1* mutants affected in their RING domain also have higher levels of γH2AX than wild type cells. γH2AX phosphorylation depends on the DNA damage checkpoint [Dickey et al, 2009], suggesting that this checkpoint is functional in *NSE1* mutant cells, although partially activated as a result of Smc5/6 deficiency. It is worth noting that the HEK293T cells used in this thesis express the large tumor antigen (T antigen) of simian virus 40 (SV40), which directly inhibits p53 [Ahuja et al., 2005]. Thus, it is highly probable that *NSE1* mutant cells escape senescence due to T-antigen mediated p53 inhibition, in spite of constitutive basal checkpoint activation.

The higher levels of endogenous DNA damage and the abrogation of the p53-branch of the DNA damage checkpoint should lead to the upregulation of genome instability markers in *NSE1* mutant cells. To corroborate this, we monitored various markers for genomic instability, such as the presence of micronuclei (MN), BLM foci and sister chromatid exchanges (SCE). We found that *NSE1* mutants show a higher incidence of micronuclei. Micronuclei are chromosomal fragments resulting from DNA breaks or lagging chromosome [Fenech et al., 2011]. The high frequency of MN may be related to an abnormal mitosis in *NSE1* mutant cells. Several other studies using plant, mice, human cell lines and patient cells deficient for Smc5/6 complex have also observed increased levels of micronuclei [Zelkowski et al, 2019, Jacome et al., 2015, Gallego-Paez et al., 2014, Payne et al., 2014, van der Crabben et al., 2016].

In addition, *NSE1* mutant cells show a significant increase in BLM foci. BLM is a helicase that regulates DNA repair by resolution of recombination intermediates. Mutations in the BLM gene cause a genetic disorder known as Bloom syndrome (BS). Cells from BS patients show high SCE levels, hyper-recombination and chromosomal instability which induce several abnormalities such as growth defects, immune deficiency and cancer susceptibility [Ellis et al, 2008]. The high number of BLM foci was also documented in previous reports using human cell lines and primary cells, derived from patients with *SMC5/6* mutations [Gallego-Paez et al., 2014, van der Crabben et al., 2016, Payne et al., 2014]. Similar to the patients' phenotype with BS, we have also detected elevated rates of SCE in *NSE1* mutant cells. This confirms an anti-crossover function the Smc5/6 complex during recombinational repair. Our result is in agreement with several other studies using chicken [Stephan et al., 2011], mice [Jacome et al., 2015, Ju et al., 2013] and primary cells from patients with impaired Smc5/6 function [Payne et al. 2014]. In addition, they indicate a conserved anti-recombinogenic function for the Smc5/6 complex at replication forks, as previously described in budding yeast [Torres-Rosell et al., 2005(1), Torres-Rosell et al., 2007(1), Torres-Rosell et al., 2007(2), Bermúdez-López et al, 2010]. In fact, BLM function at forks and joint molecules requires Smc5/6-dependent SUMOylation, a regulation that is also conserved in evolution [Bermudez-Lopez et al., 2016, Bonner et al., 2016, Pond et al., 2019].

Finally, we would like to emphasize that the similarities between the phenotype of *NSE1* RING mutants and hypomorphic yeast *smc5/6* mutants suggest that we did not have off-targets effects during Cas9 expression. To confirm this, we rescued most of the *NSE1* mutant phenotypes described in this thesis, including slow growth, expression of Smc5/6 subunits, γH2AX levels and replication fork progression, by ectopically expressing wild type *NSE1*. Thus, the genomic instability defects of 293T *NSE1* cells are perfectly reversible and can be fixed by re-expression of wild type *NSMCE1*.

Fiber analysis shows altered DNA replication fork rates in NSE1 mutant cells

The function of the Smc5/6 complex is intimately connected to S phase and to replication forks. Thus, it is possible that the defects in genome integrity in *NSE1* mutant cells stem from alterations in replication fork progression. In fact, DNA replication is delayed at repetitive regions in yeast cells with no functional Smc5/6 complex, suggesting lower fork progression rates at these loci [Torres-Rosell et al., 2007(1)]. Thus, we analyzed DNA replication in HEK293T *NSE1* mutant cells using a DNA fiber assay in collaboration with Neus Agell's group in Universitat de Barcelona. Analysis of single fibers indicates that *NSE1-ΔR* mutants exhibit a significantly slower fork progression rate, compared to wild type cells. In accordance, FACS analysis with BrdU also shows a slower progression through S phase. In addition, our analysis indicates that *NSE1-ΔR* mutant cells do not accumulate stalled replication forks, neither reduce origin firing. Therefore, we can conclude that the slower S phase in *NSE1* mutant cells can be attributed to a global lower progression rate at individual forks.

The most straightforward explanation for the effect of *NSE1* mutants in fork rates is that Smc5/6 directly promotes the movement of replication forks either directly or through local chromatin organization behind replication forks. In this sense, Smc5/6 is required to allow replication fork progression through fork blocks in budding yeast [Torres-Rosell et al., 2007 (1)]. In addition, Smc5/6 has been proposed to regulate the topology of replication forks, thus promoting fork progression [Kegel et al., 2011].

Earlier studies in yeast have proposed that inhibition of origin firing is checkpoint-dependent, whereas fork slowing and stalling can occur in the absence of checkpoint activation through a direct result of DNA damage [Iyer and Rhind, 2017, Tercero and Diffley, 2001, Kumar and Huberman, 2009]. In mammalian cells, slowing of replication forks and inhibition of origin firing seems to be both dependent on S phase checkpoint activation [Seiler et al, 2007, Unsal-Kaçmaz et al., 2007]. However, a study using human cells has proposed that the slowing of replication forks could be also a consequence of checkpoint-independent mechanisms [Merrick et al., 2004].

Our results are in contrast to previous reports from other groups, showing that Nse2 depletion does alter replication fork rates [Jacome et al., 2015, Pond et al., 2019]. Differences may be due to the fact that depletion of Nse2 does not destabilize the Smc5/6 complex, which could still be present to maintain normal replication fork rates. However, it is also worth noting that degradation of Smc5/6 subunits during the first S phase does not alter replication fork rates [Venegas et al., 2020]. In fact, transient depletion of *NSE1* with siRNA in RPE cells does not affect fork rates (Fernando Unzueta and Neus Agell, personal communication). Thus, it seems that the low replication fork rate in HEK293T *NSE1* mutant cells is most probably not a primary effect, but the consequence of cell cycling without Smc5/6 function for two or more generations. It is also possible that the alteration in fork rate is due to the combination of not having a Smc5/6 complex plus the accumulation of endogenous DNA damage (itself derived from Smc5/6 inactivity). We currently do not think that the amount of endogenous DNA damage and replicative stress is sufficiently high to mount a checkpoint response in *NSE1* cells, as we did not observe inhibition of origin firing.

Another possible explanation of our result may be the absence of p53 function in 293T cells, which could abrogate specific checkpoint responses. The function of p53 in S phase checkpoint is still not fully understood: some studies have suggested that p53 does not affect the S phase checkpoint, while others have proposed that p53 is S phase checkpoint-dependent, preventing cells from entering into mitosis with incomplete replication [Giono and Manfredi, 2006]. However, human cells lacking p53 with active S phase checkpoint show slow fork progression that is supposed to be not dependent on checkpoints [Merrick et al., 2004].

In summary, based on our results and previous findings, we propose that Nse1-deficient cells proceed into mitosis without proper completion of S phase, mainly due to the lack of Smc5/6 complex. The defects generated during this S phase are not under checkpoint surveillance. However, chromosomes suffer from non-disjunction and anaphase bridges during the first mitosis after loss of Smc5/6. This must lead to the appearance of lagging chromosomes, micronuclei and low activation of the DNA damage checkpoint in the next cell cycle, eventually triggering the gradual loss of genomic integrity. The combination of DNA damage and low Smc5/6 expression in the following cycles leads to further defects in replication fork progression. Thus, it is very likely that the initial alterations at replication forks, which are probably still present in the progeny, eventually lead to a slower replication fork progression. A future work is needed to support this assumption in human cells.

4. The Smc5/6 complex and FANCM maintain the genomic stability by regulating alternative repair pathways in human cells

The Smc5/6 complex plays a key role in chromosome disjunction by removing toxic recombination intermediates that accumulate at stalled or damaged replication forks. In budding yeast, the Smc5/6 complex seems to counteract these recombination structures facilitating their dissolution by SUMOylation of the RecQ helicase (Sgs1/BLM) or preventing their accumulation by restricting Mph1 helicase fork regression activity [Bermúdez-López et al., 2016, Chen et al., 2009, Bonner et al., 2016]. Inactivation of the helicase activity of Mph1 (the yeast homolog of human FANCM) suppresses the accumulation of recombination intermediates in *smc5/6* mutants. Besides, it allows growth of *smc5/6* knockout cells and alleviates the sensitivity to genotoxic drugs, as well as the thermo-sensitivity of *smc5/6* mutant cells [Chen et al., 2009]. This effect is a result of direct Mph1 inhibition by physical binding to Smc5 [Xue et al., 2015]. Due to the significant homology of the yeast Mph1 with the human FANCM, we hypothesized that the genetic interaction between Smc5/6 complex and FANCM would be conserved in higher eukaryotes. However, in contradiction to the previous study in budding yeast, we found that downregulation of FANCM does not rescue SMC5/6 mutants. Thus, our results indicate for the first time that unlike in budding yeast, the Smc5/6 complex and FANCM in human cells would function in distinct genetic pathways and act independently in the maintenance of genomic stability.

The synthetic sickness interaction between Smc5 and FANCM indicates that both genes act synergistically to promote genome integrity by operating through distinct DNA repair pathways. The lack of suppression of Smc5/6-depleted cells by FANCM KO indicates that the essential function of the Smc5/6 complex in human cells is not related to FANCM inhibition. Thus, the Smc5/6 complex may not be involved in the regulation of replication fork regression in human cells. However, we cannot discard that the function of Smc5/6 at forks is conserved in evolution, but through inhibition of other helicases. Numerous motor

proteins catalyze replication fork regression in higher eukaryotes. Besides FANCM, SMARCAL1, HTLF, ZRANB3 and FBH1 helicases also promote fork regression and can recognize different types of fork structures in human cells [Quinet et al., 2017]. DNA helicases SMARCAL1 and ZRANB3 are not present in yeasts, and are positively regulated by PCNA polyubiquitylation. SMARCAL1 is negatively regulated through phosphorylation by checkpoint kinases. The negative regulator for ZRANB3 has not been yet identified [Bansbach et al., 2010, Poole and Cortez, 2017]. Based on these findings, it may be also possible that these helicases are negatively regulated by other post-translational modifications, including SUMOylation or by protein-protein interactions, where the Smc5/6 complex could be implicated. In order to test if Smc5/6 complex functions as a negative regulator of some of these proteins, the genetic interactions between each type of DNA helicase and the Smc5/6 complex should be tested.

Despite the strong evolutionary conservation between Mph1 and FANCM, there are some functional and structural differences. Unlike the yeast Mph1, which is directly involved in HR repair and physically interacts with Smc5, FANCM is mainly implicated in the interstrand cross-link (ICL) repair, regulated by FA pathway, although loss-of-function mutations in FANCM cause a cancer predisposition syndrome clinically distinct from bona fide Fanconi Anemia (FA) [Bogliolo et al., 2018]. Besides, a direct interaction with the Smc5/6 complex has not yet been identified [Heyer, 2015, Yimit et al., 2016, Chen et al., 2009, Xue et al., 2008]. Additionally, a fully conserved FA-like ICL repair pathway in yeast has not been yet described, although several putative homologs of FA proteins were found [Daee et al., 2012, Xue et al., 2015]. However, the finding that the Smc5/6 complex is recruited to ICLs in mammalian cells could suggest a possible conserved connection between the Smc5/6 complex and Mph1 during the ICL repair [Räschle et al., 2015]. The specific role of the Smc5/6 complex at ICL stalled replication forks and its regulation remains to be elucidated. Probably, the Smc5/6 complex is recruited at ICL lesions in order to regulate the anti-recombinogenic function of BLM helicase or to recruit or regulate other DNA repair proteins. Apart from the functional differences, there is also some dissimilarity in the domain organization of Mph1 and FANCM. Even though, they share the same SF2 helicase domain at C-terminal part and MHF binding site, the FANCM protein is bigger and also contains non-functional ERCC4 nuclease domain, as well as RMI binding site and HhH (a tandem helix-hairpin-helix) domain at N-terminus [Xue et al., 2015]. Unlike Mph1, FANCM does not show a DNA-unwinding activity and functions as a DNA translocase promoting fork reversal and preventing formation of DSBs [Knoll et al., 2012, Wang et al., 2018 (2)].
Additionally, FANCM interacts directly with RMI1 through its RMI binding site and recruits BLM-TOPOIIIα-RMI1–RMI2 complex to stalled replication forks [Wang et al., 2013, Deans and West, 2011]. However, BLM can be also recruited by alternative mechanisms and does not depend only on the FANCM [Wang et al., 2013]. The BLM complex dissolves joint molecules in HR with the aid of Smc5/6 complex SUMOylation, and is also required in cell cycle progression during mitosis [Yang et al., 2012, Pradhan et al., 2013].

The observed differences between Mph1 and FANCM indicate that the two proteins are not fully conserved in evolution and apart from their shared role in fork regression and DNA D-loop dissociation, they can mediate also distinct functions in yeast and human cells.

Apart from its role in the FA-core complex, FANCM complex (FANCM-FAAP24-MHF1&2) exerts important functions in DNA repair. Individuals with *FANCM* mutations are associated with a higher risk of breast cancer and FANCM, as previously mentioned, has a fundamental role in recruiting Bloom complex (BLM-TOPOIIIα-RMI1-RMI2) and in remodeling stalled DNA replications forks [Deans and West, 2009]. FANCM has a role in common fragile sites (CFS) protection, in order to prevent chromosomal breakage, independently of the rest of FA-core components and the FANCI-FANCD2 complex. This function is not redundant with Rad52 or BLM [Wang et al., 2018 (1); Wang et al., 2018 (2)]. In addition, patient-derived *FANCM* mutant fibroblasts used in this thesis show slower growth rate than WT cells, present chromosome fragility, ICL sensitivity, and cell cycle alterations typical of a Fanconi Anemia (FA) cellular phenotype, but patients did not present congenital malformations or bone marrow failure (BMF), associated to FA [Bogliolo et al., 2018].

We can assume that upon endogenous DNA damage, loss of FANCM results in defective FA pathway/or defective CFS protection, and unresolved secondary structures, leading to collapsed forks that generate DSBs. Since the HR repair pathway is still active, we suggest that with the aid of the Smc5/6 complex, some of the DSBs and subsequent recombination intermediates could be further repaired. This can explain our and others results showing slower but not inhibited proliferation in FANCM deficient cells [Wang et al., 2018(1), Wang et al., 2018(2)].

Contrary to FANCM, the Smc5/6 complex is essential for cell viability. According to our results loss of Smc5 in human fibroblasts leads to gross defects in cell proliferation. This inhibitory effect is even stronger when expression of FANCM is also downregulated, leading to extremely slow cell growth. In contrast to our finding, a recent study has indicated that human cells depleted for either Smc5 or both Smc5 and FANCM show very similar proliferation rate, indicating that the Smc5/6 complex act cooperatively with some proteins of FA pathway in ICL repair [Rossi et al., 2020]. This discrepancy is probably due to different techniques of protein depletion, and/or different types of cell lines used. In fact, in HeLa cells used in that study, FANCM depletion using siRNA did not cause a slower growth rate, whereas the FANCM KO patient-derived fibroblasts used in our experiments did present a delay in growth, compared to FANCM WT cells. This difference could be explained by the the different rounds of cell cycles that cells with depleted target genes did undergo at the time of the experiment. In our experiment, *FANCM* mutant cells underwent more cell divisions at the moment we depleted Smc5, therefore, they probably had accumulated

more alterations. In the study presented above, both proteins, Smc5 and FANCM were depleted at the same time and cells underwent few cell divisions. Regarding patient-derived fibroblasts, we should expect that FANCM depletion would lead to defects in the repair of spontaneous DNA damage. Therefore, complete depletion of Smc5 in these cells would better represent the actual effect of both mutations in human cells. Unrepaired recombination intermediates induce the formation of different types of chromatin bridges [Fernández-Casañas and Chan, 2018]. Unresolved DNA bridges in turn lead to chromosomal nondisjunction and cytokinesis failure. This is in agreement with our finding showing that human cells deficient for both FANCM and Smc5/6 complex display a higher number of DNA bridges. This phenotype is also accompanied by a higher cell death rate and an increased number of micronuclei and aberrant nuclei. In accordance with these assumptions and similar to our result are two independent studies showing that cells depleted for both FANCM and BLM or FANCM and Rad52 are synthetic lethal and function independently in repair pathways [Wang et al., 2018 (1), Wang et al., 2018 (2)].

Based on this and since we know that SUMOylation of the Smc5/6 complex is required for both BLM and Rad52 to exert their functions, it seems relevant to consider that our double mutants show additive effects due to the role of the Smc5/6 complex in resolution of recombination intermediates. We can also propose that both proteins are crucial in processing of damaged forks based on their role in preventing accumulation of recombination molecules and other DNA structures. Hence, we suggest that the simultaneous depletion of FANCM and Smc5 cause defects in different repair pathways.

Based on our results, we can propose a model supposing that the increased genomic instability in human fibroblasts co-depleted for Smc5/6 complex and FANCM is due to unresolved joint molecules and DSBs as a result of the concurrent impair of Smc5/6 function in fork restart and HR, FANCM-dependent fork regression, and FA pathway. Future research is needed to better understand the exact role of the Smc5/6 complex and FANCM in repair mechanisms.

CONCLUSIONS

1. The RING domain of Nse1 is necessary for the stability of the protein and the Smc5/6 complex.

2. Human cells with mutations in the RING domain of Nse1 (*NSE1* mutants) display slow growth phenotype and prolonged mitosis.

3. *NSE1* mutant cells show sensitivity to MMS treatment.

4. *NSE1* mutants experience spontaneous endogenous DNA damage, manifesting in higher levels of γH2AX, sister chromatid exchanges (SCEs), BLM foci and micronuclei.

5. DNA fiber analysis revealed significantly slower replication fork progression in *NSE1* mutants.

6. Ectopically expressed *NSE1* rescued the wild type phenotype in *NSE1* mutant cells.

7. The Smc5/6 complex and FANCM maintain the genomic integrity by operating in distinct repair pathways indicating that the genetic interaction between the yeast Smc5/6 complex and Mph1 helicase (FANCM in humans) is not conserved in human cells.

8. Human fibroblasts deficient for both Smc5 and FANCM show extremely slow growth and higher death rates, accompanied by higher levels of chromosomal instability and failure in cytokinesis.

9. Human Nse1 physically interacts with different domains of TRUSS, whereas TRUSS interacts with the N-terminal region of Nse1.

REFERENCES

Abraham RT. Cell cycle checkpoint signaling through the ATM and ATR kinases.Genes Dev. 2001 Sep 1;15(17):2177-96. Review. PubMed PMID: 11544175.

Ait Saada A, Lambert SAE, Carr AM. Preserving replication fork integrity and competence via the homologous recombination pathway. DNA Repair (Amst). 2018;71:135-147. doi:10.1016/j.dnarep.2018.08.017

Ahuja D, Sáenz-Robles MT, Pipas JM. SV40 large T antigen targets multiple cellular pathways to elicit cellular transformation. Oncogene. 2005 Nov 21;24(52):7729-45. doi: 10.1038/sj.onc.1209046. PMID: 16299533.

Akutsu M, Dikic I, Bremm A. Ubiquitin chain diversity at a glance. J Cell Sci.2016 Mar 1;129(5):875-80. doi: 10.1242/jcs.183954. Epub 2016 Feb 15. Review.PubMed PMID: 26906419.

Al-Hakim A, Escribano-Diaz C, Landry MC, et al. The ubiquitous role of ubiquitin in the DNA damage response. DNA Repair (Amst). 2010;9(12):1229-1240. doi:10.1016/j.dnarep.2010.09.011

Allen C, Ashley AK, Hromas R, Nickoloff JA. More forks on the road to replication stress recovery. J Mol Cell Biol. 2011 Feb;3(1):4-12. doi:10.1093/jmcb/mjq049. Review. PubMed PMID: 21278446; PubMed Central PMCID:PMC3030971.

Almedawar S, Colomina N, Bermúdez-López M, Pociño-Merino I, Torres-Rosell J. A SUMO-dependent step during establishment of sister chromatid cohesion. Curr Biol.2012 Sep 11;22(17):1576-81. doi: 10.1016/j.cub.2012.06.046. Epub 2012 Jul 5.PubMed PMID: 22771040.

Ambekar S. S., Hattur S.S. and Bule P.B. DNA: Damage and Repair Mechanisms in Humans. Glob J Pharmaceu Sci. Review. Volume 3 Issue 3 - July 2017.

Ampatzidou E, Irmisch A, O'Connell MJ, Murray JM. Smc5/6 is required for repair at collapsed replication forks. Mol Cell Biol. 2006 Dec;26(24):9387-401.Epub 2006 Oct 9. PubMed PMID: 17030601; PubMed Central PMCID: PMC1698528.

Andreassen PR, Ren K. Fanconi anemia proteins, DNA interstrand crosslink repair pathways, and cancer therapy. Curr Cancer Drug Targets. 2009 Feb;9(1):101-17. Review. PubMed PMID: 19200054; PubMed Central PMCID: PMC4934657.

Andrews EA, Palecek J, Sergeant J, Taylor E, Lehmann AR, Watts FZ. Nse2, a component of the Smc5-6 complex, is a SUMO ligase required for the response to DNA damage. Mol Cell Biol. 2005 Jan;25(1):185-96. PubMed PMID: 15601841; PubMed Central PMCID: PMC538766.

Antonin W, Neumann H. Chromosome condensation and decondensation during mitosis. Curr Opin Cell Biol. 2016 Jun;40:15-22. doi: 10.1016/j.ceb.2016.01.013. Epub 2016 Feb 16. Review. PubMed PMID: 26895139.

Aragón L. The Smc5/6 Complex: New and Old Functions of the Enigmatic Long-Distance Relative. Annu Rev Genet. 2018 Nov 23;52:89-107. doi:10.1146/annurev-genet-120417-031353. PubMed PMID: 30476445.

Ardley HC, Scott GB, Rose SA, Tan NG, Markham AF, Robinson PA. Inhibition of proteasomal activity causes inclusion formation in neuronal and non-neuronal cells overexpressing Parkin. Mol Biol Cell. 2003 Nov;14(11):4541-56. doi: 10.1091/mbc.e03-02-0078. Epub 2003 Aug 22. PMID: 12937272; PMCID: PMC266771.

Au PY, Yeh WC. Physiological roles and mechanisms of signaling by TRAF2 and TRAF5. Adv Exp Med Biol. 2007;597:32-47. Review. PubMed PMID: 17633015.

Awasthi P, Foiani M, Kumar A. ATM and ATR signaling at a glance. J Cell Sci.2015 Dec 1;128(23):4255-62. doi: 10.1242/jcs.169730. Epub 2015 Nov 13. Review.Erratum in: J Cell Sci. 2016 Mar 15;129(6):1285. PubMed PMID: 26567218.

Bailey R, Priego Moreno S, Gambus A. Termination of DNA replication forks:"Breaking up is hard to do". Nucleus. 2015;6(3):187-96. doi:10.1080/19491034.2015.1035843. Epub 2015 Apr 2. PubMed PMID: 25835602; PubMed Central PMCID: PMC4615769.

Baluška F, Volkmann D, Menzel D, Barlow P. Strasburger's legacy to mitosis and cytokinesis and its relevance for the Cell Theory. Protoplasma. 2012 Oct;249(4):1151-62. Epub 2012 Apr 15. PubMed PMID: 22526203.

Bansbach CE, Boerkoel CF, Cortez D. SMARCAL1 and replication stress: an explanation for SIOD?. Nucleus. 2010;1(3):245-248. doi:10.4161/nucl.1.3.11739

Barnum KJ, O'Connell MJ. Cell cycle regulation by checkpoints. Methods Mol Biol. 2014;1170:29-40. doi: 10.1007/978-1-4939-0888-2_2. PubMed PMID: 24906307;PubMed Central PMCID: PMC4990352.

Baxter J, Oliver AW, Schalbetter SA. Are SMC Complexes Loop Extruding Factors? Linking Theory With Fact. Bioessays. 2019 Jan;41(1):e1800182. doi:10.1002/bies.201800182. Epub 2018 Dec 3. Review. PubMed PMID: 30506702.

Behlke-Steinert S, Touat-Todeschini L, Skoufias DA, Margolis RL. SMC5 and MMS21 are required for chromosome cohesion and mitotic progression. Cell Cycle. 2009;8(14):2211-2218. doi:10.4161/cc.8.14.8979

Bermúdez-López M, Ceschia A, de Piccoli G, Colomina N, Pasero P, Aragón L,Torres-Rosell J. The Smc5/6 complex is required for dissolution of DNA-mediated sister chromatid linkages. Nucleic Acids Res. 2010 Oct;38(19):6502-12. doi:10.1093/nar/gkq546. Epub 2010 Jun 22. PubMed PMID: 20571088; PubMed Central PMCID: PMC2965248.

Bermúdez-López M, Pociño-Merino I, Sánchez H, Bueno A, Guasch C, Almedawar S, Bru-Virgili S, Garí E, Wyman C, Reverter D, Colomina N, Torres-Rosell J. ATPase-dependent control of the Mms21 SUMO ligase during DNA repair. PLoS Biol. 2015 Mar 12;13(3):e1002089. doi: 10.1371/journal.pbio.1002089. PMID: 25764370; PMCID: PMC4357442.

Bermúdez-López M, Villoria MT, Esteras M, Jarmuz A, Torres-Rosell J, Clemente-Blanco A, Aragon L. Sgs1's roles in DNA end resection, HJ dissolution, and crossover suppression

require a two-step SUMO regulation dependent on Smc5/6. Genes Dev. 2016 Jun 1;30(11):1339-56. doi: 10.1101/gad.278275.116. PMID: 27298337; PMCID: PMC4911932.

Bharadwaj R, Yu H. The spindle checkpoint, aneuploidy, and cancer. Oncogene.2004 Mar 15;23(11):2016-27. Review. PubMed PMID: 15021889.

Bi X. Mechanism of DNA damage tolerance. World J Biol Chem. 2015 Aug 26;6(3):48-56. doi: 10.4331/wjbc.v6.i3.48. PubMed PMID: 26322163; PubMed Central PMCID: PMC4549768.

Bienz M. The PHD finger, a nuclear protein-interaction domain. Trends Biochem Sci. 2006;31(1):35-40. doi:10.1016/j.tibs.2005.11.001

Bischof O, Kim SH, Irving J, Beresten S, Ellis NA, Campisi J. Regulation and localization of the Bloom syndrome protein in response to DNA damage. J Cell Biol. 2001;153(2):367-380. doi:10.1083/jcb.153.2.367

Boehm EM, Gildenberg MS, Washington MT. The Many Roles of PCNA in Eukaryotic DNA Replication. Enzymes. 2016;39:231-54. doi: 10.1016/bs.enz.2016.03.003. Epub 2016 Apr 19. Review. PubMed PMID: 27241932; PubMed Central PMCID: PMC4890617.

Bogliolo M, Bluteau D, Lespinasse J, Pujol R, Vasquez N, d'Enghien CD, Stoppa-Lyonnet D, Leblanc T, Soulier J, Surrallés J. Biallelic truncating FANCM mutations cause early-onset cancer but not Fanconi anemia. Genet Med. 2018 Apr;20(4):458-463. doi: 10.1038/gim.2017.124. Epub 2017 Aug 24. PMID: 28837157.

Bologna S, Ferrari S. It takes two to tango: Ubiquitin and SUMO in the DNA damage response. Front Genet. 2013 Jun 11;4:106. doi: 10.3389/fgene.2013.00106. eCollection 2013. PubMed PMID: 23781231; PubMed Central PMCID: PMC3678106.

Bonner JN, Choi K, Xue X, Torres NP, Szakal B, Wei L, Wan B, Arter M, Matos J,Sung P, Brown GW, Branzei D, Zhao X. Smc5/6 Mediated Sumoylation of the Sgs1-Top3-Rmi1 Complex Promotes Removal of Recombination Intermediates. Cell Rep.2016 Jul 12;16(2):368-378. doi: 10.1016/j.celrep.2016.06.015. Epub 2016 Jun 30.PubMed PMID: 27373152; PubMed Central PMCID: PMC5051638.

Borden KL, Freemont PS. The RING finger domain: a recent example of a sequence-structure family. Curr Opin Struct Biol. 1996 Jun;6(3):395-401. Review. PubMed PMID: 8804826.

Borden KL. RING domains: master builders of molecular scaffolds? J Mol Biol. 2000 Feb 4;295(5):1103-12. doi: 10.1006/jmbi.1999.3429. Erratum in: J Mol Biol 2000 Apr 7;297(4):1027. PMID: 10653689.

Brandsma I, Gent DC. Pathway choice in DNA double strand break repair: observations of a balancing act. Genome Integr. 2012 Nov 27;3(1):9. doi: 10.1186/2041-9414-3-9. PMID: 23181949; PMCID: PMC3557175.

Branzei D, Foiani M. Maintaining genome stability at the replication fork. Nat Rev Mol Cell Biol. 2010 Mar;11(3):208-19. doi: 10.1038/nrm2852. Review. PubMed PMID: 20177396.

Branzei D, Sollier J, Liberi G, Zhao X, Maeda D, Seki M, Enomoto T, Ohta K,Foiani M. Ubc9- and mms21-mediated sumoylation counteracts recombinogenic events at damaged replication forks. Cell. 2006 Nov 3;127(3):509-22. PubMed PMID:17081974.

Brinkmann K, Schell M, Hoppe T, Kashkar H. Regulation of the DNA damage response by ubiquitin conjugation. Front Genet. 2015 Mar 10;6:98. doi:10.3389/fgene.2015.00098. eCollection 2015. Review. PubMed PMID: 25806049; PubMed Central PMCID: PMC4354423.

Brooker AS, Berkowitz KM. The roles of cohesins in mitosis, meiosis, and human health and disease. Methods Mol Biol. 2014;1170:229-66. doi:10.1007/978-1-4939-0888-2_11. Review. PubMed PMID: 24906316; PubMed Central PMCID: PMC4495907.

Brown JS, Jackson SP. Ubiquitylation, neddylation and the DNA damage response.Open Biol. 2015 Apr;5(4):150018. doi: 10.1098/rsob.150018. Review. PubMed PMID:25833379; PubMed Central PMCID: PMC4422126.

Buchkovich KJ, Greider CW. Telomerase regulation during entry into the cell cycle in normal human T cells. Mol Biol Cell. 1996;7(9):1443-1454. doi:10.1091/mbc.7.9.1443

Budhidarmo R, Nakatani Y, Day CL. RINGs hold the key to ubiquitin transfer. Trends Biochem Sci. 2012;37(2):58-65. doi:10.1016/j.tibs.2011.11.001

Buetow L, Huang DT. Structural insights into the catalysis and regulation of E3 ubiquitin ligases. Nat Rev Mol Cell Biol. 2016 Oct;17(10):626-42. doi: 10.1038/nrm.2016.91. Epub 2016 Aug 3. PMID: 27485899; PMCID: PMC6211636.

Burgers PMJ, Kunkel TA. Eukaryotic DNA Replication Fork. Annu Rev Biochem. 2017 Jun 20;86:417-438. doi: 10.1146/annurev-biochem-061516-044709. Epub 2017 Mar 1. PubMed PMID: 28301743; PubMed Central PMCID: PMC5597965.

Cappadocia L, Lima CD. Ubiquitin-like Protein Conjugation: Structures,Chemistry, and Mechanism. Chem Rev. 2018 Feb 14;118(3):889-918. doi:10.1021/acs.chemrev.6b00737. Epub 2017 Feb 24. Review. PubMed PMID: 28234446;PubMed Central PMCID: PMC5815371.

Caspari T. How to activate p53. Curr Biol. 2000 Apr 20;10(8):R315-7. Review.PubMed PMID: 10801407.

Castella M, Jacquemont C, Thompson EL, Yeo JE, Cheung RS, Huang JW, Sobeck A, Hendrickson EA, Taniguchi T. FANCI Regulates Recruitment of the FA Core Complex at Sites of DNA Damage Independently of FANCD2. PLoS Genet. 2015 Oct 2;11(10):e1005563. doi: 10.1371/journal.pgen.1005563. PMID: 26430909; PMCID: PMC4592014.

Ceccaldi R, Sarangi P, D'Andrea AD. The Fanconi anaemia pathway: new players and new functions. Nat Rev Mol Cell Biol. 2016;17(6):337-349. doi:10.1038/nrm.2016.48

Chan YW, Fugger K, West SC. Unresolved recombination intermediates lead to ultra-fine anaphase bridges, chromosome breaks and aberrations. Nat Cell Biol. 2018;20(1):92-103. doi:10.1038/s41556-017-0011-1

Chang DJ, Cimprich KA. DNA damage tolerance: when it's OK to make mistakes.Nat Chem Biol. 2009 Feb;5(2):82-90. doi: 10.1038/nchembio.139. Epub 2009 Jan 15. PubMed PMID: 19148176; PubMed Central PMCID: PMC2663399.

Chang DJ, Lupardus PJ, Cimprich KA. Monoubiquitination of proliferating cell nuclear antigen induced by stalled replication requires uncoupling of DNA polymerase and mini-chromosome maintenance helicase activities. J Biol Chem. 2006 Oct 27;281(43):32081-8. Epub 2006 Sep 7. PubMed PMID: 16959771.

Chang HHY, Pannunzio NR, Adachi N, Lieber MR. Non-homologous DNA end joining and alternative pathways to double-strand break repair. Nat Rev Mol Cell Biol.2017 Aug;18(8):495-506. doi: 10.1038/nrm.2017.48. Epub 2017 May 17. Review.PubMed PMID: 28512351.

Chatterjee N, Walker GC. Mechanisms of DNA damage, repair, and mutagenesis. Environ Mol Mutagen. 2017 Jun;58(5):235-263. doi: 10.1002/em.22087. Epub 2017 May 9. Review. PubMed PMID: 28485537; PubMed Central PMCID: PMC5474181.

Che R, Zhang J, Nepal M, Han B, Fei P. Multifaceted Fanconi Anemia Signaling. Trends Genet. 2018;34(3):171-183. doi:10.1016/j.tig.2017.11.006

Chen YH, Choi K, Szakal B, Arenz J, Duan X, Ye H, Branzei D, Zhao X. Interplay between the Smc5/6 complex and the Mph1 helicase in recombinational repair. Proc Natl Acad Sci U S A. 2009 Dec 15;106(50):21252-7. doi: 10.1073/pnas.0908258106.Epub 2009 Dec 7. PubMed PMID: 19995966; PubMed Central PMCID: PMC2795505.

Choi SH, Wright JB, Gerber SA, Cole MD. Myc protein is stabilized by suppression of a novel E3 ligase complex in cancer cells. Genes Dev. 2010 Jun 15;24(12):1236-41. doi: 10.1101/gad.1920310. PubMed PMID: 20551172; PubMed Central PMCID: PMC2885659.

Chu WK, Hanada K, Kanaar R, Hickson ID. BLM has early and late functions in homologous recombination repair in mouse embryonic stem cells. Oncogene. 2010;29(33):4705-4714. doi:10.1038/onc.2010.214

Cipolla L, Maffia A, Bertoletti F, Sabbioneda S. The Regulation of DNA Damage Tolerance by Ubiquitin and Ubiquitin-Like Modifiers. Front Genet. 2016 Jun 13;7:105. doi: 10.3389/fgene.2016.00105. Erratum in: Front Genet. 2016 Sep 30;7:184. PMID: 27379156; PMCID: PMC4904029.

Clauson C, Schärer OD, Niedernhofer L. Advances in understanding the complex mechanisms of DNA interstrand cross-link repair. Cold Spring Harb Perspect Biol. 2013 Oct 1;5(10):a012732. doi: 10.1101/cshperspect.a012732. Review. PubMed PMID: 24086043; PubMed Central PMCID: PMC4123742.

Cooper GM. The Cell: A Molecular Approach. 2nd edition. Sunderland (MA): Sinauer Associates; 2000. The Eukaryotic Cell Cycle.

Cortez D. Preventing replication fork collapse to maintain genome integrity.DNA Repair (Amst). 2015 Aug;32:149-157. doi: 10.1016/j.dnarep.2015.04.026. Epub 2015 May 1. Review. PubMed PMID: 25957489; PubMed Central PMCID: PMC4522347.

Couch FB, Bansbach CE, Driscoll R, Luzwick JW, Glick GG, Bétous R, Carroll CM, Jung SY, Qin J, Cimprich KA, Cortez D. ATR phosphorylates SMARCAL1 to prevent replication fork collapse. Genes Dev. 2013 Jul 15;27(14):1610-23. doi: 10.1101/gad.214080.113. PMID: 23873943; PMCID: PMC3731549.

Daee DL, Ferrari E, Longerich S, et al. Rad5-dependent DNA repair functions of the Saccharomyces cerevisiae FANCM protein homolog Mph1. J Biol Chem. 2012;287(32):26563-26575. doi:10.1074/jbc.M112.369918

Davidson IF, Bauer B, Goetz D, Tang W, Wutz G, Peters JM. DNA loop extrusion by human cohesin. Science. 2019;366(6471):1338-1345. doi:10.1126/science.aaz3418

Davis AJ, Lee KJ, Chen DJ. The N-terminal region of the DNA-dependent protein kinase catalytic subunit is required for its DNA double-stranded break-mediated activation. J Biol Chem. 2013 Mar 8;288(10):7037-46. doi:10.1074/jbc.M112.434498. Epub 2013 Jan 15. Erratum in: J Biol Chem. 2013 Jun 28;288(26):18776. PubMed PMID: 23322783; PubMed Central PMCID: PMC3591613.

De Piccoli G, Cortes-Ledesma F, Ira G, Torres-Rosell J, Uhle S, Farmer S,Hwang JY, Machin F, Ceschia A, McAleenan A, Cordon-Preciado V, Clemente-Blanco A,Vilella-Mitjana F, Ullal P, Jarmuz A, Leitao B, Bressan D, Dotiwala F, Papusha A,Zhao X, Myung K, Haber JE, Aguilera A, Aragón L. Smc5-Smc6 mediate DNA double-strand-break repair by promoting sister-chromatid recombination. Nat Cell Biol. 2006 Sep;8(9):1032-4. Epub 2006 Aug 6. PubMed PMID: 16892052; PubMed Central PMCID: PMC4493748.

Deans AJ, West SC. DNA interstrand crosslink repair and cancer. Nat Rev Cancer. 2011 Jun 24;11(7):467-80. doi: 10.1038/nrc3088. Review. PubMed PMID: 21701511; PubMed Central PMCID: PMC3560328.

Deans AJ, West SC. FANCM connects the genome instability disorders Bloom's Syndrome and Fanconi Anemia. Mol Cell. 2009 Dec 25;36(6):943-53. doi:10.1016/j.molcel.2009.12.006. PubMed PMID: 20064461.

Decorsière A, Mueller H, van Breugel PC, Abdul F, Gerossier L, Beran RK,Livingston CM, Niu C, Fletcher SP, Hantz O, Strubin M. Hepatitis B virus X protein identifies the Smc5/6 complex as a host restriction factor. Nature. 2016 Mar 17;531(7594):386-9. doi: 10.1038/nature17170. PubMed PMID: 26983541.

Deshaies RJ, Joazeiro CA. RING domain E3 ubiquitin ligases. Annu Rev Biochem. 2009;78:399-434. doi:10.1146/annurev.biochem.78.101807.093809. Review. PubMed PMID: 19489725.

Dexheimer T. (2013) DNA Repair Pathways and Mechanisms. In: Mathews L., Cabarcas S., Hurt E. (eds) DNA Repair of Cancer Stem Cells. Springer, Dordrecht.

Diaz M, Pecinka A. Scaffolding for Repair: Understanding Molecular Functions of the SMC5/6 Complex. Genes (Basel). 2018 Jan 12;9(1). pii: E36. doi:10.3390/genes9010036. Review. PubMed PMID: 29329249; PubMed Central PMCID:PMC5793187.

Díaz M, Pečinková P, Nowicka A, Baroux C, Sakamoto T, Gandha PY, Jeřábková H, Matsunaga S, Grossniklaus U, Pecinka A. The SMC5/6 Complex Subunit NSE4A Is Involved in DNA Damage Repair and Seed Development. Plant Cell. 2019 Jul;31(7):1579-1597. doi: 10.1105/tpc.18.00043. Epub 2019 Apr 29. PMID: 31036599; PMCID: PMC6635853.

Dickey JS, Redon CE, Nakamura AJ, Baird BJ, Sedelnikova OA, Bonner WM. H2AX: functional roles and potential applications. Chromosoma. 2009 Dec;118(6):683-92. doi: 10.1007/s00412-009-0234-4. Epub 2009 Aug 26. PMID: 19707781; PMCID: PMC3094848.

Donzelli M, Draetta GF. Regulating mammalian checkpoints through Cdc25 inactivation. EMBO Rep. 2003;4(7):671-677. doi:10.1038/sj.embor.embor887

Dowen JM, Young RA. SMC complexes link gene expression and genome architecture. Curr Opin Genet Dev. 2014 Apr;25:131-7. doi:10.1016/j.gde.2013.11.009. Epub 2014 May 8. Review. PubMed PMID: 24794701; PubMed Central PMCID: PMC4045092.

Doyle JM, Gao J, Wang J, Yang M, Potts PR. MAGE-RING protein complexes comprise a family of E3 ubiquitin ligases. Mol Cell. 2010 Sep 24;39(6):963-74.doi: 10.1016/j.molcel.2010.08.029. PubMed PMID: 20864041; PubMed Central PMCID:PMC4509788.

Duan X, Yang Y, Chen YH, Arenz J, Rangi GK, Zhao X, Ye H. Architecture of the Smc5/6 Complex of Saccharomyces cerevisiae Reveals a Unique Interaction between the Nse5-6 Subcomplex and the Hinge Regions of Smc5 and Smc6. J Biol Chem. 2009 Mar 27;284(13):8507-15. doi: 10.1074/jbc.M809139200. Epub 2009 Jan 13. PubMed PMID: 19141609; PubMed Central PMCID: PMC2659209.

Ellis NA, Sander M, Harris CC, Bohr VA. Bloom's syndrome workshop focuses on the functional specificities of RecQ helicases. Mech Ageing Dev. 2008 Nov;129(11):681-91. PubMed PMID: 19238688.

Eot-Houllier G, Magnaghi-Jaulin L, Fulcrand G, Moyroud FX, Monier S, Jaulin C.Aurora A-dependent CENP-A phosphorylation at inner centromeres protects bioriented chromosomes against cohesion fatigue. Nat Commun. 2018 May 14;9(1):1888. doi: 10.1038/s41467-018-04089-9. PubMed PMID: 29760389; PubMed Central PMCID: PMC5951908.

Errico A, Costanzo V. Mechanisms of replication fork protection: a safeguard for genome stability. Crit Rev Biochem Mol Biol. 2012 May-Jun;47(3):222-35. doi: 10.3109/10409238.2012.655374. Epub 2012 Feb 11. PMID: 22324461.

Fenech M, Kirsch-Volders M, Natarajan AT, et al. Molecular mechanisms of micronucleus, nucleoplasmic bridge and nuclear bud formation in mammalian and human cells. Mutagenesis. 2011;26(1):125-132. doi:10.1093/mutage/geq052

Fernández-Casañas M, Chan KL. The Unresolved Problem of DNA Bridging. Genes (Basel). 2018;9(12):623. Published 2018 Dec 12. doi:10.3390/genes9120623

Finley D, Ulrich HD, Sommer T, Kaiser P. The ubiquitin-proteasome system of Saccharomyces cerevisiae. Genetics. 2012 Oct;192(2):319-60. doi:10.1534/genetics.112.140467. Review. PubMed PMID: 23028185; PubMed Central PMCID:PMC3454868.

Fleck O, Nielsen O. DNA repair. J Cell Sci. 2004 Feb 1;117(Pt 4):515-7. Review. PubMed PMID: 14730007.

Fousteri MI, Lehmann AR. A novel SMC protein complex in Schizosaccharomyces pombe contains the Rad18 DNA repair protein. EMBO J. 2000 Apr 3;19(7):1691-702.PubMed PMID: 10747036; PubMed Central PMCID: PMC310237.

Fox JT, Lee KY, Myung K. Dynamic regulation of PCNA ubiquitylation/deubiquitylation. FEBS Lett. 2011 Sep 16;585(18):2780-5. doi:10.1016/j.febslet.2011.05.053. Epub 2011 Jun 1. Review. PubMed PMID: 21640107;PubMed Central PMCID: PMC3172383.

Fragkos M, Ganier O, Coulombe P, Méchali M. DNA replication origin activation in space and time. Nat Rev Mol Cell Biol. 2015 Jun;16(6):360-74. doi: 10.1038/nrm4002. Review. PubMed PMID: 25999062.

Fragkos M, Naim V. Rescue from replication stress during mitosis. Cell Cycle. 2017 Apr 3;16(7):613-633. doi: 10.1080/15384101.2017.1288322. Epub 2017 Feb 6. PMID: 28166452; PMCID: PMC5397263.

Freemont PS, Hanson IM, Trowsdale J. A novel cysteine-rich sequence motif. Cell. 1991 Feb 8;64(3):483-4. PubMed PMID: 1991318.

Fujioka Y, Kimata Y, Nomaguchi K, Watanabe K, Kohno K. Identification of a novel non-structural maintenance of chromosomes (SMC) component of the SMC5-SMC6 complex involved in DNA repair. J Biol Chem. 2002 Jun 14;277(24):21585-91. Epub 2002 Apr 1. PubMed PMID: 11927594.

Fukui K. DNA mismatch repair in eukaryotes and bacteria. J Nucleic Acids. 2010 Jul 27;2010. pii: 260512. doi: 10.4061/2010/260512. PubMed PMID: 20725617; PubMed Central PMCID: PMC2915661.

Furuta M, Tanaka H, Shiraishi Y, Unida T, Imamura M, Fujimoto A, Fujita M, Sasaki-Oku A, Maejima K, Nakano K, Kawakami Y, Arihiro K, Aikata H, Ueno M, Hayami S, Ariizumi SI, Yamamoto M, Gotoh K, Ohdan H, Yamaue H, Miyano S, Chayama K, Nakagawa H. Characterization of HBV integration patterns and timing in liver cancer and HBV-infected livers. Oncotarget. 2018 May 18;9(38):25075-25088. doi:10.18632/oncotarget.25308. eCollection 2018 May 18. Erratum in: Oncotarget. 2018 Aug 3;9(60):31789. PubMed PMID: 29861854; PubMed Central PMCID: PMC5982772.

Gallego-Paez LM, Tanaka H, Bando M, et al. Smc5/6-mediated regulation of replication progression contributes to chromosome assembly during mitosis in human cells. Mol Biol Cell. 2014;25(2):302-317. doi:10.1091/mbc.E13-01-0020

Ganji M, Shaltiel IA, Bisht S, et al. Real-time imaging of DNA loop extrusion by condensin. Science. 2018;360(6384):102-105. doi:10.1126/science.aar7831

Gao Y, Tateishi S, Vaziri C. Pathological trans-lesion synthesis in cancer.Cell Cycle. 2016 Nov 16;15(22):3005-3006. Epub 2016 Jul 27. PubMed PMID:27462757; PubMed Central PMCID: PMC5134697.

Gari K, Décaillet C, Stasiak AZ, Stasiak A, Constantinou A. The Fanconi anemia protein FANCM can promote branch migration of Holliday junctions and replication forks. Mol Cell. 2008 Jan 18;29(1):141-8. doi: 10.1016/j.molcel.2007.11.032.PubMed PMID: 18206976.

Garcia-Barcena C, Osinalde N, Ramirez J, Mayor U. How to Inactivate Human Ubiquitin E3 Ligases by Mutation. Front Cell Dev Biol. 2020 Feb 4;8:39. doi: 10.3389/fcell.2020.00039. PMID: 32117970; PMCID: PMC7010608.

Geenen JJJ, Schellens JHM. Molecular Pathways: Targeting the Protein Kinase Wee1 in Cancer. Clin Cancer Res. 2017 Aug 15;23(16):4540-4544. doi:10.1158/1078-0432.CCR-17-0520. Epub 2017 Apr 25. PubMed PMID: 28442503.

Gelot C, Magdalou I, Lopez BS. Replication stress in Mammalian cells and its consequences for mitosis. Genes (Basel). 2015 May 22;6(2):267-98. doi: 10.3390/genes6020267. Review. PubMed PMID: 26010955; PubMed Central PMCID:PMC4488665.

Ghosal G, Chen J. DNA damage tolerance: a double-edged sword guarding the genome. Transl Cancer Res. 2013;2(3):107-129. PubMed PMID: 24058901; PubMed Central PMCID: PMC3779140.

Ghosh S, Saha T. Central Role of Ubiquitination in Genome Maintenance: DNA Replication and Damage Repair. ISRN Mol Biol. 2012;2012:146748. Published 2012 Feb 8. doi:10.5402/2012/146748

Gibson RT, Androphy EJ. The SMC5/6 Complex Represses the Replicative Program of High-Risk Human Papillomavirus Type 31. Pathogens. 2020 Sep 25;9(10):E786. doi: 10.3390/pathogens9100786. PMID: 32992873; PMCID: PMC7599729.

Giglia-Mari G, Zotter A, Vermeulen W. DNA damage response. Cold Spring Harb Perspect Biol. 2011 Jan 1;3(1):a000745. doi: 10.1101/cshperspect.a000745. Review.PubMed PMID: 20980439; PubMed Central PMCID: PMC3003462.

Giono LE, Manfredi JJ. The p53 tumor suppressor participates in multiple cell cycle checkpoints. J Cell Physiol. 2006 Oct;209(1):13-20. Review. PubMed PMID:16741928.

Gligoris T, Löwe J. Structural Insights into Ring Formation of Cohesin and Related Smc Complexes. Trends Cell Biol. 2016 Sep;26(9):680-693. Doi:10.1016/j.tcb.2016.04.002. Epub 2016 Apr 28. Review. PubMed PMID: 27134029;PubMed Central PMCID: PMC4989898.

Golfier S, Quail T, Kimura H, Brugués J. Cohesin and condensin extrude loops in a cell-cycle dependent manner, bioRxiv 821306; 2019. doi: https://doi.org/10.1101/821306

Guilliam TA, Brissett NC, Ehlinger A, Keen BA, Kolesar P, Taylor EM, Bailey LJ, Lindsay HD, Chazin WJ, Doherty AJ. Molecular basis for PrimPol recruitment to replication forks by RPA. Nat Commun. 2017 May 23;8:15222. doi: 10.1038/ncomms15222. PMID: 28534480; PMCID: PMC5457501.

Hakem R. DNA-damage repair; the good, the bad, and the ugly. EMBO J. 2008 Feb 20;27(4):589-605. doi: 10.1038/emboj.2008.15. Review. PubMed PMID: 18285820;PubMed Central PMCID: PMC2262034.

Harashima H, Dissmeyer N, Schnittger A. Cell cycle control across the eukaryotic kingdom. Trends Cell Biol. 2013 Jul;23(7):345-56. doi:10.1016/j.tcb.2013.03.002. Epub 2013 Apr 6. Review. PubMed PMID: 23566594.

Harvey SH, Krien MJ, O'Connell MJ. Structural maintenance of chromosomes (SMC)proteins, a family of conserved ATPases. Genome Biol. 2002;3(2):REVIEWS3003. Epub 2002 Jan 30. Review. PubMed PMID: 11864377; PubMed Central PMCID: PMC139016.

Harvey SH, Sheedy DM, Cuddihy AR, O'Connell MJ. Coordination of DNA damage responses via the Smc5/Smc6 complex. Mol Cell Biol. 2004 Jan;24(2):662-74. doi: 10.1128/mcb.24.2.662-674.2004. PMID: 14701739; PMCID: PMC343814.

Hassler M, Shaltiel IA, Haering CH. Towards a Unified Model of SMC Complex Function. Curr Biol. 2018;28(21):R1266-R1281. doi:10.1016/j.cub.2018.08.034

Hauf S, Roitinger E, Koch B, Dittrich CM, Mechtler K, Peters JM. Dissociation of cohesin from chromosome arms and loss of arm cohesion during early mitosis depends on phosphorylation of SA2. PLoS Biol. 2005 Mar;3(3):e69. Epub 2005 Mar 1.PubMed PMID: 15737063; PubMed Central PMCID: PMC1054881.

Herrmann J, Lerman LO, Lerman A. Ubiquitin and ubiquitin-like proteins in protein regulation. Circ Res. 2007 May 11;100(9):1276-91. Review. PubMed PMID:17495234.

Hershko A, Ciechanover A. The ubiquitin system. Annu Rev Biochem.1998;67:425-79. Review. PubMed PMID: 9759494.

Heyer WD. Regulation of recombination and genomic maintenance. Cold Spring Harb Perspect Biol. 2015;7(8):a016501. Published 2015 Aug 3. doi:10.1101/cshperspect.a016501

Hirano T. At the heart of the chromosome: SMC proteins in action. Nat Rev Mol Cell Biol. 2006;7(5):311-322. doi:10.1038/nrm1909

Hixon ML, Gualberto A. The control of mitosis. Front Biosci. 2000 Jan 1;5:D50-7. Review. PubMed PMID: 10702375.

Hock R, Wilde F, Scheer U, Bustin M. Dynamic relocation of chromosomal protein HMG-17 in the nucleus is dependent on transcriptional activity. EMBO J. 1998 Dec 1;17(23):6992-7001. PubMed PMID: 9843505; PubMed Central PMCID: PMC1171047.

Horigome C, Bustard DE, Marcomini I, Delgoshaie N, Tsai-Pflugfelder M, Cobb JA, Gasser SM. PolySUMOylation by Siz2 and Mms21 triggers relocation of DNA breaks to nuclear pores through the Slx5/Slx8 STUbL. Genes Dev. 2016 Apr 15;30(8):931-45. doi: 10.1101/gad.277665.116. Epub 2016 Apr 7. PMID: 27056668; PMCID: PMC4840299.

Hou X, Zhang W, Xiao Z, et al. Mining and characterization of ubiquitin E3 ligases expressed in the mouse testis. BMC Genomics. 2012;13:495. Published 2012 Sep 19. doi:10.1186/1471-2164-13-495

Houtgraaf JH, Versmissen J, van der Giessen WJ. A concise review of DNA damage checkpoints and repair in mammalian cells. Cardiovasc Revasc Med. 2006 Jul-Sep;7(3):165-72. Review. PubMed PMID: 16945824.

Hu B, Liao C, Millson SH, Mollapour M, Prodromou C, Pearl LH, Piper PW,Panaretou B. Qri2/Nse4, a component of the essential Smc5/6 DNA repair complex.Mol Microbiol. 2005 Mar;55(6):1735-50. PubMed PMID: 15752197.

Huang TT, D'Andrea AD. Regulation of DNA repair by ubiquitylation. Nat Rev Mol Cell Biol. 2006 May;7(5):323-34. Review. PubMed PMID: 16633336.

Hudson JJ, Bednarova K, Kozakova L, Liao C, Guerineau M, Colnaghi R, Vidot S, Marek J, Bathula SR, Lehmann AR, Palecek J. Interactions between the Nse3 and Nse4 components

of the SMC5-6 complex identify evolutionarily conserved interactions between MAGE and EID Families. PLoS One. 2011 Feb 25;6(2):e17270.doi: 10.1371/journal.pone.0017270. PubMed PMID: 21364888; PubMed Central PMCID:PMC3045436.

Hühn D, Bolck HA, Sartori AA. Targeting DNA double-strand break signalling and repair: recent advances in cancer therapy. Swiss Med Wkly. 2013 Jul 29;143:w13837. doi: 10.4414/smw.2013.13837. eCollection 2013. Review. PubMed PMID: 23897299.

Irmisch A, Ampatzidou E, Mizuno K, O'Connell MJ, Murray JM. Smc5/6 maintains stalled replication forks in a recombination-competent conformation. EMBO J. 2009 Jan 21;28(2):144-55. doi: 10.1038/emboj.2008.273. PubMed PMID: 19158664; PubMed Central PMCID: PMC2634738.

Iyer DR , Rhind N. Checkpoint regulation of replication forks: global or local? Biochem Soc Trans. 2013 Dec;41(6):1701-5. doi: 10.1042/BST20130197. Review.PubMed PMID: 24256278; PubMed Central PMCID: PMC5074381.

Iyer DR , Rhind N. The Intra-S Checkpoint Responses to DNA Damage. Genes(Basel). 2017 Feb 17;8(2). pii: E74. doi: 10.3390/genes8020074. Review. PubMed PMID: 28218681; PubMed Central PMCID: PMC5333063.

Jackson SP, Durocher D. Regulation of DNA damage responses by ubiquitin and SUMO. Mol Cell. 2013 Mar 7;49(5):795-807. doi: 10.1016/j.molcel.2013.01.017. Epub 2013 Feb 14. Review. PubMed PMID: 23416108.

Jacome A, Gutierrez-Martinez P, Schiavoni F, Tenaglia E, Martinez P, Rodríguez-Acebes S, Lecona E, Murga M, Méndez J, Blasco MA, Fernandez-Capetillo O. NSMCE2 suppresses cancer and aging in mice independently of its SUMO ligase activity. EMBO J. 2015 Nov 3;34(21):2604-19. doi: 10.15252/embj.201591829. Epub 2015 Oct 6. PubMed PMID: 26443207; PubMed Central PMCID: PMC4641528.

Jamal A, Swarnalatha M, Sultana S, Joshi P, Panda SK, Kumar V. The G1 phase E3 ubiquitin ligase TRUSS that gets deregulated in human cancers is a novel substrate of the S-phase E3 ubiquitin ligase Skp2. Cell Cycle. 2015;14(16):2688-700. doi: 10.1080/15384101.2015.1056946. PubMed PMID: 26038816; PubMed Central PMCID: PMC4612110.

Jeppsson K (1), Carlborg KK, Nakato R, Berta DG, Lilienthal I, Kanno T, Lindqvist A, Brink MC, Dantuma NP, Katou Y, Shirahige K, Sjögren C. The chromosomal association of the Smc5/6 complex depends on cohesion and predicts the level of sister chromatid entanglement. PLoS Genet. 2014 Oct 16;10(10):e1004680. doi: 10.1371/journal.pgen.1004680. eCollection 2014 Oct. PubMed PMID: 25329383; PubMed Central PMCID: PMC4199498.

Jeppsson K (2), Kanno T, Shirahige K, Sjögren C. The maintenance of chromosome structure: positioning and functioning of SMC complexes. Nat Rev Mol Cell Biol.2014 Sep;15(9):601-14. doi: 10.1038/nrm3857. Review. PubMed PMID: 25145851.

Ji CH, Kwon YT. Crosstalk and Interplay between the Ubiquitin-Proteasome System and Autophagy. Mol Cells. 2017;40(7):441-449. doi:10.14348/molcells.2017.0115

Jones RM, Petermann E. Replication fork dynamics and the DNA damage response. Biochem J. 2012 Apr 1;443(1):13-26. doi: 10.1042/BJ20112100. Review. PubMed PMID:22417748.

Jossen R, Bermejo R. The DNA damage checkpoint response to replication stress:A Game of Forks. Front Genet. 2013 Mar 13;4:26. doi: 10.3389/fgene.2013.00026.eCollection 2013. PubMed PMID: 23493417; PubMed Central PMCID: PMC3595514.

Ju L, Wing J, Taylor E, Brandt R, Slijepcevic P, Horsch M, Rathkolb B, Rácz I, Becker L, Hans W, Adler T, Beckers J, Rozman J, Klingenspor M, Wolf E, Zimmer A, Klopstock T, Busch DH, Gailus-Durner V, Fuchs H, de Angelis MH, van der Horst G, Lehmann AR. SMC6 is an essential gene in mice, but a hypomorphic mutant in the ATPase domain has a mild phenotype with a range of subtle abnormalities. DNA Repair (Amst). 2013 May 1;12(5):356-66. doi: 10.1016/j.dnarep.2013.02.006. Epub 2013 Mar 18. PMID: 23518413.

Kakui Y, Uhlmann F. SMC complexes orchestrate the mitotic chromatin interaction landscape. Curr Genet. 2018 Apr;64(2):335-339. doi:10.1007/s00294-017-0755-y. Epub 2017 Sep 21. Review. PubMed PMID: 28936767;PubMed Central PMCID: PMC5851691.

Kang S, Kang MS, Ryu E, Myung K. Eukaryotic DNA replication: Orchestrated action of multi-subunit protein complexes. Mutat Res. 2018 May;809:58-69. doi:10.1016/j.mrfmmm.2017.04.002. Epub 2017 May 1. Review. PubMed PMID: 28501329.

Kegel A, Betts-Lindroos H, Kanno T, Jeppsson K, Ström L, Katou Y, Itoh T, Shirahige K, Sjögren C. Chromosome length influences replication-induced topological stress. Nature. 2011 Mar 17;471(7338):392-6. doi: 10.1038/nature09791. Epub 2011 Mar 2. PubMed PMID: 21368764.

Kegel A, Sjögren C. The Smc5/6 complex: more than repair? Cold Spring Harb Symp Quant Biol. 2010;75:179-87. doi: 10.1101/sqb.2010.75.047. Epub 2011 Apr 5.Review. PubMed PMID: 21467147.

Kelman Z. PCNA: structure, functions and interactions. Oncogene. 1997 Feb 13;14(6):629-40. Review. PubMed PMID: 9038370.

Kerscher O, Felberbaum R, Hochstrasser M. Modification of proteins by ubiquitin and ubiquitin-like proteins. Annu Rev Cell Dev Biol. 2006;22:159-80.Review. PubMed PMID: 16753028.

Khattar E and Tergaonkar V (November 23rd 2016). The Role of Telomeres and Telomere-associated Proteins as Components of Interactome in Cell-signaling Pathways, Telomere - A Complex End of a Chromosome, Marcelo L. Larramendy, IntechOpen, DOI: 10.5772/62130.

Kim H, D'Andrea AD. Regulation of DNA cross-link repair by the Fanconi anemia/BRCA pathway. Genes Dev. 2012 Jul 1;26(13):1393-408. doi:10.1101/gad.195248.112. Review. PubMed PMID: 22751496; PubMed Central PMCID:PMC3403008.

Kliszczak M, Stephan AK, Flanagan AM, Morrison CG. SUMO ligase activity of vertebrate Mms21/Nse2 is required for efficient DNA repair but not for Smc5/6 complex stability. DNA Repair (Amst). 2012 Oct 1;11(10):799-810. doi: 10.1016/j.dnarep.2012.06.010. Epub 2012 Aug 24. PMID: 22921571.

Kluska K, Adamczyk J, Krężel A. Metal binding properties of zinc fingers with a naturally altered metal binding site. Metallomics. 2018;10(2):248-263. doi:10.1039/c7mt00256d

Knipscheer P, Räschle M, Smogorzewska A, Enoiu M, Ho TV, Schärer OD, Elledge SJ, Walter JC. The Fanconi anemia pathway promotes replication-dependent DNA interstrand cross-link repair. Science. 2009 Dec 18;326(5960):1698-701. doi:10.1126/science.1182372. Epub 2009 Nov 12. PubMed PMID:19965384; PubMed Central PMCID: PMC2909596.

Knoll A, Higgins JD, Seeliger K, et al. The Fanconi anemia ortholog FANCM ensures ordered homologous recombination in both somatic and meiotic cells in Arabidopsis. Plant Cell. 2012;24(4):1448-1464. doi:10.1105/tpc.112.096644

Korolchuk VI, Menzies FM, Rubinsztein DC. Mechanisms of cross-talk between the ubiquitin-proteasome and autophagy-lysosome systems. FEBS Lett. 2010;584(7):1393-1398. doi:10.1016/j.febslet.2009.12.047

Kumar S, Huberman JA. Checkpoint-dependent regulation of origin firing and replication fork movement in response to DNA damage in fission yeast. Mol Cell Biol. 2009;29(2):602-611. doi:10.1128/MCB.01319-08

Kuniba H, Yoshiura K, Kondoh T, Ohashi H, Kurosawa K, Tonoki H, Nagai T,Okamoto N, Kato M, Fukushima Y, Kaname T, Naritomi K, Matsumoto T, Moriuchi H,Kishino T, Kinoshita A, Miyake N, Matsumoto N, Niikawa N. Molecular karyotyping in 17 patients and mutation screening in 41 patients with Kabuki syndrome. J Hum Genet. 2009 May;54(5):304-9. doi: 10.1038/jhg.2009.30. Epub 2009 Apr 3. PubMed PMID: 19343044.

Lafuente-Barquero J, Luke-Glaser S, Graf M, Silva S, Gómez-González B,Lockhart A, Lisby M, Aguilera A, Luke B. The Smc5/6 complex regulates the yeast Mph1 helicase at RNA-DNA hybrid-mediated DNA damage. PLoS Genet. 2017 Dec 27;13(12):e1007136. doi: 10.1371/journal.pgen.1007136. eCollection 2017 Dec.PubMed PMID: 29281624; PubMed Central PMCID: PMC5760084.

Lalan M., Bagchi T., Misra A., Chapter 1 The Cell. Challenges in Delivery of Therapeutic Genomics and Proteomics 2011, pp 1-43

Lara-Gonzalez P, Westhorpe FG, Taylor SS. The spindle assembly checkpoint.Curr Biol. 2012 Nov 20;22(22):R966-80. doi: 10.1016/j.cub.2012.10.006. Review.PubMed PMID: 23174302.

Lee AK, Potts PR. A Comprehensive Guide to the MAGE Family of Ubiquitin Ligases. J Mol Biol. 2017 Apr 21;429(8):1114-1142. doi:10.1016/j.jmb.2017.03.005. Epub 2017 Mar 11. Review. PubMed PMID: 28300603;PubMed Central PMCID: PMC5421567.

Legerski RJ. Repair of DNA interstrand cross-links during S phase of the mammalian cell cycle. Environ Mol Mutagen. 2010 Jul;51(6):540-51. doi:10.1002/em.20566. Review. PubMed PMID: 20658646; PubMed Central PMCID:PMC2911997.

Lehmann AR, Walicka M, Griffiths DJ, Murray JM, Watts FZ, McCready S, Carr AM.The rad18 gene of Schizosaccharomyces pombe defines a new subgroup of the SMC superfamily involved in DNA repair. Mol Cell Biol. 1995 Dec;15(12):7067-80.PubMed PMID: 8524274; PubMed Central PMCID: PMC230962.

Li G, Zou W, Jian L, Qian J, Deng Y, Zhao J. Non-SMC elements 1 and 3 are required for early embryo and seedling development in Arabidopsis. J Exp Bot. 2017 Feb 1;68(5):1039-1054. doi: 10.1093/jxb/erx016. PMID: 28207059; PMCID: PMC5441860.

Li Y., Barbash O., and J. Diehl A., Regulation of the Cell Cycle, Chapter 11. The Molecular Basis of Cancer, 2015, pp.165-178.e2

Liang CC, Li Z, Lopez-Martinez D, Nicholson WV, Vénien-Bryan C, Cohn MA. The FANCD2-FANCI complex is recruited to DNA interstrand crosslinks before monoubiquitination of FANCD2. Nat Commun. 2016;7:12124. Published 2016 Jul 13. doi:10.1038/ncomms12124

Liao H, Ji F, Helleday T, Ying S. Mechanisms for stalled replication fork stabilization: new targets for synthetic lethality strategies in cancer treatments. EMBO Rep. 2018 Sep;19(9):e46263. doi: 10.15252/embr.201846263. Epub 2018 Aug 13. PMID: 30108055; PMCID: PMC6123652.

Lindroos HB, Ström L, Itoh T, Katou Y, Shirahige K, Sjögren C. Chromosomal association of the Smc5/6 complex reveals that it functions in differently regulated pathways. Mol Cell. 2006 Jun 23;22(6):755-67. PubMed PMID: 16793545.

London N, Biggins S. Signalling dynamics in the spindle checkpoint response.Nat Rev Mol Cell Biol. 2014 Nov;15(11):736-doi: 10.1038/nrm3888. Epub 2014 Oct 10. Review. PubMed PMID: 25303117; PubMed Central PMCID: PMC4283840.

Lopez-Martinez D, Liang CC, Cohn MA. Cellular response to DNA interstrand crosslinks: the Fanconi anemia pathway. Cell Mol Life Sci. 2016 Aug;73(16):3097-114. doi: 10.1007/s00018-016-2218-x. Epub 2016 Apr 19. Review.PubMed PMID: 27094386; PubMed Central PMCID: PMC4951507.

Lorick KL, Jensen JP, Fang S, Ong AM, Hatakeyama S, Weissman AM. RING fingers mediate ubiquitin-conjugating enzyme (E2)-dependent ubiquitination. Proc Natl Acad Sci U S A. 1999 Sep 28;96(20):11364-9. PubMed PMID: 10500182; PubMed Central PMCID: PMC18039.

Losada A, Hirano T. Dynamic molecular linkers of the genome: the first decade of SMC proteins. Genes Dev. 2005 Jun 1;19(11):1269-87. Review. PubMed PMID:15937217.

Lundin C, North M, Erixon K, et al. Methyl methanesulfonate (MMS) produces heat-labile DNA damage but no detectable in vivo DNA double-strand breaks [published correction appears in Nucleic Acids Res. 2012 Jul;40(12):5794]. Nucleic Acids Res. 2005;33(12):3799-3811. Published 2005 Jul 11. doi:10.1093/nar/gki681

Macheret M, Halazonetis TD. DNA replication stress as a hallmark of cancer. Annu Rev Pathol. 2015;10:425-448. doi:10.1146/annurev-pathol-012414-040424

Maddox PS, Portier N, Desai A, Oegema K. Molecular analysis of mitotic chromosome condensation using a quantitative time-resolved fluorescence microscopy assay. Proc Natl Acad Sci U S A. 2006 Oct 10;103(41):15097-102. Epub 2006 Sep 27. PubMed PMID: 17005720; PubMed Central PMCID: PMC1622782.

Maeshima K, Eltsov M. Packaging the genome: the structure of mitotic chromosomes. J Biochem. 2008 Feb;143(2):145-53. Epub 2007 Nov 2. Review. PubMed PMID: 17981824; PubMed Central PMCID: PMC3943392.

Maga G, Hubscher U. Proliferating cell nuclear antigen (PCNA): a dancer with many partners. J Cell Sci. 2003 Aug 1;116(Pt 15):3051-60. Review. PubMed PMID:12829735.

Makrantoni V, Marston AL. Cohesin and chromosome segregation. Curr Biol. 2018 Jun 18;28(12):R688-R693. doi: 10.1016/j.cub.2018.05.019. PubMed PMID: 29920258;PubMed Central PMCID: PMC6013277.

Mankouri HW, Ashton TM, Hickson ID. Holliday junction-containing DNA structures persist in cells lacking Sgs1 or Top3 following exposure to DNA damage. Proc Natl Acad Sci U S A. 2011;108(12):4944-4949. doi:10.1073/pnas.1014240108

Maréchal A, Zou L. DNA damage sensing by the ATM and ATR kinases. Cold Spring Harb Perspect Biol. 2013 Sep 1;5(9). pii: a012716. doi:10.1101/cshperspect.a012716. Review. PubMed PMID: 24003211; PubMed Central PMCID:PMC3753707.

Marusyk A, Wheeler LJ, Mathews CK, DeGregori J. p53 mediates senescence-like arrest induced by chronic replicational stress. Mol Cell Biol. 2007 Aug;27(15):5336-51. Epub 2007 May 21. PubMed PMID: 17515610; PubMed Central PMCID: PMC1952086.

May KM, Hardwick KG. The spindle checkpoint. J Cell Sci. 2006 Oct 15;119(Pt20):4139-42. Review. PubMed PMID: 17038540.

Mayerova N, Cipak L, Gregan J. Cohesin Biology: From Passive Rings to Molecular Motors. Trends Genet. 2020;36(6):387-389. doi:10.1016/j.tig.2020.03.001

McAleenan A, Cordon-Preciado V, Clemente-Blanco A, Liu IC, Sen N, Leonard J,Jarmuz A, Aragón L. SUMOylation of the α-kleisin subunit of cohesin is required for DNA damage-induced cohesion. Curr Biol. 2012 Sep 11;22(17):1564-75. doi:10.1016/j.cub.2012.06.045. Epub 2012 Jul 5. PubMed PMID: 22771042.

McDonald WH, Pavlova Y, Yates JR 3rd, Boddy MN. Novel essential DNA repair proteins Nse1 and Nse2 are subunits of the fission yeast Smc5-Smc6 complex. J Biol Chem. 2003 Nov 14;278(46):45460-7. Epub 2003 Sep 8. PubMed PMID: 12966087.

McIntosh D, Blow JJ. Dormant origins, the licensing checkpoint, and the response to replicative stresses. Cold Spring Harb Perspect Biol. 2012 Oct 1;4(10). pii: a012955. doi: 10.1101/cshperspect.a012955. Review. PubMed PMID: 22904560; PubMed Central PMCID: PMC3475168.

McIntosh JR. Mitosis. Cold Spring Harb Perspect Biol. 2016 Sep 1;8(9). pii:a023218. doi: 10.1101/cshperspect.a023218. Review. PubMed PMID: 27587616; PubMed Central PMCID: PMC5008068.

Mehta A, Haber JE. Sources of DNA double-strand breaks and models of recombinational DNA repair. Cold Spring Harb Perspect Biol. 2014 Aug 7;6(9):a016428. doi: 10.1101/cshperspect.a016428. Review. PubMed PMID: 25104768; PubMed Central PMCID: PMC4142968.

Mengiste T, Revenkova E, Bechtold N, Paszkowski J. An SMC-like protein is required for efficient homologous recombination in Arabidopsis. EMBO J. 1999 Aug 16;18(16):4505-12. PubMed PMID: 10449416; PubMed Central PMCID: PMC1171525.

Merrick CJ, Jackson D, Diffley JF. Visualization of altered replication dynamics after DNA damage in human cells. J Biol Chem. 2004;279(19):20067-20075. doi:10.1074/jbc.M400022200

Metzger MB, Pruneda JN, Klevit RE, Weissman AM. RING-type E3 ligases: master manipulators of E2 ubiquitin-conjugating enzymes and ubiquitination. Biochim Biophys Acta. 2014 Jan;1843(1):47-60. doi: 10.1016/j.bbamcr.2013.05.026. Epub 2013 Jun 6. Review. PubMed PMID: 23747565; PubMed Central PMCID: PMC4109693.

Miles JA, Frost MG, Carroll E, et al. The Fanconi Anemia DNA Repair Pathway Is Regulated by an Interaction between Ubiquitin and the E2-like Fold Domain of FANCL. J Biol Chem. 2015;290(34):20995-21006. doi:10.1074/jbc.M115.675835

Mitchison TJ, Salmon ED. Mitosis: a history of division. Nat Cell Biol. 2001 Jan;3(1):E17-21. Review. Erratum in: Nat Cell Biol 2001 May;3(5):530. PubMed PMID: 11146645.

Mitra B, Guo H. Hepatitis B virus X protein crosses out Smc5/6 complex to maintain covalently closed circular DNA transcription. Hepatology. 2016 Dec;64(6):2246-2249. doi: 10.1002/hep.28834. Epub 2016 Oct 28. PubMed PMID:27639252; PubMed Central PMCID: PMC5115954.

Miyabe I, Morishita T, Hishida T, Yonei S, Shinagawa H. Rhp51-dependent recombination intermediates that do not generate checkpoint signal are accumulated in Schizosaccharomyces pombe rad60 and smc5/6 mutants after release from replication arrest. Mol Cell Biol. 2006 Jan;26(1):343-53. PubMed PMID: 16354704; PubMed Central PMCID: PMC1317627.

Mladenov E. and Iliakis G.(September 9th 2011). The Pathways of Double-Strand Break Repair, DNA Repair - On the Pathways to Fixing DNA Damage and Errors, Francesca Storici, IntechOpen, DOI: 10.5772/24572.

Moldovan GL, Pfander B, Jentsch S. PCNA, the maestro of the replication fork. Cell. 2007 May 18;129(4):665-79. Review. PubMed PMID: 17512402.

Morikawa H, Morishita T, Kawane S, Iwasaki H, Carr AM, Shinagawa H. Rad62 protein functionally and physically associates with the smc5/smc6 protein complex and is required for chromosome integrity and recombination repair in fission yeast. Mol Cell Biol. 2004 Nov;24(21):9401-13. PubMed PMID: 15485909; PubMed Central PMCID: PMC522231.

Mourtzoukou D., Drikos I., Goutas N. and Vlachodimitropoulos D. (August 1st 2018). Review of the Ubiquitin Role in DNA Repair and Tumorigenesis, with Emphasis in Breast Cancer Treatment; Current Data and Future Options, Ubiquitination Governing DNA Repair - Implications in Health and Disease, Effrossyni Boutou and Horst-Werner Stürzbecher, IntechOpen, DOI: 10.5772/intechopen.72600.

Muniandy PA, Liu J, Majumdar A, Liu ST, Seidman MM. DNA interstrand crosslink repair in mammalian cells: step by step. Crit Rev Biochem Mol Biol. 2010 Feb;45(1):23-49. doi: 10.3109/10409230903501819. Review. PubMed PMID: 20039786; PubMed Central PMCID: PMC2824768.

Murakami H. and Okayama H., Cell cycle checkpoint control. Experimental and molecular medicine, Vol. 29, No 1, 1-11, March 1997

Murphy CM, Xu Y, Li F, Nio K, Reszka-Blanco N, Li X, Wu Y, Yu Y, Xiong Y, Su L. Hepatitis B Virus X Protein Promotes Degradation of SMC5/6 to Enhance HBV Replication. Cell Rep.

2016 Sep 13;16(11):2846-2854. doi:10.1016/j.celrep.2016.08.026. PubMed PMID: 27626656; PubMed Central PMCID:PMC5078993.

Myung J, Kim KB, Crews CM. The ubiquitin-proteasome pathway and proteasome inhibitors. Med Res Rev. 2001 Jul;21(4):245-73. Review. PubMed PMID: 11410931;PubMed Central PMCID: PMC2556558.

Nalepa G, Clapp DW. Fanconi anaemia and cancer: an intricate relationship. Nat Rev Cancer. 2018 Mar;18(3):168-185. doi: 10.1038/nrc.2017.116. Epub 2018 Jan 29. Review. PubMed PMID: 29376519.

Ni HJ, Chang YN, Kao PH, Chai SP, Hsieh YH, Wang DH, Fong JC. Depletion of SUMO ligase hMMS21 impairs G1 to S transition in MCF-7 breast cancer cells. Biochim Biophys Acta. 2012 Dec;1820(12):1893-900. doi: 10.1016/j.bbagen.2012.08.002. Epub 2012 Aug 10. PMID: 22906975.

Noll DM, Mason TM, Miller PS. Formation and repair of interstrand cross-links in DNA. Chem Rev. 2006 Feb;106(2):277-301. Review. PubMed PMID: 16464006; PubMed Central PMCID: PMC2505341.

O'Connor, C. (2008) Chromosome segregation in mitosis: The role of centromeres. Nature Education 1(1):28

Ohtake F, Tsuchiya H. The emerging complexity of ubiquitin architecture. J Biochem. 2017;161(2):125-133. doi:10.1093/jb/mvw088

Onoda F, Takeda M, Seki M, et al. SMC6 is required for MMS-induced interchromosomal and sister chromatid recombinations in Saccharomyces cerevisiae. DNA Repair (Amst). 2004;3(4):429-439. doi:10.1016/j.dnarep.2003.12.007

Palecek J, Vidot S, Feng M, Doherty AJ, Lehmann AR. The Smc5-Smc6 DNA repair complex. bridging of the Smc5-Smc6 heads by the KLEISIN, Nse4, and non-Kleisin subunits. J Biol Chem. 2006 Dec 1;281(48):36952-9. Epub 2006 Sep 27. PubMed PMID:17005570

Palecek J. J. SMC5/6: Multifunctional Player in Replication. Genes (Basel). 2019 Jan; 10(1): 7.

Pannunzio NR, Watanabe G, Lieber MR. Nonhomologous DNA end-joining for repair of DNA double-strand breaks. J Biol Chem. 2018 Jul 6;293(27):10512-10523. doi:10.1074/jbc.TM117.000374. Epub 2017 Dec 14. Review. PubMed PMID: 29247009; PubMed Central PMCID: PMC6036208.

Papamichos-Chronakis M, Peterson CL. Chromatin and the genome integrity network. Nat Rev Genet. 2013 Jan;14(1):62-75. doi: 10.1038/nrg3345. PMID: 23247436; PMCID: PMC3731064.

Pardo B, Gómez-González B, Aguilera A. DNA repair in mammalian cells: DNA double-strand break repair: how to fix a broken relationship. Cell Mol Life Sci. 2009 Mar;66(6):1039-56. doi: 10.1007/s00018-009-8740-3. Review. PubMed PMID:19153654.

Pasero P, Vindigni A. Nucleases Acting at Stalled Forks: How to Reboot the Replication Program with a Few Shortcuts. Annu Rev Genet. 2017 Nov 27;51:477-499.doi: 10.1146/annurev-genet-120116-024745. Review. PubMed PMID: 29178820.

Patil M, Pabla N, Dong Z. Checkpoint kinase 1 in DNA damage response and cell cycle regulation. Cell Mol Life Sci. 2013;70(21):4009-4021. doi:10.1007/s00018-013-1307-3

Payne F, Colnaghi R, Rocha N, Seth A, Harris J, Carpenter G, Bottomley WE, Wheeler E, Wong S, Saudek V, Savage D, O'Rahilly S, Carel JC, Barroso I, O'Driscoll M, Semple R. Hypomorphism in human NSMCE2 linked to primordial dwarfism and insulin resistance. J Clin Invest. 2014 Sep;124(9):4028-38. doi: 10.1172/JCI73264. Epub 2014 Aug 8. PubMed PMID: 25105364; PubMed Central PMCID:PMC4151221.

Pebernard S, McDonald WH, Pavlova Y, Yates JR 3rd, Boddy MN. Nse1, Nse2, and a novel subunit of the Smc5-Smc6 complex, Nse3, play a crucial role in meiosis. Mol Biol Cell. 2004 Nov;15(11):4866-76. Epub 2004 Aug 25. PubMed PMID: 15331764; PubMed Central PMCID: PMC524734.

Pebernard S (1), Perry JJ, Tainer JA, Boddy MN. Nse1 RING-like domain supports functions of the Smc5-Smc6 holocomplex in genome stability. Mol Biol Cell. 2008 Oct;19(10):4099-109. doi: 10.1091/mbc.E08-02-0226. Epub 2008 Jul 30. PubMed PMID:18667531; PubMed Central PMCID: PMC2555936.

Pebernard S (2), Schaffer L, Campbell D, Head SR, Boddy MN. Localization of Smc5/6 to centromeres and telomeres requires heterochromatin and SUMO, respectively. EMBO J. 2008;27(22):3011-3023. doi:10.1038/emboj.2008.220

Pebernard S, Wohlschlegel J, McDonald WH, Yates JR 3rd, Boddy MN. The Nse5-Nse6 dimer mediates DNA repair roles of the Smc5-Smc6 complex. Mol Cell Biol. 2006 Mar;26(5):1617-30. Erratum in: Mol Cell Biol. 2006 Apr;26(8):3336.PubMed PMID: 16478984; PubMed Central PMCID: PMC1430260.

Peters JM, Tedeschi A, Schmitz J. The cohesin complex and its roles in chromosome biology. Genes Dev. 2008 Nov 15;22(22):3089-114. doi:10.1101/gad.1724308. Review. PubMed PMID: 19056890.

Pfoh R, Lacdao IK, Saridakis V. Deubiquitinases and the new therapeutic opportunities offered to cancer. Endocr Relat Cancer. 2015 Feb;22(1):T35-54. doi:10.1530/ERC-14-0516. Review. PubMed PMID: 25605410; PubMed Central PMCID:PMC4304536.

Pickart CM, Eddins MJ. Ubiquitin: structures, functions, mechanisms. Biochim Biophys Acta. 2004 Nov 29;1695(1-3):55-72. Review. PubMed PMID: 15571809.

Pilecka I, Sadowski L, Kalaidzidis Y, Miaczynska M. Recruitment of APPL1 to ubiquitin-rich aggresomes in response to proteasomal impairment. Exp Cell Res. 2011;317(8):1093-1107. doi:10.1016/j.yexcr.2011.02.002

Pinder JB, Attwood KM, Dellaire G. Reading, writing, and repair: the role of ubiquitin and the ubiquitin-like proteins in DNA damage signaling and repair. Front Genet. 2013;4:45. Published 2013 Apr 1. doi:10.3389/fgene.2013.00045

Podhorecka M, Skladanowski A, Bozko P. H2AX Phosphorylation: Its Role in DNA Damage Response and Cancer Therapy. J Nucleic Acids. 2010 Aug 3;2010. pii:920161. doi: 10.4061/2010/920161. PubMed PMID: 20811597; PubMed Central PMCID:PMC2929501.

Pond KW, de Renty C, Yagle MK, Ellis NA. Rescue of collapsed replication forks is dependent on NSMCE2 to prevent mitotic DNA damage. PLoS Genet. 2019 Feb 8;15(2):e1007942. doi:

10.1371/journal.pgen.1007942. eCollection 2019 Feb. PubMed PMID: 30735491; PubMed Central PMCID: PMC6383951.

Poole LA, Cortez D. Functions of SMARCAL1, ZRANB3, and HLTF in maintaining genome stability. Crit Rev Biochem Mol Biol. 2017;52(6):696-714. doi:10.1080/10409238.2017.1380597

Potts PR, Porteus MH, Yu H. Human SMC5/6 complex promotes sister chromatid homologous recombination by recruiting the SMC1/3 cohesin complex to double-strand breaks. EMBO J. 2006 Jul 26;25(14):3377-88. Epub 2006 Jun 29.PubMed PMID: 16810316; PubMed Central PMCID: PMC1523187.

Potts PR, Yu H. Human MMS21/NSE2 is a SUMO ligase required for DNA repair. Mol Cell Biol. 2005 Aug;25(16):7021-32. PubMed PMID: 16055714; PubMed Central PMCID: PMC1190242.

Potts PR, Yu H. The SMC5/6 complex maintains telomere length in ALT cancer cells through SUMOylation of telomere-binding proteins. Nat Struct Mol Biol. 2007 Jul;14(7):581-90. Epub 2007 Jun 24. PubMed PMID: 17589526.doi:10.1038/nsmb1259

Pradhan A, Singh TR, Ali AM, Wahengbam K, Meetei AR. Monopolar spindle 1 (MPS1) protein-dependent phosphorylation of RecQ-mediated genome instability protein 2 (RMI2) at serine 112 is essential for BLM-Topo III α-RMI1-RMI2 (BTR) protein complex function upon spindle assembly checkpoint (SAC) activation during mitosis. J Biol Chem. 2013;288(47):33500-33508. doi:10.1074/jbc.M113.470823

Prakash R, Satory D, Dray E, Papusha A, Scheller J, Kramer W, Krejci L, Klein H, Haber JE, Sung P, Ira G. Yeast Mph1 helicase dissociates Rad51-made D-loops:implications for crossover control in mitotic recombination. Genes Dev. 2009 Jan 1;23(1):67-79. doi: 10.1101/gad.1737809. PubMed PMID: 19136626; PubMed Central PMCID: PMC2632165.

Pryzhkova MV, Jordan PW. Conditional mutation of Smc5 in mouse embryonic stem cells perturbs condensin localization and mitotic progression. J Cell Sci. 2016 Apr 15;129(8):1619-34. doi: 10.1242/jcs.179036. Epub 2016 Feb 26. PubMed PMID:26919979; PubMed Central PMCID: PMC4852767.

Quinet A, Lemaçon D, Vindigni A. Replication Fork Reversal: Players and Guardians. Mol Cell. 2017 Dec 7;68(5):830-833. doi: 10.1016/j.molcel.2017.11.022.Review. PubMed PMID: 29220651; PubMed Central PMCID: PMC5895179.

Ramaekers CH, Wouters BG. Regulatory functions of ubiquitin in diverse DNA damage responses. Curr Mol Med. 2011;11(2):152-169. doi:10.2174/156652411794859269

Ran FA, Hsu PD, Wright J, Agarwala V, Scott DA, Zhang F. Genome engineering using the CRISPR-Cas9 system. Nat Protoc. 2013;8(11):2281-2308. doi:10.1038/nprot.2013.143

Räschle M, Smeenk G, Hansen RK, Temu T, Oka Y, Hein MY, Nagaraj N, Long DT,Walter JC, Hofmann K, Storchova Z, Cox J, Bekker-Jensen S, Mailand N, Mann M. DNA repair. Proteomics reveals dynamic assembly of repair complexes during bypass of DNA cross-links. Science. 2015 May 1;348(6234):1253671. doi:10.1126/science.1253671. Epub 2015 Apr 30. PubMed PMID:25931565; PubMed Central PMCID: PMC5331883.

Reusswig KU, Pfander B. Control of Eukaryotic DNA Replication Initiation-Mechanisms to Ensure Smooth Transitions. Genes (Basel). 2019 Jan 29;10(2). pii: E99. doi: 10.3390/genes10020099. Review. PubMed PMID: 30700044;PubMed Central PMCID: PMC6409694.

Rieder CL. Mitosis in vertebrates: the G2/M and M/A transitions and their associated checkpoints. Chromosome Res. 2011 Apr;19(3):291-306. doi:10.1007/s10577-010-9178-z. Review. PubMed PMID: 21194009.

Rodgers K, McVey M. Error-Prone Repair of DNA Double-Strand Breaks. J Cell Physiol. 2016 Jan;231(1):15-24. doi: 10.1002/jcp.25053. Review. PubMed PMID:26033759; PubMed Central PMCID: PMC4586358.

Rodríguez A, D'Andrea A. Fanconi anemia pathway. Curr Biol. 2017 Sep 25;27(18):R986-R988. doi: 10.1016/j.cub.2017.07.043. PubMed PMID: 28950089.

Rossi F, Helbling-Leclerc A, Kawasumi R, et al. SMC5/6 acts jointly with Fanconi anemia factors to support DNA repair and genome stability. EMBO Rep. 2020;21(2):e48222. doi:10.15252/embr.201948222

Sale JE. Competition, collaboration and coordination--determining how cells bypass DNA damage. J Cell Sci. 2012 Apr 1;125(Pt 7):1633-43. doi:10.1242/jcs.094748. Epub 2012 Apr 12. Review. PubMed PMID: 22499669.

Sancar A, Lindsey-Boltz LA, Unsal-Kaçmaz K, Linn S. Molecular mechanisms of mammalian DNA repair and the DNA damage checkpoints. Annu Rev Biochem.2004;73:39-85. Review. PubMed PMID: 15189136.

Saunus JM, Quinn MC, Patch AM, Pearson JV, Bailey PJ, Nones K, McCart Reed AE, Miller D, Wilson PJ, Al-Ejeh F, Mariasegaram M, Lau Q, Withers T, Jeffree RL, Reid LE, Da Silva L, Matsika A, Niland CM, Cummings MC, Bruxner TJ, Christ AN,Harliwong I, Idrisoglu S, Manning S, Nourse C, Nourbakhsh E, Wani S, Anderson MJ,Fink JL, Holmes O, Kazakoff S, Leonard C, Newell F, Taylor D, Waddell N, Wood S, Xu Q, Kassahn KS, Narayanan V, Taib NA, Teo SH, Chow YP, kConFab, Jat PS,Brandner S, Flanagan AM, Khanna KK, Chenevix-Trench G, Grimmond SM, Simpson PT,Waddell N, Lakhani SR. Integrated genomic and transcriptomic analysis of human brain metastases identifies alterations of potential clinical significance. J Pathol. 2015 Nov;237(3):363-78. doi: 10.1002/path.4583. Epub 2015 Aug 19. PubMed PMID: 26172396.

Saurin AJ, Borden KL, Boddy MN, Freemont PS. Does this have a familiar RING? Trends Biochem Sci. 1996 Jun;21(6):208-14. PubMed PMID: 8744354.

Schärer OD. Nucleotide excision repair in eukaryotes. Cold Spring Harb Perspect Biol. 2013 Oct 1;5(10):a012609. doi: 10.1101/cshperspect.a012609.Review. PubMed PMID: 24086042; PubMed Central PMCID: PMC3783044.

Schwab RA, Nieminuszczy J, Shah F, Langton J, Lopez Martinez D, Liang CC, Cohn MA, Gibbons RJ, Deans AJ, Niedzwiedz W. The Fanconi Anemia Pathway Maintains Genome Stability by Coordinating Replication and Transcription. Mol Cell. 2015 Nov 5;60(3):351-61. doi: 10.1016/j.molcel.2015.09.012. Epub 2015 Oct 22. PubMed PMID: 26593718; PubMed Central PMCID: PMC4644232.

Schwertman P, Bekker-Jensen S, Mailand N. Regulation of DNA double-strand break repair by ubiquitin and ubiquitin-like modifiers. Nat Rev Mol Cell Biol. 2016;17(6):379-394. doi:10.1038/nrm.2016.58

Seeger C, Mason WS. Hepatitis B virus biology. Microbiol Mol Biol Rev. 2000 Mar;64(1):51-68. Review. PubMed PMID: 10704474; PubMed Central PMCID: PMC98986.

Segurado M, Tercero JA. The S-phase checkpoint: targeting the replication fork. Biol Cell. 2009;101(11):617-627. Published 2009 Aug 19. doi:10.1042/BC20090053

Seiler JA, Conti C, Syed A, Aladjem MI, Pommier Y. The intra-S-phase checkpoint affects both DNA replication initiation and elongation: single-cell and -DNA fiber analyses. Mol Cell Biol. 2007 Aug;27(16):5806-18. Epub 2007 May 21. PubMed PMID: 17515603; PubMed Central PMCID: PMC1952133.

Sergeant J, Taylor E, Palecek J, Fousteri M, Andrews EA, Sweeney S, Shinagawa H, Watts FZ, Lehmann AR. Composition and architecture of the Schizosaccharomyces pombe Rad18 (Smc5-6) complex. Mol Cell Biol. 2005 Jan;25(1):172-84. PubMed PMID: 15601840; PubMed Central PMCID: PMC538765.

Shaltiel IA, Krenning L, Bruinsma W, Medema RH. The same, only different – DNA damage checkpoints and their reversal throughout the cell cycle. J Cell Sci. 2015 Feb 15;128(4):607-20. doi: 10.1242/jcs.163766. Epub 2015 Jan 20. Review. PubMed PMID: 25609713.

Singh TR, Ali AM, Paramasivam M, et al. ATR-dependent phosphorylation of FANCM at serine 1045 is essential for FANCM functions. Cancer Res. 2013;73(14):4300-4310. doi:10.1158/0008-5472.CAN-12-3976

Solé-Soler R, Torres-Rosell J. Smc5/6, an atypical SMC complex with two RING-type subunits. Biochem Soc Trans. 2020 Oct 30;48(5):2159-2171. doi: 10.1042/BST20200389. PMID: 32964921.

Stephan AK, Kliszczak M, Morrison CG. The Nse2/Mms21 SUMO ligase of the Smc5/6 complex in the maintenance of genome stability. FEBS Lett. 2011 Sep 16;585(18):2907-13. doi: 10.1016/j.febslet.2011.04.067. Epub 2011 May 4. Review. PubMed PMID: 21550342.

Streich FC Jr, Haas AL. Activation of ubiquitin and ubiquitin-like proteins. Subcell Biochem. 2010;54:1-16. doi: 10.1007/978-1-4419-6676-6_1. PubMed PMID:21222269.

Stringer DK, Piper RC. Terminating protein ubiquitination: Hasta la vista,ubiquitin. Cell Cycle. 2011 Sep 15;10(18):3067-71. Epub 2011 Sep 15. PubMed PMID:21926471; PubMed Central PMCID: PMC3685619.

Strunnikov A.V., Larionov V.L., Koshland D. SMC1an essential yeast gene encoding a putative head-rod-tail protein is required for nuclear division and defines a new ubiquitous protein family. J. Cell Biol. 1993;123:1635–1648.

Strzalka W, Ziemienowicz A. Proliferating cell nuclear antigen (PCNA): a key factor in DNA replication and cell cycle regulation. Ann Bot. 2011 May;107(7):1127-40. doi: 10.1093/aob/mcq243. Epub 2010 Dec 17. PubMed PMID: 21169293; PubMed Central PMCID: PMC3091797.

Subramanian M, Gonzalez RW, Patil H, et al. The nucleosome-binding protein HMGN2 modulates global genome repair. FEBS J. 2009;276(22):6646-6657. doi:10.1111/j.1742-4658.2009.07375.x

Sumpter R Jr, Levine B. Emerging functions of the Fanconi anemia pathway at a glance. J Cell Sci. 2017 Aug 15;130(16):2657-2662. doi: 10.1242/jcs.204909. Review. PubMed PMID: 28811338; PubMed Central PMCID: PMC5576063.

Swatek KN, Komander D. Ubiquitin modifications. Cell Res. 2016 Apr;26(4):399-422. doi: 10.1038/cr.2016.39. Epub 2016 Mar 25. Review. PubMed PMID: 27012465; PubMed Central PMCID: PMC4822133.

Takahashi Y, Dulev S, Liu X, Hiller NJ, Zhao X, Strunnikov A. Cooperation of sumoylated chromosomal proteins in rDNA maintenance. PLoS Genet. 2008 Oct;4(10):e1000215. doi: 10.1371/journal.pgen.1000215. Epub 2008 Oct 10. PubMed PMID: 18846224; PubMed Central PMCID: PMC2563031.

Taniguchi T, D'Andrea AD. Molecular pathogenesis of Fanconi anemia: recent progress. Blood. 2006 Jun 1;107(11):4223-33. Epub 2006 Feb 21. Review. PubMed PMID: 16493006.

Taylor EM, Copsey AC, Hudson JJ, Vidot S, Lehmann AR. Identification of the proteins, including MAGEG1, that make up the human SMC5-6 protein complex. Mol Cell Biol. 2008 Feb;28(4):1197-206. Epub 2007 Dec 17. PubMed PMID: 18086888; PubMed Central PMCID: PMC2258758.

Tercero JA, Diffley JF. Regulation of DNA replication fork progression through damaged DNA by the Mec1/Rad53 checkpoint. Nature. 2001 Aug 2;412(6846):553-7.PubMed PMID: 11484057.

Terry Powers JL, Mace KE, Parfrey H, Lee SJ, Zhang G, Riches DW. TNF receptor-1 (TNF-R1) ubiquitous scaffolding and signaling protein interacts with TNF-R1 and TRAF2 via an N-terminal docking interface. Biochemistry. 2010 Sep 14;49(36):7821-9. doi: 10.1021/bi100726n. PubMed PMID: 20704259; PubMed Central PMCID: PMC2952493.

Torres-Rosell J (1), De Piccoli G, Cordon-Preciado V, Farmer S, Jarmuz A, Machin F, Pasero P, Lisby M, Haber JE, Aragón L. Anaphase onset before complete DNA replication with intact checkpoint responses. Science. 2007 Mar 9;315(5817):1411-5. PubMed PMID: 17347440.

Torres-Rosell J (1), Machín F, Farmer S, Jarmuz A, Eydmann T, Dalgaard JZ, Aragón L. SMC5 and SMC6 genes are required for the segregation of repetitive chromosome regions. Nat Cell Biol. 2005 Apr;7(4):412-9. Epub 2005 Mar 27. PubMed PMID:15793567.

Torres-Rosell J (2), Machin F, Aragón L. Smc5-Smc6 complex preserves nucleolar integrity in S. cerevisiae. Cell Cycle. 2005 Jul;4(7):868-72. Epub 2005 Jul 5.PubMed PMID: 15917663.

Torres-Rosell J (2), Sunjevaric I, De Piccoli G, Sacher M, Eckert-Boulet N, Reid R, Jentsch S, Rothstein R, Aragón L, Lisby M. The Smc5-Smc6 complex and SUMO modification of Rad52 regulates recombinational repair at the ribosomal gene locus. Nat Cell Biol. 2007 Aug;9(8):923-31. Epub 2007 Jul 22. PubMed PMID:17643116.

Uckelmann M, Sixma TK. Histone ubiquitination in the DNA damage response. DNA Repair (Amst). 2017 Aug;56:92-101. doi: 10.1016/j.dnarep.2017.06.011. Epub 2017 Jun 9. Review. PubMed PMID: 28624371.

Ulrich HD. Ubiquitin and SUMO in DNA repair at a glance. J Cell Sci. 2012 Jan 15;125(Pt 2):249-54. doi: 10.1242/jcs.091801. Review. PubMed PMID: 22357966.

Ulrich, H. Two-way communications between ubiquitin-like modifiers and DNA. Nat Struct Mol Biol 21, 317–324 (2014). https://doi.org/10.1038/nsmb.2805

Ünal E, Arbel-Eden A, Sattler U, Shroff R, Lichten M, Haber JE, Koshland D.DNA damage response pathway uses histone modification to assemble a double-strand break-specific cohesin domain. Mol Cell. 2004 Dec 22;16(6):991-1002. PubMed PMID:15610741.

Unsal-Kaçmaz K, Chastain PD, Qu PP, Minoo P, Cordeiro-Stone M, Sancar A, Kaufmann WK. The human Tim/Tipin complex coordinates an Intra-S checkpoint response to UV that slows replication fork displacement. Mol Cell Biol. 2007 Apr;27(8):3131-42. Epub 2007 Feb 12. PubMed PMID: 17296725; PubMed Central PMCID:PMC1899931.

van der Crabben SN, Hennus MP, McGregor GA, Ritter DI, Nagamani SC, Wells OS, Harakalova M, Chinn IK, Alt A, Vondrova L, Hochstenbach R, van Montfrans JM, Terheggen-Lagro SW, van Lieshout S, van Roosmalen MJ, Renkens I, Duran K, Nijman IJ, Kloosterman WP, Hennekam E, Orange JS, van Hasselt PM, Wheeler DA, Palecek JJ, Lehmann AR, Oliver AW, Pearl LH, Plon SE, Murray JM, van Haaften G. Destabilized SMC5/6 complex leads to chromosome breakage syndrome with severe lung disease. J Clin Invest. 2016 Aug 1;126(8):2881-92. doi: 10.1172/JCI82890. Epub 2016 Jul 18. PubMed PMID: 27427983; PubMed Central PMCID: PMC4966312.

van Ruiten MS, Rowland BD. SMC Complexes: Universal DNA Looping Machines with Distinct Regulators. Trends Genet. 2018 Jun;34(6):477-487. doi:10.1016/j.tig.2018.03.003. Epub 2018 Mar 29. Review. PubMed PMID: 29606284.

Varejão N, Ibars E, Lascorz J, Colomina N, Torres-Rosell J, Reverter D. DNA activates the Nse2/Mms21 SUMO E3 ligase in the Smc5/6 complex. EMBO J. 2018 Jun 15;37(12):e98306. doi: 10.15252/embj.201798306.

Venegas AB, Natsume T, Kanemaki M, Hickson ID. Inducible Degradation of the Human SMC5/6 Complex Reveals an Essential Role Only during Interphase. Cell Rep. 2020 Apr 21;31(3):107533. doi: 10.1016/j.celrep.2020.107533. PMID: 32320646.

Vermeulen K, Van Bockstaele DR, Berneman ZN. The cell cycle: a review of regulation, deregulation and therapeutic targets in cancer. Cell Prolif. 2003 Jun;36(3):131-49. Review. PubMed PMID: 12814430.

Verver DE, Hwang GH, Jordan PW, Hamer G. Resolving complex chromosome structures during meiosis: versatile deployment of Smc5/6. Chromosoma. 2016;125(1):15-27. doi:10.1007/s00412-015-0518-9

Vesela E, Chroma K, Turi Z, Mistrik M. Common Chemical Inductors of Replication Stress: Focus on Cell-Based Studies.Biomolecules. 2017 Feb 21;7(1). pii: E19. doi: 10.3390/biom7010019. Review.PubMed PMID: 28230817; PubMed Central PMCID: PMC5372731.

Visconti R, Della Monica R, Grieco D. Cell cycle checkpoint in cancer: a therapeutically targetable double-edged sword. J Exp Clin Cancer Res. 2016 Sep 27;35(1):153. Review. PubMed PMID: 27670139; PubMed Central PMCID: PMC5037895.

Vissers JH, Nicassio F, van Lohuizen M, Di Fiore PP, Citterio E. The many faces of ubiquitinated histone H2A: insights from the DUBs. Cell Div. 2008 Apr 22;3:8. doi: 10.1186/1747-1028-3-8. PubMed PMID: 18430235; PubMed Central PMCID: PMC2373781.

Wang H (1), Li S, Zhang H, Wang Y, Hao S, Wu X. BLM prevents instability of structure-forming DNA sequences at common fragile sites. PLoS Genet. 2018;14(11):e1007816. Published 2018 Nov 29. doi:10.1371/journal.pgen.1007816

Wang H (2), Li S, Oaks J, Ren J, Li L, Wu X. The concerted roles of FANCM and Rad52 in the protection of common fragile sites. Nat Commun. 2018;9(1):2791. Published 2018 Jul 18. doi:10.1038/s41467-018-05066-y

Wang L, Chen H, Wang C, Hu Z, Yan S. Negative regulator of E2F transcription factors links cell cycle checkpoint and DNA damage repair. Proc Natl Acad Sci U S A. 2018 Apr 17;115(16):E3837-E3845. doi: 10.1073/pnas.1720094115. Epub 2018 Apr PubMed PMID: 29610335; PubMed Central PMCID: PMC5910849.

Wang Y, Leung JW, Jiang Y, et al. FANCM and FAAP24 maintain genome stability via cooperative as well as unique functions. Mol Cell. 2013;49(5):997-1009. doi:10.1016/j.molcel.2012.12.010

Wani S, Maharshi N, Kothiwal D, Mahendrawada L, Kalaivani R, Laloraya S.Interaction of the Saccharomyces cerevisiae RING-domain protein Nse1 with Nse3 and the Smc5/6 complex is required for chromosome replication and stability. Curr Genet. 2018 Jun;64(3):599-617. doi: 10.1007/s00294-017-0776-6. Epub 2017 Nov 8.PubMed PMID: 29119272.

Watanabe K, Pacher M, Dukowic S, Schubert V, Puchta H, Schubert I. The STRUCTURAL MAINTENANCE OF CHROMOSOMES 5/6 complex promotes sister chromatid alignment and homologous recombination after DNA damage in Arabidopsis thaliana. Plant Cell. 2009 Sep;21(9):2688-99. doi: 10.1105/tpc.108.060525. Epub 2009 Sep 8.PubMed PMID: 19737979; PubMed Central PMCID: PMC2768936.

Wenzel ES, Singh ATK. Cell-cycle Checkpoints and Aneuploidy on the Path to Cancer. In Vivo. 2018 Jan-Feb;32(1):1-5. Review. PubMed PMID: 29275292; PubMed Central PMCID: PMC5892633.

Weon JL, Yang SW, Potts PR. Cytosolic Iron-Sulfur Assembly Is Evolutionarily Tuned by a Cancer-Amplified Ubiquitin Ligase. Mol Cell. 2018;69(1):113-125.e6. doi:10.1016/j.molcel.2017.11.010

Westhorpe FG, Straight AF. Chromosome Segregation: Reconstituting the Kinetochore. Curr Biol. 2016;26(23):R1242-R1245. doi:10.1016/j.cub.2016.09.051

Whalen JM, Dhingra N, Wei L, Zhao X, Freudenreich CH. Relocation of Collapsed Forks to the Nuclear Pore Complex Depends on Sumoylation of DNA Repair Proteins and Permits Rad51 Association. Cell Rep. 2020;31(6):107635. doi:10.1016/j.celrep.2020.107635

Wilhelm T, Magdalou I, Barascu A, Técher H, Debatisse M, Lopez BS. Spontaneous slow replication fork progression elicits mitosis alterations in homologous recombination-deficient mammalian cells. Proc Natl Acad Sci U S A. 2014 Jan 14;111(2):763-8. doi: 10.1073/pnas.1311520111. Epub 2013 Dec 17. PMID: 24347643; PMCID: PMC3896206.

Willis N, Rhind N. Regulation of DNA replication by the S-phase DNA damage checkpoint. Cell Div. 2009 Jul 3;4:13. doi: 10.1186/1747-1028-4-13. PubMed PMID: 19575778; PubMed Central PMCID: PMC2714077.

Wilson VG. Introduction to Sumoylation. Adv Exp Med Biol. 2017;963:1-12. doi: 10.1007/978-3-319-50044-7_1. Review. PubMed PMID: 28197903.

Wojcik F, Dann GP, Beh LY, Debelouchina GT, Hofmann R, Muir TW. Functional crosstalk between histone H2B ubiquitylation and H2A modifications and variants. Nat Commun. 2018 Apr 11;9(1):1394. doi: 10.1038/s41467-018-03895-5. PubMed PMID: 29643390; PubMed Central PMCID: PMC5895630.

Wright WD, Shah SS, Heyer WD. Homologous recombination and the repair of DNA double-strand breaks. J Biol Chem. 2018 Jul 6;293(27):10524-10535. doi:10.1074/jbc.TM118.000372. Epub 2018 Mar 29. Review. PubMed PMID: 29599286; PubMed Central PMCID: PMC6036207.

Wu J (1), Kim S, Kwak MS, et al. High mobility group nucleosomal binding domain 2 (HMGN2) SUMOylation by the SUMO E3 ligase PIAS1 decreases the binding affinity to nucleosome core particles. J Biol Chem. 2014;289(29):20000-20011. doi:10.1074/jbc.M114.555425

Wu L (2), Liu Y, Kong D. Mechanism of chromosomal DNA replication initiation and replication fork stabilization in eukaryotes. Sci China Life Sci. 2014 May;57(5):482-7. doi: 10.1007/s11427-014-4631-4. Epub 2014 Apr 4. Review. PubMed PMID: 24699916.

Wu N, Kong X, Ji Z, Zeng W, Potts PR, Yokomori K, Yu H. Scc1 sumoylation by Mms21 promotes sister chromatid recombination through counteracting Wapl. Genes Dev. 2012 Jul 1;26(13):1473-85. doi: 10.1101/gad.193615.112. PubMed PMID:22751501; PubMed Central PMCID: PMC3403015.

Xiong R, Siegel D, Ross D. The activation sequence of cellular protein handling systems after proteasomal inhibition in dopaminergic cells. Chem Biol Interact. 2013 Jul 5;204(2):116-24. doi: 10.1016/j.cbi.2013.04.016. Epub 2013 May 14. PMID: 23684743; PMCID: PMC3784407.

Xu W, Ma C, Zhang Q, Zhao R, Hu D, Zhang X, Chen J, Liu F, Wu K, Liu Y, Wu J. PJA1 Coordinates with the SMC5/6 Complex To Restrict DNA Viruses and Episomal Genes in an Interferon-Independent Manner. J Virol. 2018 Oct 29;92(22):e00825-18. doi: 10.1128/JVI.00825-18. PMID: 30185588; PMCID: PMC6206484.

Xue X, Choi K, Bonner J, Chiba T, Kwon Y, Xu Y, Sanchez H, Wyman C, Niu H,Zhao X, Sung P. Restriction of replication fork regression activities by a conserved SMC complex. Mol Cell. 2014 Nov 6;56(3):436-45. doi:10.1016/j.molcel.2014.09.013. Epub 2014 Oct 16. PubMed PMID: 25439736; PubMed Central PMCID: PMC4268010.

Xue Y, Li Y, Guo R, Ling C, Wang W. FANCM of the Fanconi anemia core complex is required for both monoubiquitination and DNA repair. Hum Mol Genet. 2008 Jun 1;17(11):1641-52. doi: 10.1093/hmg/ddn054. Epub 2008 Feb 19. PMID: 18285517; PMCID: PMC2902294.

Xue X, Sung P, Zhao X. Functions and regulation of the multitasking FANCM family of DNA motor proteins. Genes Dev. 2015;29(17):1777-1788. doi:10.1101/gad.266593.115

Yan S, Wang W, Marqués J, Mohan R, Saleh A, Durrant WE, Song J, Dong X.Salicylic acid activates DNA damage responses to potentiate plant immunity. Mol Cell. 2013 Nov 21;52(4):602-10. doi: 10.1016/j.molcel.2013.09.019. Epub 2013 Oct PubMed PMID: 24207055; PubMed Central PMCID: PMC3863363.

Yang J, Bachrati CZ, Hickson ID, Brown GW. BLM and RMI1 alleviate RPA inhibition of TopoIIIα decatenase activity. PLoS One. 2012;7(7):e41208. doi:10.1371/journal.pone.0041208

Yang K, Guo R, Xu D. Non-homologous end joining: advances and frontiers. Acta Biochim Biophys Sin (Shanghai). 2016 Jul;48(7):632-40. doi: 10.1093/abbs/gmw046. Epub 2016 May 23. Review. PubMed PMID: 27217473.

Yang V.W., Chapter 8 - The Cell Cycle, Physiology of the Gastrointestinal Tract, 197-219, 2018. doi.org/10.1016/b978-0-12-809954-4.00008-6.

Yates M, Maréchal A. Ubiquitylation at the Fork: Making and Breaking Chains to Complete DNA Replication. Int J Mol Sci. 2018;19(10):2909. Published 2018 Sep 25. doi:10.3390/ijms19102909

Yekezare M, Gómez-González B, Diffley JF. Controlling DNA replication origins in response to DNA damage - inhibit globally, activate locally. J Cell Sci. 2013 Mar 15;126(Pt 6):1297-306. doi: 10.1242/jcs.096701. Review. PubMed PMID:23645160.

Yimit A, Kim T, Anand RP, et al. MTE1 Functions with MPH1 in Double-Strand Break Repair. Genetics. 2016;203(1):147-157. doi:10.1534/genetics.115.185454

Yonashiro R, Ishido S, Kyo S, et al. A novel mitochondrial ubiquitin ligase plays a critical role in mitochondrial dynamics. EMBO J. 2006;25(15):3618-3626. doi:10.1038/sj.emboj.7601249

Yoshiyama KO, Sakaguchi K, Kimura S. DNA damage response in plants: conserved and variable response compared to animals. Biology (Basel). 2013 Nov 21;2(4):1338-56. doi: 10.3390/biology2041338. PubMed PMID: 24833228; PubMed Central PMCID: PMC4009792.

Yu CJ, Wang QS, Wu MM, Song BL, Liang C, Lou J, Tang LL, Yu XD, Niu N, Yang X,Zhang BL, Qu Y, Liu Y, Dong ZC, Zhang ZR. TRUSS Exacerbates NAFLD Development by Promoting IκBα Degradation in Mice. Hepatology. 2018 Nov;68(5):1769-1785. doi:10.1002/hep.30066. Epub 2018 Oct 4. PubMed PMID: 29704259.

Yu J, Qin B, Lou Z. Ubiquitin and ubiquitin-like molecules in DNA double strand break repair. Cell Biosci. 2020 Feb 11;10:13. doi: 10.1186/s13578-020-0380-1. PMID: 32071713; PMCID: PMC7014694.

Yuen KC, Gerton JL. Taking cohesin and condensin in context. PLoS Genet. 2018 Jan 25;14(1):e1007118. doi: 10.1371/journal.pgen.1007118. PMID: 29370184; PMCID: PMC5784890.

Zapatka M, Pociño-Merino I, Heluani-Gahete H, et al. Sumoylation of Smc5 Promotes Error-free Bypass at Damaged Replication Forks. Cell Rep. 2019;29(10):3160-3172.e4. doi:10.1016/j.celrep.2019.10.123

Zelkowski M, Zelkowska K, Conrad U, et al. Arabidopsis NSE4 Proteins Act in Somatic Nuclei and Meiosis to Ensure Plant Viability and Fertility. Front Plant Sci. 2019;10:774. Published 2019 Jun 20. doi:10.3389/fpls.2019.00774

Zeman MK, Cimprich KA. Causes and consequences of replication stress. Nat Cell Biol. 2014 Jan;16(1):2-9. doi: 10.1038/ncb2897. Review. PubMed PMID: 24366029;PubMed Central PMCID: PMC4354890.

Zhang J, Dewar JM, Budzowska M, Motnenko A, Cohn MA, Walter JC. DNA interstrand cross-link repair requires replication-fork convergence. Nat Struct Mol Biol. 2015 Mar;22(3):242-7. doi: 10.1038/nsmb.2956. Epub 2015 Feb 2. PMID: 25643322; PMCID: PMC4351167.

Zhang J, Walter JC. Mechanism and regulation of incisions during DNA interstrand cross-link repair. DNA Repair (Amst). 2014 Jul;19:135-42. doi:10.1016/j.dnarep.2014.03.018. Epub 2014 Apr 24. Review. PubMed PMID: 24768452;PubMed Central PMCID: PMC4076290.

Zhang W, Qin Z, Zhang X, Xiao W. Roles of sequential ubiquitination of PCNA in DNA-damage tolerance. FEBS Lett. 2011 Sep 16;585(18):2786-94. doi:10.1016/j.febslet.2011.04.044. Epub 2011 Apr 28. Review. PubMed PMID: 21536034.

Zhao X, Blobel G. A SUMO ligase is part of a nuclear multiprotein complex that affects DNA repair and chromosomal organization. Proc Natl Acad Sci U S A. 2005 Mar 29;102(13):4777-82. Epub 2005 Feb 28. Erratum in: Proc Natl Acad Sci U S A. 2005 Jun 21;102(25):9086. PubMed PMID: 15738391; PubMed Central PMCID: PMC555716.

Zhao Y, Brickner JR, Majid MC, Mosammaparast N. Crosstalk between ubiquitin and other post-translational modifications on chromatin during double-strand break repair. Trends Cell Biol. 2014 Jul;24(7):426-34. doi:10.1016/j.tcb.2014.01.005. Epub 2014 Feb 23. Review. PubMed PMID: 24569222;PubMed Central PMCID: PMC4074573.

Zheng L, Shen B. Okazaki fragment maturation: nucleases take centre stage. J Mol Cell Biol. 2011 Feb;3(1):23-30. doi: 10.1093/jmcb/mjq048. PubMed PMID: 21278448; PubMed Central PMCID: PMC3030970.

Zheng N, Shabek N. Ubiquitin Ligases: Structure, Function, and Regulation.Annu Rev Biochem. 2017 Jun 20;86:129-157. doi:10.1146/annurev-biochem-060815-014922. Epub 2017 Mar 27. Review. PubMed PMID:28375744.

Zinngrebe J, Montinaro A, Peltzer N, Walczak H. Ubiquitin in the immune system. EMBO Rep. 2014 Jan;15(1):28-45. doi: 10.1002/embr.201338025. Epub 2013 Dec 27. Review. Erratum in: EMBO Rep. 2014 Mar;15(3):322. PubMed PMID: 24375678; PubMed Central PMCID: PMC4303447.